



HAL
open science

Study on the elaboration of highly porous materials by means of a supercritical process

Francisco Ruiz González

► **To cite this version:**

Francisco Ruiz González. Study on the elaboration of highly porous materials by means of a supercritical process. Chemical and Process Engineering. Université de Lorraine, 2015. English. NNT : 2015LORR0332 . tel-04037881

HAL Id: tel-04037881

<https://hal.univ-lorraine.fr/tel-04037881>

Submitted on 20 Mar 2023

HAL is a multi-disciplinary open access archive for the deposit and dissemination of scientific research documents, whether they are published or not. The documents may come from teaching and research institutions in France or abroad, or from public or private research centers.

L'archive ouverte pluridisciplinaire **HAL**, est destinée au dépôt et à la diffusion de documents scientifiques de niveau recherche, publiés ou non, émanant des établissements d'enseignement et de recherche français ou étrangers, des laboratoires publics ou privés.



AVERTISSEMENT

Ce document est le fruit d'un long travail approuvé par le jury de soutenance et mis à disposition de l'ensemble de la communauté universitaire élargie.

Il est soumis à la propriété intellectuelle de l'auteur. Ceci implique une obligation de citation et de référencement lors de l'utilisation de ce document.

D'autre part, toute contrefaçon, plagiat, reproduction illicite encourt une poursuite pénale.

Contact : ddoc-theses-contact@univ-lorraine.fr

LIENS

Code de la Propriété Intellectuelle. articles L 122. 4

Code de la Propriété Intellectuelle. articles L 335.2- L 335.10

http://www.cfcopies.com/V2/leg/leg_droi.php

<http://www.culture.gouv.fr/culture/infos-pratiques/droits/protection.htm>



UNIVERSITÉ
DE LORRAINE



Thèse

En vue de l'obtention du grade de

DOCTEUR DE L'UNIVERSITÉ DE LORRAINE

Spécialité : Génie des procédés et des produits

par

Francisco RUIZ GONZÁLEZ

**Etude de l'élaboration de matériaux à très haute porosité par
des procédés mettant en oeuvre des fluides supercritiques**

Soutenance prévue le 18 Décembre 2015 devant le jury composé de:

M. Arnaud RIGACCI	Professeur, Mines ParisTech-PERSEE	Rapporteur
M. Jean-Stéphane CONDORET	Professeur, INP-ENSIACET	Rapporteur
M. Jacques FAGUES	Professeur, Mines Albi - RAPSODEE	Examineur
M. Geert WOERLEE	Président, FeyeCon	Invité
M. Michel PERRUT	Président, SEPAREX S.A.S.	Co-dir. de thèse
M. Huai Zhi LI	Professeur, ENSIC - LRGP	Directeur de thèse

ACKNOWLEDGEMENTS

First and foremost I want to thank both my thesis Director, Prof. Huai Zhi LI, for the support and confidence shown over the years of thesis and the high availability at any moment to help whether at a professional or personal level. Each meeting with you was an injection of energy; and my thesis Co-Director, Dr. Michel PERRUT, for the enormous confidence placed from the very beginning and the incessant influence on my work, which allowed me to achieve many targets which I would have never imagined reaching. It has been a great pleasure to share this experience with a professional, and a person, of your level. Thanks also for all the wise counsels at the precise moments.

My deepest gratitude to the jury of my thesis, Prof. Jacques FAGUES, Prof. Jean-Stéphane CONDOLET and Prof. Arnaud RIGACCI; it has been a great honor to receive your suggestions and proposals to this work.

I will forever be thankful to SEPAREX for making me grow as a person and as an engineer. This thesis is essentially thanks to your help. To the R&D family, for giving me all your support and knowledge without hesitation while generating, tirelessly, solutions and happiness in equal measure. An especial mention to Dr. Eric FRANÇAIS, for being such a reference for me during all those years. To the equipment team, for the unconditional help and support regardless the craziness of my requests. Great professionals, better people! I would highlight the support and humanity of Dr. Jean Yves CLAVIER at any time. Thanks for giving me the opportunity to achieve this thesis and being an inspiration in my career. Jérémy LAGRUE, Nicolas DESHAYES and Romain POLANZ, without you guys the work would have never been as intense and gratifying as it was. Do never change!

In regards to my participation in the European projects partners, I will never forget the great help, patience and respect they have had with me. All of you have been an inspiration throughout my work as well as an inexhaustible source of wisdom and support.

I would like to acknowledge FeyeCon team for the great work as a whole and the fulfilling of the required gaps in my education beyond the technology. Thanks for providing me with the entrepreneurial and visionary spirit that characterizes you. In particular, my most sincere gratitude to Dr. Geert WOERLEE for the priceless coaching provided along my work; and Ian SPOELSTRA, my “battles” mate, you cannot imagine how much I have learned from you, keep the way you are.

My friends Manuel CANTERO, Juan Antonio IBÁÑEZ, Carlos BRENES and the rest of the group, who have never stopped supporting me although distance and time were not allowing us to be together.

My family in Nüremberg, always a haven of peace at any time; and my family and grandparents in Spain, the thing I am most proud of all the achievements that might be obtained.

Enrique, my brother, for looking after me everywhere and every time, you are indispensable for me. My mother Lina and my father Manolo, my greatest references. My work and personality is only a mere reflection of what you have taught me along my life. Thanks for always being there for me in good and bad times, making me feel as if there were no physical distance separating us.

Lastly, thanks to Lina, my wife, for becoming my source of energy during all these years of thesis, supporting and encouraging me with patience even if that meant not being able to see you. Thank you for always keep beside me and giving me this wonderful life I have begun with you.

I dedicate this thesis to my grandmother Manuela, because this work didn't allow me to tell you goodbye.

“Drying is a commonly practiced art but a neglected science”

R.B.Keey, 1972

TABLE OF CONTENTS

NOMENCLATURE	xi
ABSTRACT	1
RÉSUMÉ	3
RESUMEN	5

CHAPTER 1. SOL-GEL DRYING: LITERATURE AND PATENT SURVEY

1.1. INTRODUCTION	7
1.2. FREEZE DRYING (FD) OR LYOPHILIZATION	10
1.2.1. CONCEPT	10
1.2.2. HISTORY	10
1.2.3. PATENT	11
1.2.4. PUBLICATIONS	12
1.2.5. FUTURE DEVELOPMENT	13
1.3. SUBCRITICAL PRESSURE DRYING (SPD)	13
1.3.1. CONCEPT	13
1.3.2. HISTORY	16
1.3.3. PATENT	17
1.3.4. PUBLICATIONS	19
1.3.5. FUTURE DEVELOPMENT	21
1.4. SUPERCRITICAL DRYING (SCD)	21
1.4.1. CONCEPT	21
1.4.2. HISTORY	25
1.4.3. PATENT	26
1.4.4. PUBLICATIONS	29
1.4.5. FUTURE DEVELOPMENT	32
1.5. CONCLUSIONS	32

REFERENCES	33
------------------	----

**CHAPTER 2. LOW TEMPERATURE SUPERCRITICAL DRYING.
COMPREHENSIVE STUDY OF PROCESSMECHANISIMS AND PRODUCTS**

2.1. INTRODUCTION	45
2.2. EXPERIMENTAL METHODS	46
2.2.1. REAGENTS	46
2.2.2. SYNTHESIS	46
2.2.3. AGING	48
2.2.4. WASHING	48
2.3. EQUIPMENT	49
2.4. LOW TEMPERATURE SUPERCRITICAL DRYING. DRYING MECHANISIMS	51
2.4.1. RAMAN SPECTROSCOPY METHOD	53
2.4.2. RESULTS	54
2.5. AEROGEL FUNKTIONALIZATION. HYDROPHOBIZATION	56
2.5.1. REACTION	57
2.5.2. PREDICTION OF PHASE DIAGRAM ON TERNARY SYSTEM	60
2.5.2.1. Calculation Of the PT envelop	61
2.5.3. ON-LINE HYDROPHOBIZATION vs. STANDARD SILYLATION	61
2.5.3.1. Contact angle measurement	62
2.5.3.2. Water uptake	64
2.5.3.3. FTIR spectra analysis	64
2.5.4. CONCLUSIONS	66
2.6. AEROGEL PRODUCTS	67
2.6.1. SILICA GELS FROM P75E20 PRECURSOR	67
2.6.1.1. Characterization	68
2.6.2. SILICA GELS FROM TEOS58 PRECURSOR	70
2.6.2.1. Characterization	71
2.6.3. SILICA GELS FROM SODIUM SILICATE PRECURSOR	71
2.6.4. OTHER MATERIALS	72
2.6.4.1. Cellulose acetate-based aerogels	72
2.6.4.2. Polyvinyl aerogels	73
2.6.5. COMPOSITE AEROGELS: BLANKETS	74
2.7. CONCLUSIONS	75
REFERENCES	77

CHAPTER 3. APPROACHES TO THE LOW TEMPERATURE SUPERCRITICAL DRYING SCALE-UP AND MANUFACTURING

3.1. INTRODUCTION	79
3.2. PROCESS SIMULATION	79
3.2.1. FUNDAMENTALS OF THE MODELLING	80
3.2.2. THEORETICAL BACKGROUND: MASS-TRANSFER MODELLING	80
3.2.3. CONDITIONS	81
3.2.4. RESULTS	82
3.3. EQUIPMENT SCALE-UP	83
3.3.1. PLANT DESCRIPTION	83
3.3.2. SERVICE CONDITIONS AND DESIGN REQUIREMENTS	85
3.3.3. CALCULATION	86
3.3.3.1. Standards	86
3.3.3.2. Material	86
3.3.3.3. Calculation	86
3.3.4. COMISIONING	88
3.3.5. PROCESS VALIDATION	89
3.4. PRELIMINARY MANUFACTURING	89
3.4.1. PRODUCTION OF BLANKETS	89
3.4.2. CHARACTERIZATION	91
3.4.2.1. Thermal conductivity measurements	91
3.4.2.2. Mechanical properties	92
3.4.2.3. Humidity and water uptake	94
3.5. ECONOMICAL STUDY	95
3.5.1. DESCRIPTION OF STUDIED PARAMETERS AND CONSIDERATIONS	95
3.5.2. CAPITAL EXPENDITURES (CAPEX)	96
3.5.3. OPERATING EXPENSES (OPEX)	97
3.5.3.1. Equipment depreciation	97
3.5.3.2. Raw materials	97
3.5.3.3. Extraction costs	98
3.5.3.4. Man power costs	99
3.5.4. PRODUCTION COSTS	99
3.6. CONCLUSIONS	101
REFERENCES	102

CHAPTER 4. STRATEGY FOR AEROGEL MANUFACTURING DEVELOPMENT

EXECUTIVE SUMMARY	103
-------------------------	-----

4.1	COMPANY DESCRIPTION	105
4.2	MARKET ANALYSIS	106
4.2.1	HISTORY	106
4.3.	PRESENT AND FUTURE	106
4.4.	APPLICATION BY SECTOR	109
4.4.1.	CONSTRUCTION	109
4.4.2.	AEROSPACE	110
4.4.3.	PRECURSOR	111
4.4.4.	ACOUSTIC	112
4.4.5.	OIL & GAS	112
4.4.6.	AERONAUTICS	113
4.4.7.	OPTICS AND INSTRUMENTATION	113
4.4.8.	OTHERS	113
4.5.	SERVICE AND PRODUCT LINE	114
4.5.1.	PRODUCTS & APPLICATIONS	114
4.6.	COSTS AND SALES	119
4.6.1.	RAW MATERIAL. INORGANIC AEROGEL	119
4.6.2.	BLANKET SUPPLY	119
4.6.3.	EXTERNAL SYNTHESIS	119
4.6.4.	MANUFACTURING	119
4.6.5.	SALES	120
4.7.	FUNDING REQUEST	120
4.8.	FINANCIAL PROJECTIONS	123
4.9.	PROFITS AND COSTS	124
4.10.	RISK ANALYSIS	127
4.10.1.	EXTERNAL ANALYSIS. THREATS AND OPPORTUNITIES	127
4.10.1.1.	General Environment or Macro-environment	127
4.10.1.2.	Competitive Environment of Industry	128
4.10.2.	INTERNAL ANALYSIS. STRENGTHS AND WEAKNESS	129
4.10.3.	SWOT ANALYSIS	130
	REFERENCES	131
	GENERAL CONCLUSIONS	133

ANNEXES**ANNEX 1. PREDICTION TERNARY DIAGRAMM**

A1.1. BINARY MIXTURES	139
A1.2. CARBON DIOXIDE – ETHANOL SYSTEM	140
A1.3. ETHANOL – HDMS SYSTEM	141
A1.4. CARBON DIOXIDE – HDMS SYSTEM	142
A1.5. PREDICTION OF PHASE DIAGRAM ON TERNARY SYSTEM	143
REFERENCES	146

ANNEX 2. FLUID FLOW SIMULATION

A2.1. SINGLE PLATE CONSIDERATION	147
A2.1.1 PARAMETRIZATION	148
A2.2. MODULE CONSIDERATION	149
A2.3. ORIGINAL CONSIDERATION	149
A2.4. MODIFIED CONFIGURATION	152

ANNEX 3. PILOT PLANT P&ID

A3.1. PILOT PLANT P&ID	155
------------------------------	-----

ANNEX 4. PILOT PLANT INSTALLATION REUQIREMENTS

A4.1. CONNECTIONS	157
A4.2. MECHANICAL SPECIFICATIONS	157
A4.3. DESCRIPTION OF INSTALLATION ELEMENTS	158

TABLE OF FIGURES	163
-------------------------------	------------

LIST OF TABLES	167
-----------------------------	------------

ABBREVIATIONS

ACCIONA	AccionaInfraestructuras SA
AEROCOINs	Aerogel-Based Composite/Hybrid Nanomaterials for Cost-Effective Building Super-Insulation Systems
AerSUS	Aerogel European Supplying Unit for Space Applications
AIP	Alumina Isopropoxide
ARMINES	<i>Association pour la recherche et le developpement des methods et processus industriels</i>
AST	Active Space Technologies
ATEX	<i>Appareils destinés à être utilisés en ATmosphères EXplosives.</i>
BPR	Back Pressure Regulator
CAGR	Compound Annual Growth Rate
CAPEX	CAPital EXpenditures
CERN	<i>Organisation Européenne pour la Recherché Nucleaire</i>
CODAP	French Code of construction of pressure apparatus
CTP	<i>Centre Thermodynamique des Procédes</i>
CUI	Corrosion Under Insulation
DCCA	Drying Control Chemical Additives
DESY	<i>Deutches Elektronen-Synchroton</i>
DMF	N, N-dimethylformamide
EDAS	Propyltrimethoxysilane
EMPA	EidgenoessischeMaterialprufungs-und Forschungsanstalt
FD	Freeze Drying
FTIR	Fourier Transform Infrared Spectroscopy
HFIP	Hexafluoroisopropyl alcohol
HIPIN	High Performance Insulation based on Nanostructure Encapsulation of Air
HMDS	Hexamethyldisiloxane
HMDZ	Hexamethyldisilazane
HPC	High Pressure Chamber
HTSCD	High Temperature Supercritical Drying

IEA	International Energy Agency
IP	Intellectual Property
IPPC	Intergovernmental Panel on Climate Change
LNG	Liquefied Natural Gas
LRGP-CNRS	<i>Laboratoire Réactions et Génie des Procédés</i> - Centre National de la Recherche Scientifique
LTSCD	Low Temperature Supercritical Drying
ML	Manufacturing level
MLI	Multi Layer Insulation
MTES	Methyltriethoxysilane
MTMS	Methyltrimethoxysilane
NIST	National Institute of Standards and Technology
NMMO	<i>N</i> -methyl-morpholine- <i>N</i> -oxide
OPEX	OPerating EXpenses
PCAS	Produits Chimiques Auxiliaires et de Synthèse SA
OSA	Oil Shale Ash
P&ID	Piping and Instrumentation diagram
PEDS	Polyethoxydisiloxane
PEM	Proton Exchange Membrane
PES	Polyethersulfone
PFAS	Perfluoroalkylsilane
PR EoS	Peng-Robinson Equation of State
PTES	Phenyltriethoxysilane
PTFE	Polytetrafluoroethylene
PTMS	Phenyltrimethoxysilane
PVA-CNF	Cellulose nanofibril
RESSEPEE	REtrofitting Solutions and Services for the enhancement of Energy Efficiency in Public Edification
RF	Resorcinol-formaldehyde
RH	Relative Humidity
RSCE	Rapid Supercritical Extraction Process
SAS	Supercritical AntiSolvent
SEPAREX	Separex SA
SOAT	Erlangen Graduate School in Advanced Optical Technologies
SRK	Soave-Redlich-Kwong
SS	Stainless steel
SWCNT/PANI	Polyaniline
TECNALIA	Fundación Tecnalia research & Innovation
TEOS	Tetraethoxysilane
TIPS	Thermally Induced Phase Separations
TMCS	Trimethylchlorosilane

TMOS	Tetraethoxysilane
TRL	Technology Readiness Level
VTT	ValtionTeknillinen Tutkimuskeskus
ZAE	Bayerisches Zentrum für Angewandte Energieforschung ZAE
EV	

INDEX

<i>c</i>	Critical
<i>e</i>	Test pressure
<i>i</i>	Chemical species
<i>m</i>	Melting point
<i>n</i>	Nominal
<i>s</i>	Calculated pressure

NOMENCLATURE

\vec{U}	Fluid mass-averaged velocity [m/s]
<i>c</i>	Mass fraction [-]
C_{CO_2}	Gas costs [€/y]
C_{EC}	Energy consumption cost [€/y]
C_G	Gel costs [€/y]
C_I	Depreciation cost [€/y]
C_{MP}	Man power costs [€/y]
<i>d</i>	Main particle diameter [mm]
D_{AB}	Binary diffusion coefficient [m ² /s]
<i>e</i>	Thickness [mm]
<i>E</i>	Young Modulus [MPa]
<i>f</i>	Permissible Stress [MPa]

H	Enthalpy [kJ/kg]
I	Investment [€]
k	Permeability [m ²]
L/D	Length/Diameter ratio [-]
m, m'	Scaling factor [-]
M_w	Molar Mass [kg/mol]
N	Number of batch cycles [-]
P	Pressure [bar]
Q	Mass flow [kg/h]
r	Year discount rate [-]
R_m	Tensile Strength [MPa]
R_{px}	Elastic limit [MPa]
T	Temperature [°C]
t	Time [h]
v	Superficial permeation velocity [m/s]
V_T	Internal volume of vessel [m ³]
W	Working hours [h/y]
z	Welding coefficient [mm]

SYMBOLS

ω	Acentric factor [-]
σ	Relative stress [MPa]
α	Weight parameter for solvent cycle [-]
β	Weight parameter for vessel system [-]
ε	Porosity [-]
λ	Thermal conductivity [W/m·K]
μ	Dynamic viscosity [Pa·s]
ρ	Density [kg/m ³]
ν	Kinematic viscosity [m ² ·s]

ABSTRACT

Processing and drying of sol-gels is a widely practice used in industry due to the large number of existing applications for the downstream products. Among them, a specific product captures a great attention due to its high potential mainly for thermal insulation as residential, industrial and even aerospace applications. This product type, called **aerogel**, is a nanoporous material whose structure marks an extremely low density and thermal conductivity. Aerogel production can be carried out by various methods depending on the drying technique used to evacuate the liquid retained within the gel pores: Turning around the triple point (Freeze Drying), crossing the evaporation line (Subcritical Pressure Drying) or circumventing the critical point (Supercritical Drying). Each approach confers unique properties to the product at various costs. Since the industrialization of aerogels production is a growing issue, there is a lack of a comprehensive knowledge of operating cost optimization at high production volumes. This fact is an essential requirement for the techno-economic studies which will derive in new companies amplifying the aerogel offer at industrial scale.

The purpose of the present thesis is to provide the technological basis required for the development of a program for the industrial commercialization of aerogels. For this purpose, the survey shall cover the understanding and identification of the present technology maturity, the development and scaling of an optimized process and products, and evaluation of a commercial business plan for the production of aerogels. The study aims to start at a Technology Readiness Level (TRL) 1 and terminate in a TRL 6 - 7.

Chapter 1 addresses the definition and layout of the most optimal methods for producing aerogels at industrial scale for the application in thermal insulation. It is therefore necessary to begin with a thorough study of the literature and patents on the different methods of production, recent advancements and final properties of each material type. With the right information, the selection of the most sustainable and suitable process is then possible: Low Temperature Supercritical Drying (LTSCD).

Based on the use of carbon dioxide in its supercritical state as extracting solvent, LTSCD comprises removal of the liquid solvent from the gel avoiding any kind of surface tension within the pores. Hence, it provides the best quality internal structure. *Chapter 2*

focuses on the mechanisms of mass transfer during solvent extraction, as well as the possible functionalization of the final product for an optimal and effective scaling.

Success on supercritical fluids manufacturing relies on the perfect synergy between equipment design and process optimization, which is key towards low Operational Expenses (OPEX). Thus, *Chapter 3* presents the design and construction of a Pilot Plant based on simulations and optimization of this LTSCD process. Validation of a preliminary production will be the milestone to confirm the quality and characteristics of the aerogel products in real applications. Cost estimation at different production capacities will be provided.

Pilot scale results are the necessary bases for the correct processing of the techno-economic studies required for aerogels industrialization plan evolved in *Chapter 4*. This study attempts to glimpse the opportunity to create a new company dedicated to the production of aerogels for their applications in the field of thermal insulation. A semi-industrial plant is the primary objective of the company to penetrate the European market.

The environment in which takes place this thesis is comprised in two different areas. One consisted in , designing, construction and operation of a specific equipment within SEPAREX, and the other one was led in participation and management of four European projects of the 7th framework program: AEROCOINs (Grant Agreement: 260141), AerSUS (Grant Agreement: 284494) HIPIN (Grant Agreement: 260117) and RESEEPE (Grant Agreement: 609377). All of them engaged in the research and development of diverse aerogels-based materials for applications in insulation and retrofitting of buildings and insulation of spacecraft and satellites. SEPAREX participated as expert in the drying process of such materials and also as expert in the design and scale-up of equipment for the process therefore.

RÉSUMÉ

Le traitement et le séchage de sol-gels sont largement pratiqués dans l'industrie du fait du grand nombre d'applications de ces produits. Parmi ces différents produits obtenus à partir de sol-gels, celui qui suscite le plus d'intérêt, est appelé AEROGEL du fait de ses applications potentielles principalement dans l'isolation thermique (bâtiment, industries et même aérospatiale). Cet aérogel est un matériau présentant une structure nanoporeuse de densité et de conductivité thermique très faibles. La production d'aérogel peut être réalisée par diverses méthodes en fonction de la technique de séchage utilisée pour évacuer le liquide retenu dans les pores de gel: Contournement du point triple (*lyophilisation*), franchissement la ligne d'évaporation (*séchage à pression sous-critique*) ou contournement du point critique (*séchage supercritique*). Chacune de ces voies conduit à des produits ayant des propriétés différentes et également des prix de revient différents. Comme l'industrialisation de la production des aérogels est à développer, il y a une carence de connaissances approfondies sur l'optimisation des coûts d'exploitation à des volumes de production élevés. Cette optimisation est une condition fondamentale pour supporter les études technico-économiques préalables au lancement de productions d'aérogel à très grande échelle.

L'objet de cette thèse consiste à fournir les bases nécessaires pour le développement d'un programme de fabrication industrielle d'aérogels. A cet effet, nous développerons la situation actuelle de la technologie, puis le développement et la mise à l'échelle d'un processus conduisant à des produits optimisés, afin de pouvoir présenter l'évaluation d'un plan d'affaires pour la production commerciale d'aérogels. L'étude vise à débiter à un Niveau de Maturité Technologique (TRL) 1 et à terminer à un niveau TRL 6-7.

Nous présenterons au *Chapitre 1* les différentes méthodes de production des aérogels à échelle industrielle en vue de l'application à l'isolation thermique. Nous commencerons par une étude approfondie de la littérature et des brevets relatifs à ces différentes méthodes ; nous analyserons les progrès récents et présenterons les propriétés de chaque type de matériau. Sur ces bases, il apparaît que le procédé le mieux approprié est le Séchage Supercritique à Basse Température (en anglais *Low Temperature Supercritical Drying*, LTSCD).

Sur la base de l'utilisation de dioxyde de carbone dans son état supercritique en tant que solvant extracteur, LTSCD comprend l'élimination du solvant liquide dans le gel en évitant toute forme de tension superficielle à l'intérieur des pores. Par conséquent, le matériau obtenu présente la meilleure qualité de structure interne. Le *Chapitre 2* décrit les mécanismes de transfert de matière durant l'extraction du solvant, ainsi que la possible fonctionnalisation du produit final pour un dimensionnement optimal à l'échelle Pilote.

Pour mener à bien le développement du procédé LTSCD, il est nécessaire de combiner la conception de l'équipement et l'optimisation du procédé, afin d'abaisser les dépenses d'exploitation (OPEX). Ainsi, le *Chapitre 3* présente la conception et la construction d'une unité Pilote sur la base de l'optimisation et de simulations du procédé LTSCD. La validation d'une production préliminaire confirme la qualité et les caractéristiques des produits obtenus dans des applications réelles. L'estimation des coûts à différentes capacités de production sera fournie.

Les résultats à l'échelle Pilote sont les bases nécessaires pour le traitement correct des études technico-économiques nécessaires pour le plan d'industrialisation d'aérogels développé au *Chapitre 4*. Cette étude tente d'évaluer la possibilité de créer une nouvelle société dédiée à la production d'aérogels utilisables en isolation thermique. Une usine semi-industrielle est le principal objectif de la société pour pénétrer sur le marché Européen.

En fait, cette thèse a été effectuée pour une part en vue de la conception, la construction et l'opération des équipements spécifiques au sein de SEPAREX, et pour une autre part, par la participation et la gestion de quatre projets européens du 7ème *framework program*: AEROCOINs (Accord de subvention: 260141), AerSUS (Accord de subvention: 284494) HIPIN (Accord de subvention: 260117) and RESEEPE (Accord de subvention: 609377). Ces quatre programmes concernent la recherche et le développement de divers matériaux à base d'aérogels pour des applications dans l'isolation et la rénovation des bâtiments et dans l'isolation des vaisseaux spatiaux et des satellites. SEPAREX a participé en tant qu'expert dans le procédé de séchage de ces matériaux et aussi comme expert dans la conception et la mise à l'échelle d'équipements pour le processus concerné.

RESUMEN

El tratamiento y secado de sol geles es una práctica ampliamente utilizada en la industria debido al gran número de aplicaciones existentes para estos productos. Entre ellos un producto específico acapara una gran atención debido a su gran potencial en industrias tales como el aislamiento residencial e industrial o el aislamiento aeroespacial. Dicho producto, llamado **aerogel**, es un material nanoporoso cuya estructura le confiere propiedades extremadamente bajas de densidad y conductividad térmica, entre muchas otras. La producción del aerogel se puede llevar a cabo por los diversos métodos de secado según la técnica utilizada para evacuar el líquido retenido en el interior de los poros del gel: volteando el punto triple (Secado por Liofilización), cruzando la línea de evaporación (Secado por Evaporación) o traspasando el punto crítico (Secado Supercrítico). Cada método aporta al producto unas propiedades y costes singulares. Desde que la industrialización de la producción de aerogeles es un tema en expansión, no hay establecido un amplio conocimiento de optimización de los costes de operación a altos niveles de producción, requerimiento indispensable para los estudios tecno-económicos, los cuales deriven en nuevas empresas que amplifiquen la oferta del producto a escala industrial.

El objetivo de la presente tesis consiste en proveer, con las bases tecnológicas necesarias, el desarrollo de un programa de comercialización industrial de aerogeles. Para ello, el estudio abarcará desde el entendimiento e identificación de la maduración de la presente tecnología, pasando por el desarrollo y escalado de un proceso y productos optimizados; hasta el desarrollo de un plan de negocio para la producción de aerogeles. El estudio pretende comenzar con un Nivel de Desarrollo Tecnológico (TRL) 1 y terminar en un TRL 6 – 7.

El *Capítulo 1*, afronta la definición y el diseño del método más óptimo para la producción de aerogeles a escala industrial para su aplicación en el sector del aislamiento térmico. Para ello es necesario un estudio minucioso de la literatura y patentes existentes sobre los diferentes métodos de producción, los últimos avances y las propiedades finales concebidas a cada material. Con ello se podrá vislumbrar el proceso más sostenible y adecuado: Secado Supercrítico a Baja Temperatura (en inglés *Low Temperature Supercritical Drying*, LTSCD).

Basado en el uso del dióxido de carbono en su estado supercrítico como disolvente de extracción, LTSCD es un proceso consistente en la eliminación del disolvente líquido del interior del aerogel evitando todo tipo de tensión en el interior de los poros, proporcionando consecuentemente la mayor calidad de estructura interna. El *Capítulo 2* se centra en el estudio y definición de los mecanismos de transferencia de material durante la extracción, así como posibles funcionalizaciones del producto final para un escalado óptimo y exitoso.

La prosperidad de una producción basada en fluidos supercríticos se basa en una perfecta sinergia entre el diseño del equipo y la optimización del proceso. Para los aerogeles, tal sinergia representa la clave para una producción efectiva a bajos costes de operación (OPEX). Por consiguiente, el *Capítulo 3* presenta el diseño y construcción de un equipo de escala Piloto basado en la optimización y simulación del proceso de secado. Consecución de una producción preliminar será la clave para validar la calidad y propiedades de los productos en aplicaciones reales.

Los resultados a escala Piloto son las bases necesarias para la precisa elaboración de los estudios tecno-económicos necesarios para el plan industrialización de los aerogeles desarrollado en el *Capítulo 4*. Este estudio pretende vislumbrar la oportunidad de la creación de una nueva empresa dedicada a la producción de aerogeles para aplicaciones en el sector del aislamiento térmico. Una producción semi-industrial constituirá el primer objetivo de la empresa para poder penetrar en el mercado Europeo.

El entorno en el que se lleva a cabo la tesis doctoral se compone de dos áreas de trabajo diferentes. Una consiste en el diseño, construcción y uso de equipos específicos dentro de SEPAREX, y otra liderando la gestión de cuatro proyectos Europeos del 7th *framework program*: AEROCOINs (Acuerdo de subvención: 260141), AerSUS (Acuerdo de subvención: 284494) HIPIN (Acuerdo de subvención: 260117) and RESEEPE (Acuerdo de subvención: 609377). Todos ellos dedicados a la investigación y desarrollo de diversos materiales basados en aerogeles para aplicación en aislamiento y renovación de edificios y aislamiento de aeronaves espaciales y satélites. SEPAREX participaba como experto en el proceso de secado de tales materiales y como experto en el diseño y escalado de equipos para tales procesos.

Chapter 1

SOL-GEL DRYING: LITERATURE AND PATENT SURVEY

As *Aerogel* is nowadays one of the major innovative materials to be applied in normal life [1-3], therefore numerous publications are issued and patents are filed every year in order to provide a method for its manufacture. This aim is founded by the high necessity to reduce the current costs resulting from the production of aerogels and aerogels-like material, which is the first cause of the lack of widespread applications.

Despite their almost infinite applications, aerogels are of limited use in high technological and research fields, as Cherenkov radiators [4, 5] or spatial particles recovery [6, 7] among others, where limited amounts and size are required. Only some players have been able to scale up the manufacture of aerogel or aerogel-like materials, although still with too many limitations on properties, and above all, price.

The present document aims to present a survey of published knowledge classified according to the different drying methodologies established by phase transition routes: sublimation/lyophilization, evaporation or supercritical. The review does not pretend to be exhaustive but provide some basic cognition to better understand the state-of-art of the technology and processes in the manufacture of aerogels. Along this document, it will be consecutively described each process and the most important advances concerning the technology and advantages for the manufacturing.

1.1. INTRODUCTION

Aerogels, low-density open-porous solid materials, are produced by sol-gel chemistry. The aerogel structure consists in a porous solid where majority of pores are between 2 and 50 nm in diameter (mesopores). Based on this, exceptional properties such as high porosity (~95%), high specific surface area (up to 1,000 m²/g), low thermal conductivity (~0.01 W/m.K), low refractive index (~1.05), and high optical transmission (90%) might be achieved [8].

Sol-gel chemistry is based on transformation of molecular colloidal into a cross-linked gel. Depending on the precursors nature, aerogels might be inorganic (i.e. oxides from silicium-, zirconium-, titanium-based precursors), organic (i.e. polymers from

resorcinol-formaldehyde or polyurethane precursors) or hybrid (if obtained from organic-mineral precursors) [9].

Inorganic aerogels are prepared by hydrolysis and condensation of silica or metal based precursors. The first silica aerogel reported in the literature was prepared by Kistler in 1931, using sodium metasilicate, Na_2SiO_3 [10]. Nowadays, silica aerogels are prepared mostly using alkoxides of $\text{Si}(\text{OR})_4$ type, in which R and OR designate alkyl and alkoxide groups, respectively. Progress of sol-gel chemistry over the last decades has promoted innovative alkoxide-derived precursors such as methyltrimethoxysilane (MTMS) [11, 12], polyethoxydisiloxane (PEDS) [13, 14], perfluoroalkylsilane (PFAS) [15], 3-(2-aminoethylamino) propyltrimethoxysilane (EDAS) [16], etc; all rely on existence of $\equiv\text{Si-O}$ polar covalent bond that allows a random 3D-network, while additionally including built-in chemical functionality.

Organic aerogel are predominantly based on natural sources (ex. cellulose) or synthetic polymers such as formaldehyde-resorcinol, formaldehyde-melamine, polyurethanes and polyisocyanurates. Several methods for cellulose aerogels production are described in the literature [17-21]. The first cellulose aerogels were prepared by Tan et al. [22] using cellulose acetate and cellulose acetate butyrate, while “aero-cellulose” material was prepared by dissolving cellulose in aqueous NaOH or *N*-methylmorpholine-*N*-oxide (NMMO) monohydrate.

Alike to cellulose-based aerogels are polyurethane aerogels that are obtained by polycondensation of polyols with polyisocyanates, where urethane groups $-\text{O}-\text{CO}-\text{NH}-$ form a tridimensional network [23, 24]. Polyurethane aerogels exhibit low densities and very interesting thermal properties. Moreover, resorcinol-formaldehyde (RF) aerogels have been intensely studied since they are an important class of organic aerogels, although there are other types available, not only formaldehyde-based (phenol-formaldehyde, melamine-formaldehyde) but also polyimides, polyacrylates or polystyrenes [25]. Recent studies have shown that some of these materials could yield very low thermal conductivity values [26] combined with mechanical properties superior to silica aerogels [27] and a tendency to reduce dust release.

Organic aerogels can be transformed into **carbon aerogels** by pyrolysis under inert atmosphere. Carbon aerogels exhibit not only exceptionally high stiffness, strength and resilience, but also possess unusual chemical and structural properties. Chemically inert pure carbon structure, with high surface area and electrical conductivity, might be used as electrical double-layer capacitors [28], electrode and catalyst support in PEM fuel cells [29], advanced catalyst supports [30, 31] and adsorbents [32].

A new class of **composite or hybrid aerogels** has been elaborated when combining inorganic and organic precursor. Epoxy-based composites have been extensively studied [33]. Moreover, addition of biopolymers (ex. chitosan, cellulose and pectin) has significantly enhanced chemical and mechanical properties of silica based aerogels [34-36]. Zheng et al. [37] showed that cross-linked polyvinyl alcohol – cellulose nanofibril (PVA-CNF) hybrid organic aerogels exhibit excellent elasticity and mechanical durability, while demonstrating exceptional absorption performance. Novel material achieved by combining carbon nanotubes and polyaniline (SWCNT/PANI) nano-ribbons can be applied as lithium ion battery electrodes due to their high capacity (185 mAh/g) and good cycle performance (up to 200 times) [38].

The first step on Aerogel manufacture consists in the preparation of a colloidal solution of the material or “sol”, which leads to a “gel” after a “maturation” period of time: An “aquasol” if the liquid phase is water, leading to an “aquagel”, or “alcosol” if the liquid phase is an alcohol, leading to an “alcogel”. The second step, an economically most important, consists in the drying of the gel. The sol-gel drying process basis relies

on solvent elimination from the matrix without generating a two-phase system and the related capillary forces [39] that cause partial or total destruction of the gel nanostructure. If the liquid phase is removed from the gel in a non-destructive manner, a solid porous would be left with approximately the same shape and volume as the original gel. Several techniques have been developed and improved in order to obtain the best solid material out of each sol-gel method. This is due to the drying process has a big impact on the properties [40] and economics of the final material [41, 42] since the porous structure is concerned.

In order to remove the liquid phase from the gel structure, three ways can be chosen concerning the phase transition of the solvent. As shown in Figure 1.1, the routes to pass from liquid phase to gas phase for all the substances concern either to go around the triple point cross the gas/phase equilibrium line or surround the critical point.

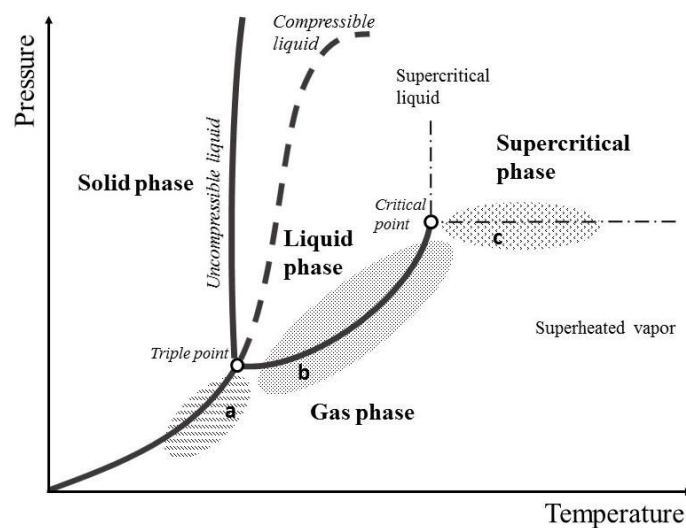


Figure 1.1. Phase transition routes to pass from liquid to gas phase.

In relation to the different phase change routes, three main processes have been highly developed and optimized:

- Sublimation of the solvent below the triple point so called “Freeze Drying”, and the resulting solid material called “Cryogel”.
- Evaporation of the solvent through the liquid-gas interphase line, so called “Subcritical Pressure Drying” and the resulting material called “Xerogel”
- Increase of temperature and pressure to go around over the critical point of the solvent, so called “Supercritical Drying” and the resulting material called “Aerogel”.

1.2. FREEZE DRYING (FD) OR LYOPHILIZATION

1.2.1. CONCEPT

Upon heating of frozen substances, liquefaction generally precedes vaporization. However, when high-vacuum is also applied (Figure 1.1), solvent can be evacuated directly into gas phase by sublimation. This process is called Freeze-drying and can be successfully performed on sol-gels in order to avoid liquid phase meniscus stress and obtain crack-free materials with high porosity [43].

Three stages are governing the process, so called Lyophilization Cycle: (a) reduction of temperature of the soaked solvent below its triple point; (b) reduction to high vacuum pressures and (c) controlled sublimation at isobaric conditions. Therefore, Freeze-drying process is performed at conditions which comprise very low temperatures depending on the solvent involved. Water (T_m : 0 °C) is commonly used but organic solvents as acetone (T_m : -95 °C), methanol (T_m : -97 °C) or ethanol (T_m : -114 °C), among others, while liquid nitrogen or external sources are used to reduce temperature. Main drawback in the process are addressed as the time and energy consuming to reach the required lyophilization cycle [44, 45] and the different freezing/sublimation ratios which can promote the formation of microcrystalline structures within the samples.

Freeze-drying becomes an important method for heat-sensitive gels which degrade at high temperatures or are very sensible to moisture (e.g. cellulose, biopolymer gels) but also well applied to silica- [46], organic gels [47, 48] and their equivalent carbon cryogels [49-51]. Studies have reported that final structure of the material is highly influenced by the freezing rate, sublimation temperature and solvent nature (which affects the freezing rate and temperature). Major efforts have been performed in order to optimize cryogels production, which mainly deal with the procurement of monolithic nanoporous materials, since this process allow generally to obtain granular and powders material [52]. Among the different processes investigated, one promising result concern the exchange of the soaked solvent for a second one with higher melting temperature as *tert*-butanol (T_m : 25.7 °C) [53, 54]. Although the exchange time can last a couple of weeks, the final results show monolithic materials with high porosity and internal surface area compared to their analog aerogels or xerogels.

1.2.2. HISTORY

Freeze drying process is well established in industry to mainly dry food related compounds. Related to aerogels, the production of the so called “Cryogel” has been always limited to research purposes but never applied at industrial scale due to the lower cost of other solutions as Subcritical Pressure Drying (see below), for similar properties.

Nevertheless, since freeze drying was used to prepare the first organic-based sol-gels (based on cellulose or organic compounds as Resorcinol-Formaldehyde), this process played an important role since the procedure could be implemented by the freezing of the aqueous solvent instead of proceed with long solvent exchanges. Nowadays, the increase of research on graphene and carbon aerogels, above all as clay templates, also enlarged the use of FD technology to produce capacitors and batteries.

Even if the technology at large scale is well developed, the use of large quantities of energy and solvents are evading the implement of such method at commercial scale.

1.2.3. PATENT

- Earliest production of silica cryogels was claimed by Henri A. Aboutboul et al. at Nat Petro Chemical Co. Inc. for the preparation of narrow pore diameter materials directly from water [55]. Vacuum subliming drying of water was performed at temperatures between -1 and 10 °C.
- Cabot Corp., for silica based [56], and American Aerogel, for their organic foams [57, 58], has claimed the production of cryogel materials but it has been the research institutes as Case Western Reserve University [59], Chinese Academy of Science [60, 61], University of Florida [62], Lawrence Livermore National Security Llc. [63], etc. who really got advantage of FD method to develop new materials.
- Recently, Kunshan Lansheng Building Materials Co. Ltd. claimed the production of large blocks of hydrophobic cellulose aerogel by FD [64, 65]. The material consists of a combination of reticular cellulose nano-fiber skeleton and a sol. Different basic of cellulose were processed at -80 °C and down to 20 Pa. Hydrophobization it was made by plasma treatment in a later stage. Thermal conductivity of material was reported to achieve 29 mW/mK at ambient conditions while elastic modulus was up to 150 MPa.
- Tyco Electronics Corp. (former Tyco International) claimed the production of graphene, graphene oxide aerogels by FD as suitable method [66]. In a similar way, Ferro Corp. [67] and BASF SE. [68] has developed comparable techniques to produce cryogels materials, but without major advantages compared to the basic methodology.

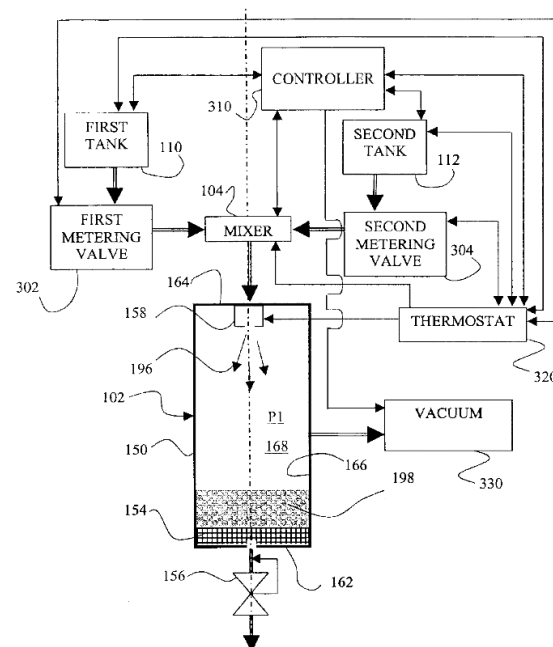


Figure 1.2. Boris Y et al. FD process system [67].

1.2.4. PUBLICATIONS

Table 1.1. Process and Simulation of Cryogel drying.

Gel type	Process	Solvent	Result and Observations	References
Clay cryogels	FD	Water	Low densities achieved with improved mechanical properties	[69]
Silica	FD	<i>Tert</i> - Butanol	Lower exergy process. Monoliticity achieved at one-step freezing-drying.	[54]
Cellulose-Phenol-Formaldehyde	FD	<i>Tert</i> -Butanol Ethanol (SCD)	Similar pore distribution between cryogels and aerogels. Cryogels possess less porosity than aerogels.	[70]
Cellulose	FD	Water	Young's Modulus up to 3.86 MPa.	[71]
Cellulose (Chitosan)	SFEP	Acetone Acetic Acid	Combination of Thermally Induced Phase Separations (TIPS) with SCD. Faster dryings were achieved for macroporous scaffolds.	[72]
Graphene-based	FD-Pyrolysis	-	Densities below 4 mg/cm ³ and surface areas up to 1019 m ² /g.	[73, 74]
Polyacrylamide based	FD	Water	Rapid freezing cryo-polymerization process assisted by dry-ice. Reduction of overall process cost for granular.	[75]
RF	FD	-	FD method provide the highest surface area (>2500 m ² /g) but less stability in carbon cryogel.	[50, 76]
Porous mater.	FD	-	Simulation of sublimation-transport-condensation process. Increase drying rate by a factor of 2.2by modifications. Reduction of cycle times	[77-79]
Porous mater.	FD-Microwave	-	Theoretical simulation of the FD assisted by microwave heating.	[80]
Porous mater.	FD	-	Reduction of total exergy losses over 50% Optimal operational conditions.	[44, 45]

1.2.5. FUTURE DEVELOPMENT

The foreseen development of Freeze Dried gels at industrial scale still remains doubtful even if the total cost reduction has been proven and the technological development is very low. Xerogel materials have overcome the market for aerogel-like material with limited properties at a price and simple technology very similar to the required for cryogels, placing this method to other industries or very specific applications as biomedical scaffolds.

Nevertheless, a potential manufacture for the future is monolithic cryogels which are further developed due to the limit-less of the plate production (up to 10 to 50 m² of shelf area per batch [81]), being able to acquire the dimensions demanded by construction industry. This advantage will allow the use of cryogels over xerogels and, maybe, aerogels materials in building insulation. The only drawback at such industrial scale would be the scale up factor of the OPEX, that is higher than the ones of two other counterparts routes.

1.3. SUBCRITICAL PRESSURE DRYING (SPD)

1.3.1. CONCEPT

Subcritical Pressure Drying (or Ambient Pressure Drying) is the most immediate method to evacuate the solvent within the porous material. The reaction solvent is brought over its bubble point in order to be displaced in gas form. Such process can be performed at conditions all along the liquid-gas phase from the triple to the critical point of the solvent. In consequence, pressure for evacuation is from vacuum to subcritical conditions.

Since the drying process starts, three regions of solvent phases coexist in the sample: the confined liquid in the pores, the liquid-gas transition line and the gas phase. The drying will be completed when liquid-gas transition line reaches the core of the material and the totality of the solvent is evacuated in gas state. However, evaporation of liquids from gels results in large capillary pressures (up to 100 – 200 bar [39]) within the pores and, thus, the final materials may have reduced porosity or may highly crack due to a fragile solid skeleton even if at such a scale the macro physical law like Laplace disjunction pressure is meaningless.

Silica-based aerogels are produced from silicon alkoxides or alkylsilicas of Si(OR)₄ type, in which R and OR designate alkyl and alkoxide groups, respectively. Generally, the alkoxide group is designed with a methyl or ethyl compound obtaining tetraethoxysilane (TMOS) and tetraethoxysilane (TEOS) respectively. By nature, the silica backbone of TMOS and TEOS contains hydroxyl radical groups that highly react with water by hydrogen bonds.

This method is mainly able to provide xerogels in granular and impregnated-mat shape due to the difficulties of guarding the nanostructure of the primary gel during the drying. In order to achieve nanoporous aerogel-like material, major modifications in both gel pre-treatment and drying processing must be taking into account.

Gel pre-treatment

Besides of what it concerns to normal sol-gel synthesis procedure, SPD requires a pre-treatment on the gel or modification on the synthesis which essentially consists in surface alteration and/or pore strengthening.

The main issue addressed during SPD is the structure collapse due to the stress formed for the phase change of the solvent within the pores, which produces shrinkage of the structure. This derives in a condensation of reactive groups on the pore walls, what disengages the structure. In order to avoid this reaction, a treatment of the internal surface is then required for the annulation of the H bond from the active radical Si – OH and the consequence condensation defeat. Such process is done by the reaction of an alkoxysilane compound in the presence of a solvent (i. e. methyltrimethoxysilane – MTMS–, methyltriethoxysilane –MTES–, phenyltrimethoxysilane –PTMS, phenyltriethoxysilane –PTES–, hexamethyldisilazane –HMDZ–, hexamethyldisiloxane –HMDS–, trimethylchlorosilane –TMCS–, etc.[82]) to form hydrolytically stable Si – R groups.

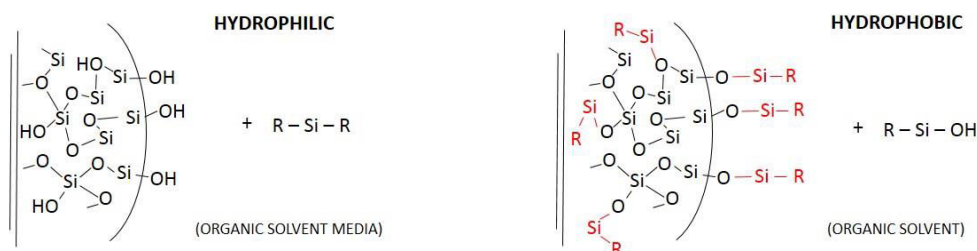


Figure 1.3. Surface representation of hydrophilic (left) and hydrophobic (right) silica aerogel.

Sililation reaction is performed with the gel under a mixture of solvent with the alkoxysilane compound (up to 15% w.) in acidic conditions. The reaction takes place at temperature over 50 °C for 24h. This step is followed by several wash steps in order to evacuate excess of reactant and sub-products (e.g. ammonium) from the sample gels. The washing period can last several hours until the concentration of the solvent in the gel over 99% and is performed over 50 °C. When samples are “hydrophobized” by the described pre-treatment method, the evaporative drying process is performed.

Second modification used to produce xerogel materials with high surface area and pore volume with a minimal shrinkage of the sample concern the addition of “Drying Control Chemical Additives” (DCCA). The addition of glycerol, formamide, dimethyl formamide, oxalic acid or tetramethylammonium hydroxide, among others, during the synthesis will lead to a very uniform pore size distribution within the gel structure (either large or small pores). Such modification will provide the material with a better performance towards the pores stress during evaporative drying obtaining a considerable diminution of shrinkage. The addition of DCCA also has major consequence in the nucleation mechanism of the silica during the condensation stage of gelation [83, 84]. Those variations can be tunable in order to obtain bigger and stronger silica necks and the consequence lower shrinkage.

Drying

Evaporative drying of sol-gel has been reported to be very inefficient concerning the maintenance of the pore structure if no pre-treatment modifications are carried out. Together with the pre-treatment of the samples described before, the Subcritical Pressure Drying can be performed by two different methods: direct evaporation or controlled atmosphere drying.

The first one, direct evaporation, consists in the evacuation of the solvent within the gel by increasing the temperature of the system over the bubble point of the solvent by

the injection of heated gas (for granular and powder) or via a superheated surface contact (blankets). In both cases, the process is done in one step at saturated temperature and low pressure.

Direct evaporative drying is composed of three drying stages [85]:

- I. Constant drying rate period when the fully saturated gel reduces its volume to a critical moisture content where the volume of liquid and evaporated gas are in balance;
- II. First decreasing drying rate period when non evacuated liquid flows through partially empty pores;
- III. Second decreasing drying rate period when liquid escapes from the drying gel only via diffusive vapor transport to the exterior surface.

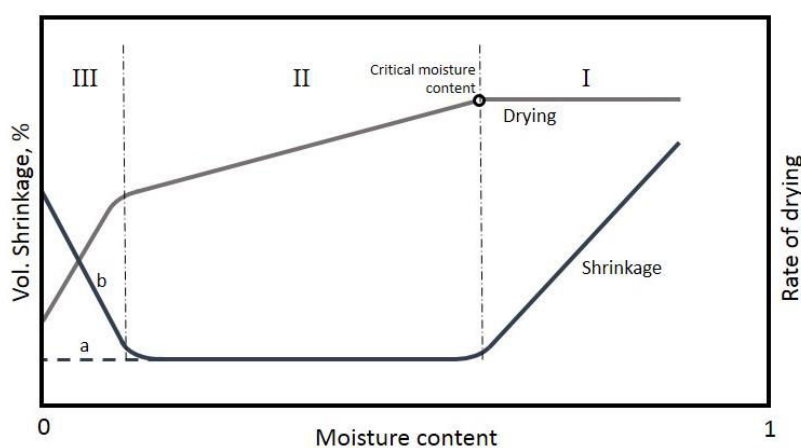


Figure 1.4. SPD rate and shrinkage of porous materials: (a) untreated and (b) treated gel.

In the first step (I), the highest rate of shrinkage takes place on the samples due to the capillary forces acting on it until a critical moisture content is reached, where many particles within the structure come into contact. During the second stage of drying (II), there are already many empty pores within the gel network and they are connected through many pores which are still liquid filled. Evaporation from the liquid pore filled interfaces causes a gradual decrease of the total surface area of those pores and thus a continuous decrease of the drying rate. After all solvent in liquid form has been removed from the pores, the capillary forces disappear and release their grip on the fragile particle network. At this point, and only if the surface does not contain R–OH groups, the sample will partially expand again and recover its preliminary gel volume (up to 95%) by a so-called “spring-back effect” [86] caused by the van der Waals repulsion between Si – R groups present in the surface, which detaches each other with a feasible low activation energy [82]. In this third region of drying (III), the drying rate drops is even faster since mostly gaseous solvent molecules are present in the gel, they are pushed out from the gel by a diffusion process.

This technique is able to maintain the xerogels structure with limited high surface area and low density that even in some cases can be exposed in the range of properties exhibits by supercritically dried aerogels.

However, the method that shows more versatility and handling for the scale up is the drying of granular and powder sol-gel under heated air injection. This process has been

successfully scaled up as fluidized bed systems [87] due to the low density of the particles and continuous of the process. Fluidization technique has extensively been used for the efficient drying of the materials in granule as well as in powder forms. The basic principle of this technique is that the agglomerated sol-gel particles in the slurry are dried and dispersed fine by passing a heated gas through them at a temperature over 150 °C.

Homogeneous and reliable monolith xerogels can be obtained when pre-treatment modifications are accompanied by a controlled atmosphere drying instead of a direct evaporation. This comprises the controlled parameters: temperature (over the bubble point of the solvent), pressure (all along the liquid-gas interface, covering the subcritical region), solvent concentration and convective gas flow.

A saturated atmosphere of the solvent allows to control the evacuation of the gas within the gel in a less aggressive manner. This route can be tailored in order to maintain the developed tensile stress of the structure below the destructive stress of the material during the different drying steps. Generally, the process is conducted in a set of consecutive steps at different temperatures for different periods of time depending on the thickness and nature of the gel. The temperature conditions can reach values as higher as than 180 °C for several hours as peak of the process, being reduced in a controlled manner to ambient conditions. Such process may involve the use of pressured conditions in the subcritical region.

A successful approach for a specific application is the called *pinhole* method to dry highly refractive index monoliths. The technique relies on the control of the shrinkage rate by design of the pinhole-containers and temperature to avoid any cracks. Tailored refractive index is obtained by monitoring the weight of the gel during drying. Due to the slowly of the evacuation of the gas, shrinkage of the sample is linear to the final volume without any *spring-back effect*.

1.3.2. HISTORY

Silica particle material has been used since the 50'ies as construction material, thickening agent, polymerization catalysts of normally gaseous unsaturated hydrocarbons in petrochemical industry, among other applications. They have been extensively manufactured in different shapes with a wide range of properties as non-porous fumed silica or silica fume with limited properties.

Xerogel powder was firstly produced by evaporative drying of an inorganic silicon oxide colloidal sol-gel at high temperatures from both aqueous and organic solvents. This material was still very limited in surface area and porosity due to the high grade of shrinkage submitted during the drying step.

During the 80'ies, the first boom on aerogel manufacture relied on innovative procedures to reducing the OPEX of the drying process, and led to an aerogel-like material that could be used instead of fume silica. Brinker (University of New Mexico) provided the best approach by implementing the already existing functionalization of internal surface of the porous material to experience the so-called Springback Effect. This system allowed making xerogels with minimized shrinkage and properties similar to the aerogels. The process was exploited by the company Nanopore in USA.

The "open-door" provided by Brinker led into a faster development of xerogel materials at industrial scale in early 90'ies. Companies that worked with silica materials found the key to reduce considerably the production costs and started to produce xerogels materials with high porosity for different applications. Hoechst AG, Degussa, Basf AG, among many others, made great advancements on different materials and

functionalization. In June 2003, Cabot Corporation took over the aerogel IP of Hoechst AG and other researcher to start a production of 10,000 Ton/year semi-industrial plant in the nearby of Frankfurt. Siemens Axiva was in charge of the construction of the manufacturing line.

In the present time, many emerging companies are using SPD process in order to produce aerogel-like materials displaying very small difference with those dried by SCD. Enersens, MeroTech are entering the aerogel market with granules similar to those provided by Cabot, which still keep the leadership on the production. Other player as ActiveAerogels are producing flexible monolith xerogels based on hybrids ormosils.

1.3.3. PATENT

- Drying of inorganic jellies and gels by direct evaporation is a technique highly used in industry to obtain porous dried silica by different manners reaching temperatures up to 480 °C for several hours [88-91]. Such processes allow producing silica particles with limited porosity, but being produced in a continuous process as showed in Figure 1.5.

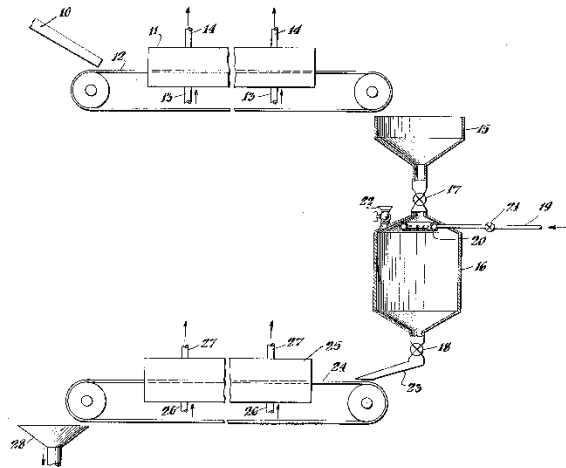


Figure 1.5. Example of continuous process for inorganic xerogel production by Socony Mobil Oil Co. [89].

- Up to the 80's many patents were filled for the production of fine silica xerogels. Companies as Du Pont [92, 93], General Electric[94] and Degussa (Actual Evonik) [95, 96] claimed different methods to obtain the material from spray drying, fluidized bed or direct evaporation. Final material achieved low apparent densities between 10 – 100 kg/m³, and surfaces areas between 80 – 500 m²/g. Those methods allowed reducing considerably the price of such material for applications additives or thickening agents.
- McDaniel claimed in 1978 that inserting organosilicon compounds in the hydrogel matrix prior the evaporative drying, the pore size of the material could be maintained [97], avoiding the large shrinkage of standard xerogel. This process was the first step that would precede the development of the *Springback effect* for xerogel drying.
- Brinker et al. improved the system by controlling the internal chemical reaction of the organic compound [98]. This modification allowed producing xerogels

material with a limited shrinkage during drying at vacuum or ambient pressures due to the re-expansion of the pores derived of the repulsion of silane ends. Drying was carried out by venting hexane at different temperatures steps from room temperature to 50 °C and 140 °C during 24 h each. Dried gels achieved low densities from 50 Kg/m³ to 100 Kg/m³.

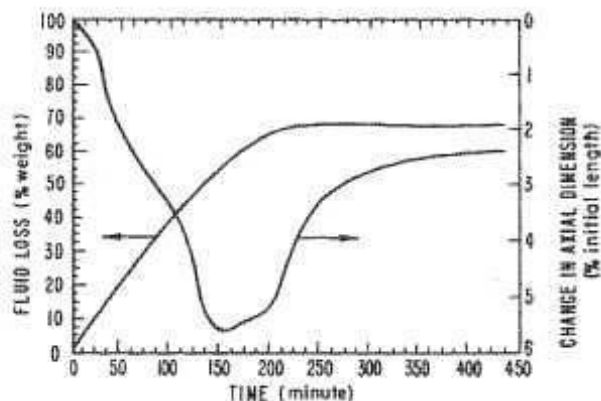


Figure 1.6. Shrinkage during SPD moisture reduction.

- The use of Drying Control Chemical Additives (DCCA) was firstly claimed by Hench and Orcel (University of Florida) [99] for the use of glycerol, formamide, oxalic acid or monocarboxylic acids on the production of monolithic xerogels. The process claimed reduction of the total overall drying time from several days to 18 hours at temperatures between 70 °C to 150 °C. Final material could reach surfaces areas up to 850 m²/g. The presented process was later implemented by other companies as Texas Instruments Inc. [100] to obtain porosities greater than 80%.
- Hoechst AG (now Sanofi S.A.) [101-104], BASF AG [105] (for fluidized bed drying) and Cabot [106] made great advancements on both functionalized materials and drying process that would allow to further decrease the OPEX of SPD. Those advancements did not imply a new procedure but the optimization of the conditions to dry the sililated silica gels in order to obtain granular xerogels via *Springback effect*. Normally the conditions comprise between 100°C to 200°C of inert gas at pressures up to 5 bar. Pressure difference along the samples has been one of fastest advancements applied to the process. From 1999 to Jun 2003, Cabot Corporation took over all the patents concerning aerogels of Hoechst AG and its subsidiary to exploit them at semi-industrial scale.
- Pinhole drying process is known to manufacture materials [107], but it was in later 90's when it was started to be applied on porous sol-gels in order to obtain narrow porous xerogels by Yazaki Corp. [108] among others. The standard pinhole method was shortly improved by using subcritical conditions in a controlled vessel [109, 110].
- The latest advancement on xerogel drying was provided by emerging companies as Enersens, which claimed a process to dry inorganic gels by a sequential temperature ramping process to allow a continuous manufacturing [111]. The

Swiss Federal Laboratories for Material Science and Technology recently claimed a process that produce aerogels within few hours, further decreasing the process.

1.3.4. PUBLICATIONS

Whereas the main drawback of the SPD process is preservation of the initial porous structure, the primary effort has been dedicated to the procurement of modified routes to strength the gel structure. Diverse methodologies have been proposed and investigated concerning, among others, the modification from synthesis and optimization and control of the drying steps. It is factual that great advancements have been achieved but mainly at lab-scale.

Table 1.2. Process and Simulation of Xerogel drying.

Gel type	Process	Solvent	Result and Observations	References
TEOS:TMCS	SPD	MeOH	Reduction of total processing time to 40 h. Optimization of synthesis and mechanical vibration to increase diffusion.	[112, 113]
Na ₂ SiO ₄	SPD	<i>n</i> -Hexane	Crack-free monoliths of sodium silicate. Drying from ambient temperature to up to 230 °C in 74 h.	[114-116]
TMOS	Pinhole	N, N-dimethylformamide (DMF) MeOH	Refractive index over a range of 1.0026 – 1.26. Extremely low densities: 0.01 g/cm ³ . Process time over several months.	[117-119]
Na ₂ SiO ₄ Oil Shale Ash (OSA)	Fluidized bed drying	Organic	Continuous powder drying manufacture. Up to x2 higher surface area than conventional SPD.	[120-122]
Resorcinol-Formaldehyde	SPD	H ₂ O	Structure Simulation Carbon aerogel microporosity does not depend on drying method as mesoporosity.	[123-126]
SiO-based	SPD	Alcohol	<i>Spring back effect</i> simulation	[127, 128]
Porous mater.	SPD	-	Use of dissolved Sodium Chloride as a crystallized salt layer to control evaporative drying rate.	[129]
Porous mater.	SPD	-	Theoretical Simulation of porous formation and behavior at different drying conditions and states.	[130-133]

Table 1.3. Different solvent and reactions.

Gel type	Process	Solvent	Result and Observations	References
TEOS	SPD HTSCD	Ethanol <i>Iso</i> -Butanol 2-Pentanol <i>Iso</i> -Octane	Comparison between HTSCD and SPD for different organic solvents. Lower surface tension of solvent can decrease the evaporation pressures to avoid cracks.	[134]
TMOS : Diisocyanate	SPD	Pentane	Dried of cross-linked aerogel with similar properties as SCD counterparts.	[135]
TEOS	SPD	Acetonitrile	Optically transparent silica aerogels with low density	[136]
TEOS	SPD	Alcohol	Effect of synthesis on drying shrinkage	[137, 138]
TEOS	SPD- DCCA	Glycerol Formamide Oxalic acid	Uniform pore distribution formed from large (basic formamide) or small (oxalic acid)	[139]
TMOS TEOS	SPD - DCCA	Glycerol N,N-dimethylformamide (DMF)	Narrow and more uniform pore size distribution obtained.	[83, 140]

1.3.5. FUTURE DEVELOPMENT

SPD is the most developed method for sol-gel process due to its wide use in industry for decades. For the production of xerogels, this fact together with the strong dependence of the synthesis in the global cycle, has formed a more practical, fast and economical objective than other scaling, however not the case on the final properties of the product.

The greatest advance has been realized on the development of sol-gels with higher mechanical properties that can withstand the tension forces produced within the pores allowing maintaining higher pore volumes. Therefore, it is understood that the maximum volume recovery is improved the final material could be compared with their counterparts. It is also noted that the production of both impregnated blankets and monoliths are reaching levels of final porosity and consistence similar to those produced by SCD.

The key points for the scaling of the SPD technology are based on the proper use and recycling of the large amounts of solvents that are required in the production, which would otherwise not be feasible. For example, some interesting results to decrease solvent by optimizing the hydrolysis of TEOS to produce ethanol as by-product that directly interacts in the gelation has been demonstrated to reduce considerably the production cost. Likewise, the control of dust is a factor into account when SPD is applied.

1.4. SUPERCRITICAL DRYING (SCD)

1.4.2. CONCEPT

Supercritical Drying is the process according to which the liquid inside the sol-gel material is transferred into gas in the entirely absence of surface tension and capillary stress. SCD involves pressurizing and heating the liquid solvent in the sol-gel over its critical point, at which it is changed into supercritical phase. Beyond this point, the supercritical fluid can be removed from the pores of the material by depressurizing the fluid in isothermal conditions (keeping the temperature above its critical temperature). If the fluid temperature drops below the critical one, liquid will start to rain out of the fluid. After a certain time, enough of the fluid will have been removed from the pressure vessel so that when it is cooled below its critical point there just is not enough substance to recondense to a liquid (the fluid is too low in density) and instead reverts to a gas. According to this process, the solvent within the sol-gel can be vented by two possible means: i) venting the solvent above its critical point or ii) by solvent exchange with a second solvent, generally carbon dioxide (CO₂), in which the former solvent is completely soluble, followed by supercritical venting of the second solvent. The first one is known as High Temperature Supercritical Drying (HTSCD); and the second, as Low Temperature Supercritical Drying (LTSCD).

High Temperature Supercritical Drying (HTSCD)

High Temperature Supercritical Drying process has been the first way to dry aerogel since it was implemented by Kistler in 1931 [10].

The basis of the process relies on the vent of the organic solvent used for the sol-gel synthesis over its critical point. Process is performed in five defined steps:

1. Samples washed of chemical reaction exceed are placed in a high pressure/temperature autoclave covered with the same solvent within the gel.
2. Autoclave is filled with pressurized inert gas (e.g. N_2) to avoid oxygen in the lines. Then autoclave is heated under control to avoid rapid thermal expansion [39, 141]. Pressure and temperature will rise and adjusted to the desired values over the critical point depending on the organic solvent used.
3. Stationary condition is then established for an interval defined by the major thickness of the samples. Heat diffusion through the sample will lead the duration of the step. Supercritical state must be reached in the entirely volume of the sample.
4. Solvent is slowly vented isothermally. Accurate control of parameters is required in order to avoid condensation of solvent in the pores and apparition of the capillary stress. Pressure drops until to ambient pressure.
5. At ambient pressure, the autoclave is fluxed with inert gas in order to extract the excess of solvent and cooled down to ambient temperature.

Since the critical point of most organic solvents used in sol-gel science is relatively high, up to 200-500 °C (Figure 1.7), the resulting material treated by this process normally exhibits some special properties. Most of those properties are related to the hydrophobic behavior of the resulting material due to its chemical reorganization of hydroxyl groups (OH), which are replaced by hydrolytically stable organo-functional alkoxy groups (e.g. $R=CH_3$), activated at those high temperatures. However, the stability of the hydrophobic compound during time is highly dependent on the silica precursor and the solvent (e.g. TEOS silica aerogel dried with in supercritical ethanol lose the hydrophobicity properties in only some hours).

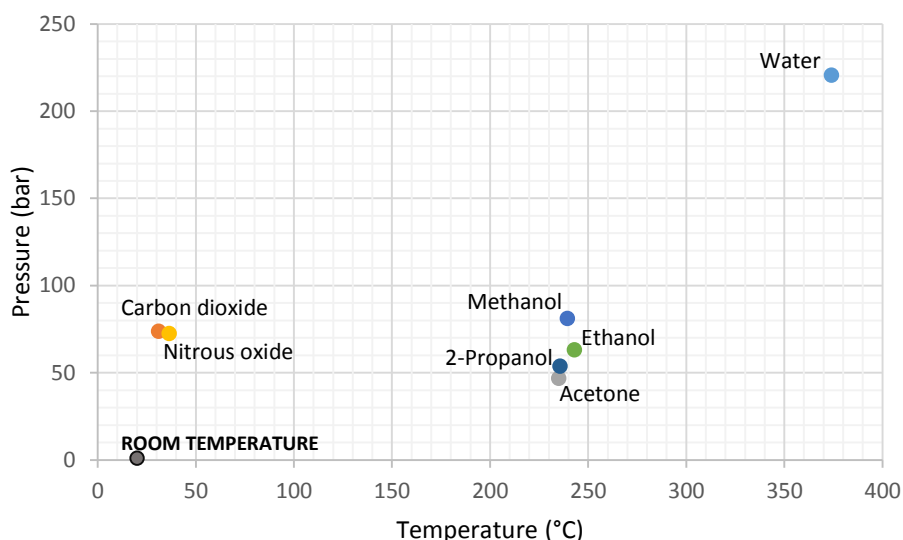


Figure 1.7. Critical point of common solvents

It has been reported that HTSCD from organic solvents is the best way to minimize shrinkage of the gel, leading to much lower-density gels than those prepared by other drying methods. However, certain aerogels, such as organic [23] or cellulose-based [20]

aerogels, cannot be generated by using HTSCD because they decompose or react at the temperatures at which most organic solvents are supercritical.

Another side effect of this process is related to flammability and explosivity of the solvents at these severe conditions. In the case of supercritical ethanol, it becomes extremely corrosive with the equipment and seals. For this reason, development of this procedure at large scale is not-satisfactory due to the special safety precautions [142].

Low Temperature Supercritical Drying (LTSCD)

In order to avoid the use of flammable and explosive solvents, an adjustment of the process consists in the use of safer and non-flammable process solvents. This modification relies on the replacement of the synthesis solvent within the sol-gel by one with a lower critical point. The most used solvent is carbon dioxide due to its relatively low critical point (for CO₂: T_c = 31.1°C, P_c = 7.4 MPa) and its properties at the supercritical state are suitable for the extraction of most of the organic solvents used in the synthesis.

In this process, the organic solvent in a gel can be replaced with liquid or supercritical carbon dioxide by soaking or extraction, respectively. As a practical example for the normal LTSCD procedure, sol-gels prepared in an organic solvent is described below:

1. The sol-gel is placed in an autoclave that is filled up with additional solvent and then closed. Liquid CO₂ is pumped to purge the excess of solvent and then working pressure is achieved.
2. Replacement of organic solvent by carbon dioxide can be achieved by two different techniques:
 - a. CO₂ at liquid state is pumped into the autoclave in order to supplant the organic solvent by fluid exchange. Such process can be done in static (gravimetric) or in dynamic conditions. When organic solvent has been fully replaced, temperature and pressure are slowly increased over the critical point. This route is recommended for sol-gels with narrow porous.
 - b. CO₂ at temperature and pressure larger than its critical temperature and pressure is flushed through the autoclave until the solvent has been totally extracted from the sol-gel [143].

The operation can last from several hours to days, depending on the gel thickness since the transport mechanism of the process is governed by convection and, particularly by diffusion in confined pores. However, it has been reported that extraction with supercritical CO₂ is in the order of magnitude of 3 times faster than with liquid CO₂ fluid replacement [144].

3. Autoclave is then slowly and isothermally depressurized until reaching ambient pressure. This step can last several hours as CO₂ has to be removed very slowly to avoid i) phase change due to depressurization and related capillary forces that may damage the gel nanostructure, and ii) strong mechanical stress on the material that can also alter its morphology.
4. The vessel is cooled down to room temperature and opened, then aerogel withdrawn.

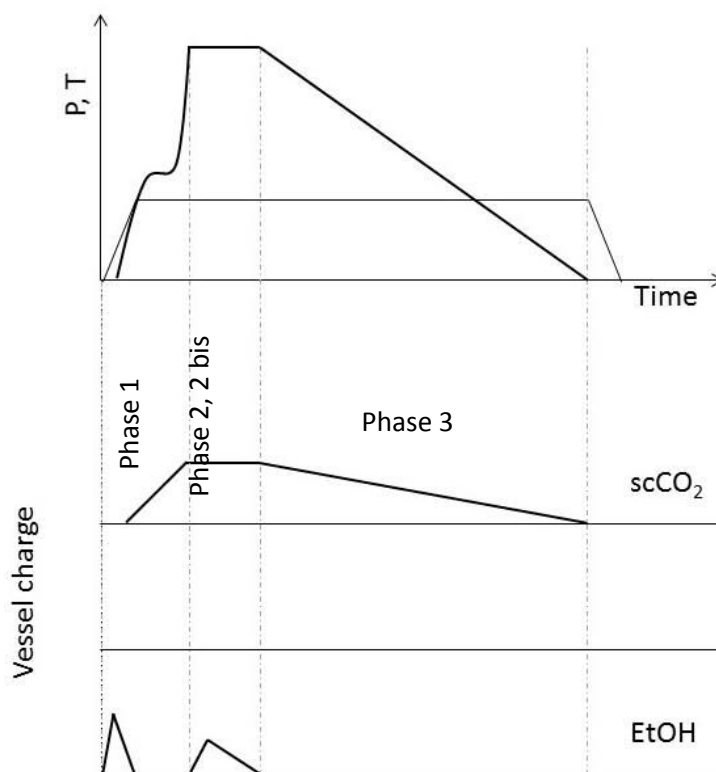


Figure 1.8. LTSCD process conditions.

As shown before, steps 2 and 3 can have duration of several hours depending on the thickness of the aerogel, due to the fact that the diffusion within the sample is independent of the environment of the sample. Optimization of the conditions and understanding of its causal effects with the diffusion can allow a better performance of the drying. Many studies were reported for the simulation of diffusion time [145], morphology of resulting material [146] and depressurization [147, 148], in order to shorten the main issues related to this process: time.

LTSCD of aerogel is a procedure governed by a fine control of the fluid conditions in order to avoid capillary forces during fluid replacement or extraction. Hence, the technology for this purpose must allow a process regulated with high accuracy in each measurement. The critical factors for the aerogel LTSCD have been defined as those ones that directly control the state of the CO_2 -solvent mixture: pressure and temperature.

The repercussion of the temperature has been reported as non-viable factor to take into account due to the high consumption of energy (with the increasing of temperature) which is not justifiable by the low process enhancement that can be achieved. Therefore, this factor can be considered constant and non-critical since it is over the T_c of the solvent in the process. On the other hand, small variations on the pressure around the aerogel can easily derive in a light shrinkage within the sample due to the expansion of the solvent or possible phase separation, Figure 1.9. To avoid this issue of shrinkage, the solvents have to remain over the liquid-gas line of the scCO_2 - organic solvent during the whole extraction process.

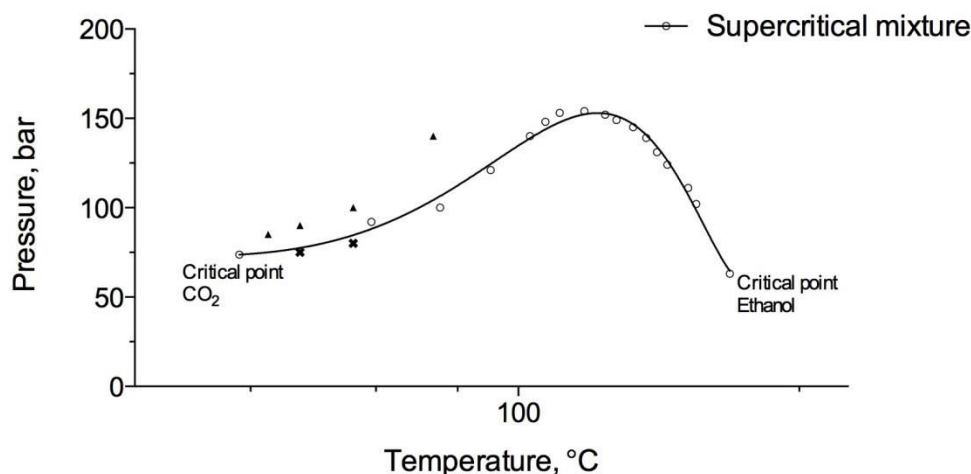


Figure 1.9. Exchange CO₂/ethanol [143]: (x) Shrinkage, (▲) no shrinkage

LTSCD conditions do not favor the replacement of the hydroxyl groups (OH) of the surface by hydrolytically stable organo-functional alkoxy groups (e.g. R=CH₃), and as a consequence, the final material leads to more hydrophilic solids (if the original sol-gel has not been prior modified).

This method has also the inconvenience that it cannot be applied to some aerogels, such as certain metal oxides, because they react with carbon dioxide to form metal carbonates.

1.4.2. HISTORY

In 1931, and in the concept of a bet between colleagues, Kistler produced the first Aerogel material by HTSCD of waterglass-precursor silica gel in methanol [10]. Later this method was adjusted by Monsanto Chemical Co. to produce granular and powder aerogels for diverse applications.

The aerogel drying was based entirely in HTSCD process, and even some player as BASF AG and Du Pont enter the production, it was still very limited due to high operational costs and risk. That reason, together with the wide development of xerogel powder materials in that period, made aerogel manufacture to decrease in the 60'ies and 70'ies.

Europe got back the attention of Aerogels when a new simplification in the synthesis by Teichner impulsed the manufacturing of aerogel monoliths for the application in Cherenkov detectors at DESY (*Deutsches Elektronen-Synchrotron*) and at CERN (*Organisation Européenne pour la Recherche Nucléaire*). Those aerogel tiles were mainly produced at Airglass AB. by HTSCD of methanol, which facilities suffered a problem due to the manipulation of high volume of methanol at supercritical conditions.

In 1984, Graser and Stange from BASF AG developed the LTSCD in order to reduce cost and risk in the production of hundred cubic meter or granular aerogel which was abandoned in 1996. The invention of LTSCD has been also attributed to Hunt and Tewari from the Microstructured Materials Group (University of California,), which exploited the process under the companies Aerotherm L.P. (until 1990) and Thermalux L.P. The last one, based the production in a 300 L equipment to produce granular/powder aerogel. When Thermalux L.P. activities ceased in 1992, the facilities were taken over by Aerojet Corp. (Sacramento) in collaboration with Lawrence Berkeley National Laboratory, in order to drive again the development of the production of different types of aerogels by LTSCD until 1996.

Aspen Systems started in 1984 when many patents on LTSCD process with some modifications were filed. In 1993, Aspen Systems started a contract with NASA for the development of aerogels for space application. After manufacturing of aerogel monoliths, in 1995, Aspen Systems developed a flexible aerogel blanket insulator for Space Suits, consisting in a fibre matrix within the sol-gel. In 2001, Aspen Aerogels expanded its facilities in parallel with the market. The products developed are used for example by the Elite Special Forces of the US army. Since the expansion of the plant, the revenue was growing steadily while its net losses have been shrinking until an IPO in May 2014. A third facility is planned for 2015 in East Europe or China.

Presently, Aspen Aerogels Inc. remains the main SCD player with its modified LTSCD process. HTSCD has been displaced to research purpose even for Airglass AB, which also moved to LTSCD for a limited production of large aerogel monoliths 60x60x2 cm³ which was declined in 2014.

1.4.3. PATENT

- *“This invention relates to improvements in the art and process of producing dry gels from colloidal solutions, and the present specification is particularly directed to the production of a gel, one continuous phase of which is a gas, and which I therefore define as an aerogel.”* [149]. With those words Kistler defined his discovery of producing highly porous silica material by the vent of an alcohol solvent within the gel at its supercritical state, so called HTSCD. Kistler claimed in this patent and succeeding ones [150-152] the HTSCD of mainly waterglass-based aerogels from different liquid solvents as alcohols ($T_c > 239$ °C), acetone ($T_c = 235$ °C) or liquid propane ($T_c = 94$ °C) or liquid dimethyl ether ($T_c = 126.9$ °C) and their mixtures. Kistler also assumed the necessity of a lower critical point solvent to be exchanged prior the supercritical drying step.
- Monsanto Chemicals Co. (Boston, US), with the license agreement of Kistler and a variation on the synthesis by Marshall [153], developed a process to manufacture the silica aerogel in powder ($d = 15\mu\text{m}$) shape in a continuous HTSCD process [154-159]. The process relies on the continuous feed of a silica colloid solution into a tubular reactor conditioned at supercritical conditions (up to 500 °C and 130 bars). The tubular reactor hosts both the gelation of the silica colloid and the achievement of the supercritical state of the organic solvent used. The pressure was controlled by an automatic control valve that allowed the discharge of the gel and the supercritical solvent into a conditioned vessel over 110 °C, avoiding the condensation of the organic solvent inside the porous material. Collected aerogel powder was recirculated by air to a separator where residual gas was separated while the aerogel solid material was automatically stored in a vessel.
- Same basis but with a simplified procedure was developed later by several companies as Universal Oil Products Company [160] which modified their already existing procedures to dry silica xerogels (e.g. Oil Product Co. [90]) in order to dry aerogel powders by HTSCD.
- Nicolaon and Teichner [161, 162] claimed the elaboration of aerogel monoliths by HTSCD of different alcohol solvents inside a high pressure vessel in batch mode. The real novelty of the patent was the use of a new silica based precursor of silica dispersed on alcohol, tetraethyl orthosilicate (so called TEOS). However, the

discontinuous batch process disclosed served for the industrial scale undertaken by Airglass AB until 1984. This process is the most established manner to HTSCD aerogel at research level nowadays.

- In 1984, Graser and Stange, at BASF AG., filled the patent of the development of a high potential variation of the HTSCD, the LTSCD [163, 164]. The modification was demanded in order to avoid the use of high temperatures and risky procedure and it was a consequence of the knowledge generated by the authors in the near-critical drying of finely divided pigments at low temperature (to do not decompose or damage the organic pigments) [165]. The process relies on the exchange of the organic solvent (free of water) within the gel by other with a lower critical point: liquid or supercritical carbon dioxide. When the gel is virtually free of the organic medium, CO₂ is removed at supercritical state by isothermal depressurization. The new step: *exchange organic solvent by a second solvent with low critical point*, was an inflexion point on the process due to the availability to work in more ambient-like temperature and friendly atmosphere. However, the process become longer due to the new step, and several days were needed for each batch. Hunt and Tewari [166] also claimed the same process to elaborate transparent aerogel insulating arrays by the same LTSCD process as described by *Graser et al.* including other compounds as possible low critical point solvents (i.e. Nitrous Oxide, Freon 13, Freon 23 and Freon 116. These two patents complete the open-door left by Kistler in the search of a solvent with lower critical point than organic ones, which already tried with DME- or propane-alcohol mixtures.
- Up to the end of the 20th century, many patents were filled for aerogel-based materials and their applications, but only a few about the process and manufacture. Among them, the most interesting is that developed by Hunt and Tewari in the development and commercialization of aerogel powder and monoliths by their LTSCD process under the company THERMALUX [167]. MATSUSHITA Electric Works Ltd. (future Panasonic) developed, a part from many different applications [168, 169], various optimizations and improvements in both supercritical drying processes [170] and, more importantly, the hydrophobization of silica aerogels during the LTSCD with CO₂ as solvent [171, 172].
- In 1997, SEPAREX S.A.S. claimed a semi-continuous process [173] to manufacture aerogel materials based on a simulated moving bed system as used for supercritical chromatography. The equipment was designed to host several vessels in where in each one a step of the whole process would be carried out, reducing substantially the process Operating Expenses (OPEX).

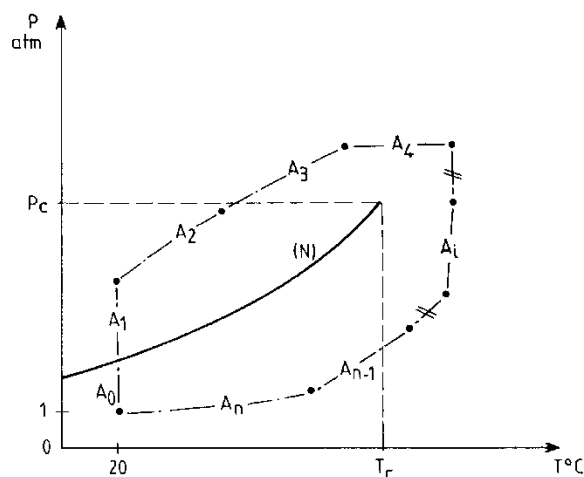


Figure 1.10. Separex S.A.'s semi-continuous LTSCD process with $n+1$ vessels and n steps.

- The past decade, many companies joined the development of aerogel manufacture. Most of them based their processes on LTSCD in order to avoid the HTSCD risks and costs. Among others the most significant patents for each process are the following. HTSCD: Philips Electronics N. V. [174], BASF AG [175], Henkel AG [176], General Ideas Ltd. (lately assigned to American Aerogel Corporation) [177, 178], Yazaki Corporation [110], etc. LTSCD: Gegussa Novara Technology Spa [179], Aspen Systems Inc. (lately assigned to Aspen Aerogel Inc.) [180, 181], Aspen Aerogel Inc. [182, 183], etc.
- Coronado et al., (University of California) implemented, in 1995, a process in order to produce monolithic aerogels by a “*Rapid Supercritical Extraction Process*” (RSCE) [184]. The method minimized the time of gelation and HTSCD by physically confining the gel during the process to avoid the stress formed by the rapid heating of the solvent and its subsequently dilatation. Thus, heating rate could be highly increased. The process is based on the same precept as Monsanto Chemical Co's process where gelation and HTSCD of the synthesis solvent is done at the same and only step, but obtaining a monolithic shape by avoiding internal stress. Process is as follows: Colloidal solution or existing gel is placed inside a pressure vessel where the whole volume must be occupied, and then by fast heating (at 20 °C/min) the gelation will take place. At the same time supercritical phase of the solvent will arise and evacuation of supercritical solvent will be done through one valve (at 5 bar/min), as shown in Figure 1.11. The authors reported that a single batch can be done within 1 - 4 hours with sizes up to 20 cm diameter sample.
A variation of RSCE process is the evacuation of the organic solvent within the gel by applying a pressurized gas (i.e. carbon dioxide) from one side and evacuating the solvent in the other side through a strong porous frit. This method is similar to that applied by Cabot with low pressurized gas.
- An improvement of RSCE method was claimed by Gauthier, Aet al. (Union College)[185]. The process relies in the same procedure but modifies the pressure application via hot press plates which at a first step will seal and pressurize the vessel, and at the end, will be the medium from where to control the release of pressure by restraining force conditions. The advantage of this method compared to

the original RSCE is that no high pressure vessel is needed and manufacture of multiples aerogel monoliths can be performed easily in the same hot press plate.

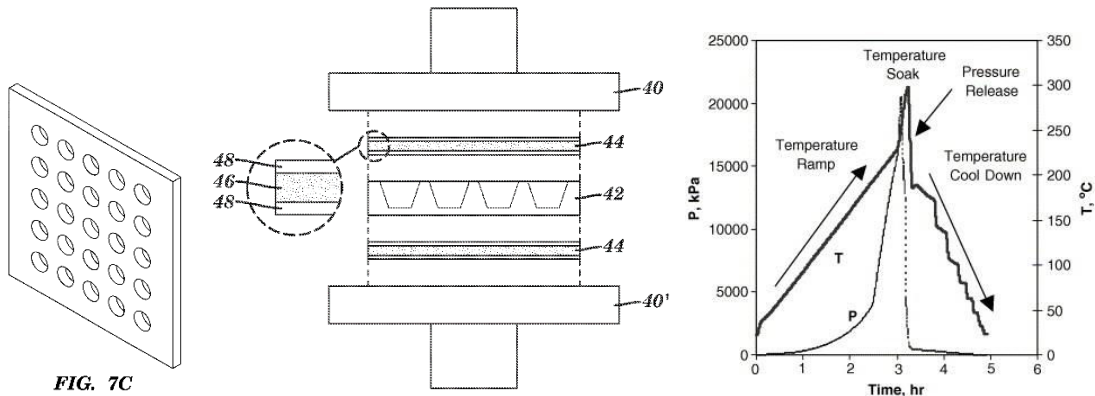


Figure 1.11. Rapid Supercritical Extraction Process (RSCE) equipment (left – middle) and process conditions (right).

- Aspen Systems Inc. claimed in 1999 for a process that would become the most scaled one on LTSCD [186]. It mainly comprises the implementation of each step of the LTSCD process in order to speed up the global cycle time. Fluid exchange and depressurization are the main point to be optimized by: a) insert supercritical rather than liquid CO₂ at the pressurization step, b) apply pressure pulse of two different frequencies (1 – 100,000 Hz and 0.0001 – 10 Hz) to enhance solvent exchange [187], and c) use of pressure waves during the depressurization step in order to increase the evacuation of CO₂ without damage the aerogel structure. The last step, pulses can be performed with the assistance of a non-supercritical gas in order to increase the CO₂ evacuation.

1.4.4. PUBLICATIONS

Ever since the first Aerogel was synthesized and dried, much effort has been placed into research on supercritical drying. Above all, the research has been more focused on understanding the process behavior and the repercussion on the properties of the Aerogel, than the exploration for new processes and scale-up. However, many improvements and sub-processes have been developed in order to enhance both the drying time and the final properties of the material.

In to the following Table 1.4 and Table 1.5, the most interesting currents research and discoveries are disclosed.

Table 1.4. Process and simulation of Aerogel drying.

Gel type	Process	Supercritical Solvent	Result and Observations	References
TMOS SiO ₄	HTSCD	Alcohol	Numerical simulation of stress Greater stress in cylinder than in a sphere	[39]
TMOS SiO ₄	HTSCD	Ethanol	Numerical simulation of depressurization For ethanol, the compressibility rises rapidly below ~4 MPa, use fast depressurization rate above, and slower rate at lower pressures. x30 faster than conventional HTSCD	[188]
TMOS SiO ₄	RSCE	Methanol	Liq. waste reduced by 40% x3 times less energy required	[189, 190]
TMOS SiO ₄ Alumina isopropoxide (AIP)	Union College RSCE	Methanol	7 – 15 h for hydrophobic aerogels with up to 155° contact angle 7.5 h for Alumina aerogel	[191-194]
TEOS SiO ₄	LTSCD	CO ₂	scCO ₂ flow velocity dependence (Optimum: < critical value) Optimized for transparent aerogel: Low temperature, high pressure, low flow velocity and thick gel. Diffusion and convective transport ratio (16 – 20)	[195]
SiO ₄ - Starch	LTSCD	CO ₂	Drying mass transfer modeling Diffusion kinetics vary of 1 order-of-magnitude between SiO and Starch.	[145]
TEOS SiO ₄	LTSCD	CO ₂	Drying time independent of the temperature (if above T _c of CO ₂) Optimal economic conditions (85 bar, 35 °C)	[143]
TEOS SiO ₄	LTSCD	CO ₂	Dynamic pressurization model (1 – 8 MPa) Permeability on pressure obeys Klinkenberg's model The mass transfer by convection in the earliest stages.	[147]
TEOS SiO ₄	LTSCD	CO ₂	Direct relationship between drying rate and CO ₂ flow. In the later stages, diffusion of the remaining organic solvent through the alcogel determined the mass transfer process.	[196]
SiO ₄	LTSCD	CO ₂	Numerical simulation of diffusion Diffusion of scCO ₂ is 3 order-of-magnitude than liq. CO ₂ Max. diffusion range: 0 ≤ P ≤ 74 bar; 0 ≤ ρ _{CO₂} ≤ 0.4 g/cm ³	[144, 196-199]
SiO ₄	LTSCD	CO ₂	Numerical simulation of stress Stress in LTSCD is lower than in HTSCD at low temperatures. Stress in circular plates are 3 – 4 order of magnitude less than for cylindrical for LTSCD and HTSCD, respectively.	[141]
SiO ₄ Resorcinol- Formaldehyde	LTSCD/HTSCD	CO ₂	Numerical simulation of structure	[200-203]

Table 1.5. Different solvent and reactions.

Gel type	Process	Supercritical Solvent	Result and Observations	References
Zinc Borates ($2\text{ZnO} \cdot 3\text{B}_2\text{O}_3 \cdot 3\text{H}_2\text{O}$ and $\text{ZnO} \cdot \text{B}_2\text{O}_3 \cdot 2\text{H}_2\text{O}$)	HTSCD	Ethanol	Decomposition of ZnO into boric acid	[204]
$\text{TiO}_2\text{-SiO}_2$	HTSCD	Ethanol	80% porosity 868 m ² /g surface area 40 nm particle size	[205]
Resorcinol-formaldehyde (RF)	HTSCD	Acetone	700 – 820 m ² /g surface area 34 – 15 % shrinkage Larger pore than in CO ₂ (Less surface area) Shrinkage diminished with vol. of ethanol to the reactor and pressure	[206-209]
TEOS SiO ₄	HTSCD	Ethanol	>91% porosity Increasing ethanol vol. in reactor, increase surface area. Increase of N ₂ pressure, decrease surface area	[210]
Resorcinol-formaldehyde (RF)	HTSCD	Ethanol / Methanol	Density 0.8 – 1.0 g/cm ³	[211]
Silica-, alumina-, zirconia based	HTSCD	Hexafluoroisopropyl alcohol (HFIP) Diethyl ether Methyl- <i>tert</i> -butyl ether	New solvents for aerogel synthesis. Novel solvents have twice higher specific surface area than ethanol-dried ones.	[212, 213]
Resorcinol-formaldehyde (RF)	HTSCD	2-Propanol	557 - 656 m ² /g surface area Density 0,48 – 0,15 g/cm ³	[214]
Agar (Mw ~120,000)	HTSCD	Acetone	Aerogel synthesis in supercritical acetone as synthesis porogenic solvent	[215]
	LTSCD	CO ₂ CO ₂ /EtOH(6%)	Addition of co-solvent increase the water solubility and its extraction. Co-solvent addition induce microstructural changes on the gel.	[216]
TEOS SiO ₄ TMOS SiO ₄ Polymer ZrO ₂	LTSCD	CO ₂	Use of liq. or supercritical CO ₂ as porogenic solvent during aerogel synthesis. Higher kinetic reaction: at high temperature and lower pressures Issue: high acid CO ₂ behavior	[217-221]
TEOS SiO ₄	SAS	CO ₂	Particle size 1 – 2.5 μm	[222]
TEOS SiO ₄	LTSCD	CO ₂ /HMDS	Surface modification by reaction of silanol in supercritical CO ₂ solution. Contact angle up to 130°	[223-227]

1.4.5. FUTURE DEVELOPMENT

It is remarkable the high interest and the efforts to scale up the supercritical drying processes, either HTSCD or LTSCD, since that method provides the best quality material from a same initial gel. However, only few players arise to develop a manufacture of aerogels but always hauling the high costs related to the drying.

Further developments are required in order to establish an aerogel manufacturing line at a price that can compete with their counterparts in the different areas of applications. For such purpose, improvements in both faster processes and efficient high pressure equipment must be achieved within the next years.

1.5. CONCLUSIONS

A broad description of the State-of-the-Art of sol-gel drying methods and technology have been provided in order to established a strong base wherefrom to consider the manufacturing of aerogel products. Despite the quantity of product developed at lab scale, it has been shown the few successful cases of industrialization. However, the growing of industrials applications will encourage the optimization and escalation of the different methods.

FD methods showed a great performance for hydrophilic and organic materials, being successful on maintaining the porous structure in contrast with SPD. Conversely, the OPEX is too high for large manufactures where SPD of hydrophobic silica materials is appropriate. The author strongly believes that the most potential development is found in the LTSCD, since the OPEX and operational conditions are very low and the implantation of this technology in the world is coming prevalent [228]. Hence, high pressure systems have suffered an impressive CAPEX reduction. This fact together with the optimization of the process could turn into a high versatility method to produce top quality aerogel products.

Furthermore, regardless of the application, all processes that comprise supercritical fluids share numerous benefits compared with those traditional ones for the same purpose.

- It is a green technology.as it avoid the use of organic solvents harmful to the environment and which must be recycled in various purification processes.
- The use of carbon dioxide as waste from industry to add value. This technology does not produce CO₂, but reuses.
- Recycling of all compounds and solvents up to 98% makes this technology sustainable and products derived from it suffers minimal impact in Life Cycle Assessment.

REFERENCES

1. Baetens, R., B.P. Jelle, and A. Gustavsen, *Aerogel insulation for building applications: A state-of-the-art review*. Energy and Buildings, 2011. **43**(4): p. 761-769.
2. Ulker, Z. and C. Erkey, *An emerging platform for drug delivery: Aerogel based systems*. Journal of Controlled Release, 2014. **177**(0): p. 51-63.
3. Cuce, E., et al., *Toward aerogel based thermal superinsulation in buildings: A comprehensive review*. Renewable and Sustainable Energy Reviews, 2014. **34**(0): p. 273-299.
4. Nishida, S., et al., *Aerogel RICH for the Belle II forward PID*. Nuclear Instruments and Methods in Physics Research Section A: Accelerators, Spectrometers, Detectors and Associated Equipment, (0).
5. Tabata, M., et al., *Recent Progress in Silica Aerogel Cherenkov Radiator*. Physics Procedia, 2012. **37**(0): p. 642-649.
6. Kissel, J., et al., *The Probable Chemical Nature of Interstellar Dust Particles Detected by "CIDA" Onboard "STARDUST"*, in *COSPAR Colloquia Series*, H.F.H.J.F. Klaus Scherer and M. Eckart, Editors. 2001, Pergamon. p. 351-359.
7. Burchell, M.J., et al., *Hypervelocity capture of particles in aerogel: Dependence on aerogel properties*. Planetary and Space Science, 2009. **57**(1): p. 58-70.
8. Hüsing, N. and U. Schubert, *Aerogels—Airy Materials: Chemistry, Structure, and Properties*. Angewandte Chemie International Edition, 1998. **37**(1-2): p. 22-45.
9. Brinker, J.C. and G.W. Scherer, *Sol-Gel Science, The Physics and Chemistry of Sol-Gel Processing*, ed. s. Edition 1990, New York: Academic Press.
10. Kistler, S.S., *Coherent Expanded Aerogels and Jellies*. Nature, 1931. **227**: p. 741-741.
11. El Rassy, H., et al., *Surface Characterization of Silica Aerogels with Different Proportions of Hydrophobic Groups, Dried by the CO₂ Supercritical Method*. Langmuir, 2002. **19**(2): p. 358-363.
12. Venkateswara Rao, A., et al., *Synthesis of flexible silica aerogels using methyltrimethoxysilane (MTMS) precursor*. Journal of Colloid and Interface Science, 2006. **300**(1): p. 279-285.
13. Deng, Z., et al., *Physical Properties of Silica Aerogels Prepared with Polyethoxydisiloxanes*. Journal of Sol-Gel Science and Technology, 2000. **19**(1-3): p. 677-680.
14. Einarsrud, M.-A., et al., *Strengthening of silica gels and aerogels by washing and aging processes*. Journal of Non-Crystalline Solids, 2001. **285**(1-3): p. 1-7.
15. Zhou, B., et al., *Hydrophobic silica aerogels derived from polyethoxydisiloxane and perfluoroalkylsilane*. Materials Science and Engineering: C, 2007. **27**(5-8): p. 1291-1294.
16. Alié, C., et al., *Preparation of low-density xerogels through additives to TEOS-based alcogels*. Journal of Non-Crystalline Solids, 1999. **246**(3): p. 216-228.
17. Sescousse, R. and T. Budtova, *Influence of processing parameters on regeneration kinetics and morphology of porous cellulose from cellulose–NaOH–water solutions*. Cellulose, 2009. **16**(3): p. 417-426.
18. Pinnow, M., et al., *Characterization of Highly Porous Materials from Cellulose Carbamate*. Macromolecular Symposia, 2008. **262**(1): p. 129-139.
19. Hoepfner, S., L. Ratke, and B. Milow, *Synthesis and characterisation of nanofibrillar cellulose aerogels*. Cellulose, 2008. **15**(1): p. 121-129.

20. Gavillon, R. and T. Budtova, *Aerocellulose: New Highly Porous Cellulose Prepared from Cellulose–NaOH Aqueous Solutions*. *Biomacromolecules*, 2007. **9**(1): p. 269-277.
21. Innerlohinger, J., H.K. Weber, and G. Kraft, *Aerocellulose: Aerogels and Aerogel-like Materials made from Cellulose*. *Macromolecular Symposia*, 2006. **244**(1): p. 126-135.
22. Tan, C., et al., *Organic Aerogels with Very High Impact Strength*. *Advanced Materials*, 2001. **13**(9): p. 644-646.
23. Biesmans, G., et al., *Polyurethane-Based Aerogels for Use as Environmentally Acceptable Super Insulants in the Future Appliance Market*. *Journal of Cellular Plastics*, 1998. **34**(5): p. 396-411.
24. Rigacci, A. and P. Achard, *Cellulosic and Polyurethane Aerogels*, in *Aerogels Handbook*, M.A. Aegerter, N. Leventis, and M.M. Koebel, Editors. 2011, Springer New York. p. 191-214.
25. Pierre, A.C. and G.M. Pajonk, *Chemistry of Aerogels and Their Applications*. *Chemical Reviews*, 2002. **102**(11): p. 4243-4266.
26. Lu, X., et al., *Correlation between structure and thermal conductivity of organic aerogels*. *Journal of Non-Crystalline Solids*, 1995. **188**(3): p. 226-234.
27. Pekala, R.W., C.T. Alviso, and J.D. LeMay, *Organic aerogels: microstructural dependence of mechanical properties in compression*. *Journal of Non-Crystalline Solids*, 1990. **125**(1-2): p. 67-75.
28. Pekala, R.W., *Organic aerogels from the polycondensation of resorcinol with formaldehyde*. *Journal of Materials Science*, 1989. **24**(9): p. 3221-3227.
29. Smirnova, A., et al., *Novel carbon aerogel-supported catalysts for PEM fuel cell application*. *International Journal of Hydrogen Energy*, 2005. **30**(2): p. 149-158.
30. Moreno-Castilla, C., et al., *Group 6 metal oxide-carbon aerogels. Their synthesis, characterization and catalytic activity in the skeletal isomerization of 1-butene*. *Applied Catalysis A: General*, 1999. **183**(2): p. 345-356.
31. Maldonado-Hódar, F.J., C. Moreno-Castilla, and A.F. Pérez-Cadenas, *Catalytic combustion of toluene on platinum-containing monolithic carbon aerogels*. *Applied Catalysis B: Environmental*, 2004. **54**(4): p. 217-224.
32. Haji, S. and C. Erkey, *Removal of Dibenzothiophene from Model Diesel by Adsorption on Carbon Aerogels for Fuel Cell Applications*. *Industrial & Engineering Chemistry Research*, 2003. **42**(26): p. 6933-6937.
33. Gupta, N. and W. Ricci, *Processing and compressive properties of aerogel/epoxy composites*. *Journal of Materials Processing Technology*, 2008. **198**(1-3): p. 178-182.
34. Cai, J., et al., *Cellulose–Silica Nanocomposite Aerogels by In Situ Formation of Silica in Cellulose Gel*. *Angewandte Chemie International Edition*, 2012. **51**(9): p. 2076-2079.
35. Risen, W.M., Jr. and X. Liu, *Chitosan Biopolymer-Silica Hybrid Aerogels*, in *Natural Fibers, Plastics and Composites*, F. Wallenberger and N. Weston, Editors. 2004, Springer US. p. 227-246.
36. Garcia-Gonzalez, C.A., et al., *Design of biocompatible magnetic pectin aerogel monoliths and microspheres*. *RSC Advances*, 2012. **2**(26): p. 9816-9823.
37. Zheng, Q., Z. Cai, and S. Gong, *Green synthesis of polyvinyl alcohol (PVA)-cellulose nanofibril (CNF) hybrid aerogels and their use as superabsorbents*. *Journal of Materials Chemistry A*, 2014. **2**(9): p. 3110-3118.

38. Ge, D., et al., *In Situ Synthesis of Hybrid Aerogels from Single-Walled Carbon Nanotubes and Polyaniline Nanoribbons as Free-Standing, Flexible Energy Storage Electrodes*. Chemistry of Materials, 2014. **26**(4): p. 1678-1685.
39. Scherer, G., *Stress in aerogel during depressurization of autoclave: I. theory*. Journal of Sol-Gel Science and Technology, 1994. **3**(2): p. 127-139.
40. Dowson, M., et al., *Streamlined life cycle assessment of transparent silica aerogel made by supercritical drying*. Applied Energy, 2012. **97**(0): p. 396-404.
41. Fricke, J. and T. Tillotson, *Aerogels: production, characterization, and applications*. Thin Solid Films, 1997. **297**(1-2): p. 212-223.
42. Carlson, G., et al., *Aerogel commercialization: technology, markets and costs*. Journal of Non-Crystalline Solids, 1995. **186**(0): p. 372-379.
43. Bhaduri, S.B., *THE PHYSICS AND CHEMISTRY OF SOL-GEL PROCESSING edited by C.J. Brinker and G.W. Scherer Academic Press, Inc., San Diego, CA 908 pages, hard cover, 1990*. Materials and Manufacturing Processes, 1993. **8**(3): p. 391-392.
44. Liu, Y., Y. Zhao, and X. Feng, *Exergy analysis for a freeze-drying process*. Applied Thermal Engineering, 2008. **28**(7): p. 675-690.
45. Aghbashlo, M., et al., *A review on exergy analysis of drying processes and systems*. Renewable and Sustainable Energy Reviews, 2013. **22**(0): p. 1-22.
46. Su, L.F., et al., *Low-cost and fast synthesis of nanoporous silica cryogels for thermal insulation applications*. Science and Technology of Advanced Materials, 2012. **13**(3): p. 035003.
47. Mathieu, B., et al., *Freeze-dried resorcinol-formaldehyde gels*. Journal of Non-Crystalline Solids, 1997. **212**(2-3): p. 250-261.
48. Bruno, M.M., et al., *A novel way to maintain resorcinol-formaldehyde porosity during drying: Stabilization of the sol-gel nanostructure using a cationic polyelectrolyte*. Colloids and Surfaces A: Physicochemical and Engineering Aspects, 2010. **362**(1-3): p. 28-32.
49. Yamamoto, T., et al., *The effects of different synthetic conditions on the porous properties of carbon cryogel microspheres*. Carbon, 2005. **43**(6): p. 1231-1238.
50. Babić, B., et al., *Characterization of carbon cryogel synthesized by sol-gel polycondensation and freeze-drying*. Carbon, 2004. **42**(12-13): p. 2617-2624.
51. Sánchez-Silva, L., et al., *Tailor-Made Aerogels Based on Carbon Nanofibers by Freeze-Drying*. Science of Advanced Materials, 2014. **6**(4): p. 665-673.
52. Jafarzadeh, M., I.A. Rahman, and C.S. Sipaut, *Synthesis of silica nanoparticles by modified sol-gel process: the effect of mixing modes of the reactants and drying techniques*. Journal of Sol-Gel Science and Technology, 2009. **50**(3): p. 328-336.
53. Tamon, H., et al., *FREEZE DRYING FOR PREPARATION OF AEROGEL-LIKE CARBON*. Drying Technology, 2001. **19**(2): p. 313-324.
54. Pons, A., et al., *A new route to aerogels: Monolithic silica cryogels*. Journal of Non-Crystalline Solids, 2012. **358**(3): p. 461-469.
55. Aboutboul, H.A., W. Kirch, and J.H. Krekeler, *Preparation of silica gels*, 1972, Google Patents.
56. Wallace, S., D.M. Smith, and W.C. Ackerman, *Drying wet gel comprising gel solids and a drying agent to remove drying agent to produce dried gel*, 2001, Google Patents.
57. Albert, D.F., G.R. Andrews, and J.W. Bruno, *Organic, open cell foam materials*, 2011, Google Patents.

58. Albert, D.F., G.R. Andrews, and J.W. Bruno, *Organic, low density microcellular materials*, 2001, Google Patents.
59. Schiraldi, D.A., M.D. Gawryla, and S.A. Bandi, *Clay aerogel-based polymer composites, materials and methods*, 2007, Google Patents.
60. *One kind of block airgel composite material and method*, 2014, Google Patents.
61. *A flexible airgel block and its preparation method*, 2014, Google Patents.
62. Zhai, L. and J. ZOU, *Carbon nanotube or graphene-based aerogels*, 2011, Google Patents.
63. Pauzauskie, P.J., et al., *Graphene aerogels*, 2012, Google Patents.
64. *Block aerogel composite material and preparation method thereof*, 2012, Google Patents.
65. *Method for preparing hydrophobic block cellulose aerogel thermal insulation material*, 2014, Google Patents.
66. Wang, J. and M.W. Ellsworth, *Graphene and graphene oxide aerogels*, 2010, Google Patents.
67. Shekunov, B.Y., P. Chattopadhyay, and J.S. Seitzinger, *Lyophilization method and apparatus for producing particles*, 2005, Google Patents.
68. SCHWAB, M.G., et al., *Aerogel based on doped graphene*, 2013, Google Patents.
69. Pojanavaraphan, T., D.A. Schiraldi, and R. Magaraphan, *Mechanical, rheological, and swelling behavior of natural rubber/montmorillonite aerogels prepared by freeze-drying*. Applied Clay Science, 2010. **50**(2): p. 271-279.
70. Grishechko, L.I., et al., *Lignin–phenol–formaldehyde aerogels and cryogels*. Microporous and Mesoporous Materials, 2013. **168**(0): p. 19-29.
71. Donius, A.E., et al., *Superior mechanical performance of highly porous, anisotropic nanocellulose–montmorillonite aerogels prepared by freeze casting*. Journal of the Mechanical Behavior of Biomedical Materials, 2014. **37**(0): p. 88-99.
72. Baldino, L., et al., *Chitosan scaffolds formation by a supercritical freeze extraction process*. The Journal of Supercritical Fluids, 2014. **90**(0): p. 27-34.
73. Qian, Y., I.M. Ismail, and A. Stein, *Ultralight, high-surface-area, multifunctional graphene-based aerogels from self-assembly of graphene oxide and resol*. Carbon, 2014. **68**(0): p. 221-231.
74. Ji, C.-C., et al., *Self-assembly of three-dimensional interconnected graphene-based aerogels and its application in supercapacitors*. Journal of Colloid and Interface Science, 2013. **407**(0): p. 416-424.
75. Yun, J., et al., *Rapid freezing cryo-polymerization and microchannel liquid-flow focusing for cryogel beads: Adsorbent preparation and characterization of supermacroporous bead-packed bed*. Journal of Chromatography A, 2013. **1284**(0): p. 148-154.
76. Czakkel, O., et al., *Influence of drying on the morphology of resorcinol–formaldehyde-based carbon gels*. Microporous and Mesoporous Materials, 2005. **86**(1–3): p. 124-133.
77. Ganguly, A., et al., *Freeze-drying simulation framework coupling product attributes and equipment capability: Toward accelerating process by equipment modifications*. European Journal of Pharmaceutics and Biopharmaceutics, 2013. **85**(2): p. 223-235.
78. Schoen, M.P., et al., *A simulation model for the primary drying phase of the freeze-drying cycle*. International Journal of Pharmaceutics, 1995. **114**(2): p. 159-170.

79. Carullo, A. and A. Vallan, *Measurement uncertainty issues in freeze-drying processes*. Measurement, 2012. **45**(7): p. 1706-1712.
80. Nastaj, J.F., K. Witkiewicz, and B. Wilczyńska, *Experimental and simulation studies of primary vacuum freeze-drying process of random solids at microwave heating*. International Communications in Heat and Mass Transfer, 2008. **35**(4): p. 430-438.
81. STEFAN C. SCHNEID, H.G., *Rational approaches and transfer strategies for the scale-up of freeze-drying cycles*. Chemistry today, 2012. **30**(2).
82. Shewale, P.M., A.V. Rao, and A.P. Rao, *Effect of different trimethyl silylating agents on the hydrophobic and physical properties of silica aerogels*. Applied Surface Science, 2008. **254**(21): p. 6902-6907.
83. Rao, A.V. and M.M. Kulkarni, *Effect of glycerol additive on physical properties of hydrophobic silica aerogels*. Materials Chemistry and Physics, 2003. **77**(3): p. 819-825.
84. Blanco, E., et al., *Processing of silica xerogels using sonocatalysis and an additive*. Journal of Non-Crystalline Solids, 1992. **147-148**(0): p. 296-302.
85. Brinker, C.J. and G.W. Scherer, *CHAPTER 8 - Drying*, in *Sol-Gel Science*, C.J. Brinker and G.W. Scherer, Editors. 1990, Academic Press: San Diego. p. 452-513.
86. Prakash, S.S., et al., *Silica aerogel films prepared at ambient pressure by using surface derivatization to induce reversible drying shrinkage*. Nature, 1995. **374**(6521): p. 439-443.
87. Bhagat, S.D., et al., *A continuous production process for silica aerogel powders based on sodium silicate by fluidized bed drying of wet-gel slurry*. Solid State Sciences, 2008. **10**(9): p. 1113-1116.
88. K, K.K., *Method of producing easily pulverized xerogel*, 1947, Google Patents.
89. Weisz, P.B., *Process for drying inorganic hydrogels particles*, 1956, Google Patents.
90. Owen, J.J., *Process for drying hydrogel catalysts*, 1949, Google Patents.
91. Marisic, M.M., *Process of drying inorganic oxide gels*, 1950, Google Patents.
92. Alexander, G.B., R.K. Iler, and F.J. Wolter, *Process of preparing dense amorphous silica aggregates and product*, 1956, Google Patents.
93. B, A.G., *Pulverulent silica products*, 1962, Google Patents.
94. M, B.E., *Halosilane hydrolysis with tetrahydrofuran and water*, 1959, Google Patents.
95. Schmidt, F., K. Spitznagel, and A. Wagner, *Process for the production of silica with an aerogel type structure*, 1979, Google Patents.
96. Laufer, S. and W. Roy, *Highly-active, finely divided super-dry silicon dioxide*, 1977, Google Patents.
97. McDaniel, M.P., *Contacting with organosilicon compound, drying, increasing pore volume*, 1980, Google Patents.
98. Deshpande, R., D.M. Smith, and C.J. Brinker, *Preparation of high porosity xerogels by chemical surface modification*, 1994, Google Patents.
99. Hench, L.L. and G.F. Orcel, *Glycerol, formamide, oxalic acid and monocarboxylic acids*, 1989, Google Patents.
100. Smith, D.M., et al., *Low volatility solvent-based method for forming thin film nanoporous aerogels on semiconductor substrates*, 1999, Google Patents.
101. Jansen, R.M. and A. Zimmermann, *Process for the preparation of xerogels*, 1997, Google Patents.

102. Jansen, R.M., et al., *Method for the subcritical drying of aerogels*, 1998, Google Patents.
103. Schwertfeger, F. and A. Zimmermann, *Process for preparing organically modified aerogels using alcohols*, 2000, Google Patents.
104. Jansen, R.M.D. and A.D. Zimmermann, *Xerogels, process for their preparation and their use*, 1996, Google Patents.
105. Teich, F., et al., *Feeding as moving bed countercurrently to a drying fluid; reduction of fluid interfacial tension*, 2003, Google Patents.
106. C, A.W., S.D. M, and W. Stephen, *Process for producing low density gel compositions*, 1998, Google Patents.
107. Firestone, R.A., *Device for maintaining dry conditions in vessels*, 1985, Google Patents.
108. Wang, S., S. Raychaudhuri, and A. Sarkar, *Sol-gel process for providing a tailored gel microstructure*, 1996, Google Patents.
109. Wang, S., et al., *Apparatus for rapidly drying a wet, porous gel monolith*, 1994, Google Patents.
110. Wang, S., et al., *Process for rapidly drying a wet, porous gel monolith*, 1993, Google Patents.
111. BESSELIEVRE, E., et al., *Process for manufacturing xerogels*, 2013, Google Patents.
112. Mahadik, D.B., et al., *Reduction of processing time by mechanical shaking of the ambient pressure dried TEOS based silica aerogel granules*. Journal of Porous Materials, 2012. **19**(1): p. 87-94.
113. Venkateswara Rao, A., et al., *Influence of preparation conditions on nanoporous structure and optical transmission of sodium silicate based ambient pressure dried aerogels employing shaking*. Journal of Porous Materials, 2011. **18**(6): p. 751-759.
114. Hwang, S.-W., et al., *Effective preparation of crack-free silica aerogels via ambient drying*. Journal of Sol-Gel Science and Technology, 2007. **41**(2): p. 139-146.
115. Rao, A.V., et al., *Sodium Silicate Based Aerogels via Ambient Pressure Drying*, in *Aerogels Handbook*, M.A. Aegerter, N. Leventis, and M.M. Koebel, Editors. 2011, Springer New York. p. 103-124.
116. Hwang, S.-W., T.-Y. Kim, and S.-H. Hyun, *Effect of surface modification conditions on the synthesis of mesoporous crack-free silica aerogel monoliths from waterglass via ambient-drying*. Microporous and Mesoporous Materials, 2010. **130**(1-3): p. 295-302.
117. Adachi, I., et al., *Study of transparent silica aerogel with high refractive index*. Nuclear Instruments and Methods in Physics Research Section A: Accelerators, Spectrometers, Detectors and Associated Equipment, 2011. **639**(1): p. 222-224.
118. Barnyakov, A.Y., et al., *Status of aerogel production in Novosibirsk*. Nuclear Instruments and Methods in Physics Research Section A: Accelerators, Spectrometers, Detectors and Associated Equipment, 2011. **639**(1): p. 225-226.
119. Tabata, M., et al., *Silica aerogel radiator for use in the A-RICH system utilized in the Belle II experiment*. Nuclear Instruments and Methods in Physics Research Section A: Accelerators, Spectrometers, Detectors and Associated Equipment, (0).
120. Gao, G.-M., et al., *Preparation of silica aerogel from oil shale ash by fluidized bed drying*. Powder Technology, 2010. **197**(3): p. 283-287.

121. Gao, G.-M., et al., *Synthesis of ultrafine silica powders based on oil shale ash by fluidized bed drying of wet-gel slurry*. *Fuel*, 2009. **88**(7): p. 1223-1227.
122. Li, H., et al., *Hydrodynamic behaviour of aerogel powders in high-velocity fluidized beds*. *Powder Technology*, 1990. **60**(2): p. 121-129.
123. Léonard, A., et al., *Evolution of mechanical properties and final textural properties of resorcinol-formaldehyde xerogels during ambient air drying*. *Journal of Non-Crystalline Solids*, 2008. **354**(10-11): p. 831-838.
124. Léonard, A., et al., *Suitability of convective air drying for the production of porous resorcinol-formaldehyde and carbon xerogels*. *Carbon*, 2005. **43**(8): p. 1808-1811.
125. Job, N., et al., *Towards the production of carbon xerogel monoliths by optimizing convective drying conditions*. *Carbon*, 2006. **44**(12): p. 2534-2542.
126. Gallegos-Suárez, E., et al., *On the micro- and mesoporosity of carbon aerogels and xerogels. The role of the drying conditions during the synthesis processes*. *Chemical Engineering Journal*, 2012. **181-182**(0): p. 851-855.
127. Khalloufi, S., et al., *Mathematical Model for Simulating the Springback Effect of Gel Matrixes During Drying Processes and Its Experimental Validation*. *Drying Technology*, 2011. **29**(16): p. 1972-1980.
128. Prakash, S.S., C.J. Brinker, and A.J. Hurd, *Silica aerogel films at ambient pressure*. *Journal of Non-Crystalline Solids*, 1995. **190**(3): p. 264-275.
129. Eloukabi, H., et al., *Experimental study of the effect of sodium chloride on drying of porous media: The crusty-patchy efflorescence transition*. *International Journal of Heat and Mass Transfer*, 2013. **56**(1-2): p. 80-93.
130. Prat, M., *Recent advances in pore-scale models for drying of porous media*. *Chemical Engineering Journal*, 2002. **86**(1-2): p. 153-164.
131. Plourde, F. and M. Prat, *Pore network simulations of drying of capillary porous media. Influence of thermal gradients*. *International Journal of Heat and Mass Transfer*, 2003. **46**(7): p. 1293-1307.
132. Prat, M., *On the influence of pore shape, contact angle and film flows on drying of capillary porous media*. *International Journal of Heat and Mass Transfer*, 2007. **50**(7-8): p. 1455-1468.
133. Surasani, V.K., T. Metzger, and E. Tsotsas, *Consideration of heat transfer in pore network modelling of convective drying*. *International Journal of Heat and Mass Transfer*, 2008. **51**(9-10): p. 2506-2518.
134. Kirkbir, F., et al., *Drying of aerogels in different solvents between atmospheric and supercritical pressures*. *Journal of Non-Crystalline Solids*, 1998. **225**(0): p. 14-18.
135. Leventis, N., et al., *Nanoengineered Silica-Polymer Composite Aerogels with No Need for Supercritical Fluid Drying*. *Journal of Sol-Gel Science and Technology*, 2005. **35**(2): p. 99-105.
136. Bangi, U.K.H., et al., *Improvement in optical and physical properties of TEOS based aerogels using acetonitrile via ambient pressure drying*. *Ceramics International*, 2012. **38**(8): p. 6883-6888.
137. Nilsen, E., M.A. Einarsrud, and G.W. Scherer, *Effect of precursor and hydrolysis conditions on drying shrinkage*. *Journal of Non-Crystalline Solids*, 1997. **221**(2-3): p. 135-143.
138. Jung, S.-B., et al., *Effect of solvent on the preparation of ambient pressure-dried SiO₂ aerogel films*. *Microelectronic Engineering*, 2003. **65**(1-2): p. 113-122.

139. Nikolić, L. and L. Radonjić, *Effect of drying control chemical additives in Sol-Gel-Glass Monolith processing*. Ceramics International, 1994. **20**(5): p. 309-313.
140. Venkateswara Rao, A., et al., *Influence of N,N-dimethylformamide additive on the physical properties of citric acid catalyzed TEOS silica aerogels*. Materials Chemistry and Physics, 1999. **60**(3): p. 268-273.
141. Unlusu, B., S.G. Sunol, and A.K. Sunol, *Stress formation during heating in supercritical drying*. Journal of Non-Crystalline Solids, 2001. **279**(2-3): p. 110-118.
142. LI, H.Z. and M. PERRUT, *Flash discharge of supercritical fluid and high pressure gas through pipes: experimental results and modelling*. Chemical Engineering Communications, 1992. **117**(1): p. 415-431.
143. van Bommel, M.J. and A.B. de Haan, *Drying of silica aerogel with supercritical carbon dioxide*. Journal of Non-Crystalline Solids, 1995. **186**(0): p. 78-82.
144. Wawrzyniak, P., et al., *Diffusion of ethanol-carbon dioxide in silica gel*. Journal of Non-Crystalline Solids, 1998. **225**(0): p. 86-90.
145. García-González, C.A., et al., *Supercritical drying of aerogels using CO₂: Effect of extraction time on the end material textural properties*. The Journal of Supercritical Fluids, 2012. **66**(0): p. 297-306.
146. Griffin, J.S., et al., *Continuous Extraction Rate Measurements During Supercritical CO₂ Drying of Silica Alcogel*. The Journal of Supercritical Fluids, (0).
147. Gross, J. and G.W. Scherer, *Dynamic pressurization: novel method for measuring fluid permeability*. Journal of Non-Crystalline Solids, 2003. **325**(1-3): p. 34-47.
148. Scherer, G.W., J.J. Valenza II, and G. Simmons, *New methods to measure liquid permeability in porous materials*. Cement and Concrete Research, 2007. **37**(3): p. 386-397.
149. Kistler, S.S., *Method of producing aerogels*, 1937, Google Patents.
150. Kistler, S.S., *Inorganic aerogel compositions*, 1940, Google Patents.
151. Kistler, S.S., *Buffing and polishing composition*, 1940, Google Patents.
152. Kistler, S.S., *Treatment of aerogels to render them waterproof*, 1952, Google Patents.
153. D, M.M., *Method of producing sols and aerogels*, 1942, Google Patents.
154. F, W.J. and W.W. S, *Methods of preparing hydrogels and aerogels*, 1957, Google Patents.
155. M, D.W. and S.N. A, *Method for producing aerogels*, 1959, Google Patents.
156. Allen, L.S., *Coating composition and process of preparation*, 1959, Google Patents.
157. F, N.R., *Process for the preparation of silica gel and silica aerogels*, 1960, Google Patents.
158. A, T.T., *Novel silica aerogels and processes for preparing same*, 1964, Google Patents.
159. Marotta, R. and H. Teicher, *Organic liquids thickened with treated silica materials*, 1969, Google Patents.
160. Deanesly, R.M., *Preparation of fine powders from gel materials*, 1951, Google Patents.
161. Andre, N.G. and T.S. Jean, *Method of preparing inorganic aerogels*, 1972, Google Patents.

162. Andre, N.G., T.S. Jean, and V.M. Adrien, *Production of aerogels of alumina and - titania*, 1970, Google Patents.
163. Graser, F.D. and A.D. Stange, *Verfahren zur herstellung von aerogelen*, 1986, Google Patents.
164. Graser, F. and A. Stange, *Replacing water with solvent, then replacing solvent with carbon dioxide and drying*, 1987, Google Patents.
165. Graser, F.D.C.D. and G.D.I. Wickenhaeuser, *Verfahren zum trocknen von feinteiligen pigmenten*, 1981, Google Patents.
166. Tewari, P.H. and A.J. Hunt, *Hydrolysis and condensation of alkoxides to form alcogels; window, appliance insulation*, 1986, Google Patents.
167. Martin, M.R., *Monolithic aerogel insulation cast and dried within a support structure and method*, 1992, Google Patents.
168. Kamae, T., et al., *Optical fiber with silica aerogel cladding*, 1998, Google Patents.
169. Kawano, K., et al., *Substrat d'aerogel et son procédé de preparation*, 2010, Google Patents.
170. Sonoda, K., et al., *Process for producing aerogel*, 2005, Google Patents.
171. Takahama, K., et al., *Process for producing hydrophobic aerogel*, 1993, Google Patents.
172. Yokogawa, H., et al., *Process of forming a hydrophobic aerogel*, 1998, Google Patents.
173. Perrut, M. and E. Francais, *Process and equipment for drying a polymeric aerogel in the presence of a supercritical fluid*, 1999, Google Patents.
174. Boonstra, A.H., L.J.G. Van, and W.C.P.M. Meerman, *Method of manufacturing a monolithic silica aerogel*, 1990, Google Patents.
175. Teich, F., et al., *Process for drying microporous particles used in production of thermal insulating materials*, 1999, Google Patents.
176. Dolhaine, H.D. and I.D. Wolf-Leistikow, *Verfahren zur herstellung von SiO_2 (pfeil abwärts) $_2$ (pfeil abwärts)-aerogelen (i)*, 1991, Google Patents.
177. Mendenhall, R.S., et al., *Process whereby organic solvent in which gel is immersed is directly extracted supercritically without exchanging with low temperature solvent prior to extraction of pore fluid*, 2000, Google Patents.
178. Mendenhall, R.S., et al., *The organic liquid solvent which has completely filled the pores of the gel, is extracted under supercritical conditions, without the need to first exchange said organic liquid solvent with an alternate liquid*, 2000, Google Patents.
179. Boara, G., F. Costa, and A. RÜCKEMANN, *Process for the production of monoliths by means of the sol-gel process*, 2007, Google Patents.
180. Ryu, J., *Flexible aerogel superinsulation and its manufacture*, 2000, Google Patents.
181. Lee, K., *Enhancement of fluid replacement in porous media through pressure modulation*, 2004, Google Patents.
182. Ou, D., et al., *Methods for manufacture of aerogels*, 2006, Google Patents.
183. Stepanian, C.J., G.L. Gould, and R. Begag, *Method of Manufacturing of Aerogel Composites*, 2009, Google Patents.
184. Coronado, P.R., et al., *Method for rapidly producing microporous and mesoporous materials*, 1997, Google Patents.
185. Gauthier, B.M., et al., *Simultaneously heating and applying restraining force to sealed vessel via hot press plates then controllably releasing; minimizing*

- venting; embedded chemical sensing agents; fast, simple, easily automated, industrial scale, 2008, Google Patents.
186. Lee, K.P., R. Begag, and Z. Altiparmakov, *Rapid aerogel production process*, 2003, Google Patents.
 187. Kang, P.L., *Remplacement ameliore des fluides dans des milieux poreux par modulation de pression*, 2002, Google Patents.
 188. Woignier, T., G. Scherer, and A. Alaoui, *Stress in aerogel during depressurization of autoclave: II. Silica gels*. *Journal of Sol-Gel Science and Technology*, 1994. **3**(2): p. 141-150.
 189. Poco, J.F., et al., *A rapid supercritical extraction process for the production of silica aerogels* 1996. Medium: ED; Size: 6 p.
 190. Scherer, G.W., et al., *Optimization of the rapid supercritical extraction process for aerogels*. *Journal of Non-Crystalline Solids*, 2002. **311**(3): p. 259-272.
 191. Gauthier, B.M., et al., *A fast supercritical extraction technique for aerogel fabrication*. *Journal of Non-Crystalline Solids*, 2004. **350**(0): p. 238-243.
 192. Roth, T.B., A.M. Anderson, and M.K. Carroll, *Analysis of a rapid supercritical extraction aerogel fabrication process: Prediction of thermodynamic conditions during processing*. *Journal of Non-Crystalline Solids*, 2008. **354**(31): p. 3685-3693.
 193. Anderson, A.M., C.W. Wattlely, and M.K. Carroll, *Silica aerogels prepared via rapid supercritical extraction: Effect of process variables on aerogel properties*. *Journal of Non-Crystalline Solids*, 2009. **355**(2): p. 101-108.
 194. Bono, M., Jr., A. Anderson, and M. Carroll, *Alumina aerogels prepared via rapid supercritical extraction*. *Journal of Sol-Gel Science and Technology*, 2010. **53**(2): p. 216-226.
 195. Mukhopadhyay, M. and B.S. Rao, *Modeling of supercritical drying of ethanol-soaked silica aerogels with carbon dioxide*. *Journal of Chemical Technology & Biotechnology*, 2008. **83**(8): p. 1101-1109.
 196. Sanz-Moral, L.M., et al., *View cell investigation of silica aerogels during supercritical drying: Analysis of size variation and mass transfer mechanisms*. *The Journal of Supercritical Fluids*, 2014. **92**(0): p. 24-30.
 197. Melnichenko, Y.B., et al., *Adsorption of supercritical CO₂ in aerogels as studied by small-angle neutron scattering and neutron transmission techniques*. *The Journal of Chemical Physics*, 2006. **124**(20): p. -.
 198. Saugey, A., et al., *Diffusion in pores and its dependence on boundary conditions*. *Journal of Physics: Condensed Matter*, 2005. **17**(49): p. S4075.
 199. Griffin, J.S., et al., *Continuous extraction rate measurements during supercritical CO₂ drying of silica alcogel*. *The Journal of Supercritical Fluids*, 2014. **94**(0): p. 38-47.
 200. Ma, H.-S., et al., *Computer simulation of mechanical structure–property relationship of aerogels*. *Journal of Non-Crystalline Solids*, 2001. **285**(1–3): p. 216-221.
 201. Ma, H.-S., et al., *Mechanical structure–property relationship of aerogels*. *Journal of Non-Crystalline Solids*, 2000. **277**(2–3): p. 127-141.
 202. Schenker, I., et al., *Generation of porous particle structures using the void expansion method*. *Granular Matter*, 2009. **11**(3): p. 201-208.
 203. Czakkel, O., et al., *In situ SAXS investigation of structural changes in soft resorcinol–formaldehyde polymer gels during CO₂-drying*. *The Journal of Supercritical Fluids*, 2013. **75**(0): p. 112-119.

204. Gönen, M., D. Balköse, and S. Ülkü, *Supercritical ethanol drying of zinc borates of $2\text{ZnO}\cdot 3\text{B}_2\text{O}_3\cdot 3\text{H}_2\text{O}$ and $\text{ZnO}\cdot \text{B}_2\text{O}_3\cdot 2\text{H}_2\text{O}$* . The Journal of Supercritical Fluids, 2011. **59**(0): p. 43-52.
205. Ismail, A.A. and I.A. Ibrahim, *Impact of supercritical drying and heat treatment on physical properties of titania/silica aerogel monolithic and its applications*. Applied Catalysis A: General, 2008. **346**(1–2): p. 200-205.
206. Liang, C., G. Sha, and S. Guo, *Resorcinol–formaldehyde aerogels prepared by supercritical acetone drying*. Journal of Non-Crystalline Solids, 2000. **271**(1–2): p. 167-170.
207. Szczurek, A., et al., *Porosity of resorcinol-formaldehyde organic and carbon aerogels exchanged and dried with supercritical organic solvents*. Materials Chemistry and Physics, 2011. **129**(3): p. 1221-1232.
208. Czakkel, O., et al., *Drying of resorcinol–formaldehyde gels with CO_2 medium*. Microporous and Mesoporous Materials, 2012. **148**(1): p. 34-42.
209. Amaral-Labat, G., et al., *Impact of depressurizing rate on the porosity of aerogels*. Microporous and Mesoporous Materials, 2012. **152**(0): p. 240-245.
210. Estella, J., et al., *Effect of supercritical drying conditions in ethanol on the structural and textural properties of silica aerogels*. Journal of Porous Materials, 2008. **15**(6): p. 705-713.
211. Liu, N., et al., *Carbon aerogel spheres prepared via alcohol supercritical drying*. Carbon, 2006. **44**(12): p. 2430-2436.
212. Lermontov, S., et al., *Hexafluoroisopropyl alcohol as a new solvent for aerogels preparation*. The Journal of Supercritical Fluids, 2014. **89**(0): p. 28-32.
213. Lermontov, S.A., et al., *Diethyl and methyl-tert-butyl ethers as new solvents for aerogels preparation*. Materials Letters, 2014. **116**(0): p. 116-119.
214. Fu, R., et al., *The Fabrication and Characterization of Carbon Aerogels by Gelation and Supercritical Drying in Isopropanol*. Advanced Functional Materials, 2003. **13**(7): p. 558-562.
215. Moner-Girona, M., et al., *Sol-Gel Route to Direct Formation of Silica Aerogel Microparticles Using Supercritical Solvents*. Journal of Sol-Gel Science and Technology, 2003. **26**(1-3): p. 645-649.
216. Brown, Z.K., et al., *Drying of agar gels using supercritical carbon dioxide*. The Journal of Supercritical Fluids, 2010. **54**(1): p. 89-95.
217. Cooper, A.I. and A.B. Holmes, *Synthesis of Molded Monolithic Porous Polymers Using Supercritical Carbon Dioxide as the Porogenic Solvent*. Advanced Materials, 1999. **11**(15): p. 1270-1274.
218. Cooper, A.I., C.D. Wood, and A.B. Holmes, *Synthesis of Well-Defined Macroporous Polymer Monoliths by Sol–Gel Polymerization in Supercritical CO_2* . Industrial & Engineering Chemistry Research, 2000. **39**(12): p. 4741-4744.
219. Sui, R., A.S. Rizkalla, and P.A. Charpentier, *Direct Synthesis of Zirconia Aerogel Nanoarchitecture in Supercritical CO_2* . Langmuir, 2006. **22**(9): p. 4390-4396.
220. Sui, R., A.S. Rizkalla, and P.A. Charpentier, *Synthesis and Formation of Silica Aerogel Particles By a Novel Sol–Gel Route in Supercritical Carbon Dioxide*. The Journal of Physical Chemistry B, 2004. **108**(32): p. 11886-11892.
221. Smirnova, I. and W. Arlt, *Synthesis of Silica Aerogels: Influence of the Supercritical CO_2 on the Sol-Gel Process*. Journal of Sol-Gel Science and Technology, 2003. **28**(2): p. 175-184.

222. Montes, A., et al., *Silica microparticles precipitation by two processes using supercritical fluids*. The Journal of Supercritical Fluids, 2013. **75**(0): p. 88-93.
223. Kartal, A.M. and C. Erkey, *Surface modification of silica aerogels by hexamethyldisilazane-carbon dioxide mixtures and their phase behavior*. The Journal of Supercritical Fluids, 2010. **53**(1-3): p. 115-120.
224. Sanli, D. and C. Erkey, *Demixing pressures of hydroxy-terminated poly(dimethylsiloxane)-carbon dioxide binary mixtures at 313.2 K, 323.2 K and 333.2 K*. The Journal of Supercritical Fluids, 2014. **92**(0): p. 264-271.
225. Sanz-Moral, L.M., et al., *Gradual hydrophobic surface functionalization of dry silica aerogels by reaction with silane precursors dissolved in supercritical carbon dioxide*. The Journal of Supercritical Fluids, 2013. **84**(0): p. 74-79.
226. Shin, Y., et al., *Supercritical processing of functionalized size selective microporous materials*. Microporous and Mesoporous Materials, 2000. **37**(1-2): p. 49-56.
227. Purcar, V., et al., *Surface modification of silica particles assisted by CO₂*. The Journal of Supercritical Fluids, 2014. **87**(0): p. 34-39.
228. Machida, H., M. Takesue, and R.L. Smith Jr, *Green chemical processes with supercritical fluids: Properties, materials, separations and energy*. The Journal of Supercritical Fluids, 2011. **60**(0): p. 2-15.

Chapter 2

LOW TEMPERATURE SUPERCRITICAL DRYING. COMPREHENSIVE STUDY OF PROCESS MECHANISMS AND PRODUCTS

2.1. INTRODUCTION

An extensive description of existing procedures and state-of-the-art on the technology to transform sol-gel materials into dried porous matters was described in *Chapter 1*. The main conclusion is the fact that higher properties from the same original gel are obtained from supercritical drying process, so called Aerogel. However, it has been reported that the scale up manufacturing is more convenient by APD, even if some properties of the final product are compromised. Since many years, different approaches have been followed in order to obtain a material with a wide range of different properties but always aiming at achieving a low OPEX. A cost balance compromising the final properties has been the only method to achieve de cost reduction, selecting therefore xerogel materials route. The LTSCD process was then selected only for the study and development of very specific materials in which the production cost is not an important parameter. The author considers that the failure to wrongly establish a high OPEX in LTSCD is directly derived from a misuse of supercritical technology and an incorrect scaling. Even being higher CAPEX than the other drying solutions, it is known that scaling up LTSCD leads to a strong reduction of OPEX.

For all those facts concluded in *Chapter 1*, and with the aim of producing aerogels with the highest quality possible, the author desired to investigate the development of an optimized LTSCD processes to reduce cost without compromising the quality of material or form. The present study was in the framework of four European founded projects for the development of aerogel based products. Diverse gels were produced for the different applications targeted although the drying step remained similar for all the cases of study. Functionalization was also required in all the silica-base cases due to the hydrophilic nature of the aerogel backbone.

2.2. EXPERIMENTAL METHODS

2.2.1. REAGENTS

Different silica precursors were used in the present study considered each one to a different European project FP7 and/or internal research:

Pre-hydrolyzed Tetraethyl Orthosilicate (P75E20 – 20% Silica content) was provided by PCAS (FR). Tetraethyl Orthosilicate – TEOS- (98% Purity) was purchased from Sigma-Aldrich (FR) or provided by Evonik Industries AG (GE). Aqueous Sodium Silicate (Waterglass) solution (30 % Silica content) was purchased from Sigma-Aldrich (GE). Modified TEOS, so-called TEOS58 (58% Silica content), for the HIPIN synthesis was provided by Thomas Swan (UK). Technical Ethanol (99.8 % Purity) and 2-Propanol (99.8% Purity) was purchased from SolvEst (FR). Aqueous NH_4OH (28.0 – 30.0 % Purity) and Amberlite IR120 resin were purchased from Sigma-Aldrich (FR). Hexamethyldisiloxane – HMDS – (>98% Purity) was purchased from Acros Organics (BE). Self-deionized water was used in all experiments.

Cryogenic CO_2 (>98% Purity) was provided in the general tank by Air Liquide (FR).

All chemical were used as delivered, no further modification were applied.

2.2.2. SYNTHESIS

Sol-gel synthesis is the formation of an oxide network by the polycondensation reaction of a sequence of molecular colloids solution (so called “precursor”) in a liquid. The consecutive agglomeration of colloidal particles will built a three dimensional continuous network so called “gel”. Generally, the sol particles interact through van der Waals forces or hydrogen bonds.

Most of the sol-gels developed for aerogel production are based on alkoxy-silanes of the type $\text{R}_n\text{SiX}(4-n)$, where the X functional group is involved in the reaction with the inorganic substrate. X is a hydrolysable group, typically, alkoxy, acyloxy, amine or chlorine. The most common used alkoxy groups are methoxy (TMOS) and ethoxy (TEOS) due to the production of methanol and ethanol as byproduct during the reaction respectively. R is a non-hydrolyzable organic radical that possesses a functionality which enables the coupling agent to bond with organic resins and polymers.

The silanes are subjected to hydrolysis to activate the surface to form a silanol group. The silanol groups can consequently condense with other groups to form siloxane linkages (Figure 2.1). The hydrolyzing agent is water which is added to the precursor and solvent mixture.

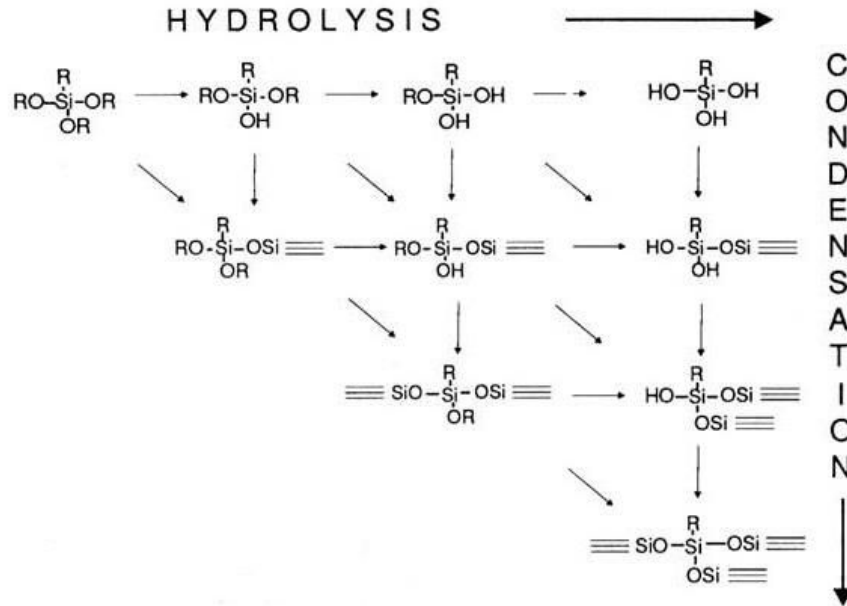


Figure 2.1. Hydrolyzation and condensation of alkoxy silanes [1].

Hydrolysis can be performed under different pH solutions. The rate of acid hydrolysis is significantly greater than the base hydrolysis and is related to their steric bulk: $\text{CH}_3\text{O} > \text{C}_2\text{H}_5\text{O} > t\text{-C}_4\text{H}_9\text{O}$. Thus, a methoxysilane hydrolyzes at 6 – 10 times the rate of an ethoxysilane. Condensation of agglomerated groups to create the three dimensional network is dynamic and may it steered in different direction by adjusting parameters. The electron density on Si element will influence the reaction rate: $\text{Si-R} > \text{Si-OR} > \text{Si-OH} > \text{Si-O-Si}$. Low pH reactions demand high electron density, forming more straight chains as consequence; accordingly, high pH reactions require low electron density, triggering more branched networks, Figure 2.2. The role of the pH in the kinetics of the reaction is also notable due to its strong dependence on the hydrolysis and condensation rates.

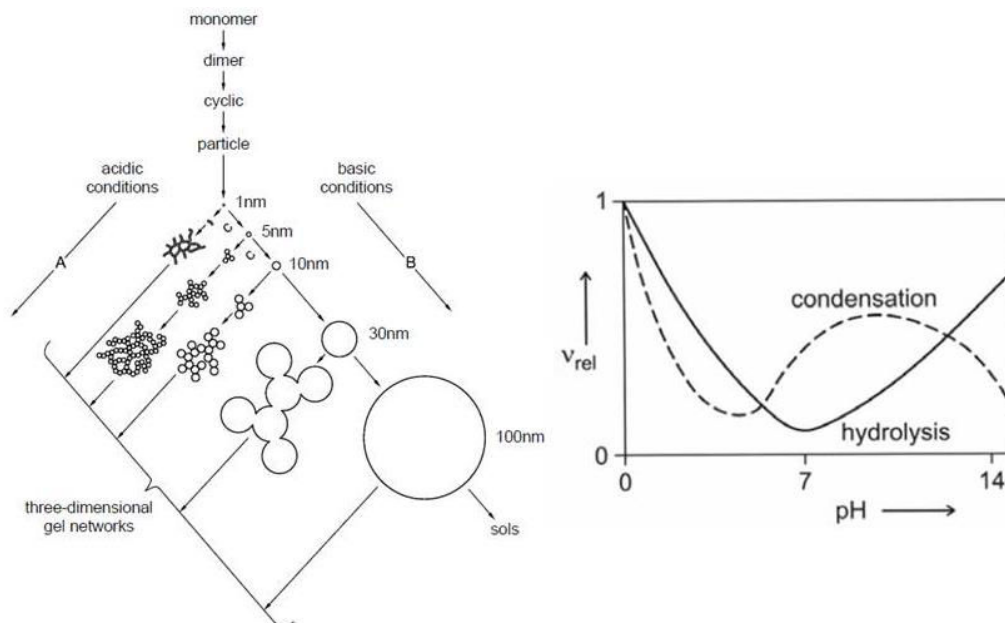


Figure 2.2. $\text{Si}(\text{OR})_4$ particle and chain formation at different pH (left), dependence of relative rates of hydrolysis and condensation reactions on pH (right).

The sol-gel reaction is performed during the mix of the silica precursor with solvent, hydrolyzer agent and catalysts. This operation can be done by mixing all compounds at the same time or by mixing several solutions separately and putting them together in a second stage. The first one is called 1-step synthesis while the second, 2-step synthesis.

2.2.3. AGING

Once the gel is formed, a large number of sol particles and clusters have not yet reacted. Aging step is the generally applied in order to ensure the complete reaction of the network. During aging, the structure may change considerably depending on time, pH, solvent mixture and temperature. Practically, and for the present study, it consists on an overnight maceration of the gel in a solution based on the same composition of solvent, hydrolyzer agent and catalyst as the original synthesis. This step will allow to finalizing the overall internal connections to provide strength to the gel [2]. A final step is the washing of reaction exceed and impurities that could remain within the pores.

2.2.4. WASHING

Washing step is performed equally to every synthesis after aging. The samples are immersed in pure ethanol solution to dilute existing non-reacted compounds and impurities from the porous network. Most of these impurities are catalyst (i.e. NH_4OH) and water. This step is very important due to the poor solubility of water in supercritical CO_2 under working conditions (<2vol. %). Therefore the existence of aqueous solutions during the LTSCD will lead in the collapse of the aerogel samples. Cracking of the sample caused by water content has a specific

pattern which was defined by Bisson et al .[3]. Solvent exchange is performed during 3 days with 2 exchanges per day at lab scale.

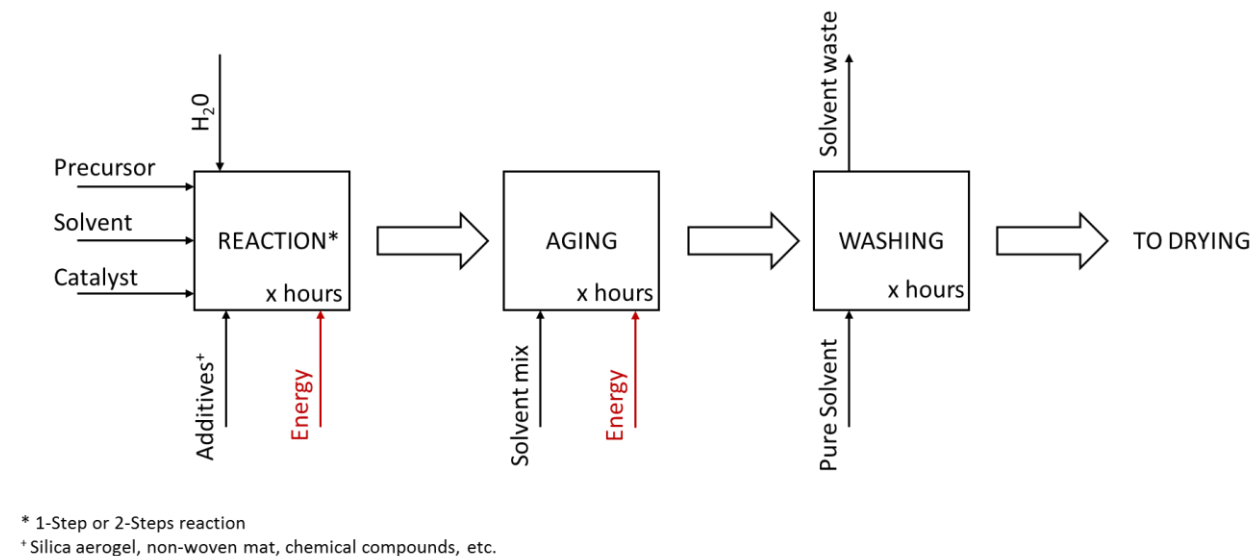


Figure 2.3. Synthesis steps diagram.

Several recipes based on silica were performed during the work to accomplish the objectives defined for each application or project.

2.3. EQUIPMENT

The high pressure equipment used for the drying of aerogel-based materials at lab-scale by the LTSCD process was specifically made for the present study and was composed by the following systems:

- Liquid CO₂ pump system: a condenser and a high pressure piston pump (Flow: 6 kg/h)
- Pre-treatment system: a heated line for supercritical drying and a non-heated line for liquid state drying. Both lines possess a damper volume to avoid excessive pulsation in the drying vessel.
- Co-solvent injection system: a solvent tank and a high pressure piston pump (Interchim LabAlliance).
- Drying vessel: a high pressure vessel (Vol.: 2 litre, P_{max}: 700 bar, T_{max}: 150 °C) with an electrical jacket and 2 sapphire windows.
- Pressure regulation system: a Back Pressure Regulator (TESCOM) and an electrical heating device.
- Separator system: a cyclonic separator (Vol.: 200 mL) with heating system.

Equipment is supplied with a recycle line to reduce the CO₂ consumption. Versatility of the equipment configuration was highly required in order to try different procedures.

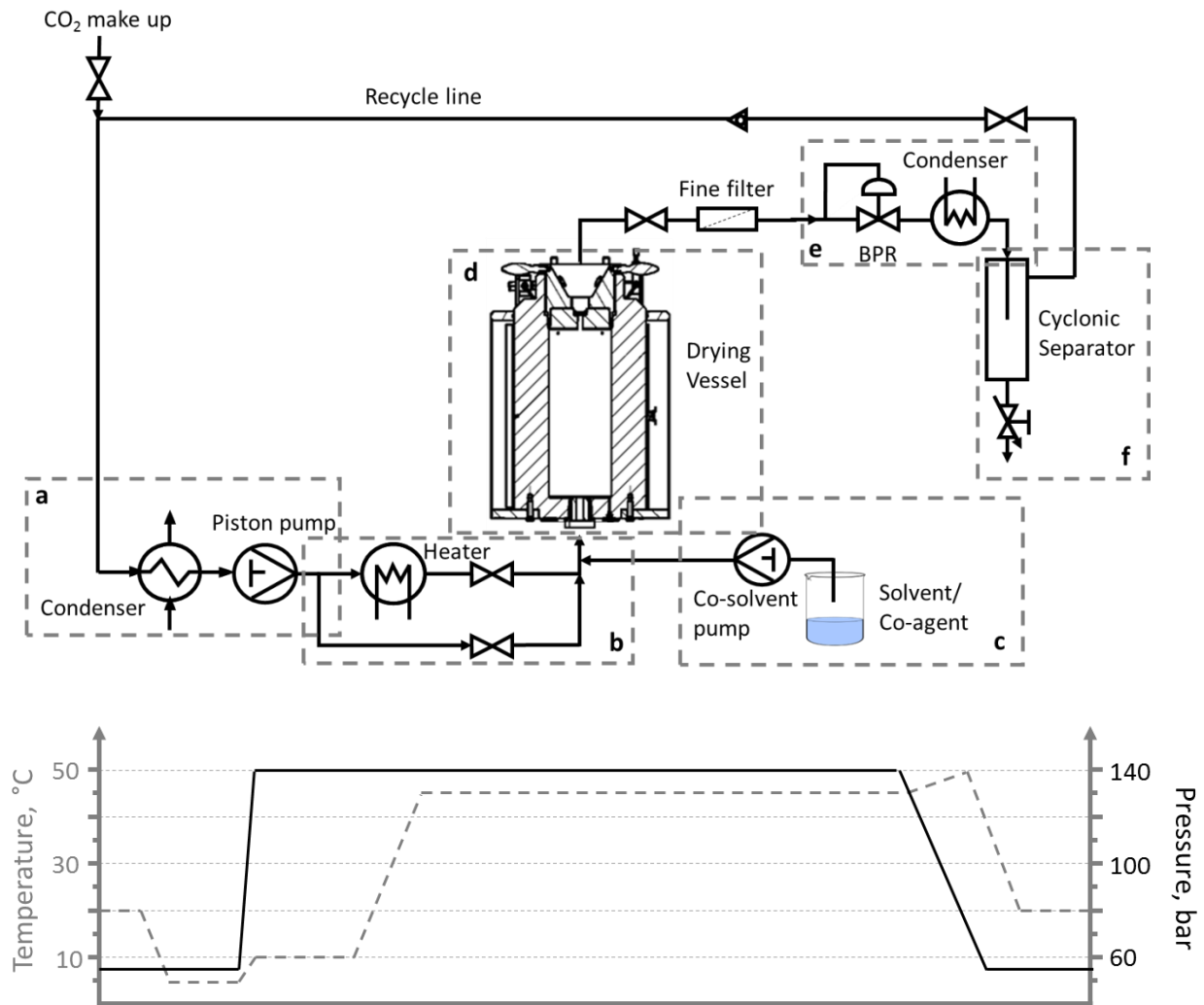


Figure 2.4. Flow sheet of lab-scale aerogel dried by LTSCD process with CO₂
Pressure/Temperature profile.

As showed in Figure 2.4, the equipment allows to receive the CO₂ from the general system in gas form (50-60 bar, 20 °C) and is liquefied at isobaric conditions (50-60 bar, 5 °C). Liquid CO₂ is pressurized and inserted in the vessel through the heater to working conditions (130 bar, 45 °C) or directly kept at liquid state. Then CO₂ is depressurized at controlled temperature conditions to separate the solubilized compound by phase separation. Gasified CO₂ is recycled while liquid extract is purged from the cyclonic separator.

Total energy demand for the CO₂ cycle is below 550 kJ per kg of CO₂. At lab-scale, the average energy consumption is up to 15 kWh which are neglected for research purposes.



Figure 2.5. Appearance of tailored lab-scale equipment.

2.4. LOW TEMPERATURE SUPERCRITICAL DRYING. DRYING MECHANISIMS

After the synthesis stage and the consecutive aging and washing, samples are ready to be dried. This step is performed in batch mode in a high pressure equipment.

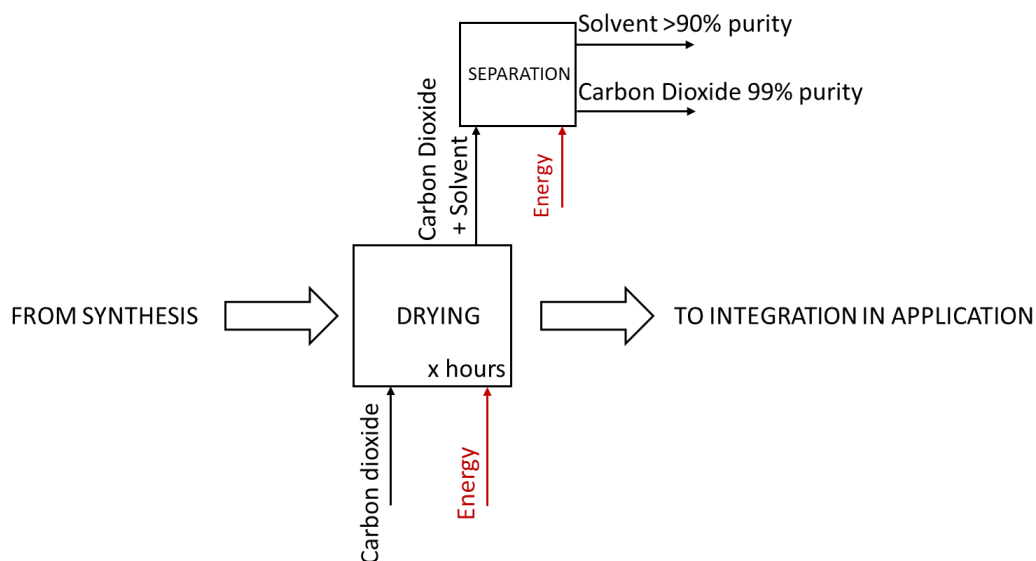


Figure 2.6. Drying process diagram.

As described in *Chapter 1*, the drying of sol-gels by supercritical drying provides the finest quality materials in terms of nanostructure. The fact of working with carbon dioxide in supercritical state involves numerous optimizations and very precise control conditions, since minimal changes in the process can cause large fluctuations in the properties of both the fluid and solvent which impacts on the final properties of the material. The temperature and pressure being the main operating parameters, viscosity and solubility are accordingly defined.

In LTSCD process, the organic solvent solubility in the carbon dioxide is critical since the viability of the extraction as well as the processing time is directly related. This parameter being high, LTSCD is regarded as an extraction process not limited by the extract solubility in the fluid, but by the solvent diffusion through the extract matrix and the confined liquid [4].

The mass transfer mechanisms governing the aerogel material drying have been described by Garcia et al. [5] and correspond to two stages involving different process. The first stage starts when the sample soaked with organic solvent get in contact with the supercritical CO₂. Organic solvent and CO₂ will engage in one single phase mixture along the sample. This mechanism is control by solubility and convection. Expansion of mixture will occurs, but crack will not take place if pressurization is down slowly [6]. In the second stage, the supercritical fluid mixture composed of organic solvent and CO₂ starts to get diluted in organic solvent by the diffusion to the exterior. This stage is controlled by an effective diffusion coefficient defined by the porosity of the material and the diffusion of the organic solvent on the CO₂ under working conditions.

Therefore it can be defined the aerogel drying as a process which implies two different stages of the extraction at supercritical state: convection-controlled and diffusion-controlled drying.

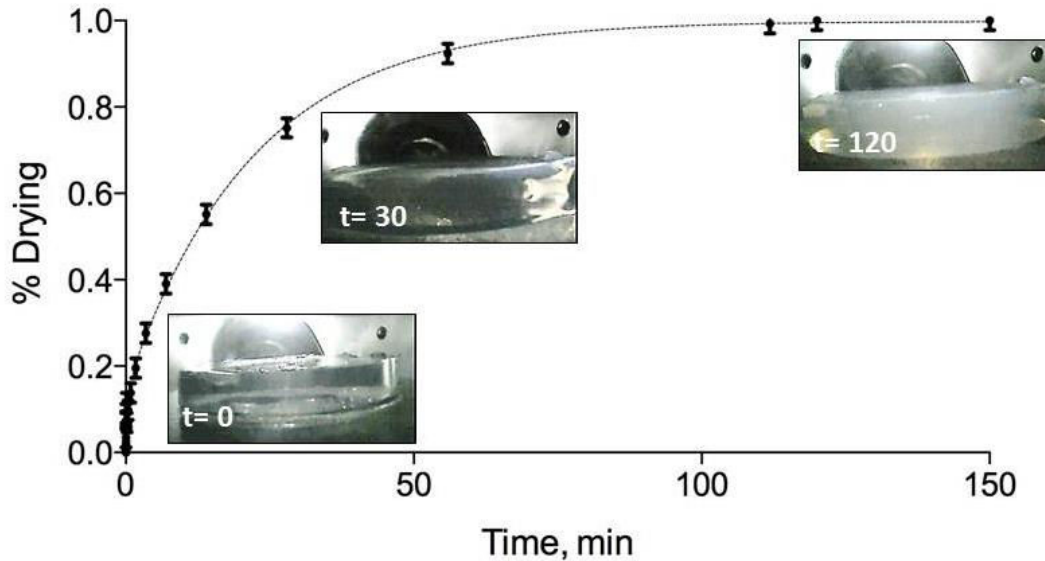


Figure 2.7. Standard drying curve for 10-mm thickness P75E20 sample with the image at each stage of the drying. Curve fixed from Fick's second Law with laboratory data.

In the first stage of the process (convection), carbon dioxide penetrates the porous matrix rapidly to solubilize the organic solvent, in this case ethanol. Once that the whole mixture becomes one phase, the second stage control the process (diffusion) by diluting the interior of the sample of organic solvent and increasing the concentration of carbon dioxide. This diffusion is highly dependent on the nature of the organic solvent and operating conditions. Effective drying ends when the dilution within the vessel achieves a level where the remaining solvent below the critical minimum that avoids the re-condensation of the solvent in the depressurization step.

Published studies determine the effective diffusion by the control of the organic solvent carried by CO₂ outlet of the vessel together with the measurement of the remaining solvent in the sample over time. Organic solvent at the outlet can be measured by volumetric methods or more accurately by refraction index or as chromatography. Remaining solvent is measured by the

weight difference of the sample after inducing evaporation. Those methods provide reliable information which can be easily used for the mathematical simulation of the drying mechanisms (Figure 2.7). However, the evolution of concentration profiles and mass transport inside the sample cannot be determined with by such methods, even if visualization of the sample during the process is available.

2.4.1. RAMAN SPECTROSCOPY METHOD

In order to directly quantify the mass transfer mechanisms occurring within the porous structure of the gel, the one-dimensional Raman Spectroscopy technique was applied. This method has been already applied to derive the diffusion coefficients from measured compositions profiles of miscible liquids at ambient conditions [7, 8]. In collaboration with Erlangen Graduate School in Advanced Optical Technologies (SAOT) in Germany, the study of P75E20 based aerogels was performed.

The one-dimensional Raman technique consists on different measurements locations of the Raman spectra aligned along one imaginary line placed inside the gel. Consequently, the whole image of compositions during time can be recorded at different levels within the gel. By means of the state equation, the measured composition can be transformed on concentration profiles, which allows a more detailed study of mass transport mechanisms during the LTSCD. It must be outlined that this procedure can only be applied to those aerogels whose solid network does not provide a Raman signal.

In Figure 2.8 a sketch of the experimental setup for the Raman analysis is described. The aerogel probe is place on the High Pressure Chamber (HPC) designed for single sample measurement. The system counts with a high pressure pump (SP), pressure and temperature regulator and a Back Pressure Regulator (BPR). The Raman Spectroscopy system consists in a laser beam, aperture (A), mirror (M), focusing lens (L) and the beam dump (BD). The detection part consists of achromatic lenses (AC1 and AC2), dichoric mirror (DM), long pass filter (LP), polarization analyzer (PA), spectrometer, and charge-coupled device (CCD) detectors.

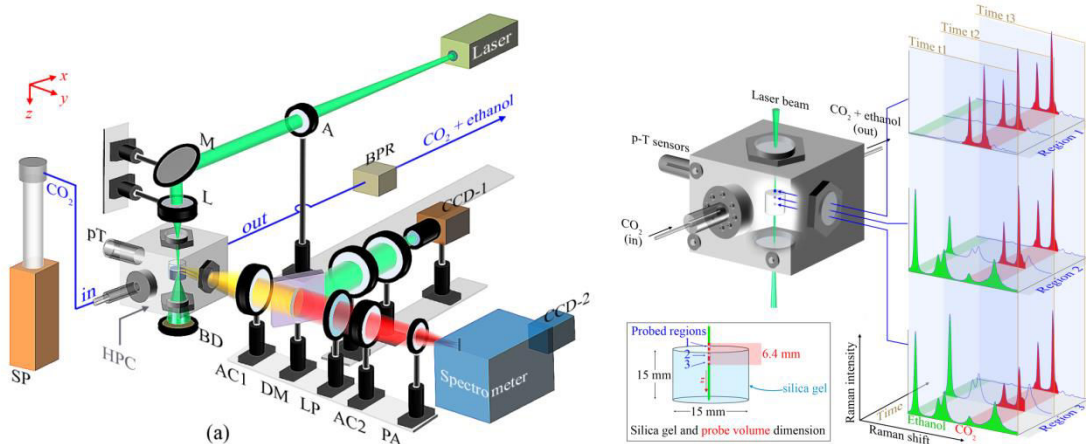


Figure 2.8. Raman measurement display and example of three measurements from the sample (SAOT).

Measurements were carried out in a long distance of 6.4 mm, being 0.64 mm out of the gel and 5.76 mm inside the gel. The diameter of the sample was 15 mm, therefore it was assumed that the mass transport path measured is not in the radial direction but perpendicular to the length.

2.4.2. RESULTS

The present study will be performed in different steps. Those steps will be disclosed but not discussed in the present document since the main work was performed by the SAOT team.

In order to quantify the mass transport mechanisms within the gel, the evolution of concentration must be determined. Raman Spectroscopy does not directly measure the concentration but the composition, which is proportional to the ratio of existing substances. Conversion to concentration values was performed through a modified version of the Soave-Redlich-Kwong (SRK) equation of state. The equation was also fitted to the obtained values according to the literature. As a result, Figure 2.9 shows the concentration of the mixture and single elements computed as a function of the CO₂ molar fraction. Due to the non-ideal mixing behavior of ethanol and CO₂, density of the mixtures of both components can exceed those of the pure elements.

It is noticeable that the changes on concentration depend on CO₂ mole fraction. Three regimes are differentiated concerning the variations speed. It is shown that ethanol concentration decreases during the whole process while the concentration of CO₂ increases first and then decrease until the gel is completely filled with the gas. We can conclude that in the regime 1 the mass transfer of CO₂ to the interior of the gel is faster than the mass transfer of organic solvent to the exterior. In the regime 2, the concentration of CO₂ reaches a maximum but the ratio of mass transport is considerably lower than before. CO₂ keeps entering the sample at a ratio lowered than the ethanol that it is going out. In the regime 3, the concentration of CO₂ and ethanol decreases. Both compounds leave the sample in the same direction.

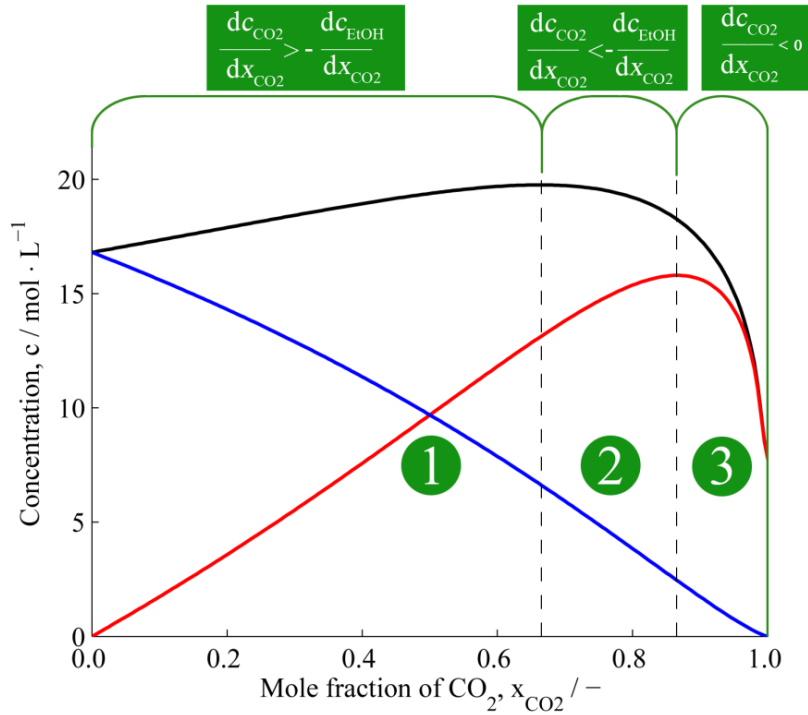


Figure 2.9. Concentration of CO₂ (red), ethanol (blue) and mixture (black) as function of the CO₂ molar fraction (SAOT).

Three regimens can be considered for the different drying mechanisms encountered in the aerogel.

Effective binary diffusion can be calculated from the results by fitting the data corresponding to evolution of concentration in points inside the sample (to avoid the values of convective mass transport regime) to the experimentally measured evolutions. Second Fick's law was then used for the computation of concentration profiles:

$$\frac{\partial c_i^*(z^*, t)}{\partial t} = D_{ij} \frac{\partial^2 c_i^*(z^*, t)}{\partial z^{*2}} \quad 2.1$$

D_{ij} is the adjusting parameters. As it was showed in Figure 2.9, during the drying process neither the quantity of ethanol or CO₂ remains constant. Therefore to keep one quantity as reference system constant, the method described by Crank [9].

The resulting best fitted effective binary diffusion value obtained were $D_{CO_2/EtOH} = 4.684 \times 10^{-9} \text{ m}^2 \cdot \text{s}^{-1}$. Those values will be used for the scaling up simulations in Chapter 3.

Present study represent the first reported *in situ* measurement of the of the diffusion mechanisms of the solvent within the aerogel sample. This tool has a great potential to further understand the details of the drying to improve the scaling up of the process towards an optimized industrialization. Further development will be performed in collaboration with SAOT in order to define more accurately the mass transfer mechanisms for different materials (porosity) and conditions.

2.5. AEROGEL FUNCTIONALIZATION. HYDROPHOBIZATION

Silica-based aerogels are produced from silicon alkoxides or alkylsilicas of $\text{Si}(\text{OR})_4$ type, in which R and OR designate alkyl and alkoxide groups, respectively. The methyl group and ethyl group are often used in alkoxide groups, termed tetramethoxysilane (TMOS) and tetraethoxysilane (TEOS) respectively. By nature, the silica backbone contains hydroxyl radical groups that highly react with water or moisture (Figure 2.10a), degrading then the properties or even collapsing the structure. For that reason, for plenty applications of aerogels, the material needs to be treated in order to provide hydrophobicity properties.

The state-of-the-art of hydrophobization process for sol-gel, and sub-consequence xerogel or aerogel materials concern a wide range of chemical modifications in different solutions. The reaction consists of the interchange of the hydroxyl radical group of the surface of the aerogel backbone by a hydrolytically stable -R groups that will not form hydroxyl bounds with water. The compounds suitable as -R radical are usually alkoxysilanes as hexamethyldisilazane -HMDZ-, hexamethyldisiloxane -HMDS-, trimethylchlorosilane -TMCS- or similar.

Reaction is performed in the sol-gel under a mixture of solvent with the alkoxysilane compound in acidic conditions. The volume ratio of the alkoxysilane in the mixture can be up to 15%vol. and the temperature over 50 °C. The silylation reaction will take place through 24 h. (overnight).

Once that the reaction is over, excess of reactant are washed out by fluxing clean solvent until the internal porous contain no trace of reactant. Such process can last several hours up to 36h. Resulting gel can then be dried by evaporative drying to obtain hydrophobic xerogel, or by supercritical drying to obtain an aerogel.

This method allows producing materials with a high level of hydrophobicity in the whole silica structure. However, some disadvantages are related to this limited method:

- Hydrophobization is performed at its maximal capacity, obtaining super-hydrophobic materials whose application can be limited or restricted.
- Transparency is highly degraded by this method. Silica aerogel can be tailored to obtain very low refraction index (down to 1.005), but once that hydrophobization is required, transparency will be comprised.
- Silylation reaction solvent is a very corrosive and hazardous mixture for its use in large quantities.
- Alkoxysilane compound must be used up to 15%vol. to perform the reaction [10].
- In applications like building construction, product hydrophobized by this method does not achieve the grade of fire resistance required for the certifications.
- Life Cycle Assessment (LCA) of products treated with this method does not achieve the minimum CO_2 footprint defined for applications as building insulation [11].

This process is mandatory for ambient drying, but for supercritical drying those disadvantages become issues when the hydrophobic aerogel is required with the same characteristics as the raw hydrophilic one.

For that reason, a process to functionalize aerogel in order to provide hydrophobic properties without compromising any properties from those defined by the raw hydrophilic aerogel is required.

Also, the application of this process on cellulose-containing silica gel composites, however, has proven to be difficult as cellulose degrades on contact with HCl. Therefore, an alternative hydrophobization process applicable on silica gels and cellulose has to be searched for. Silica gels, as well as cellulose, have previously been hydrophobized with hexamethyldisiloxane HMDS.

2.5.1. REACTION

The present study aims to provide an alternative method to control the functionalization of the aerogel materials without adding further steps in the manufacture to obtain the same properties as the raw hydrophilic aerogel.

This method is based on the high solubility capacity and acidic conditions of carbon dioxide in supercritical state. Common alkoxy silanes used for the silylation of silica gel are highly soluble in supercritical CO_2 , what provides a great dispersion of compound in the solvent. This advantage together with the fact that supercritical CO_2 is a very acidic solution, the silylation reaction with the $-\text{OH}$ radical of the gel would be very favorable and homogenous in the whole volume of the aerogel. This reaction is performed without the assistant of organic solvent. Depending on alkoxy silane content, the samples can be hydrophobized from moisture resistant to high hydrophobic (contact angle over 120°) as schematized in Figure 2.10. Alkoxy silane used for the present study was hexamethyldisiloxane (HMDS).

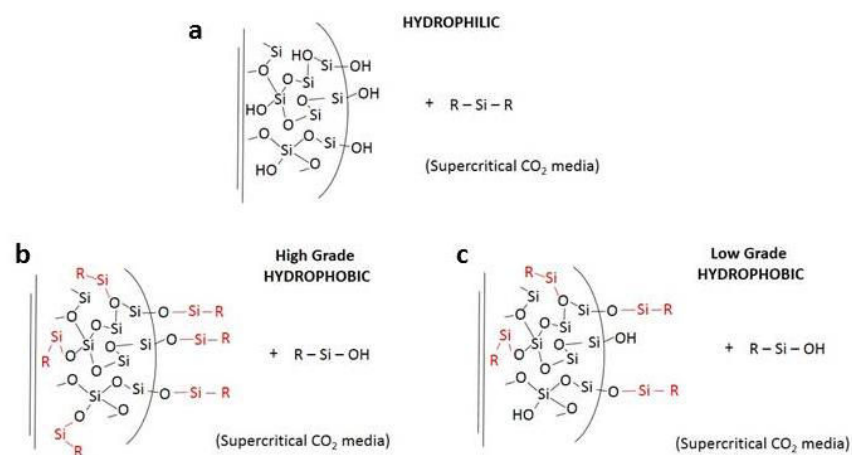


Figure 2.10. Structure reaction of alkoxy silane with the aerogel backbone. a) Hydrophilic backbone, b) super-hydrophobic backbone and c) moisture-resistant backbone.

The process can be performed by two different procedures depending on the quantities of samples to be treated per batch and the thickness.

For the treatment at lab scale of single samples, the hydrophobization method 1 is described:

Silica sol-gel produced from colloidal suspensions of TEOS, P75E20, Waterglass or TEOS58 were synthesized, as prior described, in different casting molds depending on the desired shape, granulated or implemented in a fibrous mat. Once that samples are washed, without further steps, they are immersed in the high-pressure autoclave, which is filled with solvent. Autoclave is closed and exceed of organic solvent purged out by pressurized CO₂ gas, or other inert/water-free gas. Pressure (50-200 bars) and Temperature (20 – 50°C) are raised over supercritical conditions with pressurized CO₂ in liquid or supercritical state. Supercritical CO₂ is then fluxed through the vessel in order to replace the organic solvent within the sol-gel/aerogel. Required time depends on thickness and quantity of the samples. When organic solvent remaining inside the sample is below the estimated value for the reaction, alkoxy silane compound is fluxed into the reactor at desired ratio (depending on the grade of hydrophobization, normally up to 3 vol.% HMDSO) and mechanically homogenized by stirred or reflux pump. Vessel is then isolated and reaction occurs in less than 4 hours. Clean CO₂ is pumped into the vessel in supercritical state to wash exceed of alkoxy silane. Vessel is slowly depressurized in rigorous adiabatic conditions and hydrophobic aerogel withdraw. Silylating agent is introduced through the HPLC co-solvent pump.

For the treatment of larger or several samples, the alkoxy silane is added prior the drying. The hydrophobization method 2 is as follows:

Silica sol-gels are synthesized as in method 1 with its respective aging and washing steps. Once the batch of samples is washed, they are introduced in a bath of organic solvent with the alkoxy silane in the rate defined by the hydrophobization rate (normally 3 vol.% HMDS). This batch is kept overnight at room conditions to allow homogenization of mixture within the gels. After this step, samples are inserted in the vessel and dried as standard LTSCD. Hydrophobization method 2 was preferred as standard process due to its less energy and time consuming.

As disclosed in the general FTIR spectra for treated and untreated samples in Figure 2.11, the surface treatment described is able to reduce the hydroxyl radical – OH (intensities of the broad Si – OH band around 950 cm⁻¹). Besides, the treated material shows the picks typical from polymers, and a sharp peak that reveals the presence of Si – CH₃ links around wavelength of 2900 cm⁻¹ and 1000 cm⁻¹. Figure 2.11, manifests the effectiveness of the reaction.

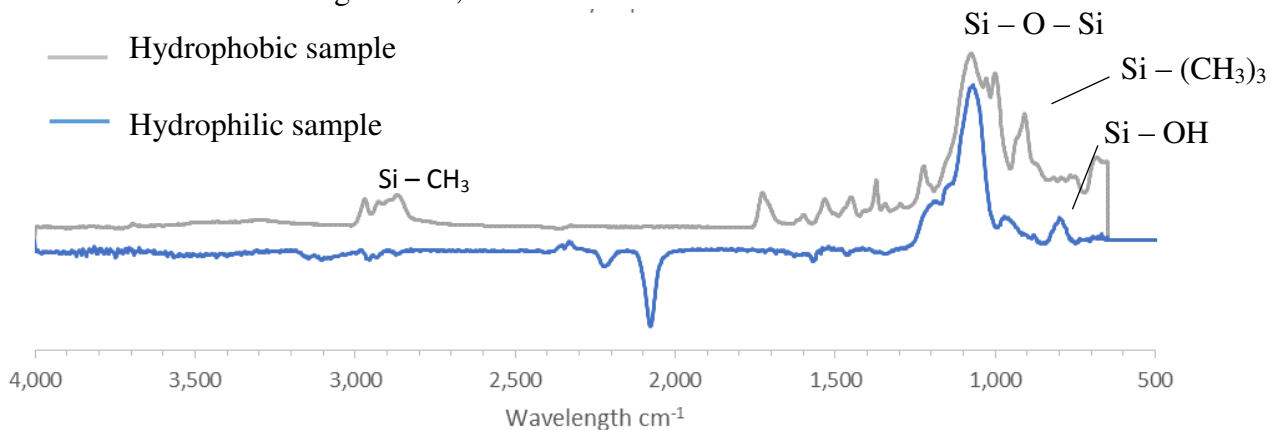


Figure 2.11. FTIR measurements. It is clearly observed that treated sample possess more Si – R groups in the place of Si – OH groups (predominant in untreated sample).

In order to obtain homogeneous hydrophobization within the whole volume of the aerogel but with different range of substitution, different concentration parameter were studied. Figure 2.12, shows the FTIR spectra of samples treated with different concentrations of alkoxy silane HMDS.

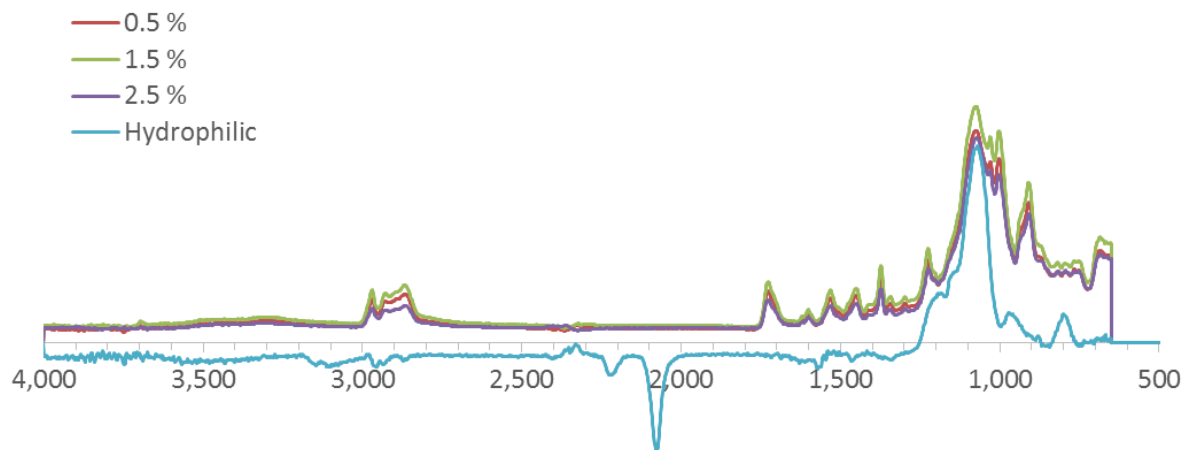


Figure 2.12. FTIR spectra of different concentrations of hydrophobization.

As qualitative measurement, FTIR spectra shows a very similar slope for the three samples with the characteristic peaks at 2900 cm^{-1} and 1000 cm^{-1} and the absence of Si – OH bonding at 950 cm^{-1} corresponding to untreated hydrophilic samples. Reaction is performed similarly with the different concentrations

Else, precipitation of HMDS may occur when 2-phases system is generated in the reactor. This precipitation may damage the sample (if it is produced within the porous) or cover the sample avoiding homogenization and silylation reaction (Figure 2.13). Due to the issues generated by the phase separation within the scaling-up of the process, a study of the ternary diagram of the mixture was performed.

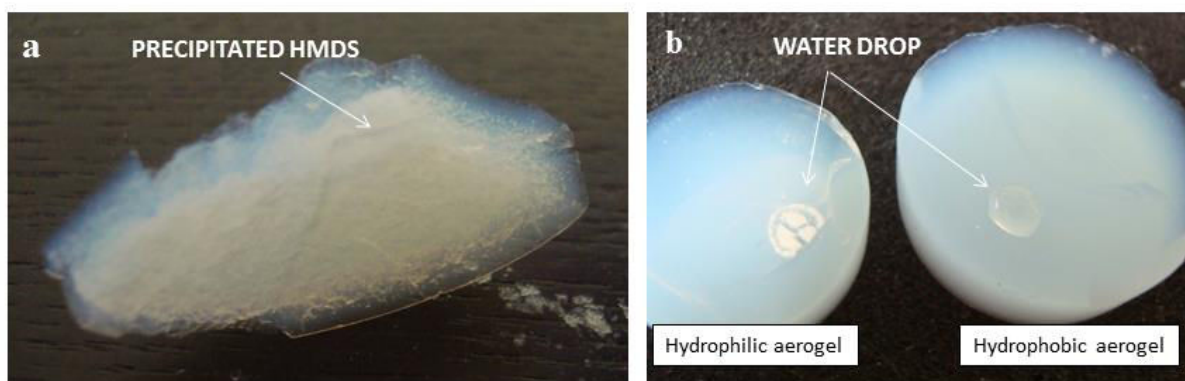


Figure 2.13. a) Precipitation of HMDS inside the sample and b) reaction towards a water droplet for a hydrophilic and an hydrophobic silica aerogel.

Such precipitation can be observed also in the upstream of the process (i.e. filters, separator, etc.) if the content of silylating agent in the reactor is excessive or the mechanical homogenization is inefficient. Risk of blockage of the system is high if the process is not well controlled.

2.5.2. PREDICTION OF PHASE DIAGRAM ON TERNARY SYSTEM

In order to establish the best conditions for the surface modification reaction at supercritical state, a simulation of the phase diagram of the mixture was performed. Due to the lack of phase equilibrium of the mixture HMDS-CO₂-EtOH, a bibliographic study and modeling concerning the thermodynamic behavior of the ternary systems composed of carbon dioxide (CO₂), ethanol and hexamethyldisiloxane has been performed in close collaboration with Coquelet, (CTP of Mines ParisTech). The literature review was done using the NIST Standard Reference Database (2008) and the Simulis Thermodynamic software.

Table 2.1. Physical properties of components (Compilation from DIPPR available in Simulis Thermodynamic software from PROSIM France).

Components	Chemical Formulae	Molar Mass g. mol ⁻¹	Boiling point K	Melting Point K	Critical temperature K	Critical Pressure MPa	Acentric Factor ω
Carbon dioxide	CO ₂	44	194.7	216.58	304.21	7.38	0.22362 1
Ethanol	C ₂ H ₆ O	46.069	351.44	159.05	513.92	6.147	0.64524 5
Hexamethyl disiloxane	C ₆ H ₁₈ OSi ₂	162.379	373.67	204.93	518.7	1.91	0.41515

In *ANNEX 1*, the detailed description of the simulation procedure is disclosed, as well as the method to generate the two-phase diagram of the three binary mixtures. Table 2.2 presents the parameters obtained after data treatment using Simulis Thermodynamics (Remark: no Temperature dependence).

Table 2.2. Values of the binary interaction parameters.

Component i	Component j	A _{ij}	A _{ji}
CO ₂	Ethanol	224.1	144.7
CO ₂	HDMS	1035.2	-420.0
Ethanol	HDMS	-209.8	1124.0

2.5.2.1. Calculation of the PT envelop

Using the thermodynamic model with the adjusted binary interaction parameters, it was determined the PT envelop of a mixture composed of $z_{\text{CO}_2}=0.950$, $z_{\text{Ethanol}}=0.045$ and $z_{\text{HMDS}}=0.005$. Figure 2.14 presents the calculated phase diagram. We can easily observe a cricondentherm and a cricondenbar.

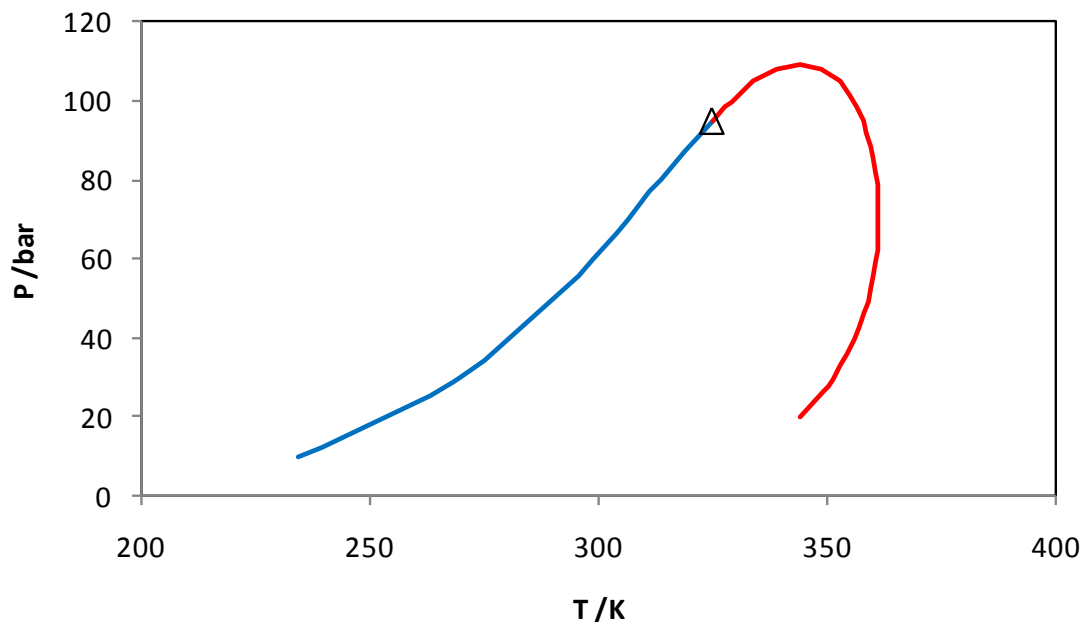


Figure 2.14. PT envelop of the mixture $\text{CO}_2/\text{Ethanol}/\text{HMDS}$ (0.950/0.045/0.005).

The thermodynamic model was based on the literature database, no experimental test could be performed, however, the simulations agreed with the experimented issues of precipitation originated in the process. The surface modification reaction also produce NH_3OH as sub-product [12], this component could not be added in the study.

Further works to improve the model will be necessary by considering BIP temperature dependent. To do that, data base must be completed by doing experimental work concerning the two binary systems CO_2/HMDS and ethanol/HMDS. Validation of the model can be done using vapor liquid equilibrium data on the ternary system.

2.5.3. ON-LINE HYDROPHOBIZATION vs. STANDARD SILYLATION

In order to compare different method of hydrophobization, a study was carried out in close collaboration with ARMINES. In order to evaluate the efficiency of the different hydrophobization processes on silica gels, silica/cellulose composites, and cellulose, the characterization of the samples after different hydrophobization method and drying in supercritical CO_2 was performed. Measurements of density by powder pycnometry and contact

angle were determined for a series of samples by ARMINES, as well as the water uptake. In addition, FTIR spectra of a series of samples have been compared.

Table 2.3 shows number and references of samples treated and/or supercritically dried. Aerogel densities have been estimated based on sample mass and geometric volume measured at SEPAREX after drying, as well as by powder pycnometry using the Micromeritics Pycnometer GeoPyc 1360, at their arrival to ARMINES.

For those that were required, drying and hydrophobization were performed as described *Hydrophobization method 1* at 45 °C and 130 bar. Quantity of silane used was 0.5%, 1.5%, 2.5% and 5%. The highest concentration was not considered in the results due to the difficulties of homogenization within the samples that triggered the crack of the samples, Figure 2.15a.

Table 2.3. Gels treated and densities.

Gel type	Aerogel type	Ref.	HMDS Vol. %	ρ (kg/m ³)
SiO ₂	(SiO ₂ / HMDS)	B	0.5	155
	Supercritical	C	2.5	178
	hydrophobization	D	1.5	211
SiO ₂ / HMDSO	Standard hydrophobization	A1	0	135
SiO ₂	Hydrophilic	A2	0	143
Aerocellulose	(Aerocellulose/HMDS)	E	1.5	323
	Supercritical hydrophobization	F	0.5	198
Composites SiO ₂ / Avicel2.5	(SiO ₂ /Av2.5/HMDS)	G	0.5	227
		H	2.5	191
		I	1.5	185
		J	1.5	194

2.5.3.1. Contact angle measurement

Contact Angles of samples A1, A2, B, F, and Si_HMDSO-ARM were determined:

Table 2.4. Contact Angles of HMDS and HMDSO silylated samples

Gel type	Reference	Contact Angle
SiO ₂ /HMDS	B	97.59°
SiO ₂ /HMDS	A1	123.11°
SiO ₂	A2	Non measurable
Aerocellulose/HMDS	F	Non measurable

SiO₂/HMDS
(ARMINES)

Si_HMDS-
ARMINES

115.89°

Images used for determining the contact angle of sample A1, a silica gel treated in HMDSO/HCl solution at ARMINES and dried in supercritical CO₂ at SEPAREX, can be seen in Figure 2.15a. The contact angle has been determined to be 123.11°. Upon trying to determine the contact angle of sample A2, a silica gel without any hydrophobization treatment and dried in supercritical CO₂ at SEPAREX, sample A2 absorbed the water drop immediately. No measure of the contact angle was possible.

Images used for determining the contact angle of sample Si_HMDSO-ARM, a silica gel treated in an alkane solution of HMDS at ARMINES and subsequently dried in supercritical CO₂, can be seen in Figure 2.15b. The contact angle has been determined to be 115.89°.

Images used for determining the contact angle of sample B, a silica gel hydrophobized with HMDZ during drying in supercritical CO₂ at SEPAREX, can be seen in Figure 2.15c. The contact angle has been determined to be 97,59°.

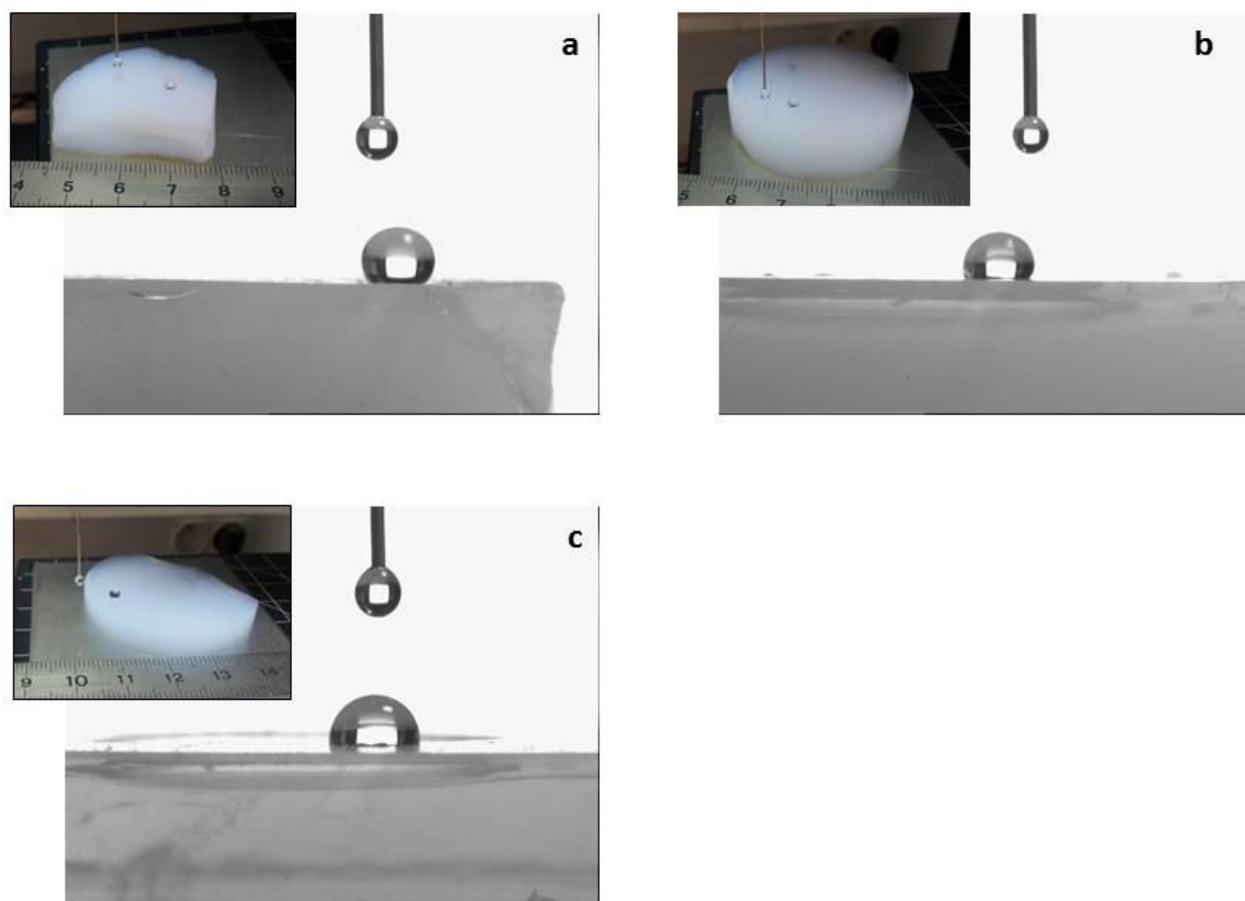


Figure 2.15. Contact angle measurements on samples a) A1, b) Si_HMDSO-ARMINES and c) B. (ARMINES)

Upon trying to determine the contact angle of sample F, coagulated cellulose exposed to HMDS during drying in supercritical CO₂ at SEPAREX, it was found that the water drop was absorbed immediately. No measure of the contact angle was possible. Furthermore, the spot where water was absorbed became yellowed, shrank, and deformed to the point of exposing fractures.

Hydrophobization of silica gels is feasible using HMDS. Nonetheless contact angles are lower for HMDS-treated samples. The contact angle determined for sample B is lowest, indicating a lesser degree of hydrophobization if samples are exposed to HMDS during supercritical CO₂ drying as compared to hydrophobization in a solution. Coagulated cellulose has not been hydrophobized by an exposure to HMDS during supercritical CO₂ drying; such treatment even seems to be detrimental to the sample's reaction to water.

Also, contact angle measurement on HMDS treated cellulose samples was not possible either: the water drop sank into the sample instantaneously; the spot where the water touched became all yellowish-orange, shrank and fractured. This is not the typical behavior of aerocellulose.

2.5.3.2. Water uptake

Water uptake has been measured between a dry point at 20 °C and 20% relative humidity for 24h and a humid point at 20 °C and 80% relative humidity for 48 h.

Table 2.5. Water uptake of HMDSO silylated samples.

Ref.	Sample Description	Mass uptake dry → humid
A1	SiO ₂ /HMDS	-0.6%
D	SiO ₂ /HMDS-CO ₂	12.7%
E	Aerocellulose/HMDS-CO ₂	27.3%
G	SiO ₂ /Avicel/HMDS-CO ₂	8.4%
H	SiO ₂ /Avicel/HMDS-CO ₂	0.1%

Sample A1 seems to have been well hydrophobized. Sample D, however, features a water uptake similar to that of non-treated silica gels of about 10%. Sample E showed a very important water uptake; obviously no hydrophobization has taken place. It even seems as if the treatment of coagulated cellulose with HMDS during supercritical CO₂ drying had induced a different behavior of resulting aerocellulose in contact with water. As for samples G and H, although they are supposed to be of the same formulation, their water uptakes differ sensibly. Whereas sample H seems well hydrophobized, sample G's water uptake comes close to that of a non-treated silica aerogel.

2.5.3.3. FTIR spectra analysis

FTIR spectra of samples A1, A2, B, F, and Si_HMDS-ARM have been taken and compared to standard silica aerogel and standard silica gel treated in HMDS solution.

In Figure 2.16, Samples A2 (in blue) and B (in green) have been compared to a standard silica aerogel (in black) and a HMDS treated standard silica aerogel (in red). The FTIR spectra of sample A2 follow the standard hydrophilic silica gels spectra very closely. The spectrum of sample B (green) resembles that of the standard HMDS-treated silica aerogel (red), only with a lower intensity. This finding bears out the results of the contact angle, indicating a lesser degree of silylation/hydrophobization for sample B treated with the lowest degree of HMDS during supercritical CO₂ drying.

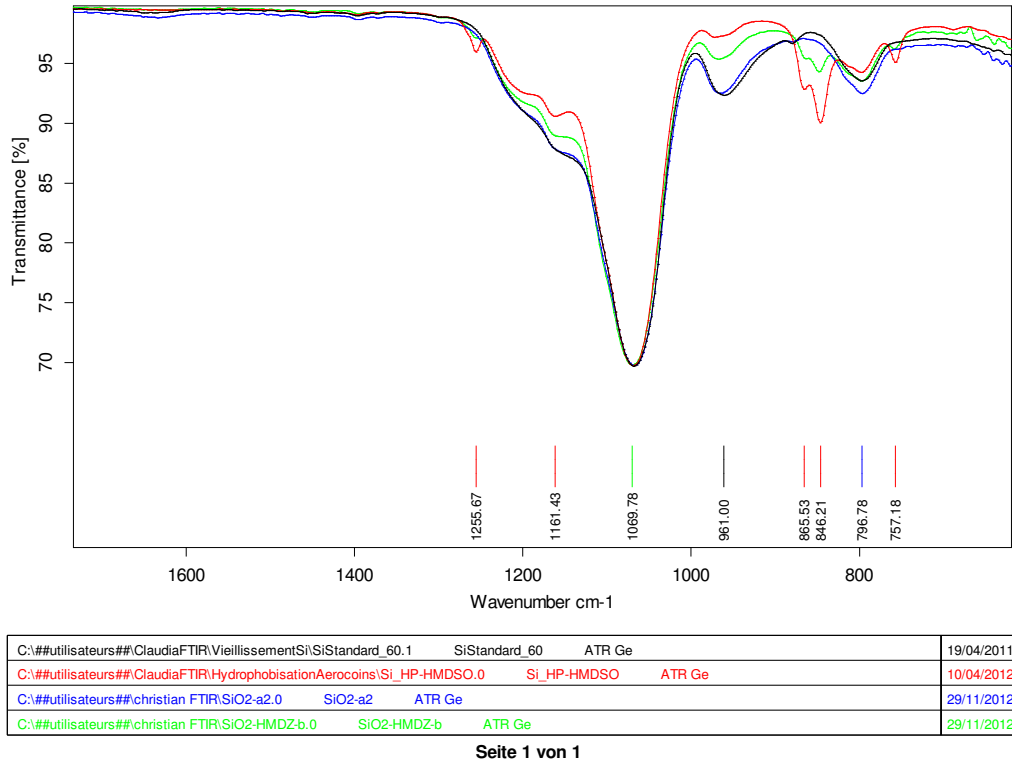


Figure 2.16. FTIR spectra of samples A2 (blue), B (green), a standard silica aerogel (black), and a standard silica aerogel hydrophobized in HMDS solution (red). (ARMINES)

Figure 2.17 corroborates the above mentioned findings. Whereas the spectra of sample A1 (pink) is comparable to that of a standard HMDSO-treated silica aerogel (red), the spectra of sample A2 (orange) practically overlays the spectra of a standard silica aerogel (black) rather than that of sample A1 supposed to be of the same formulation. In conclusion, A1 seems to have been hydrophobized, A2 is unlikely to have undergone any kind of hydrophobization treatment.

The FTIR spectrum of sample Si_HMDS-ARMINES (blue) overlays more or less as well with the spectra of A1 (pink) and the standard HMDSO-treated silica aerogel (red). However, Si_HMDSO-ARMINES (blue) spectrum intensity lies also above that of sample B (light blue). Silylation with HMDSO seems to be more efficient if carried out in solution, rather than in supercritical CO₂.

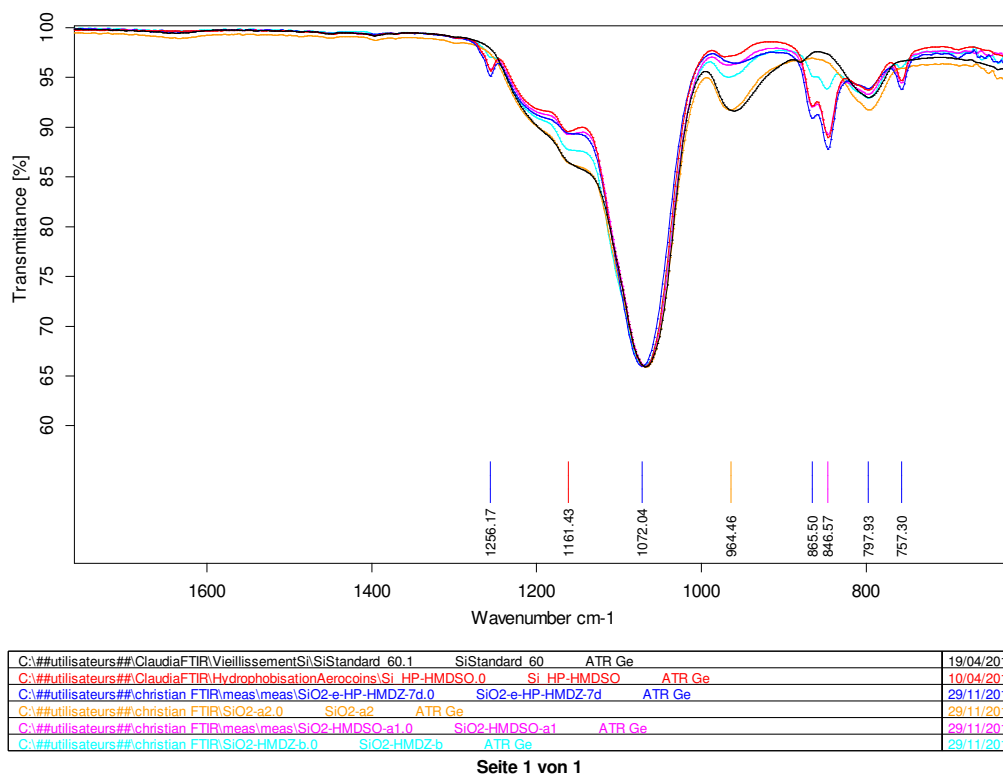


Figure 2.17. FTIR spectra of samples Si_HMDS-ARMINES (blue), A2 (orange), A1 (pink), B (light blue), a standard silica aerogel (black), and a standard silica aerogel hydrophobized in HMDS solution (red). (*ARMINES*)

2.5.4. CONCLUSION

Silica gels may be hydrophobized using HMDS and HMDS. Hydrophobization in HMDS solution yields the results similar to hydrophobization of silica gels in a HMDS/HCl solution. Treatment of silica gels with HMDS during drying in supercritical CO₂ resulted in the hydrophobization of silica gels as well. However, the degree of hydrophobization seems to be higher for HMDS/alcane solutions and lower for HMDS/supercritical CO₂ mixes. Treatment of coagulated cellulose in HMDS during supercritical CO₂ drying is detrimental to the aerocellulose response to water contact. The effect of HMDS treatment during supercritical CO₂ drying on silica gel/avicel composites is not clear yet, more tests have to be effectuated. In general, silica hydrophobization through treatment with HMDS during supercritical CO₂ drying is feasible and can allow to obtain aerogels with lower hydrophobization degrees and using up to 80% less silylation agent.

For scaling up of the material, the presented hydrophobization reaction in supercritical media may have several important advantages:

- The reaction of alkoxy silane compound can be tailored in order to have an optimal hydrophobicity desired in the material from moisture-resistant to super-hydrophobic grade.

- Hydrophobization is homogeneously achieved in the whole volume of the aerogel without any modification of the structure, achieving a highly transparent material.
- The Si-R radical will avoid the shrinkage of the material (normally up to 10% by scCO₂ drying) by a so call “springback” effect of the silicon backbone, obtaining materials with a linear shrinkage <2%. This process must be further studied to obtain final conclusions.
- This method also allows to dry aerogels with very narrow porous without cracks, only possible by performing the solvent exchange with liquid CO₂ which is x3 times more slowly than supercritical CO₂.
- Homogeneous hydrophobization of the aerogel is performed with the minimum quantity of alkoxy silane required (<3% vol.).
- The present process supposes a potential manufacturing advantage for those aerogels that must be hydrophobized.

2.6. AEROGELS PRODUCTS

2.6.1. SILICA GELS FROM P75E20 PRECURSOR.

Adapted from the synthesis developed by ARMINES [3], the original synthesis was performed with solutions from P-XERO diluted in isopropanol (so-called IPA) under ammonia catalysis with or without additional water. The reaction was maintained under 60 °C for the gelation. The current recipe was based on the composition IPA : Ethanol : P75E20 : NH₄OH (30 w%) : H₂O = 29.6 vol.% : 29.6 vol.% : 38.5 vol.% : 1.3 vol.% : 1.0 vol.%. The sol composed by IPA, Ethanol, P75E20 and H₂O is gently stirred with a magnetic bar at room temperature for one hour to induce hydrolysis. NH₄OH is slowly added at strong stirring. After 5 minutes, the solution is poured in a Teflon mold to allow condensation. The mold is closed to avoid evaporation during the gelation process. After gelation, which takes between 5 and 10 minutes at room conditions, an excess of ethanol is poured on the gel to maintain saturation of solvent in the gas phase of the closed mold. Wet gels are aged in a mixture of IPA, Ethanol, NH₄OH (30 w%) and H₂O with the same composition as in the synthesis at room temperature overnight. Washing with organic solvent (generally ethanol) is performed after aging period.

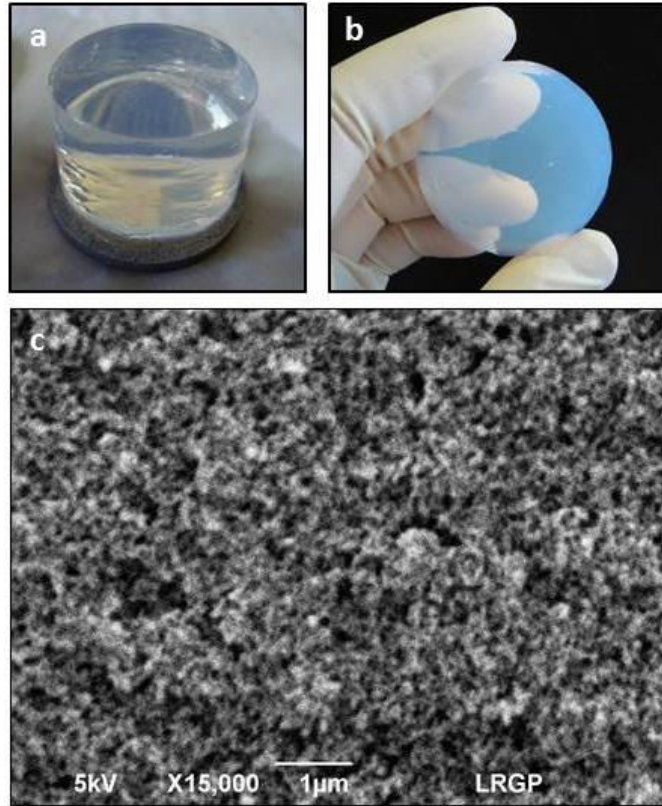


Figure 2.18. a) Basic silica Alcolgel, b) Aerogel and c) SEM Image of P75E20 based gel.

2.6.1.1. Characterization

Mechanical properties of P75E20-based aerogel were investigated in EMPA's laboratories using a universal material testing machine equipped with a 2 kN force transducer in a controlled environment. Tensile strength of the aerogel were estimated using the Brazilian test method where the compressive force applied along the length of the samples is proportional to the tensile stress field perpendicular to both the length of the sample and the direction of the compressive load [13]. Hence, compressive force and sample geometry results in the tensile strength.

Very interesting results were obtained in comparison with other kind of pure silica aerogel (e.g. silicic acid) even if they are still too brittle for most applications. Compression test shows an exponential dependence with the density as it was expected, Figure 2.19; and three domains were defined into the samples: brittle, elastic and compressible.

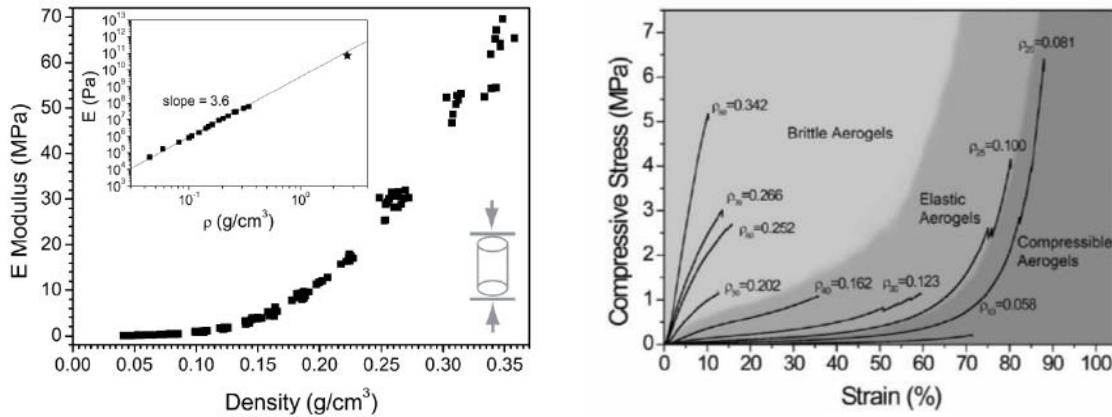


Figure 2.19. E Modulus and Compressive Stress of P75E20 based aerogels (*AEROCOINs project*).

Tensile strength measurements show a similar exponential result depending on the density of the aerogel, but it remains between 10 to 100 times lower than the one observed by compression (Figure 2.20).

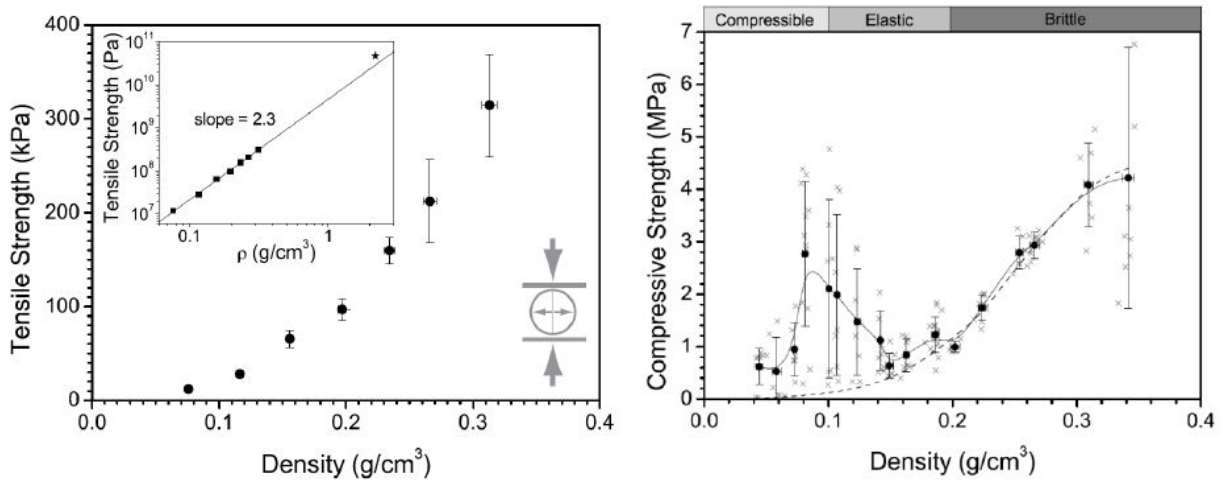


Figure 2.20. Tensile Strength and Compressive Strength of P75E20 based aerogels (*AEROCOINs project*).

As shown in Figure 2.19 and Figure 2.20, mechanical properties of P75E20 silica aerogels are still too low compared with most commercial insulation materials. Therefore further implementations are needed in order to apply reinforcement with external agents as fibers.

Investigation of thermal conductivities was performed in collaboration with EMPA and ZAE Bayern using the hot-wire method with a 50 μm platinum wire placed between two identical aerogel samples. The method uses the electrical wire - as heating element and temperature sensor simultaneously - that is heated with a constant power during the experiment. The variation of the hot-wire temperature is directly proportional to the temperature- dependent resistance of the wire and the thermal conductivity of the aerogel. The thermal conductivity is then calculated by fitting an analytical solution to the temperature over time [14].

The thermal conductivity of the silica samples at ambient pressure used for the process optimization is presented in Figure 2.21.

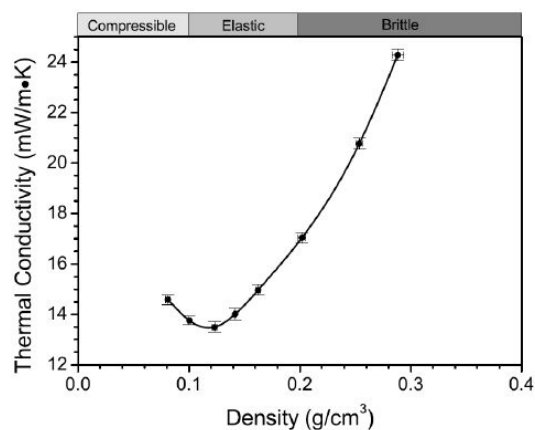


Figure 2.21. Thermal conductivity of P75E20 based aerogel for different densities (*AEROCOINs project*).

Regarding Figure 2.21, and comparing with and Figure 2.20, we observe that the highest values of both compressible and tensile stresses are located in the regime of lowest thermal conductivity.

2.6.2. SILICA GELS FROM TEOS58 PRECURSOR.

HIPIN synthesis was developed at SEPAREX from the high-silica content precursor TEOS58. The 1-Step reaction is carried out under base catalysis with water a hydrolyzer agent. The final recipe was based on the composition IPA: EtOH : TEOS58 : NH₄OH (30 w%) = 24.0 vol.% : 23.7 vol.% : 47.4 vol.% : 4.5 vol.% : 0.4 vol.%. The mixture of IPA, EtOH, water and precursor is stirred for 1 hour at room conditions until hydrolysis is performed. Then ammonium hydroxide is added slowly under strong stirring. Gel was casted in the mold. Gelation takes place between 10 – 15 min at room conditions. Samples were immersed in aging solvent overnight and then washed with pure ethanol solution.

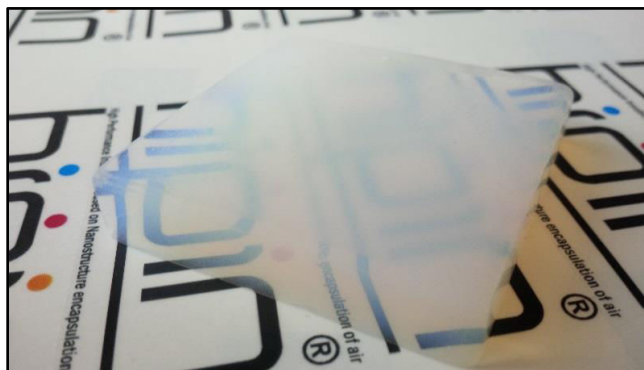


Figure 2.22. TEOS58 based aerogel monolith.

A particular level of aerogel hydrophobicity was required in order to incorporate it in the final products. Different formulations of aerogel produced in SEPAREX were supplied to the partners (TWI, Vimark, Methodo, ICI) for studying their integration in the final products.

2.6.2.1. Characterization

Thermal conductivity measurements of the final aerogel were carried out by ZAE Bayern with the same method as used for the P75E20 samples. It was measured for three different shapes of aerogel, monolith 5x5x1 cm³, granular (main particle diameter, d = 1-4 mm) and powder (d = < 100 μm) by using a hot-wire method. The results are presented in Table 2.6.

Table 2.6. Experimental thermal conductivity (W.(mK)⁻¹) of aerogels from HIPIN58 precursor.

Gas pressure / mbar	GRANULAR (d< 100mm)	GRANULAR (4 mm> d>1 mm)		MONOLITH (10 mm thickness)
	Hydrophobic	Hydrophilic	Hydrophobic	Hydrophobic
Ambient	0.0241 ± 0.0012	0.0843 ± 0.0042	0.0299 ± 0.0015	0.0158 ± 0.0008
1			0.0217 ± 0.0011	0.109 ± 0.0005
10			0.0267 ± 0.0013	0.0111 ± 0.0006
100			0.0267 ± 0.0013	0.0118 ± 0.0006

Different methods in order to characterize the hydrophobicity of the samples were developed in collaboration with TWI. The objective was to establish a test to define the hydrophobicity of the aerogel beyond the contact angle method which can only be applied to flat monolith and not to granular. Results were not conclusive before the end of the project.

2.6.3. SILICA GELS FROM SODIUM SILICATE PRECURSOR.

The sol used for gel preparation consists of silicic acid (H₂SiO₃) and its oligomers (polysilicic acids), which are produced by exchanging Na⁺ ions of sodium silicate with H⁺. To remove sodium ions in the sodium silicate solution, a dilute sodium silicate is passed through a column filled with strongly acidic, cationic ion-exchange resin which is generally based on sulfonated polystyrene. Practically, a 6% vol. silica content solution in H₂O is passed through the Amberlite resin by gravity. The quantity of resin is 1:1 on volume to the treated silica acid. The pH of the native sodium silicate solution is ~11.5 and but once passed through the ion exchange resin drops into the acidic range with typical values ~2.5 [15]. pH of resulting silica acid solution is adjusted to pH 4-5 by adding NH₄OH (30 w%) while stirring to induce gelation. Sol is casted in a Teflon mold and closed. Gelation takes place after 20-30 minutes at room temperature. The sample is aged with a solution of H₂O and NH₄OH with the same composition as the original synthesis overnight. Washing is performed after aging period with pure Ethanol.

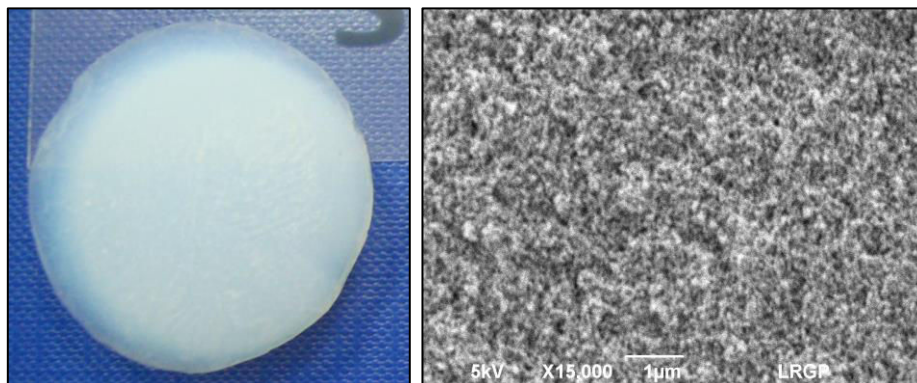


Figure 2.23. Waterglass-based aerogel and SEM image.

No in-deep characterization was performed on the sodium silicate samples due to the clear lower mechanical properties and the lack of direct application of the material.

2.6.4. OTHER MATERIALS

2.6.4.1. Cellulose acetate-based aerogels

Cellulose acetate-based aerogels are obtained by drying cellulose acetate-based gels through standard supercritical CO_2 drying. Cellulose acetate-based gels are synthesized by sol-gel method, based on a protocol established by ARMINES. The sol-gel synthesis of the corresponding cellulose acetate-based gels proceeds in three main steps as follows:

- i) First cellulose acetate is dispersed in acetone.
- ii) A catalyst is then added, to activate the sol-gel process and to accelerate the kinetics of the subsequent condensation reaction between the precursor and cross-linker molecules.
- iii) Upon the addition of a polyisocyanate compound, the cross-linking process is triggered: covalent bonds in the form of urethane links ($-\text{NH}(\text{CO})\text{O}-$) form between the isocyanate groups ($-\text{N}=\text{C}=\text{O}$) of the polyisocyanate compound and the hydroxyl functional groups of the cellulose acetate ($-\text{O}-\text{H}$).

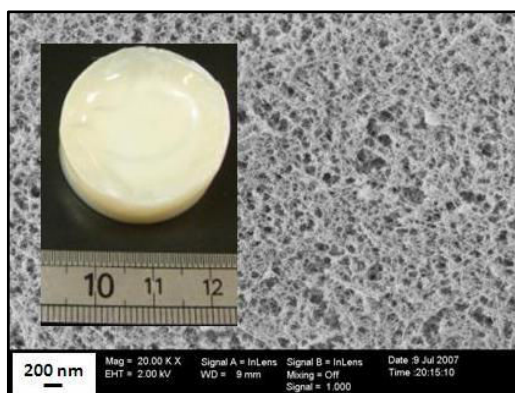


Figure 2.24. Standard cellulose acetate-based aerogel and SEM image. (ARMINES)

This aerogel-based material has the peculiarity of reducing its volume around 90% during low temperature supercritical drying, with a change of solvent by CO₂.

2.6.4.2. Polyvinyl aerogels

One approach carried out within the Project AEROCOINS in order to perform the fundamental cross-linking work for the reinforcement of the silica aerogel consisted in using a reference family of vinyl-based polymers. The main methods described in the literature so far have used epoxy, polyurethane and partly polystyrene for the preparation of cross-linked aerogel samples. Because polystyrene-based samples yield hydrophobic material it was considered that vinyl-based monomers could be considered as cross-linker agent as a suitable starting point. Leventis and coworkers [16] have attempted several strategies to obtain mechanically strong aerogel composites. One method they used was to modify wet gels with amine groups, which then can react with epoxy.

Tecnalia partner in AEROCOINS was in charge of this synthesis to go one step further: both modes of addition of vinyl monomers, after and before the gelation step, will be studied in parallel. The goal is to obtain a material with lower densities than those reported in the literature, and with a compromise in their mechanical properties as to obtain an aerogel-like material board with a value of $\lambda < 0.018$ W/mK. By using co-gelation monomers and/or precursors, a better control of the final material structure could be achieved and the homogeneity of the final material could be enhanced.

The modified polyvinyl synthesis showed a better performance on the drying. Samples with different concentration of polymer from 59 wt% - 39wt% - 29wt% are showed in Table 2.7.

Table 2.7. Polyvynil aerogel properties.

		59 wt%	39 wt%	29 wt%	Normal silica
Density	kg/m³	200	180	110	180
Volume shrinkage	%	15	20	25	30
Thermal conductivity	mW/mK	25	18	15	16

The performance of the aerogel-based material is quiet good in terms of shrinkage and thermal conductivity without exceed on a densification of the aerogel. Further characterization of the samples in order to define the mechanical response to compression and tensile strength is needed so that the reinforcement of the aerogel can be measured. In Figure 2.25, the sample with 29% polyvinyl can be observed.



Figure 2.25. Polyvinyl cross-linked aerogel with different compositions. (*AEROCOINs project*)

2.6.5. COMPOSITE AEROGELS: BLANKETS

As it has been discussed in Figure 2.19, pure aerogels show great fragility and low elasticity. Thus, different methods of reinforcement have been studied to improve the mechanical capabilities of silica aerogels: co-polymerization [17, 18], coating [19] (X-Aerogel [16]), aging [2] and many more have shown promising results. However, the most successful method to increase the mechanical properties of silica aerogels to be applied in the industry has been the impregnation of fibrous matrices. This method developed by Aspen Aerogel provides the ability to obtain large amounts of reinforced aerogels without changing the process of synthesis and drying.

The method involves impregnating the fibrous matter with the alcogel before gelation thereof. Impregnation process must be done uniformly throughout the volume of the blanket and avoiding the accumulation of air inside (by low vibration or compound dumping). Tailored product can be obtained by described procedure depending on supporting matrix and aerogel synthesis. Rigid panels developed for AEROCOINs project were synthesized from P75E20 precursor in Polyethersulfone (PES) fiber matrix of 400 g/m², Figure 2.26. Prior drying, impregnated composite gels were submitted to the same steps as the aerogels based on P75E20.

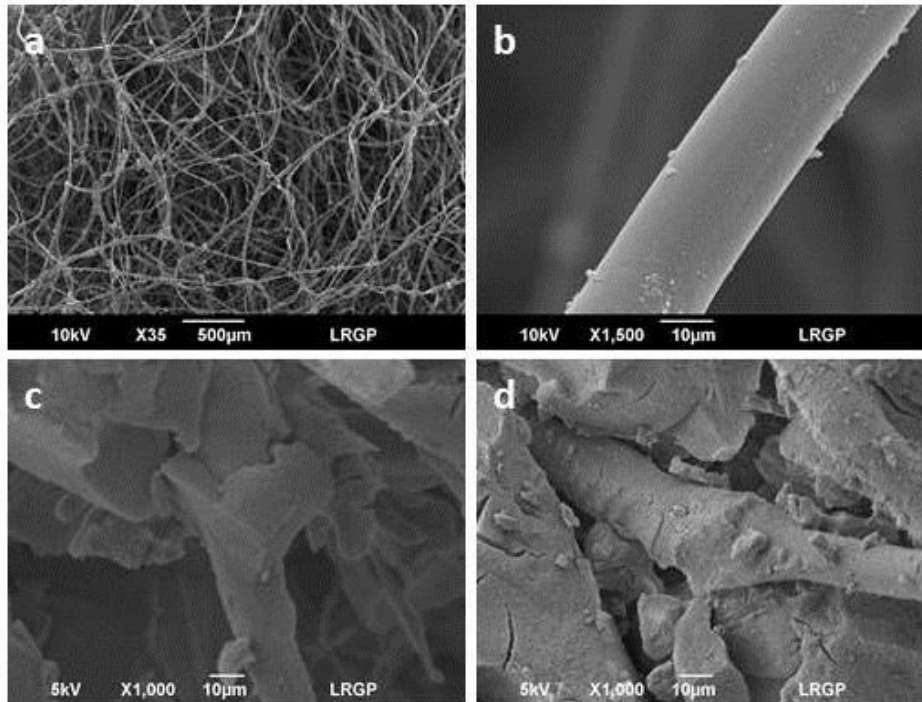


Figure 2.26. a) Original PES fiber matrix, b) single PES fiber, c) impregnated fiber with waterglass-based aerogel and d) impregnated fiber with P75E20-based aerogel. (LRGP-CNRS)

Characterization of the material will be exposed in *Chapter 3* together with the scale-up of the production.

2.7. CONCLUSIONS

Clear understanding of the mass transfer mechanisms governing the LTSCD for different aerogel products is the base to provide an efficient scaling of the manufacture. In the present chapter, the description of the effective diffusion of solvents within the porous structure was observed, defining three separate regimens regarding concentration variation speeds. The results offer a great opportunity to adjust the process parameters in dynamic wise in order to optimize the energy efficiency of the process while maximizing the organic solvent removal.

Functionalization of the hydrophilic samples has been achieved by the reaction of an alkoxy silane (i.e. Hexamethyldisiloxane) with the silica aerogel assisted by CO_2 in supercritical conditions. Study of the ternary diagram of the mixture $\text{CO}_2/\text{HMDS}/\text{EtOH}$ was also conducted in order to establish the optimal operating conditions for the process. Reaction has been successfully demonstrated for different silane concentrations, allowing tailoring the hydrophobization grade of the product. This factor represents a great advancement for the tailoring of products for different applications without reverting in mayor modifications on the process. However, hydrophobization level of standard hydrophobization has been shown to be higher than the provided by the supercritical reaction. Functionalization process assisted by supercritical CO_2 involves less than 20% of the alkoxy silane required for standard hydrophobization of the same material, assuming a great cost reduction. Hence, the possibility to functionalize the aerogel

during the LTSCD eliminates one entire step in the synthesis process, achieving a considerably costs reduction at higher manufacturing levels.

Manufacture of diverse aerogel products was achieved based on the process optimization described. Fully characterization of the materials revealed their superior quality concerning structure preserving and the linked physical properties as low thermal conductivity and density. Product based on P75E20 and HIPIN precursor were validated for their escalation at Pilot Scale in order to apply them in different real applications.

REFERENCES

1. Arkles, B., et al., *Factors contributing to the stability of alkoxy silanes in aqueous solution*. Journal of adhesion science and technology, 1992. **6**(1): p. 193-206.
2. Reichenauer, G., *Thermal aging of silica gels in water*. Journal of Non-Crystalline Solids, 2004. **350**(0): p. 189-195.
3. Bisson, A., et al., *Drying of Silica Gels to Obtain Aerogels: Phenomenology and Basic Techniques*. Drying Technology, 2003. **21**(4): p. 593-628.
4. van Bommel, M.J. and A.B. de Haan, *Drying of silica aerogel with supercritical carbon dioxide*. Journal of Non-Crystalline Solids, 1995. **186**(0): p. 78-82.
5. García-González, C.A., et al., *Supercritical drying of aerogels using CO₂: Effect of extraction time on the end material textural properties*. The Journal of Supercritical Fluids, 2012. **66**(0): p. 297-306.
6. Amaral-Labat, G., et al., *Impact of depressurizing rate on the porosity of aerogels*. Microporous and Mesoporous Materials, 2012. **152**(0): p. 240-245.
7. Bardow, A., et al., *Concentration-dependent diffusion coefficients from a single experiment using model-based Raman spectroscopy*. Fluid Phase Equilibria, 2005. **228–229**(0): p. 357-366.
8. Kriesten, E., et al., *Direct determination of the concentration dependence of diffusivities using combined model-based Raman and NMR experiments*. Fluid Phase Equilibria, 2009. **277**(2): p. 96-106.
9. Crank, J., *The mathematics of diffusion* 1979: Oxford university press.
10. Wong, J.C.H., et al., *Mechanical properties of monolithic silica aerogels made from polyethoxydisiloxanes*. Microporous and Mesoporous Materials, 2014. **183**(0): p. 23-29.
11. Gao, T., L.I.C. Sandberg, and B.P. Jelle, *Nano Insulation Materials: Synthesis and Life Cycle Assessment*. Procedia CIRP, 2014. **15**(0): p. 490-495.
12. Slavov, S.V., A.R. Sanger, and K.T. Chuang, *Mechanism of silation of silica with hexamethyldisilazane*. The Journal of Physical Chemistry B, 2000. **104**(5): p. 983-989.
13. Proveti, J.R.C. and G. Michot, *The Brazilian test: a tool for measuring the toughness of a material and its brittle to ductile transition*. International journal of fracture, 2006. **139**(3-4): p. 455-460.
14. Reichenauer, G., U. Heinemann, and H.-P. Ebert, *Relationship between pore size and the gas pressure dependence of the gaseous thermal conductivity*. Colloids and Surfaces A: Physicochemical and Engineering Aspects, 2007. **300**(1): p. 204-210.
15. Lee, C.J., G.S. Kim, and S.H. Hyun, *Synthesis of silica aerogels from waterglass via new modified ambient drying*. Journal of Materials Science, 2002. **37**(11): p. 2237-2241.
16. Leventis, N. *Mechanically strong lightweight materials for aerospace applications (X-aerogels)*. in *56th International Astronautical Congress*. 2005.
17. Fu, B., et al., *Simulation of the microstructural evolution of a polymer crosslinked templated silica aerogel under high-strain-rate compression*. Journal of Non-Crystalline Solids, 2011. **357**(10): p. 2063-2074.
18. Zhang, G., et al., *Isocyanate-crosslinked silica aerogel monoliths: preparation and characterization*. Journal of Non-Crystalline Solids, 2004. **350**(0): p. 152-164.
19. Fazli, Y., et al., *PMMA-grafted silica aerogel nanoparticles via in situ SR&NI ATRP: Grafting through approach*. Microporous and Mesoporous Materials, 2015. **214**(0): p. 70-79.

Chapter 3

APPROACHES TO THE LOW TEMPERATURE SUPERCRITICAL DRYING SCALE-UP AND MANUFACTURING

3.1. INTRODUCTION

Supercritical processes are a proven tool for a large number of industrial applications and many new ones. In almost all cases, this technology supposes a better option than the common method employed concerning OPEX and sustainability. As discussed in the previous chapters, LTSCD represents the most feasible practice to produce top quality porous materials at industrial scale. In addition, this process also experiences a massive reduction of OPEX within the scaling, which is not experimented by any counterpart process. Therefore, and on the basis of the experimental results, a scale-up of the LTSCD process at Pilot scale will be performed in order to asset industrialization and commercialization of aerogel materials.

For scaling towards an aerogel industrialization of the, the author relies on the mechanisms of the drying process studied in *Chapter 2* to make an analysis based on different consecutive steps: First, a simulation of batches drying for the optimal arrangement of the samples, mechanical design and process conditions. Second, design and construction of a Pilot Plant based on the optimal parameters obtained beforehand. Third, the commissioning and validation of the both the process carried out in the Pilot Plant, as well as the product obtained. To finalize, the study of the economic impact of the different factors governing the manufacturing will be conducted to assess the opportunity of this production line in a growing, while competitive, market.

3.2. PROCESS SIMULATION

The present study is part of the collaboration generated between the company Active Aerospace and Separex within the AerSUS - Aerogel European Supplying Unit for Space

Applications project (Agreement No: 284494), an initiative funded by the Seventh Framework Program of the European Union.

The purpose is to provide a first approach to the simulation of the alcogel drying within the supercritical Pilot Plant, in order to predict the drying time, understand the development of the flow during the process and provide inputs for optimizing the geometry inside the vessel.

3.2.1. FUNDAMENTALS OF THE MODELLING

The process to simulate is considered as a porous matrix (alcogel) in a two-phase flow, since two species are present in the fluid (carbon dioxide and organic solvent).

The assumptions for this simulation are:

- The flow is considered incompressible since the velocity is below Mack 0.3 [1];
- The flow is considered isothermal;
- A two-phase flow is considered because carbon dioxide and organic solvent are two involved fluids inside the vessel;
- Since the flow is isothermal, the diffusion coefficient D_{AB} is assumed constant [2];
- There are no sources or sinks in the medium that generate or deplete the diffusing species (e.g., no heat generation and mass conservation);

The main topics addressed for the simulation are mass transfer and percolation in porous media. To describe the flow behavior inside the porous media, Darcy's law was used due to its simplicity and versatility. Darcy's law is a simple, phenomenological proportional relationship between the instantaneous discharge rate through a porous medium, the viscosity of the fluid, and the pressure drop over a given distance. It describes well the phenomenon performed during aerogel drying.

3.2.2. THEORETICAL BACKGROUND: MASS-TRANSFER MODELLING

In this section the set of equations used in the simulations is presented. The momentum conservation equation for a fluid in the vector form is:

$$\frac{\partial \varepsilon \vec{U}}{\partial t} + \nabla(\vec{U} \cdot \vec{U}) - \nabla \cdot (\vartheta \nabla \vec{U}) = -\nabla P + S_y \quad 3.1$$

where ε is the porosity of the porous matrix, \vec{U} is the fluid mass-averaged velocity, ν is the fluid kinematic viscosity, P is the pressure and S_y stands for the volumetric mass sources or sinks, in this case is replaced by the Darcy term. Note that the variables ε and S_y are only applied in the porous media and the gravity is neglected. The continuity equation for an incompressible fluid:

$$\nabla \vec{U} = 0 \quad 3.2$$

The Darcy term is given by:

$$S_y = -\frac{\mu}{k} \vartheta \quad 3.3$$

Where μ is the fluid viscosity, k is the permeability of the porous matrix and v represents the superficial permeation velocity of the fluid through the porous medium.

The equation for the conservation of chemical species i is:

$$\frac{\partial c_i}{\partial t} + \nabla(c_i \vec{U}) - \nabla(D_{12} \nabla c_i) = S_{yi} \quad 3.4$$

Where c_i is the mass fraction of species i and D_{12} is the binary diffusivity. The aerogel permeability and porosity are considered constant even, if it has been observed variation of volume during the different step of the drying. Nevertheless, those values are not available or are difficult to estimate accurately.

PARAMETRIZATION

In order to understand the behavior of the system that govern the drying, the simulation would be compared with the experimental drying performed by the University of Coimbra for reverse, since it allowed to dry single samples. The variables and main parameter of the models are listed in Table 3.1.

Table 3.1. Parametrization and variables used in the simulation model.

Variables	Parameters
Velocity	Flow
Pressure	Outlet pressure
Carbon dioxide concentration	Viscosity
Organic solvent concentration	Permeability/ Porosity
	Diffusivity
	Density

3.2.3. CONDITIONS

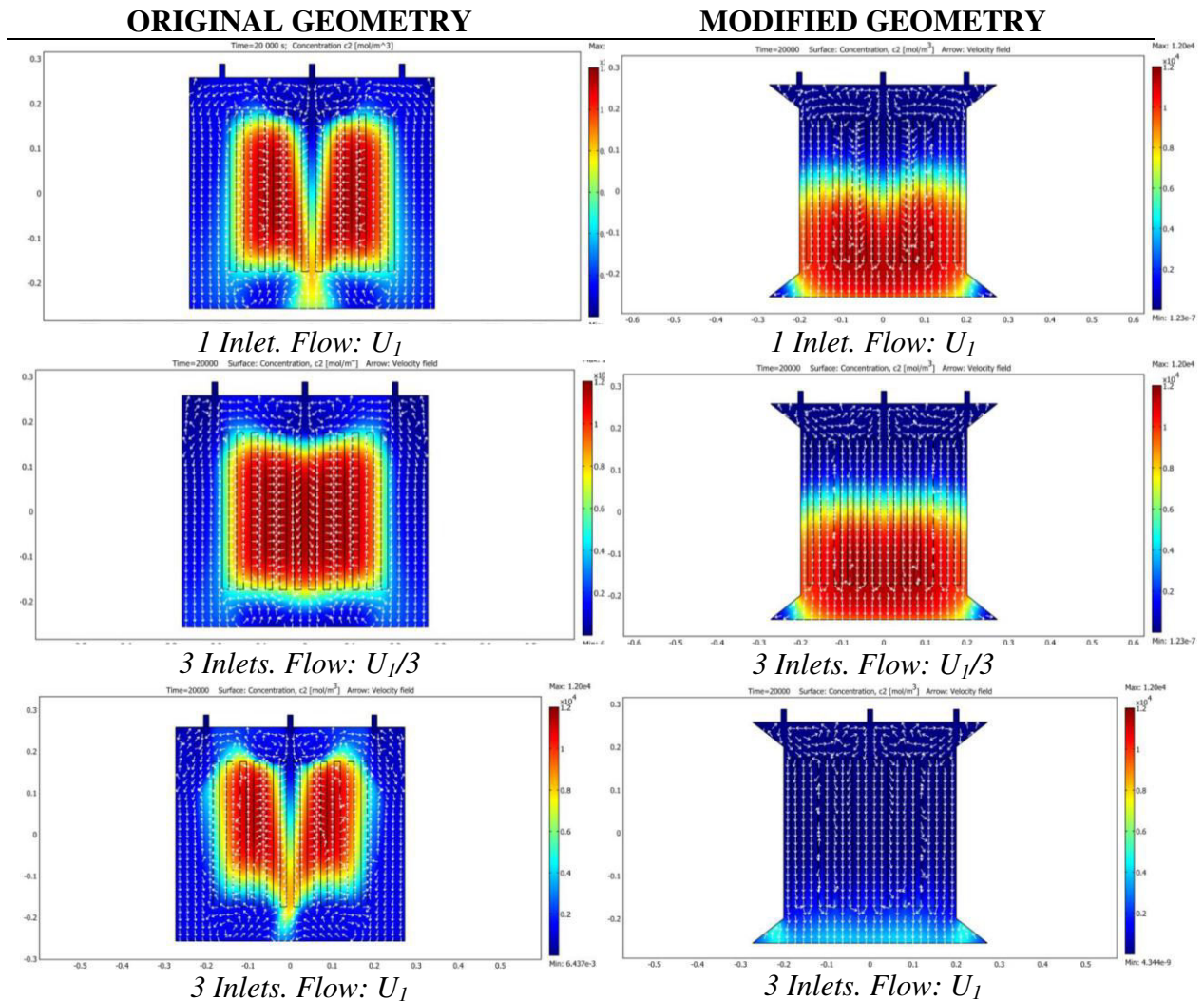
Boundary conditions for fluid velocity and pressure as well as for the concentrations of carbon dioxide and organic solvent were considered. It was generally adopted a constant velocity boundary condition for the inlet and a constant pressure boundary value for the outlet.

The boundary conditions for velocity were assumed as $U=0$ (no slip condition) for the walls; and a parabolic distribution of the velocity field where the vector field is perpendicular to the inlet cross section, for the inlet. The boundary conditions for the mass transport equations were assumed as insulation conditions on walls; constant in the inlets (CO_2 pure); and constant total density of CO_2 – organic solvent mixture, in the outlet. Initial conditions are established as: starting flow in a steady state; starting homogeneous pressure and CO_2 concentration in aerogel is zero as the organic solvent is 1.

3.2.4. RESULTS

At Pilot Scale, the numerical resolution of the model was performed to simulate the drying of single sample and the whole system, which is of paramount importance for the industrialization. Different numbers of inlets as well as flows were considered in order to identify the most suitable conditions to reduce drying time. As a consequence of the study, a modification on the internal geometry of the vessel was proposed for the case of drying of rectangular panels, in order to force the fluid to be conducted through the samples. In Table 3.2, the organic solvent concentration at a common drying time of 5.5 hour is exposed for the diverse options studied. Further parametrization of the different conditions and their representation can be found in ANNEX 2.

Table 3.2. Organic solvent concentration at 5.5 h of drying time for different configurations.



It is remarkable that the modified geometry (with the flow constraint and forcing the flow along the aerogel plates) presents a significant decrease in the drying time. In fact, in the original geometry the flow has a preferred path between the aerogel panels and the autoclave wall and little fluid is actually flowing along and between the plates and effectively drying the aerogel. The decrease in drying time for the modified geometry is around one order of magnitude. The use of 3 inlets instead of 1, for the same flux, does not provide a consistent result for the original and the modified geometries.

The uniformity of the flow is important since it enables a more efficient and uniform extraction across the different aerogel plates. Aerogel plates closer to the inlet dry faster and the plates farther from the inlet take longer to dry. The use of three inlets also contributes to a more uniform flow, thus reducing the overall drying time.

The geometry of the autoclave is of paramount importance: because the autoclave vessel is a cylinder and the aerogel panels are square, there is quite a large volume of unused space inside the vessel. Aerogel plates fill only on the largest square contained within the circle defined by the vessel diameter. This means the unused space ends up being the preferred streamline path for the flow, decreasing the drying efficiency. This space can be used to dry small samples when used in real dryings.

The present study corresponds to a preliminary understanding of the behavior of the drying at Pilot Scale. Further studies must be carried out in order to validate many particularities observed in this work. However, one can say that as the inlet velocity increases, the expected drying time decreases. In fact the inlet velocity is one of the most important variables to control the drying time, but only at large scale. This fact occurs since it does not affect the internal diffusion in the samples as demonstrated by Özbakir *et al.* [3] but the convection in the external layer by reducing the concentration of organic solvent around the sample.

In the case of binary system, the expected drying time increases with the decrease of diffusivity. This parameter does not affect significantly the expected total drying time. Practically, a binary diffusivity decrease of almost two orders of magnitude produces a variation of the drying time by only ~25 s. This is a very important fact to consider in the scale-up: modification of pressure/temperature conditions to increase diffusivity will not impact on the economics of the process.

The expected drying time increases with the decrease of permeability. Aerogel type will play an important role in this parameter since its permeability varies by several orders of magnitude among different references.

3.3. EQUIPMENT SCALE-UP

3.3.1. PLANT DESCRIPTION

To satisfy the production for the European projects AerSUS, AEROCOINs and HIPIN, a Pilot Plant was designed and constructed to manufacture aerogels in different shapes. Process knowledge developed in *Chapter 2* and *Section 3.2.Process Simulation* were applied as input on the design of the equipment, with the budget restriction.

Main purpose of the equipment is the multi-functional research capacity of the plant in order to allow easy modifications in both the process and the mechanical configuration. Different designs of internal supports are also required for performing the drying of a wider

range of materials and shapes without further great increase of drying time due to malfunction of the flow.

The Pilot plant was designed to comprise different steps:

- Charge of Material
- Pressurization
- Supercritical drying in dynamic conditions
- Controlled depressurization.

Each step must be operated under an absolute control due to the fragility of the manufactured material and the risk of the high quantities of organic solvent to be handled.

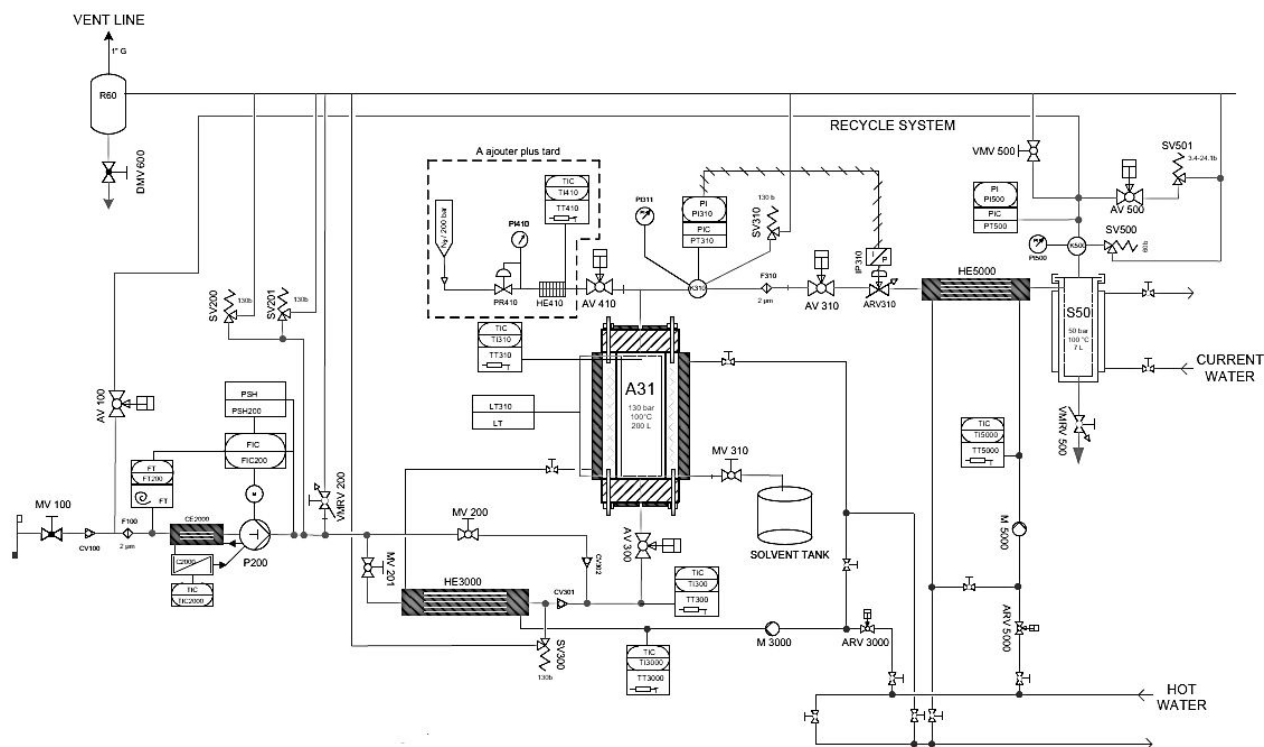


Figure 3.1. Process P&ID diagram.

The process is designed in order to reduce energy costs by increasing the efficiency of the CO₂ circulation and recycling of the solvents. Figure 3.1 shows a schematic diagram of the equipment which will perform the LTSCD process as described in *Chapter 2*. Detailed P&ID can be found in *ANNEX 3*.

Design concerns the following improvements:

- Recycling of the liquid (organic solvent) and gaseous (carbon dioxide) solvents. 95% separation in the cyclone separator.
- Homogeneous operating conditions within the vessel. No temperature gradient along the vessel due to a pre-heater.
- Optimized CO₂ flow through the vessel to decrease drying time.

- Fine depressurization rate control (< 0.2 bar max. fluctuation) to avoid cracks in the sample.

3.3.2. SERVICE CONDITIONS AND DESIGN REQUIREMENT

Service conditions required for the projected Pilot plant are described:

CO ₂ flow rate:	Min. 100 kg/h
Operating Pressure:	150 bar min. per reactor First separator: 200 bar
Operating temperature:	+20 to 100 °C for the reactor Ambient to 80 °C for the rest
Samples requirement:	Min. of 20 rigid samples 350x350 mm ² per batch Min. 100 L of granular per batch

The equipment consists in the following elements:

- Skid 1
 - 100 kg/h CO₂ process piston pump with ATEX motor.
 - 220-litre Reactor
 - Separator
 - 20-litre tank on vent line
 - Electrical cabinet
- 2x50-litre Storage tank
- Heaters
- Heaters:
 - Separation Heater HE5000
 - reactor/pre-Heater HE3000
- Chiller
- Computer control
- Ancillaries
 - Internal support for panels and granules.
 - Metallic spill pallet
 - Solvent pump

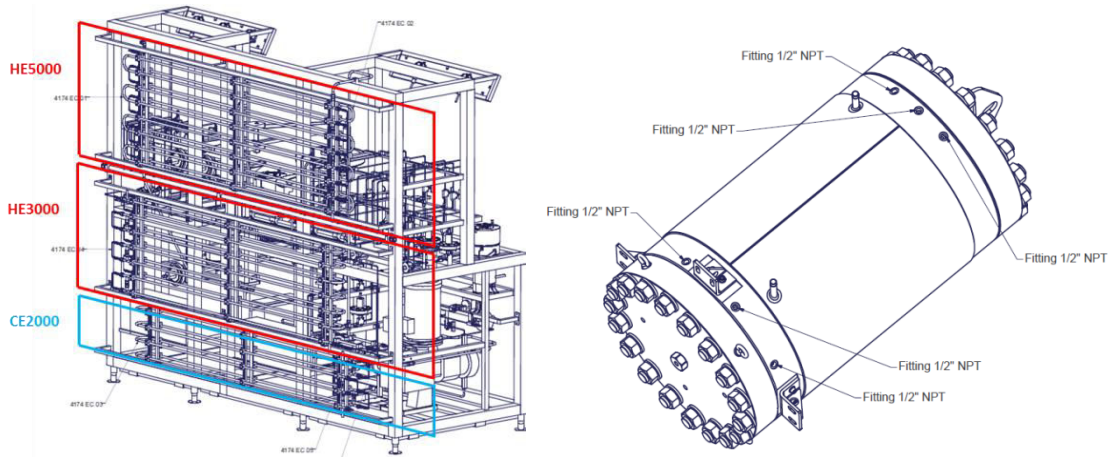


Figure 3.2. Heat exchangers configuration (left); Autoclave A31 connections (right).

Further description of the equipment part can be found in *ANNEX 4*.

3.3.3. CALCULATION

3.3.3.1. Standards

The calculation has been done in base to the “French Code of Construction of Pressure Apparatus” CODAP 2010 and the following norms:

- CODETI 2006
- Norm NF EN 10088-3 / 10088-2 Stainless steel.
- Norm NF EN 10222-5 Stainless steel forged components for pressure apparatus

3.3.3.2. Material

The material relative to the norm 10088-3 and 10888-2 to be used for the construction of the reactor elements are:

- M42 Bolt : X4 Cr Ni Mo 16-5-1 (Stainless Steel 1.4418)
- Double jacket : X 2 Cr Ni Mo 17-12-2 (Stainless Steel 1.4404)

The material relative to the norm 10222-5, to be used for the construction of the reactor is:

- Body, top and bottom closures : X 2 Cr Ni Mo 17-12-2 (Stainless Steel 1.4404)

3.3.3.3. Calculation

The reactor was machine-tooled from an existing metal piece. Therefore the project is restricted to a maximal working pressure defined by the existing material thickness. In

order to guarantee the working conditions, the calculation of the minimum permissible stress for the defined dimensions and material will be conducted.

Calculation of the permissible stress of the body and covers is performed with the required data from the norm NF EN 10222-5 for issued material. Tensile strength (R_m) and Elastic limit at 1% ($R_{px 1.0}$) for both ambient and maximal temperature are then obtained. Permissible stress (f) is calculated from Equation 3.5, for $x = 1$ for ambient temperature; and $x = 2$ for max. temperature.

$$f = f_x = \frac{R_{P_x 1.0}^T}{1.5} \quad 3.5$$

Permissible stress for testing conditions (max capacity) is calculated from Equation 3.6:

$$f = \max \left\{ (0.95 \times R_{P_2 1.0}^T); \left(\frac{R_m^T}{2} \right) \right\} \quad 3.6$$

Permissible stress for Body and top and bottom lids (SS 1.4404) at working conditions is $f_2 = 132.7 \text{ MPa}$ with a maximal permissible stress of $f = 245 \text{ MPa}$. For the bolts (SS1.4418) the elastic limit is calculated at 0.2%, obtaining a permissible stress of $f_2 = 180 \text{ MPa}$ with a maximal permissible stress of $f = 350 \text{ MPa}$. Double jacket (SS 1.4404) has a permissible stress of $f_2 = 133.3 \text{ MPa}$, being the maximal permissible of $f_2 = 250 \text{ MPa}$.

Being the minimum permissible stress at working conditions defined by the body part ($f_2 = 180 \text{ MPa}$), the dimensional requirements of the vessel are disclosed in Table 3.3:

Table 3.3. Dimensional requirements of autoclave A31.

Verification of body thickness (<i>Calculation with internal diameter, Di</i>)		
Interior design pressure	$P =$	13 MPa
Nominal stress	$f =$	132,7 MPa
Internal diameter	$D_i =$	545 mm
Nominal Thickness	$e_n =$	35 mm
	$5.e =$	175 mm
Average diameter	$D_m =$	580 mm
Ring outer diameter	$D_e =$	615 mm
	$D_e/D_i =$	1,128
Terms respected from CODAP norm: $D_m > 5e$		
Following calculation C2.1.4-1		
Welding coefficient	$z =$	1 mm
Minimum thickness required	$e = \frac{P \cdot D_i}{2 \cdot f \cdot z - P}$	$e =$ 28,08 mm
Acceptable Thickness: $e_n = 35 \text{ mm} > e_{\min} = 28,08 \text{ mm}$		

As showed in table above, the vessel to be recuperated is suitable to work at operational conditions since the existing thickness is over the minimum required.

3.3.4. COMMISSIONING

The plant was designed, assembled and installed at SEPAREX facilities. Additional systems as CO₂ storage tanks, ventilation systems, chiller and hot utilities were also attached to the equipment. The final assembly of the plant can be observed in Figure 3.3.



Figure 3.3. Final assembly of the plant.

Internal structures to hold the samples during drying were design in order to use self-supporting samples (vertical disposition) and non-self-supporting samples (horizontal disposition). The structures have been designed in stainless steel and are able to host ca. 40 samples of 35x35x1 cm³ per batch.

Certifications can be found in the related documentation retained by the fabricator and Separex. Calibration and verification of single devises installed on the plant as flowmeter, safety valves, indicators, temperature and pressure probes and variator speed were performed by the project manager engineer.

Hydraulic test certification was performed together with the assigned certification authority. Test pressure was calculated for each part of the equipment concerning the material and norm by the Equation 3.7.

$$P_e = \max\left(\frac{1.25 \times P_s \times f_1}{f_2}\right); 1.43 \times P_s \quad 3.7$$

The ratio P_e/P_s must be lower than the relation between the nominal stress at room temperature in an exceptional service situation with the nominal stress at working temperature in a normal service situation. Thus, the internal pressure calculated for each

segment of the equipment will be dimensioned regarding the test analysis. For the piping circuit and vessel, the test pressure calculated was 18.6 MPa. For the double jacket it is 0.74 MPa.

The test was performed with pressurized water as incompressible fluid at ambient temperature during 15 min. The plant was modified in order to protect all the measuring devices and concentrate the pressure only in those segments issued. A security protocol plan was also filled in order to prevent all the issues of the process relative to the high quantity of organic solvent to be used.

3.3.5. PROCESS VALIDATION

In order to validate the operational function of the equipment tests at working conditions were carried out in order to validate the following parameters:

Table 3.4. Validated parameters.

Max. working pressure	Alarms
Stability working pressure at max/min flow	Depressurization control
Max. working temperature	Depressurization Stability
Facilities temperature	Solvent recovery
Stability of temperature at max/min flow	Valves Automation

The final conclusion of the tests is that the equipment is validated for the drying of aerogels by the Low Temperature Supercritical Drying process with an accurate control over the conditions. High quality nanostructured materials can be obtained without any cracks or other kind of issues relative to the process.

3.4. PRELIMINARY MANUFACTURING

The general objective of this study is to produce and characterize the scaled-up aerogel material obtained in the Pilot Plant. Different materials and shapes were synthesized and dried in order to perform with the low manufacturing required for the European Projects. This production concerned up to 1.3 m³ of silica aerogel in granular form, 120 silica reinforced boards (400x400x20 mm³) and ca. 50 silica monoliths (350x350x15 mm³).

3.4.1. PRODUCTION OF BLANKETS

Granular aerogels from HIPIN precursor were dried and hydrophobized in the facilities, however, the major product to develop consisted of the aerogel composite boards based on silica gel impregnated in PES blankets.

The preparation and recipes for the relating prototype aerogel boards were described in *Chapter 2* from P75E20 based aerogel reinforced with PES fibrous matrix. Organic reinforcing material was provided by the partners already shaped to the required dimensions. No further treatment was applied to the fibers. Synthesis was performed individually in a horizontal mold where the raw blanket was placed while colloidal solution was mixed as previously described. Gelation time was similar to those at lab scale (i.e. 10

minutes). Before the gelation took place, the gel was pored over the blanket in the mold and slightly pressed in order to prevent air bubbles from staying in the interior of the sample. When the gelation was occurring, the blanket was turned over a metallic net to maintain both sides of the blanket free of gel accumulation. This method provides very homogeneous composite blankets without heterogenic areas.

Following the protocol, the sample was kept overnight in an aging solution prior the steps of washing. A control of the solvent quality was performed by measuring the refraction index of the solution over time. The minimum quantity of water in solution was established concerning the ternary diagram of the mixture $\text{CO}_2/\text{EtOH}/\text{Water}$ at working conditions, to ensure that the water content would not be an issue to arise a single phase within the porous during the drying.

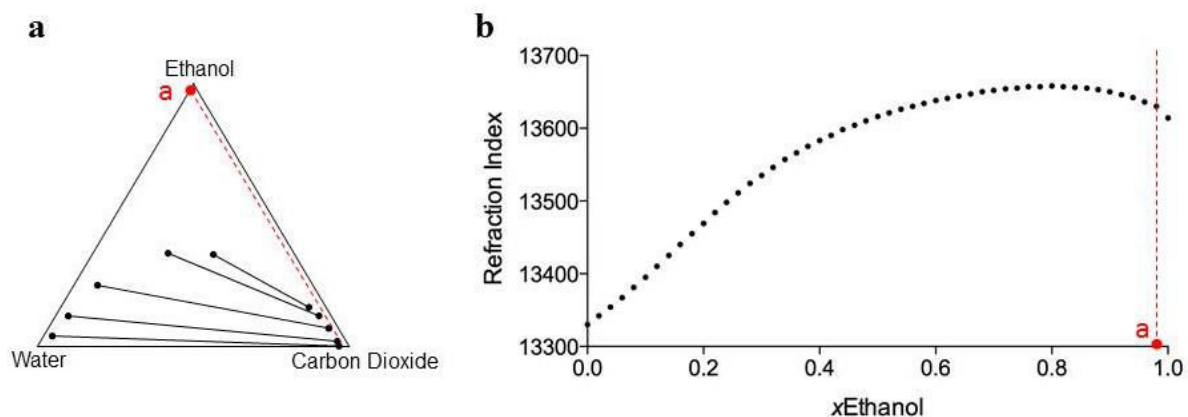


Figure 3.4. a) Critical Point of the mixture $\text{CO}_2/\text{Water}/\text{Ethanol}$ at operating conditions and b) Refraction index of water/Ethanol mixture. Point *a* (in red), determines the maximal allowance of water in the supercritical mixture in order to acquire one phase.

In Figure 3.4-right, a maximal allowance of 2 vol. % of water for a 98 vol.% rich CO_2 mixture with Ethanol for one phase is disclosed at operating conditions (SEPAREX's private database). This quantity belongs to a minimum purity of 0.98 during washing steps (Figure 3.4-left).

Once the samples were free of impurities and water, they were inserted on the vessel (to obtain hydrophilic samples) or inserted in a solution of organic solvent with a 3% vol. of HMDS overnight. The second solution would allow the aerogel to carry the silane in its interior in order to react with the CO_2 to hydrophobize the silica during the LTSCD.

Drying was performed in batches of 15 – 20 samples placed horizontally. Process time was determined simultaneously by the simulation described in *Section 3.2. Process Simulation* and the measurement of the recuperated organic solvent in the separator S50.

Supercritically dried samples were processed successfully by SEPAREX (see Figure 3.5). The boards ($40 \times 40 \times 2 \text{ cm}^3$) were dried and hydrophobized under supercritical conditions for further analyzing and installation in demonstration prototypes.

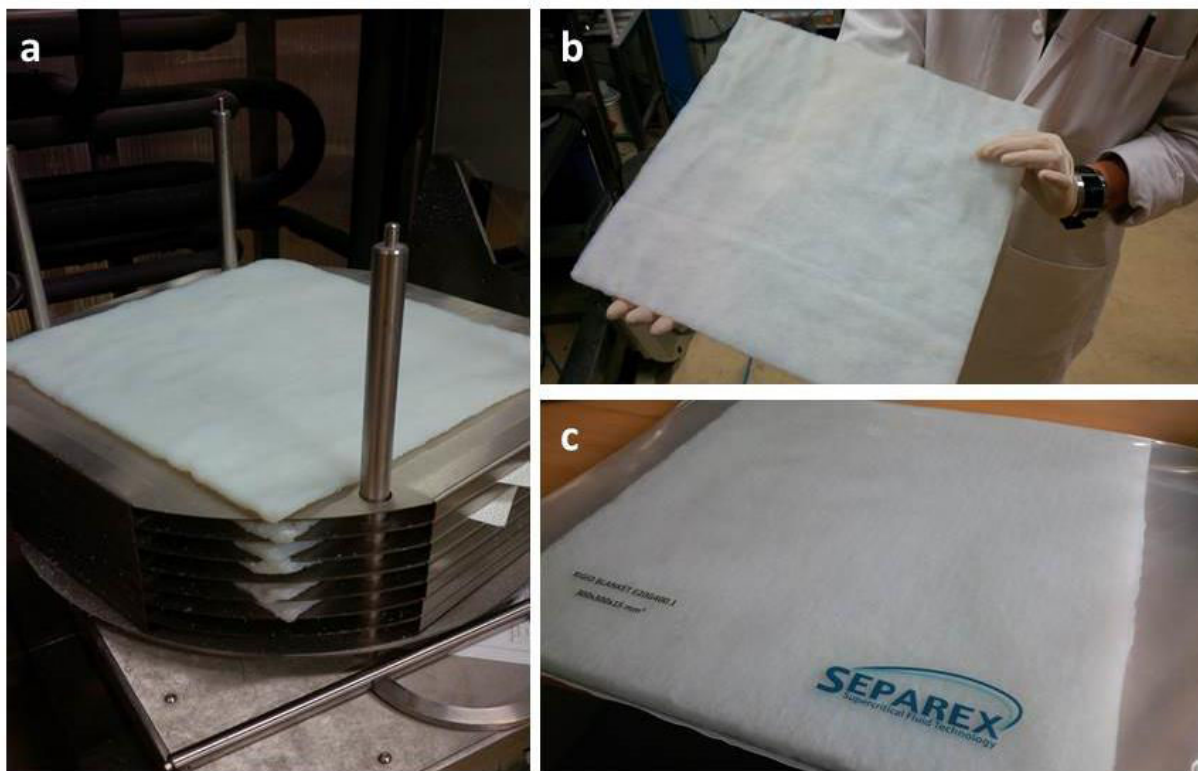


Figure 3.5. a) Boards in the horizontal drying structure, b) aerogel dried board and c) final package and labeling prior sending to partners.

3.4.2. CHARACTERIZATION

3.4.2.1. Thermal conductivity measurements

Thermal analysis for supercritical dried silica boards was measured at ZAE with hot-plate instruments Netzsch HFM 436/3/1E Lambda for a size of 300x 300x20-30 mm at ambient conditions. All samples investigated provide thermal conductivities (measured in parallel by ZAE) in the range between 16.3 and 18.2×10^{-3} W/(m K), listed in Table 3.5. The results were compared with those boards dried at ambient conditions by a third partner. No clear trend was found that connects low conductivities with any of the two drying methods, although the densities of the supercritical dried aerogels were 25 % higher than the ones ambient dried (100 Kg/m^3) due to the consistency of the material.

Table 3.5. Thermal conductivities of supercritically dried boards measured (ZAE)

$\rho \text{ (kg/m}^3\text{)}$	$\lambda_{\text{ZAE}} \text{ (} 10^{-3} \text{ W/(m K))}$
134.0	16.9 ± 0.9
128.0	17.4 ± 0.9

3.4.2.2. Mechanical properties

To characterize the mechanical behavior of the reinforced silica aerogel boards a quasi-static uniaxial compression test was applied by ZAE. The stress-strain characteristics of the samples were measured for short term loads of up to 20 % strain.

Compression tests were performed using a Zwick Roell Z20 equipped with a 20 kN load cell. Displacement and force were measured continuously with an accuracy of ± 0.5 mm and $\pm 1\%$ (for loads > 60 N), respectively.



Figure 3.6. Experimental setup for compression testing with two parallel plates. (ZAE)

Test was performed according to EU standard EN 826 (Determination of Compression Behavior of Thermal Insulation Products) samples were placed centrally between the two plates, preloaded with (250 ± 10) Pa and compressed with a constant rate of displacement of 5 mm/min. The zero deformation point was defined as the deformation at a stress of (250 ± 10) Pa. In contrast to the standard, where deformations of 10 % are recommended for evaluation of elastic constants, the aerogel boards were compressed until 20 % of strain was reached. Only at very low deformation (< 2 %) and around 20 % strain a linear increase of the stress strain curve was observed (Figure 3.7). This is a typical behavior found for aerogels that soften after an initial Hooke's law upon minor strain resulting in a buckling of the backbone chains at the microscopic scale.

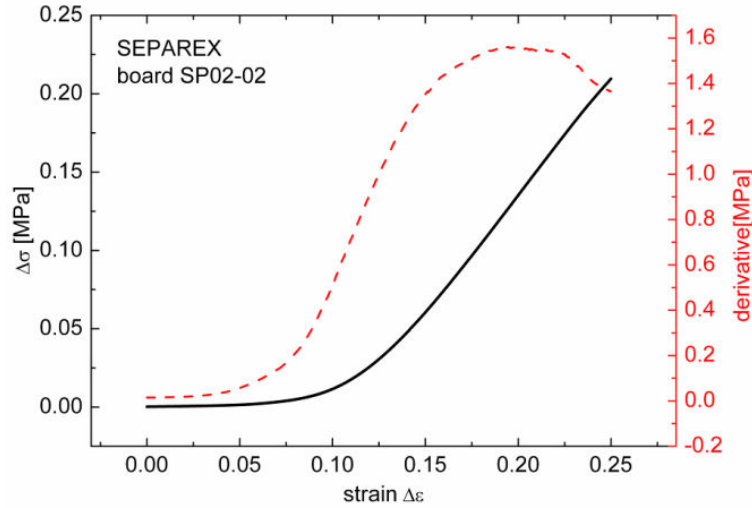


Figure 3.7. Black: Stress strain curve recorded for sample SP02-02 (SEPAREX); red: corresponding derivative. (ZAE)

The Young modulus E was calculated from the linear portion of the force-displacement curve (constant derivative, Figure 3. right) using the following formula:

$$E = \frac{\Delta\sigma}{\Delta\varepsilon} \quad 3.8$$

Where $\Delta\sigma$ denotes the relative stress (pressure applied) and $\Delta\varepsilon = (\Delta d/\Delta d_0)$ the relative strain (i.e. relative change in sample thickness $\Delta d/\Delta d_0$) in different regimes of linear relationship.

All boards essentially show two linear regimes. While the first region characterizes the mechanical stiffness of the undeformed sample, the second region characterizes the resistance against mechanical of the deformed material. Using Equation 3.8 the compression modulus of elasticity E was determined for each of the two regions. Results are summarized for the respective samples in the Tables below.

Table 3.6. Summary of elastic moduli determined in different regimes of deformation for supercritical dried samples; the boards analyzed had a size of 290 x 290 mm² and a thickness of about 16 mm. (ZAE)

Sample name	Deformation < 1%		Deformation: 20 %	
	E MPa	Error E 10 ⁻⁴ MPa	E MPa	Error E 10 ⁻⁴ MPa
SP02-02v1	(0.025)	7.3	--	--
SP02-02v2	0.019	0.23	1.2	6.9
SP02-02v3	0.018	0.13	1.3	6.1
SP02-02v4	0.015	0.22	1.5	3.4
SP02-02v5	0.015	0.16	1.6	3.0

The values are significantly lower than the values for pure silica aerogels that are well above 1 MPa for densities of 100 kg/m³ and above [4]; here the moduli were calculated at (3±2 %) strain. This effect is likely due to the reinforcement that increases the tensile strength of the overall composite but seems to reduce the compressive strength. In addition, the two types of aerogel composites dried by ambient and supercritical conditions have very similar behavior at very small strain; however, reveal a different characteristic in the range of about 5 to 12 % strain.

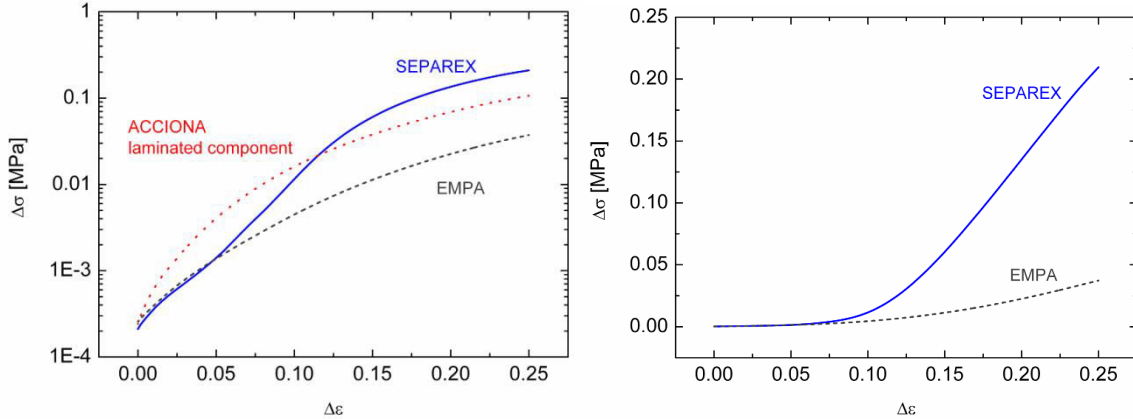


Figure 3.8. Stress-strain curve for the silica aerogel boards ambient dried (EMPA) and supercritically dried (SEPALEX), as well as the laminated component (ACCIONA). (ZAE)

In contrast, the laminated component provides higher compression stiffness at low strain while at high strains falling in between the ambient and the supercritical dried boards.

Table 3.7. Summary of elastic properties determined.

Sample name	Density (kg/m ³)	Deformation < 1 %		Deformation 20 to 25 %	
		E[MPa]	E[MPa]	E[MPa]	E[MPa]
Supercritically dried	130	0.017	1.4		
Ambient pressure dried	95	0.020	0.32		

3.4.2.3. Humidity and water uptake

Moisture behavior of large samples from ambient drying and supercritical drying was measured at VTT facilities. Moisture uptaking in different humidity environments has been measured by monitoring the samples weight after exposure to defined humidity.

A remarkable difference between the two types of aerogel board samples was observed due to the different hydrophobization methods. The ambient dried boards hydrophobization was more effective than those hydrophobized during the supercritical drying. Water uptake for supercritical dried samples ascended to 8 % of water content at 80% of relative humidity, while ambient dried samples were below 1 %. At 100% relative humidity, supercritical dried samples raised 14% in contrast with ambient dried, below 2%.

The water vapor permeability was determined (for the large test samples) under about 50 % / 0 % RH humidity conditions (Figure 3.9). The test samples were large enough so that they could be placed in a diffusion cup frame. Diameter for measuring diffusion rate was

145 mm. The vapor diffusion through the samples was monitored by weighing the test sample and the cup including salt solution (desiccant). In these tests the surrounding air humidity (50 % RH, +23 C) caused moisture flow through the samples into the salt solution (0 % RH) of the diffusion cup. The mass flow, time, free surface area and thickness of the samples are needed to calculate the water vapor resistance factors μ for the samples under investigation.

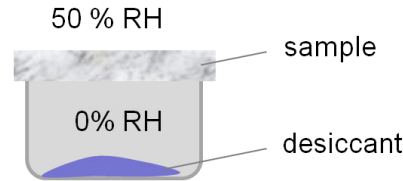


Figure 3.9. Set-up of the cup test applied to determine the water vapor permeability under 50 % / 0 % RH humidity condition. (VTT)

Table 3.8 presents the water vapor resistance factors for test samples. Both of these materials can be considered very vapor open materials. The PES fibrous material prior the impregnation with aerogel had values of 1.3-1.4. The aerogel samples had about 7-8 times higher resistance as the untreated fiber material.

Table 3.8. Water vapor resistance factors μ for test samples. (VTT)

	μ
Ambient dried	9.6
Supercritically dried	11.7

3.5. ECONOMICAL STUDY

Aerogel production volumes are still low compared with other insulation materials. High production capacity is not yet a realistic approach for new companies since each application would require a slightly different material and volume. Hence, the economic study presented for the aerogel production will aim to provide a general overview of the cost ratio for different volume capacity to become a tool to assist on manufacturing design decisions. Later, for each specific scenario, a more detailed calculation must be done based on the general data obtained hereafter.

The estimation will only include the cost relative the high pressure supercritical plant and the operational expenditures consequence of the aerogel drying. Civil engineering or taxes are not included in the present study for diverse regulation concerns which would require a more specific revision in each case.

3.5.1. DESCRIPTION OF STUDIED PARAMETERS AND CONSIDERATIONS

Targeting a wide production capacities range (from hundred liters to several m³) several assumptions are taken. Constant parameters of manufacturing are related to volume

capacity. Most significant capacity-dependent parameters used in the present study are described below.

Working hours per year will be divided in three manufacturing levels (ML) as described in Table 3.9. The reference system is established based on the experience of SEPAREX's clients and supercritical extraction plant customers.

Table 3.9. Manufacture level (ML) assumption.

Capacity, m ³	Working hours (W), h/y	Manufacture level
< 0.5	2440	Low
0.5 < V < 2	7200	Medium
>2	8064	High

Vessel geometry is restricted to an internal length/ diameter (L/D) ratio of 4 to maximize the blanket production. This value is slightly below the recommended values of 5 for supercritical extractor. Such determination is proposed since extractors with high ratio L/D are aiming to increase the linear velocity of the fluid to reduce processing cycles. In our case, mass transfer mechanisms are not dependent on the fluid velocity, bringing the emphasis on maximizing the production per cycle.

Labor costs are labelled for the region of Lorraine (France) in 2014. Two operators must be in place always during manipulation of the pressurize equipments. Rates are 53 €/h for managers and 35 €/h for operators.

The model will include also the use of direct driven pump or compressors depending on the ML of the plant, being more favorable the use of pumps at lower level and the compressor at medium and high levels.

3.5.2. CAPITAL EXPENDITURES (CAPEX)

Fixed assets costs estimation for the high pressure plant is based on the data collected by SEPAREX in the last 10 years for solid treatment plants with operating conditions similar to the one used for drying the aerogels in the previous chapters. To homogenize the plant cost, a modified function integrating the mass flow, vessel capacity and number of vessels will be considered as defined by Perrut [5] and modified by Núñez *et al.* [6].

The cost of supercritical plants can be defined as a function of the flow and the volume with a scaling factor which represents the cost reduction of the plant with the increase of the size, Equation 3.9.

$$I \propto (Q \cdot V_T)^{m'} \quad 3.9$$

Where I is the cost, Q is the CO₂ mass flow in kg/h, V_T is the internal volume of the vessel in liters and m' is the scaling factor which vary between 0.5 – 0.6 [7]. Perrut reported a scaling factor of 0.24 for the supercritical equipment manufactured at SEPAREX. Núñez *et al.* proposed a modification in order to introduce also the parametrization of the number of vessels. Computation is based on considering the plant as two systems: the vessel (defined by the internal volume) and the CO₂ cycle (defined by the mass flow). Equation

3.10 describes the equipment cost for supercritical extraction plant base on a reference equipment conditions and cost.

$$I = I_r * \left[\frac{\alpha}{\alpha + n_r \beta} \left(\frac{Q}{Q_r} \right)^{m_1} + \frac{\beta n}{\alpha + n_r \beta} \left(\frac{V_E}{V_r} \right)^{m_2} \right] \quad 3.10$$

I_r , Q_r , n_r and V_r are the reference price, mass flow, number of vessels and internal volume, respectively. The coefficients m_1 and m_2 are the scaling factors for the solvent cycle and vessel system, respectively. In bibliography they are considered as $m' = m/2$ as well $m_1 = m_2 = m$; therefore we will use the value $m = 0.48$. α and β are the weighting parameter for the solvent cycle and the vessel system, respectively. They are correlated from values of SEPAREX equipment to obtain $\alpha = 0.55$ and $\beta = 0.15$.

3.5.3. OPERATING EXPENSES (OPEX).

The contributions of the diverse costs related to the manufacture of the aerogel products are hereafter disclosed.

3.5.3.1. Equipment depreciation

Depreciation of the equipment is considered for 10 year with a discount rate of 6% ($r = 0.06$). Equation 3.11 represents the depreciation of the equipment per year.

$$C_I = \left[\frac{r(1+r)^{10}}{(1+r)^{10} - 1} \right] I \quad 3.11$$

C_I represent the depreciation cost in €/y.

3.5.3.2. Raw materials

Inorganic aerogel can be prepared by different silica precursors as it has been described in prior chapters. In Table 3.10, the price per volume of common precursors is showed. The cost hereby exposed is based on raw material price over 1 MT min. supply and considering recycled solvent. The calculation for granular aerogel cost is in the basis of 1.8 L of granular aerogel production per liter of gel.

Table 3.10. Inorganic gel raw material cost from different precursors (C_G).

	C_G €/L _{gel}	Contribution gel cost	
		Panel/blanket* €/m ² _{aerogel}	Granular €/m ³ _{aerogel}
Tetra ethoxysilane (TEOS)	1.9	19	1,056
P75E20 (TEOS-based)	2.97	29.7	1,650
HIPIN (TEOS-based)	2.15	21.5	1,194
Tetramethylorthosilicate (MTMS)	2.0	20	1,111

Sodium silicate (Na ₂ SiO ₃)	0.49	4.9	272
Rice hull ash	0.29	2.9	161

* 10 mm thickness panel/blanket

The gel cost is based mainly on the precursor cost since the chemicals used during synthesis are fully recycled or are negligible on the calculation (e.g. < 3% water or NH₄OH per liter of gel). It is notable that difference between the costs of the alkoxysilanes with those based on sodium silicate is very important.

Solvent contribution during LTSCD is negligible since it is fully recycled and reused on the process. Cost of gases is labelled for high supply of carbon dioxide in cryogenic tanks at a cost of 0.16 €/Kg and recycled 92%. Consumption of assistant gases as nitrogen or pressurized air are neglected. CO₂ consumed per year is described in Equation 3.12.

$$C_{CO_2} = 0.92 \cdot 0.16 \cdot \rho_{CO_2}(@buffer\ conditions) \cdot V_E \cdot N \quad 3.12$$

$$N = \text{Int} \left[\frac{W - (n - 2)t_s}{t_s} \right]; \text{Extraction batches} \quad 3.13$$

3.5.3.3.Extraction costs

Drying cycle time is defined by the different steps of pressurization, dynamic drying and depressurization. Focused on the production of 10 mm thickness samples and regarding the simulation carried out in *Section 3.2 Process Simulation*, the different stages time are are: Pressurization time (t_{pre.})= 0.5 h; Depressurization time (t_{dep.})= 7 h and Switch time (t_s) = 0.5 h.

Energy requirement for the process is defined by Enthalpy variation of the fluid through the different operating conditions. Data is provided by Mollier diagram for Carbon dioxide. Following the operating conditions presented in Figure 2.13, the energy consumption of each stage (C_{EC,i}) is calculated following Equation 3.14 and Equation 3.15.

$$C_{EC,i} = 0.00028 \cdot t_i \cdot EP \cdot \Delta H_i \cdot Q_i \cdot N \quad 3.14$$

$$C_{EC} = \sum C_{EC,i} \quad 3.15$$

t_i is the stage time previously defined, EP represent the energy price of the labelled country (France: 0.10 €/kWh), ΔH_i represents the Enthalpy variation between stages in kJ/kg, Q_i is the mass flow in each stage in kg/h. For the stage of pressurization, the coefficient η_i is added to represent the efficiency of the pump or compressor (30 % for both cases).

3.5.3.4. Man power costs

Person month rate required for the equipment is related to the size of plant. The approach is considered with the criteria as in Table 3.9. Man power cost is described by Equation 3.16 using two operators and a ¼ of management per working hour.

$$C_{MP} = 83 \text{ €/h} \cdot N \tag{3.16}$$

3.5.4. PRODUCTION COSTS

The manufacturing of the aerogel-based materials must be well designed from the two key points of the production: The sol-gel synthesis and the supercritical drying process. Both have the inconvenient of having a high cost compared with the manufacturing of normal insulation materials, but a good synergy between the equipment manufacturing and an optimized drying is the solution to obtain economically competitive products.

Aim relies on the maximization of the production volume at a lower cost. Study of different manufacturing systems (different number of vessel for cascade production) are considered, as well the final production capacity, Figure 3.10.

Production costs of aerogel blanket manufacturing highly decrease with the rise of vessel volume. The use of single vessel systems at low ML is notable recommendable. Inflexion point at medium ML triggers the use of 2 vessels systems while 3 vessels system, at high ML. The reason of the inflexion point is the intensification of production capacity while optimizing the efficiency of the process cycle.

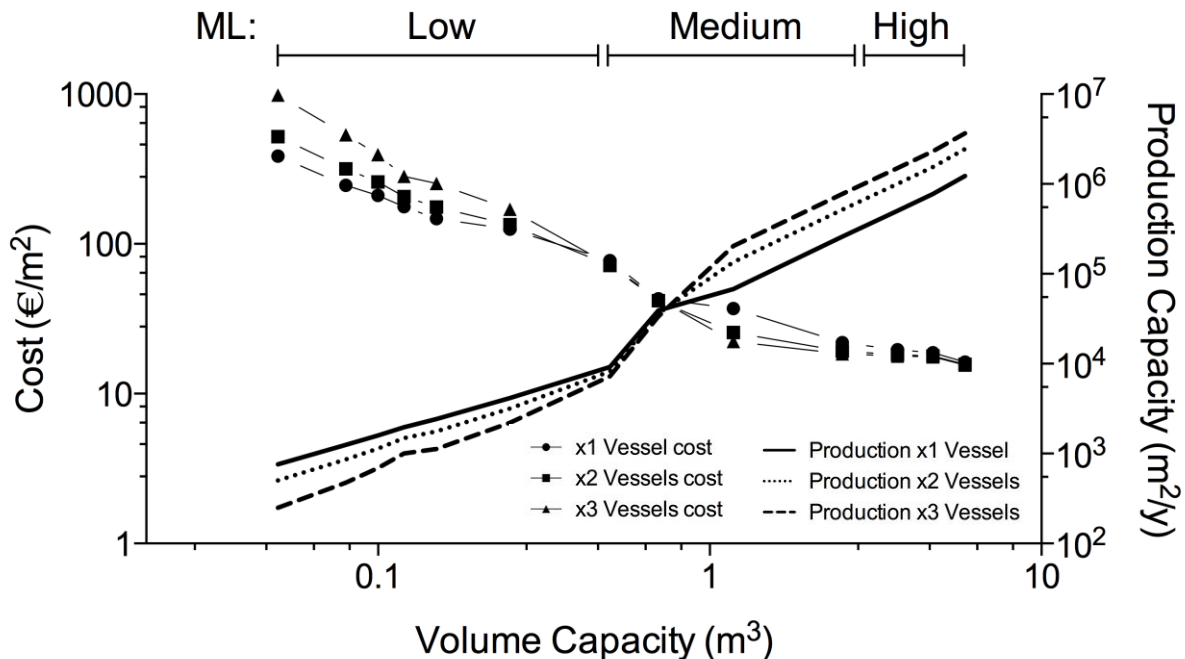


Figure 3.10. Production costs and capacity of aerogel blanket manufacturing at different MLs.

The cost contribution of the final product is described in Figure 3.11. It is notable that the final cost is highly dependent on the precursor cost at medium and high ML meaning over

80% of the costs. The higher automation linked to higher ML is observed by the reduction of the contribution of the Man Power cost.

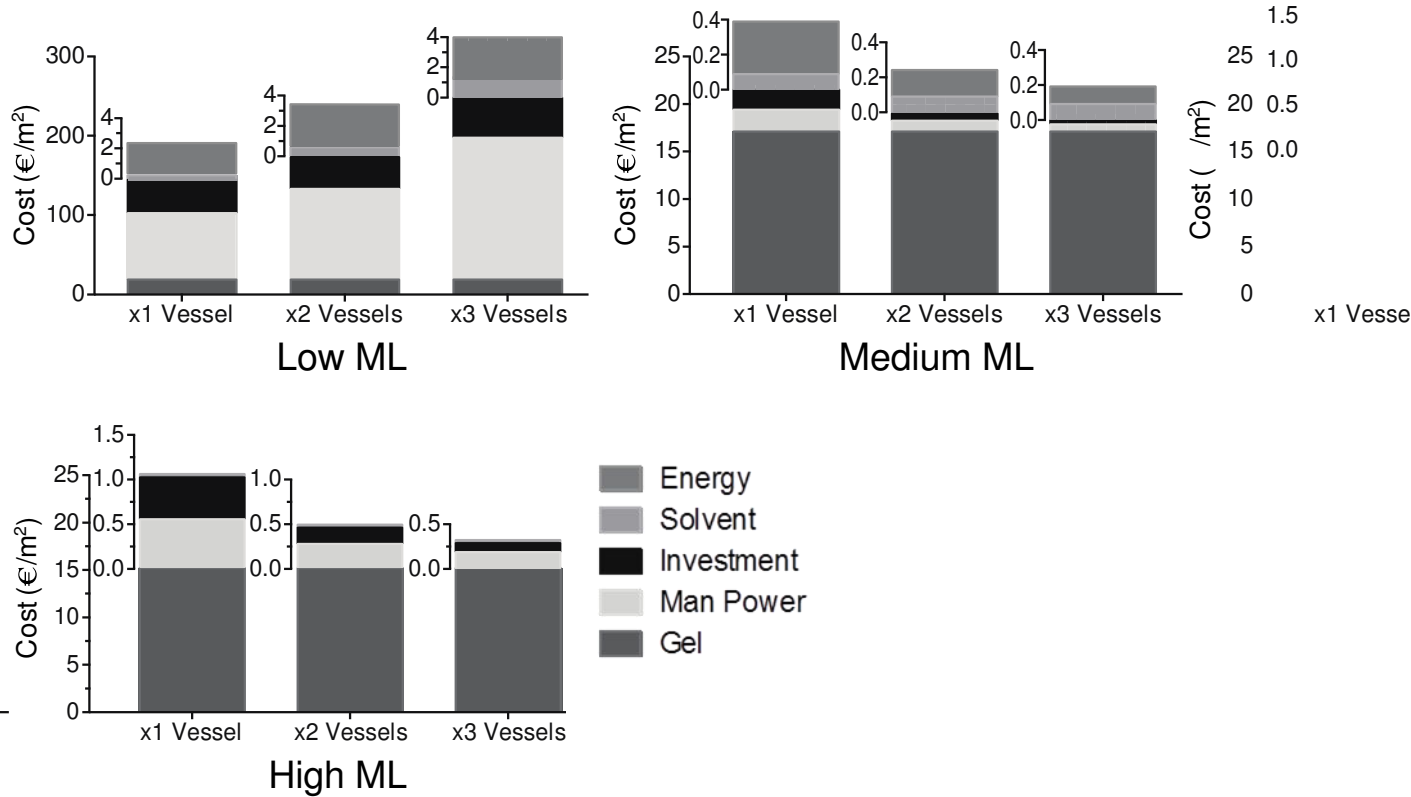


Figure 3.11. Cost contribution on aerogel blankets at different MLs for TEOS based materials.

Considering the production of other samples based on the same precursor, the cost reduction is comparable to the observed on the 10mm thickness blanket. Figure 3.12 discloses the cost reduction of different aerogel product from a similar precursor (i.e. TEOS) using the same system of vessels (i.e. 1 vessel system). Comparison of two type of blanket manufacturing (10 mm and 5 mm thickness) and granular aerogel (2 mm main particle diameter) is displayed.

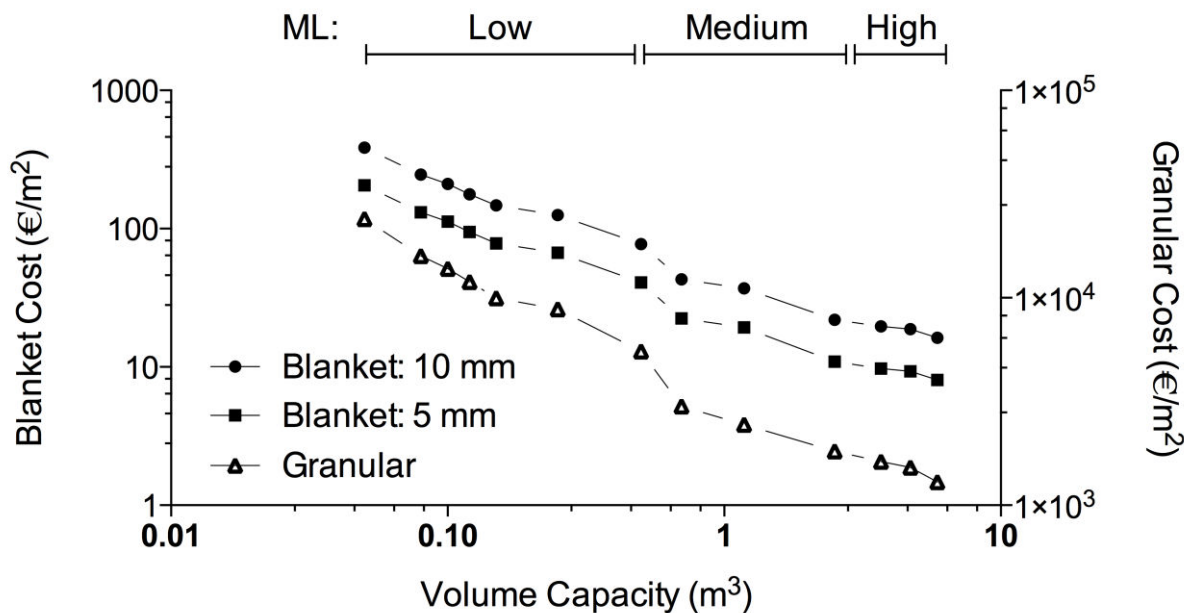


Figure 3.12. Production costs for different aerogel products.

It can be observed that cost of 5mm thickness blankets are below the half of the cost of 10 mm thickness. This evaluation could be erroneously interpreted for 5mm thickness blanket as the most suitable thickness for production, applying a double layer in the application. Practically, 5mm thickness conveys a higher labor not indicated in this study.

3.6. CONCLUSIONS

Design and construction of a tailored 0.2 m³ supercritical aerogel dryer plant has been achieved based on the process simulations carried out. Optimized Pilot Plant allowed producing up to 1.3 m³ of silica aerogel product in granular form, 120 silica reinforced boards (400x400x20 mm³) and ca. 50 silica monoliths (350x350x15 mm³). Low manufacture of diverse aerogel product was then validated for the different European founded projects.

Techno-economical study of the production of aerogels was performed in order to disclose the costs and production capacities obtained at the divers manufacturing levels. Strong cost reduction is achieved by increasing the volume capacity of the equipment. Regarding to several vessels, this reduction is achieved at medium and high manufacturing levels compared to a single vessel system which is more suitable for low levels. Production of different products was also accomplished. For blankets manufacturing, the reduction of thickness by half conveys a higher impact in the drying cost decrease, however this concept is partly incorrect since extra labor costs are not included in the study.

Cost contribution on the aerogel manufacture reveals that the heaviest burden is caused by the precursor cost, becoming this fact more remarkable at medium and high MLs, where reaches up to 95% of the total cost of production. This circumstance expresses the highly necessity to find low cost precursors at industrial scales.

REFERENCES

1. Anderson, J.D., *Fundamentals of aerodynamics*, 2001, McGraw-Hill, Boston, Massachusetts.
2. Swartzendruber, D., *DARCY'S LAW*, in *Encyclopedia of Soils in the Environment*, D. Hillel, Editor 2005, Elsevier: Oxford. p. 363-369.
3. Özbakır, Y. and C. Erkey, *Experimental and theoretical investigation of supercritical drying of silica alcogels*. The Journal of Supercritical Fluids, 2015. **98**(0): p. 153-166.
4. Wong, J.C.H., et al., *Mechanical properties of monolithic silica aerogels made from polyethoxydisiloxanes*. Microporous and Mesoporous Materials, 2014. **183**(0): p. 23-29.
5. Perrut, M., *Supercritical fluid applications: industrial developments and economic issues*. Industrial & engineering chemistry research, 2000. **39**(12): p. 4531-4535.
6. Núñez, G.A. and J.M. del Valle, *Supercritical CO₂ oilseed extraction in multi-vessel plants. 2. Effect of number and geometry of extractors on production cost*. The Journal of Supercritical Fluids, 2014. **92**: p. 324-334.
7. Green, D.W., *Perry's chemical engineers' handbook*. Vol. 796. 2008: McGraw-hill New York.

Chapter 4

STRATEGY FOR AEROGEL MANUFACTURING DEVELOPMENT

EXECUTIVE SUMMARY

Building and industrial insulation business is a huge market of over 1,000 billions € covered by non-effective materials. In the best cases is required several centimeters of thickness to perform an essential insulation.

AEROGEL is a new nanoporous material with the best thermal insulation performance in ambient conditions. Compared with available materials, only the 15% of the thickness is required for the same thermal insulation factor, plus an extra of acoustic protection not reached by the commercial options. This aerogel material has also great applications for the technology of the future of automotive and aerospace market and that it's willing to be brought to next step on the manufacturing.

This document emphasizes the high interest and benefits of the possession of effective large-scale production equipment as the key to cover a big part of the demand of aerogel at an European scale. For that task the present company joins a group of experts with the knowledge and the experience in both Aerogel synthesis and supercritical drying process. The present business opportunity intent to be an investment on the proof of manufacturing concept towards the industrialization of aerogels products.

What it is then here proposed is the development of a manufacturing line of Aerogel-based materials with a price similar to the common insulation material. The main application would be the renovation of existing buildings (about 80% in Europe were built before 1981) and industrial insulation, especially pipe insulation. The secondary market would be focused in the Aerospace insulation where aerogel products compete against the common used material (MLI) with a 11% lighter and 36% cheaper, being also the solo company to manufacture it in Europe.

Mission:

- Supply high quality aerogel products at a reduced cost.
- Provide implemented products for different applications.
- Offer research services to develop new applications and markets.

The investment for this business adventure will be performed in two rounds, a first one up to 1 million € for the establishment of the laboratory and start-up of the existing pilot facilities; and a second one after validation of final product manufacturing to build the semi-industrial plant to acquire a 8% of the market. The present business will be profitable in the third year obtaining a global pay-back of 6 years.

Key to success:

- Highly skilled team with more than 25 years of experience and more 10 successful projects in the different technologies involved in the aerogel business.
- Optimized drying process. High manufacturing cost reduction.
- Improved properties of final product by innovative synthesis.
- Well established Aerogel network in Europe.

4.1 COMPANY DESCRIPTION

The new proposed company (hereinafter *NewCo*) is a consequence of the strategic combination of several experts in the underlying technologies in producing aerogels. They all share the responsibility of working to provide a technology that will contribute to the benefit of today's society and our environment. With this objective, the *NewCo* aims to implement a production of aerogels at low cost and high quality, promoting the comprehensive introduction of this superinsulator in the industry.

The *NewCo* will focus their activities into bring the current aerogel development to the next level of production since their manufacturing process will decrease the bottleneck-cost of the last two decades, the supercritical drying process. The own developed technology is able to manufacture aerogels with the maximal quality at a reduced cost.

The headquarter & product development center of the *NewCo* will be located in the facilities of Separex S.A.S. as part of a Joint Venture. The *NewCo*'s expected facilities includes an equipped chemical laboratory for the development and characterization of nanoporous materials and implemented lab-scale equipment for supercritical drying of high porosity materials. For scaled development, the group will be equipped with a pilot-scale supercritical drying plant for processing products and further industrialization studies.

The interdisciplinary group is initially comprised by experts in the field of technology: sol-gel science, supercritical technology and aerogels drying processes; as business development. Their background has nearly a ten of European projects which have participated as managers, more than a dozen successful private projects and over 25 years of experience in various fields of this technology.



Figure 4.1. SEPREX S.A.S. Facilities in Champigneulle France.

4.2. MARKET ANALYSIS

Due to their “abnormally” high nanoporosity, aerogels are firstly considered for thermal insulation. But, other specific applications are also becoming attractive in high-tech systems.

4.2.1. HISTORY

Utilization of supercritical CO₂ as drying fluid instead of alcohols makes the process much more secure, as CO₂ is non-explosive and allows to proceed at lower reaction temperatures, close to room temperature. On this basis, some companies such as BASF, Henkel, Thermolux, Aerojet, and Airglass developed large-scale production. For experimental purposes, BASF manufactured aerogels in granular form instead of rectangular blocks in the early 1990s, using sodium silicate as precursor dissolved in an acidic solution that is sprayed through a nozzle. BASF produced these aerogels under the trade name "BASOGEL" until 1996.

Along the 90ies, intensive research was dedicated to developing simpler and cheaper production methods in order to reach commercially interesting materials. For this reason, it was investigated how to bypass the most costly step, the drying, by using current atmospheric pressures conditions. Synthesis methods and a drying process under atmospheric pressure providing material with lower properties but at much affordable cost. In particular, companies like Hoechst and Nanopore (USA), implemented this new method which soon led to first successes.

In the early 90ies, Siemens Axiva (part of Hoechst AG, later Aventis) developed a new process based on conventional drying for large-scale production of aerogels. Moreover, in order to optimize the mechanical material properties, they developed a specific forming process. The US company Cabot acquired this Sanofi division, gaining the patent rights and taking advantage of a pilot plant in which the process had already been tested at a significant scale, and first samples were produced. After intensive testing, in 2003 Cabot built up a plant with a capacity of 10,000 Tons per year near Frankfurt (Germany).

The main competitor of Cabot is Aspen Aerogel. The history of Aspen Systems starts in 1984 and many patents on CO₂ drying process (Tewari and Hunt) were filed. In 1993, Aspen Systems started a contract with NASA for the development of aerogels for space application. After manufacturing aerogel monoliths, in 1995, Aspen Systems developed a flexible aerogel blanket insulator for Space Suits, consisting in a fibre matrix within the sol-gel. In 2001, Aspen Aerogels expanded its facilities in parallel with the market. Since the expansion of the plant, the sales were growing steadily while its net losses have been shrinking. It had \$43.2 million in revenue in 2010, up from \$28.6 million the previous year. In May 2014, Aspen Aerogels succeed with their second attempt to launch an IPO with an anticipated price per share of \$14 to \$16, which is drop to \$10 at their open.

4.3. PRESENT AND FUTURE

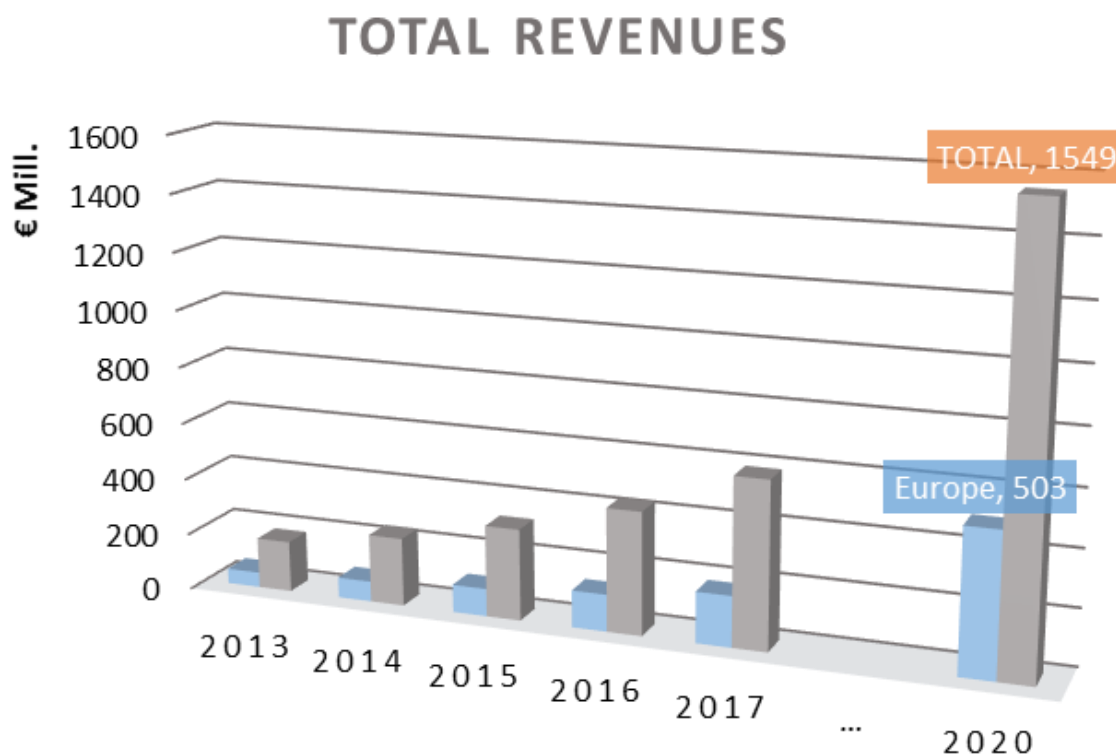
The market of aerogels has been considered small and only a limited number of manufactures play an important role. However, latest advancements on the manufacture have induced the so-called “third revolution” on aerogels. Table 4.1 emphasizes the current European weakness and the dominance of North America.

Table 4.1. Major companies involved in Aerogels production.

Company	Country	Annual Revenue*	Comments
Aerogel Composite, LLC	USA	\$1-10 mil	
Aspen Aerogel, Inc. ASPN	USA	\$10-50 mil	Joint collaboration in the IEA Annex 65
Cabot Corp. (Aerogel section) CBT	USA	\$10-20 mil	Joint collaboration in the IEA Annex 65
Taasi Aerogel Technologies	USA	\$1-10 mil	
Thermablok Inc.	USA	N/A	
Enersens	FR	N/A	Joint collaboration in AEROCOINs project
American Aerogel Corp.	USA	\$1-10 mil	
NanoPore Inc.	USA	\$1.8 mil	
MaeroTech SDN BHD	MALAYSIA	N/A	
Allison Aerogel	CHINA	N/A	
Nano Hi-Tech	CHINA	N/A	
Active Aerogels	PORTUGAL	N/A	Joint collaboration in AerSUS project
Airglass	SWEDEN	N/A	Joint collaboration in HIPIN project
Svenska Aerogel	SWEDEN	N/A	

* Revenue figures may include income generated by other products and operations

The global market for aerogels grew from the €67 million in 2008 to the valued €180 million in 2013. The most recent studies expect a total revenue of €1,500 million by 2020 with a Compound Annual Growth Rate (CAGR) of 35 – 40 % (Clark, 2014).

**Figure 4.2.** Total revenues of Aerogel manufacturing.

Blanket aerogel is and would be the largest revenue-generating segment in the overall aerogel market by form type, through 2020. This segment is expected to reach €515 million by 2020, from 2013 market value of € 90 million, at a CAGR of 33.6% during 2014-2020.

Major factor contributing for this growth is applications in oil & gas industry for piping insulation purposes. Particle/powder aerogel form is the second largest revenue-generating segment, which is projected to generate revenue of €450 million by 2020, from 2013 market value of €46 million, at a CAGR of 39% during the forecast period. This is mainly due to convenience offered by this form while developing coatings. The fastest growing segment observed in the market study is panel form of aerogel with CAGR 41%.

Consumption of blanket form of aerogel was highest in the year 2013, which was estimated to be 4.6 million m² and is expected to reach 36 million m² by 2020. Granular/powder form is second leading segment, which is expected to reach the adoption of 21,000 Tons by 2020 from the 2013 market adoption of 2,500 Tons with CAGR of 37.4% during the analysis period. Panel form of aerogel is expected to grow with highest CAGR of 45.6% during the forecast period.

High production cost is the primary restraining factor for this market, as the burden eventually slides towards the consumers. Moreover, the industries such as petroleum, construction, power generation, etc. are vulnerable to cross-boundary economic conditions and hence, the dependent markets such as aerogel face sales side pressure in adverse economic conditions. On the other hand, the global aerogel market has numerous opportunities in future.

The degree of novelty of the technology itself is considered to be low, but the product potential may be classified as high. The key factor for commercial success is an economic production of the aerogel material. However, in the medium term, aerogel materials could achieve a significant share of the global market for thermal insulation products.

Within geography markets, North America was the largest revenue-generating region market. European region is the fastest growing geographical segment with a CAGR of 38.4% during the later years. European governments' green initiatives are pushing the market growth by catalyzing the need of building and industrial insulators.

Though aerogel is turned out to be a better-insulation solution compared to conventional material, manufacturers have to increase the product price to meet their production cost, which is still at the higher side. Therefore, the high cost results high threat of substitutes. Top investment pocket analysis evaluated building insulation as the most promising sector for investments in future. This market possesses huge growth potential; however, cash flow in this sector at present is comparatively low. Although the market is dominated by the conventional insulation solutions, aerogel manufacturers are expected to have increasing share with the segment during the coming period.

4.4. APPLICATION BY SECTORS

Here below will be more detailed the characteristic and market of each real application of aerogel-based material.

4.4.1. CONSTRUCTION

With the absolute need to save energy and reduce CO₂ emissions, building insulation represents an immense market worldwide, both for new constructions and for renovation.

Buildings in Europe account for approximately 40% of the total global energy demand and hence come with a CO₂ footprint of a similar magnitude. The main target for the Intergovernmental Panel on Climate Change (IPCC) is to reduce the CO₂ emission by 80% by 2050 (World Business Council for Sustainable Development 2014). For that reason and given the relative weight of existing buildings (70-80% of buildings in Europe were built before 1981 (International Energy Agency, 2014)) one of the simplest ways to achieve this “energy performance” target is to reduce their energy consumption by decreasing heating and cooling energy demands.

How will that affect to the aerogel business? This task can only be reach with aerogel-based insulation materials. This means that even at higher cost, aerogel will be applied in the insulation of retrofiting of existing building as well as in new construction. To give an appraisal of this huge market, we could remind that the energy consumption of buildings in central Europe is around 20 liters of heating oil per square meter per year, whilst the current standards for energy efficient buildings is about 7 liters and pilot projects are ready being implemented for “3-litre houses”.

In Figure 4.3, the different insulation materials used for buildings are compared. This data can give an idea of the direct secondary benefit of the aerogel: The saving in space for the same performance of insulation is greatly persuasive.

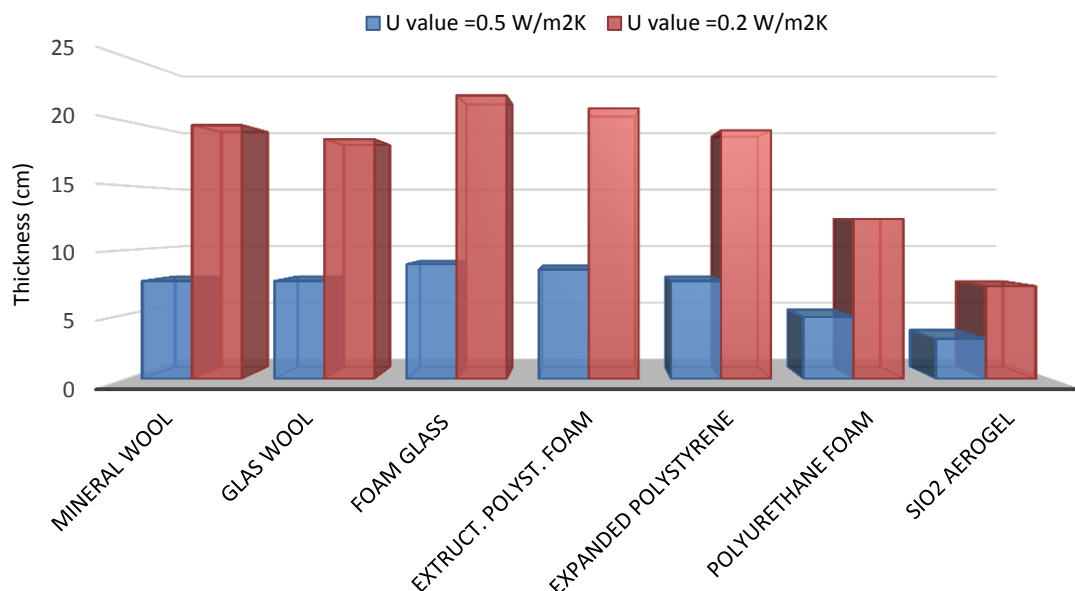


Figure 4.3. Layer thickness of building insulation material required to reach a U value of 0.5 and 0.2 W/m²K (AEROCOINS project)

Aerogel in construction can be applied as common insulation materials in form of panels or blankets, but also more convenient as an additive. In this approach, granular and powder aerogels can be inserted in cement, plaster and paints. Obtaining advantageous benefits beside the high thermal resistance provided, as the reduction of the total weight of the component.

4.4.2. AEROSPACE

A first rough splitting of these technologies depends on the field of application, mainly if the mission is mainly in an almost vacuum environment (satellite or space probe) or if there is an atmospheric environment, with presence of gas pressure (launchers, “on-surface” operations with landers or probes on planetary bodies like Mars or asteroids).



Figure 4.4. Satellite prototype insulation based on encapsulated aerogel (AerSUS project).

Multi-Layer Insulation (MLI) is the most used thermal insulation material for space applications. It is composed by multiple foils, with low emissivity, separated by polyester, resulting in blankets that impede the radiative heat exchange. It is clear that MLI’s best application is in space environment (no atmospheric conditions) although it is also used in ground test facilities. Aerogels appear as the greater potential next generation material for the thermal insulation in aeronautic applications. Reduced integrated cost and time, grounding, and modelling errors have been pushing for alternative solutions to MLI and other insulating materials. Moreover, several studies (Sun, Wu, Zhang, Xu, & Jiang, 2009) reveal that for the same thickness of insulation, the aerogel materials perform almost as the 30 layer MLI while being 11% lighter, and that the aerogel was 48% less labor intensive and 36% cheaper.

Table 4.2. Properties of aerospace insulation materials (AerSUS project).

Material	k (mW/mk) (p bar)	k (mW/mk) (low p)	ρ (kg/m ³)	E (MPa)	σ (MPa) (tens/comp)
Aerogel (Not encaps.)	10-50 (T=300K)	4 -25 (P=10mbar)	19 - 350	0.01-10	0.016 / 0.3
MLI (STC Handbook, 2002)	20-80 (T=300K)	15-80 (P=10mbar)	50 (5mm thick)	-	- / -
Fiberglass –Polyester resin	30-40 (T=300K)	25 (P=10mbar)	9 - 48	15	40/100

Carbon Dioxide (CO₂) (Heinemann, 2002)	17	15 -20 (P=10mbar)	1.97	0	0
PMI Foams (Rohacell 71) (Swiss Composite)	30 (T=300K)	-	75	71	2.7 / 1.5

The major advantage of Aerogel materials in Aerospace applications are the low density and the low thermal conductivity at reduced pressures. However, the lack of flight heritage is the major drawback for the moment together with the cleanness of the integration process.

Table 4.3. Advantages and disadvantages of insulation materials for aerospace applications

Property	Advantages	Disadvantages	Critical
Aerogel	Low density Low thermal conductivity Space qualified Low thermal conductivity Reliable, performance well characterized with considerable heritage Clean	Dusty Lack of flight heritage Expensive Difficult integration / manufacturing Easy to damage	Dirty Integration processes not well developed
MLI	Cheaper than active thermal control Easy to modify and repair during integration Choice of thermal control coating	Long material lead time ITAR issues with certain types of material Blankets are geometry specifics	Highly priced Difficult integration Not suitable for p> 2 mbar (TBC)
Glass Fiber	Low density	Not able to support mechanical loads Only applicable to landers/rovers	
CO ₂ (<0.1mbar)	Available in a number of atmospheres	Only applicable to internal structures No thermal inertia	
Foams: Eccofoam/ Rohacell	Inexpensive Easy to integrate Acceptable insulation in atmosphere	Not self-sustainable Weak mechanical properties	

4.4.3. PRECURSOR

For long, aerogels were considered as adsorbent or catalyst support in relation with their open porous morphology and very high specific area. Nearly all oxides relevant for catalytic applications may be manufactured in form of aerogel. Catalytic metals can be smoothly deposited inside the aerogel structure by vapor diffusion, which considerably increases the active surface. However, applications were hindered by the poor mechanical properties that are incompatible with using such material in packed-bed reactors, and of course in fluidized-bed reactors. Aerogel materials can also improve the flow properties of powders more effectively than conventional additives (such as Aerosil)

Since carbon aerogels are characterized by an excellent chemical stability, they are suitable for robust use in water treatment and extraction. Further applications in the environmental sector may be seen in the area of air purification (air filters) or waste water remediation. Aerogel composites are suitable to efficiently extract gaseous pollutants from air by adsorption. TiO_2 -impregnated aerogels are well suited to remove volatile organic compounds such as benzene from air by adsorption and subsequent photocatalytic cleavage. Hydrophobic aerogels can also be used in wastewater treatment for removal of organic solvents.

4.4.4. ACOUSTIC

The sound speed of aerogels is around 40 to 300 m/s (Forest *et al.*, 2001), with the remarkable peculiarity of decrease by increasing the ambient pressure. As a result of this property, aerogel become an excellent candidate to be applied in noise protection in many different sectors. Especially in the range of low frequencies aerogel offer and improved sound insulation compared with conventional insulation materials. Due to the high insulation effect, the thickness of the insulation layers could be reduced significantly resulting in lower space requirements, and by not needing to be modified, it can be applied together with the thermal insulation.

The applications can go from house and automobile acoustic insulation applications to aircraft, noise barriers and high-quality loudspeakers. It is remarkable that granular aerogels are exceptional reflectors of audible sound and, by combining multiple layers with different granular sizes, average attenuations of -60 dB have been measured for a thickness of 70mm (Ricciardi *et al.*, 2002).

4.4.5. OIL & GAS

The business for oil & gas insulation systems with aerogel-based materials is also one of the biggest and promising markets. It is known that oil typically comes out from subsea wells at temperatures significantly higher than the water temperature. If such oil would cool down as the result of those temperatures, pipelines would become inoperative.

In a similar way, but the inverse situation, Liquefied Natural Gas (LNG) must be maintained in liquid phase at cryogenic temperatures until it reaches onshore refueling terminals. This is a reality not only in offshore terminals, but also in the pipe lines as well. For that reason, oil well lines, LNG tankers and transfer lines must be heated, super cooled or insulated to maintain product temperature, thereby insuring efficient and uninterrupted operation. Aerogel provides then an exceptional thermal conductivity for any oil & gas application with a reduction of diameter between 3-4 times of the commercial insulation material, Figure 4.5. For pipes that can reach several tens of kilometers, this reduction of insulation material can suppose a big investment saving to highly consider.



Figure 4.5. Common insulation of industrial pipes (left). Thickness comparison between normal insulation (lower part), aerogel-based insulation (Aspen Aerogel) (middle part) and row pipe (upper part) (right).

4.4.6. AERONAUTICS

Aeronautics business is maybe the sector with more issues to introduce aerogel materials due to the restrictions and the lack of certification. Besides, many applications are being developed for the future implantation in airplanes and stratospheric vehicles (HIAD Flight project). Aerogel can be used as a thermal and acoustic insulation material for the motors and cabin components, but also as air cleaners (Smirnova *et al.*, 2012).

4.4.7. OPTICS AND INSTRUMENTATION

Silica aerogel monoliths are transparent, but are very difficult to manufacture without any “crack”; it is why the wide use envisaged for window pane insulation. Moreover, they transmit light as a birefringent material. This property is used in *non-linear* optics systems, e.g. Cherenkov radiators (Adachi *et al.*, 2008)

As market needs faster and more powerful computer and memory chips, limits might be soon reached when using the current means of chip design and materials processing. Some aerogels, in particular those made of metal-chalcogenide composites, open up application perspectives in the semiconductor industry. Aerogels made of cadmium selenide quantum dots have been fabricated in a three dimensional network.

4.4.8. OTHERS

Just to cite a rather curious application: Aerogel was used in a NASA space vehicle (Tsou *et al.*, 1995) to trap comet dust that was then collected after return on earth.

Aerogels are also gaining interest in energy storage applications. Due to their large internal surface aerogels are able to quickly incorporate electric charges or ions, to store them at small space and to release them quickly (Pai *et al.*, 2003) (Saliger *et al.*, 1998), graphene aerogels are growing space in this application in parallel at their production growth. Those materials are also investigated as substrates, adsorbents, and chemical concentrators for new sensor applications (such as lab-on-a-chip systems) (Tenorio *et al.*, 2011).

Many studies focus on the application of aerogels as an alternative to the conventional micronization of drugs to provide solubility. Applied in tablet production aerogels may serve both as drug carriers and to improve the flow properties (Gacria *et*

al., 2011) (Masmoudi *et al.*, 2011). However, this application is still far from commercial as acceptance of such materials might be a very long way to prove both efficacy and harmlessness.

As a direct industrial application of Aerogels, thermal packaging systems (American aerogel) can be designed to withstand the abuse of multiple shipments for a long period of time. This robust container is ideal for transporting temperature sensitive products within an organization, say between research and development centers in different countries. This container can be ideal for express shipments of biomedical, pharmaceutical and medical in device products.

4.5. SERVICE AND PRODUCT LINE

Primary: Supply of raw aerogel

Secondary: R&D services and License.

The *NewCo* will have a clear primary service: supply of raw high-quality silica-based aerogel material. *NewCo* will obtain an exclusive license on the product developed by SEPAREX . This service model will be validated when the production scale achieve the volume necessary to decrease the price to the target value. Samples will be available before for demonstration and optimization for final applications in close collaboration with the partners.

The secondary service will be R&D and license. This service will be considered from a specific implementation in the process to a full research program of a specific material or application. License will be awarded to certain products which application and manufacture will be limited.

At the early stage of the *NewCo*, the service presented will be shared from 20:80 for primary and secondary service respectively. After second investment round, the service share will be changed to 80:20 for primary and secondary service, respectively. This change will be produced by the synergy of both increase of production capacity and consequence of the intense application development in close collaboration with the clients.

4.5.1. PRODUCTS & APPLICATIONS

The main product to be developed will be silica-based aerogel in different shapes depending on the area of application. The possibility of developing organic aerogels will be considered for specific applications but its manufacture will be limited and may submit to exclusive licenses.

In Table 4., a relation between the shape and the nature of the aerogel-based material developed is disclosed. This selection has been made in base on the final applications, properties and effective production cost (synthesis and drying).

Table 4.4. Aerogel Nature vs. Shape

	<i>Inorganic</i>	<i>Organic</i>
<i>Powder</i>	X	-
<i>Granular</i>	X	-
<i>Monolith</i>	X	X
<i>Blanket</i>	X	-

❖ Powder

This product can be produced as secondary sub-product from the treatment of granular ones. The main particle size is between 1 – 500 μm with an apparent density around 90 kg/m^3 . Its nature is hydrophobic and opaque.

The direct application of the raw silica powder can cover from oil or water absorbers, thickening agents and thermal insulation to cosmetics and coated paint uses.

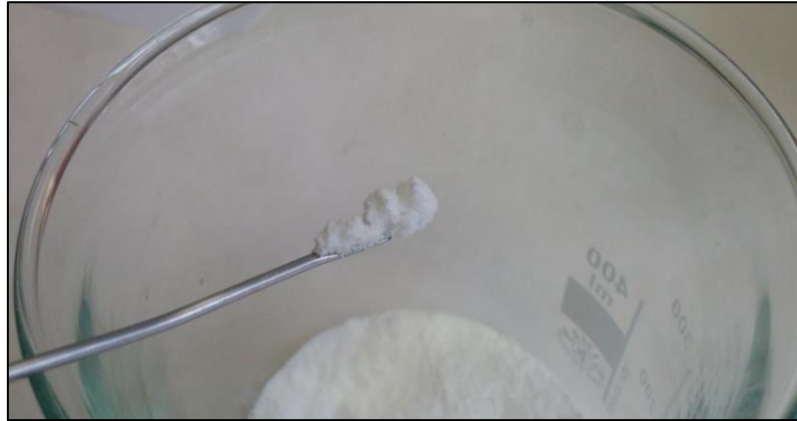


Figure 4.6. Powder aerogel sample.

❖ Granular

Granular aerogel products can be produced from 0.5 – 2 mm particle size with a relative low production cost. The specific density varies from 60 to 120 kg/m^3 depending on particle size and package.

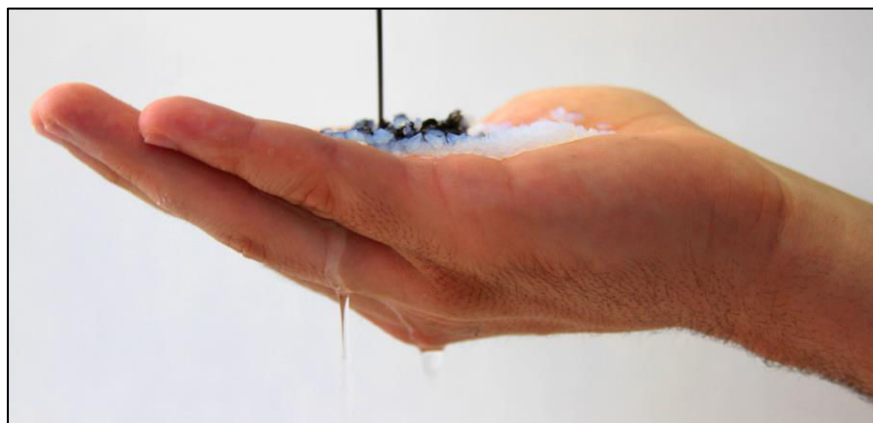


Figure 4.7. Granular aerogel absorbing oil from water.

The granular products are hydrophobic and the light transmittance of the final material can reach from opaque to up to 80%.

The direct main applications of this product are the thermal & acoustic insulation and skylights. Encapsulated in different covertures, they can be directly applied over oil & gas pipes, house insulation and translucent windows.

Other important application area for base inorganic silica aerogel are as adsorbents, fillers and air cleaners in specific close environments as airplanes cabins. Modifying the synthesis and adding some metallic or functional groups, the same granular aerogel can be applied from catalyst, drug delivers, and waste-treatment agent to batteries and sensors. Such modification is not costly and the drying process keeps being the same, for a final product with a very high added value.

❖ Monolith

The *NewCo* aims to be the first major supplier of monolithic inorganic aerogels. This shape has always been restricted to a very small dimension due to the difficulty of the manufacture. Conversely, the production method used by the *NewCo* will allow supplying such product.

The main properties of the inorganic monoliths are described in Table 4.5.

Table 4.5. Inorganic monolith's main properties.

Properties		Values
Thermal conductivity	W/mK	14
Density	kg/m ³	150
Modulus of rupture (MOR)	MPa	0.02
Pore diameter	nm	20

Due to the high transmittance of this aerogel, it could be also implemented as glazing systems for buildings and optical instrumentations.

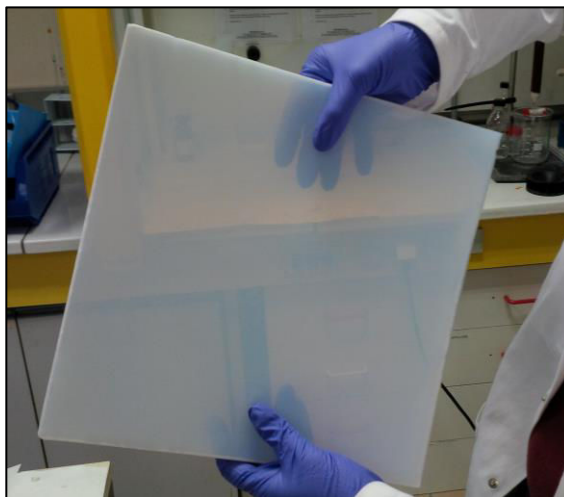


Figure 4.8. Inorganic monolith panel.

❖ Blanket

Blanket is the major product in the market due to its versatility in the different applications. They are composed by inorganic aerogel reinforced by a fiber matrix (organic or inorganic). The synergy results in an extremely flexible material that can be applied for the thermal insulation of different bodies without no restriction of shape. Blankets are hydrophobic and opaque.



Figure 4.9. Inorganic aerogel board (left) and blanket (right).

The *NewCo*'s blanket product are designed to have an extremely limited dust release since it is the major drawback of available products, conferring a major add value in real applications. Thermal conductivity of the flexible product is below 16 mW/mK and a density of 150 Kg/m³.

The main application of blanket products is in industrial insulation, mainly in pipe insulation as well as in boilers. The reduction of thickness and avoidance of common issues (e.g. Degradation, CUI ...) are the main benefit of the use of aerogels in this application.

In Table 4.6, a relation of the most extended applications and the desired shape of the material to be used is described.

Table 4.6. General Aerogel applications and final manufacture.

■ Not applicable. □ Applicable.

Application		MONOLITH		GRANULAR		BLANKET
		Encapsulated	Not Encap.	Encapsulated	Not Encap.	
House / Buildings	Thermal insulation	□	■	□	■	□
	Acoustic insulation	□	■	□	■	□
	Lightweight construction material	■	■	□	□	□
	Skylights	□	■	□	■	■
Aeronautics	Thermal insulation	□	■	■	■	□
	Acoustic insulation	□	■	■	■	□
Aerospace	Thermal insulation	□	■	□	■	□
	Acoustic insulation	□	■	□	■	□
Energy / Environment	Supercapacitor / batteries / fuel cells	■	□	■	□	■
	Waste treatment	■	□	■	□	■
	Catalyst	■	□	■	□	□
Biomedical	Drug deliver / hygiene / cosmetics	■	■	□	□	■
	Medical implants	□	□	■	■	■
Others	Shock absorbers	□	□	□	■	■
	Adsorbents / additives / fillers	■	□	■	□	■
	Sensors / optics	■	□	■	□	■

4.6. COSTS AND SALES

The key for a strong and successful aerogel manufacturing release in a variety of high quality products at a reduced cost, covering all the nature of such material: powder, granular, monolith and blankets. Each one needs a special synthesis and treatment prior and after the drying. Here below, the cost for each synthesis is analyzed.

4.6.1. RAW MATERIAL. INORGANIC AEROGEL

Inorganic aerogel manufactured will be based on the different synthesis developed by SEPAREX which will be granted to the *NewCo*. Price of related precursor is showed in Table 3.10 from *Chapter 3*. The production of P75E20 based aerogel will be the main target due to the superior properties and its well described characterization. Further internal development will be focused on a second aerogel generation aiming the manufacture of co-polymerized based TEOS and MTMS products. This optimized generation will break the gap between low-cost raw materials based on Sodium Silicate (Na_2SiO_3) which have a limited performance, and the expensive siloxanes.

4.6.2. BLANKET SUPPLY

The *NewCo* works in close association with different blanket suppliers of different nature. Those suppliers are based in Europe and are able to modify their material if it is required in a very short delay. Pre-shape of blankets is also possible.

4.6.3. EXTERNAL SYNTHESIS

In order to cover some certain and selected applications or business, *NewCo* can request the external support from any of the partners related to sol-gel synthesis. They constitute the best network on Aerogel research in Europe.

All of them own high values synthesis procedures that can be exploited through the *NewCo* aerogel manufacturing. The advantage of the *NewCo* is that its supercritical drying process could manufacture a larger range of aerogels materials that cannot be dried by other methods. The cost of the royalties can suppose a rate between a 4 – 6 % of the final sales (Kemmerer *et al.*, 2008).

4.6.4. MANUFACTURING

The manufacturing of the aerogel-based materials is based on the synergy between the equipment manufacturing and an optimized drying process to obtain an economically competitive product. The production will be divided in two stages, a first one based on a Pilot Plant (Low Manufacturing Level) for the validation of product and application; and a later stage, where it will be achieved a production over 500,000 m²/y.

In Figure 3.10 and Figure 3.12 in *Chapter 3*, the cost reduction of the manufacturing by the increase of capability has been exposed for different technologies and products. It is pertinent to notice that with the *NewCo* technology, the reduction of price is achieved at higher manufacturing levels. Hence, Pilot Plant will not aim to sell products but achieve clients. This fact offers a great versatility for both the mass production of raw material and the licenses.

It can be appreciated a strong dependence on the raw material cost when higher volume is considered. Therefore the importance of further implements the raw material

supply with the partners to achieve a much lower price. This policy will be present during the development towards Milestone 3 and 4.

In Figure 4.10, the contribution of each cost to the final price of the Pilot Plant and the Semi-Industrial plant are disclosed.

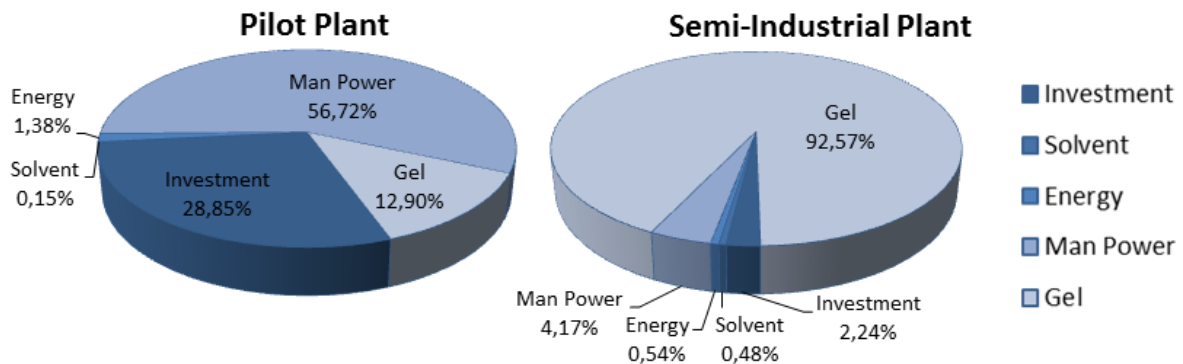


Figure 4.10. Inorganic Aerogel production cost contribution at different scales.

Final aerogel manufacturing in Milestone 4 must achieve a production capacity up to 80% of the maximal capacity of the equipment, producing materials in all shapes. Inorganic flexible blankets and granular are the first material to produce, being the inorganic rigid blankets and panels the second class manufacturing.

4.6.5. SALES

Material sales will be performed by two main procedures: direct sales and close collaboration with final users and on-line/email inquiries. Most of the inquiries in the within the Pilot Scale manufacturing will be proposed as joint development with the client in order to obtain the feedback on the performance and hence optimize the product.

In the semi-industrial stage, sales will be performed automatically while further contact and collaboration will be performed with strategic clients and partners.

4.7. FUNDING REQUEST

The disclosed proposal does not aim to be an investment in research, but an investment on the proof of manufacturing concept for the rapid industrialization of the aerogel products.

In order to validate the business plan's activities described in the present document, the working strategy is divided in four milestones and two investment rounds.

FIRST INVESTMENT ROUND: Up to 300 k€.

Objective: Milestone 1, 2, 3.

Strategic partner: Up to 20%

Own investment: Up to 60%

Public investor: Up to 20%

MILESTONE 1: “SETTING UP I”**OBJECTIVES**

- Creation of the *NewCo* legal entity and launch the laboratory.
- Regulation of contracts of Man Power
- Client portfolio creation

Headquarter laboratories: Separex S.A.S. Champigneulles (FR)

The already available laboratory will allow the rapid installation and startup the activities. The great connection with whole Europe will be highly beneficial.

Required capital: 50 k€

Timing: M3

MILESTONE 2: “TAKE-OFF”**OBJECTIVES**

- Start-up pilot facilities with current technology for low manufacturing validation
- Validation Technology (escalation x100)

Facility 2: Separex S.A.S. Champigneulles (FR)

The existing plant will be installed and commissioned by the *NewCo*. Accommodations and resources will be provided by the Separex S.A.S.

Required capital: 70k€

Timing: M6 – M8

MILESTONE 3: “DEMONSTRATION”**OBJECTIVES**

- Validation of final product manufacturing
 - Engineering of manufacturing (full batches)
 - Optimization for applications
- Validation of process manufacturing
- Client establishment

Validation of final product quality and manufacture will be mandatory to continue for the industrialization. Evaluation and approval of product from client side is mandatory.

Required capital: 150 k€

Timing: M12

SECOND INVESTMENT ROUND: Up to €10 Mill.

Objective: Milestone 4

Strategic partner: Up to 30%

Own investment: Up to 50%

Public investor: Up to 20%

MILESTONE 4: “FIRST INDUSTRIALIZATION”

OBJECTIVES

- Construction of manufacturing line. 5 m³ min. (e.g. Figure 4.)
- Validation process manufacturing
- Validation final product manufacturing
- Validation in final application
- Enter market

The construction of a semi-industrial plant will allow validating the present business plan concerning mass production manufacturing and final targeted price. Enter the market with satisfied client mandatory.

Required capital: 10 Mill. €

Timing: M22



Figure 4.11. Representation of a desired 5 m³ scale (DyeCoo Textile Systems B.V.).

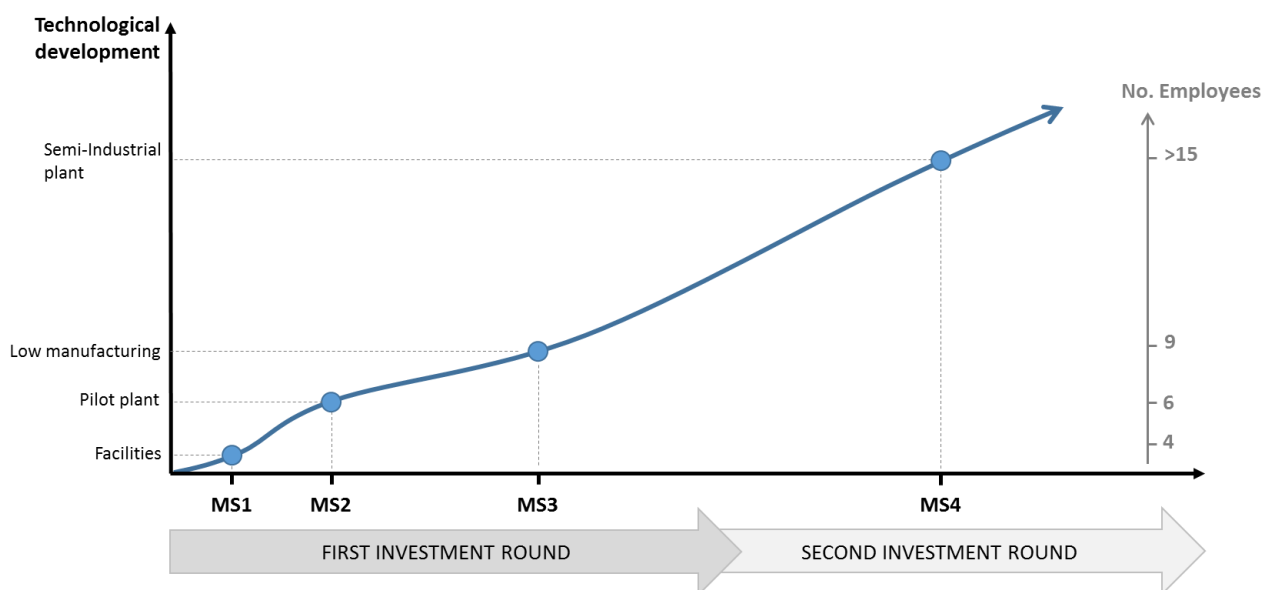


Figure 4.12. Overview of funding request and development plan.

4.8. FINANCIAL PROJECTIONS

For the development of the present Business Plan, all the assumptions are based on a provisional analysis for 3 years with the starting point in 2015.

The required investment for the present business covers the cost of the plant and equipment necessary for the aerogel manufacturing. This amount accounts also the setting up of the business, premises and starting operations.

The following assumptions were established in order to estimate the total revenues:

Table 4.7. Business assumption for 2017 production.

		Blanket	Granular
<i>Annual potential market in Europe</i>	$m^2 - m^3$	>5 mill.	> 1 mill.
<i>Selling price</i>	€/m ² - €/m ³	22 - 25	1,800 – 2,500
<i>Starting Vol. Capacity of Manufacture</i>	%	55	30

The considered market penetration and global annual sales:

Table 4.8. Market penetration and annual sales.

		2017	2018	2019
<i>Production increase</i>	%	10	15	20
<i>Market penetration</i>	%	8	10	15
<i>Annual sales</i>	<i>Blanket</i>	360,000	410,000	500,000
	<i>Granular</i>	200	220	260

4.9. PROFITS AND COSTS

The following profit and costs statements include the two stages of the present proposal: First start-up at pilot scale and a second, industrialization.

The revenues for the 3 years are based in the Annual sales (m² or m³) of the material and services. Within the first two years, sales are based in R&D services and grants while 2017 is expected to be the start-up of the manufacturing of the semi-industrial plant, increasing profit.

Table 4.9. 3 years profits and costs.

	2015		2016		2017		TOTAL
	<i>Pilot plant</i>		<i>Semi-Industrial</i>				
<i>Sales</i>	€	70,000	€	240,000	€	7,080,000	€ 7,390,000
<i>Product</i>	€	35,000	€	90,000	€	6,880,000	€ 7,005,000
<i>Services</i>	€	35,000	€	150,000	€	200,000	€ 385,000
<i>Costs of goods sold</i>	€	40,000	€	190,000	€	4,230,000	€ 4,460,000
<i>Product</i>	€	20,000	€	40,000	€	4,080,000	€ 4,140,000
<i>Services</i>	€	20,000	€	150,000	€	150,000	€ 320,000
<i>Gross profit (loss)</i>	€	30,000	€	50,000	€	2,850,000	€ 2,930,000
<i>Expenses</i>	€	250,000	€	250,000	€	10,400,000	€ 10,900,000
<i>Investment</i>	€	1,000,000	€	15,000,000	€	-	€ 16,000,000
<i>Net profit</i>	€	(220,000)	€	(200,000)	€	(7,550,000)	€ (7,970,000)
<i>Cash</i>	€	780,000	€	15,580,000	€	8,030,000	€ 8,030,000
<i>Gross profit margin</i>		0.43		0.21		0.40	0.40
<i>Net profit margin</i>		-3.14		-0.83		-1.07	-1.08

It is appreciated that the investment for the semi-industrial plant will be done in the first quarter of the third year (2017), while the second round investment is expected to be achieved by the second half of the second year (2016).

Table 4.10. 5 years profits and costs.

	2015		2016		2017		2018		2019		TOTAL	
	Pilot plant				Semi-Industrial plant							
<i>Sales</i>	€	70,000	€	240,000	€	7,080,000	€	7,820,000	€	9,520,000	€	24,730,000
<i>Product</i>	€	35,000	€	90,000	€	6,880,000	€	7,820,000	€	9,520,000	€	24,345,000
<i>Services</i>	€	35,000	€	150,000	€	200,000	€	220,000	€	300,000	€	905,000
<i>Costs of goods sold</i>	€	40,000	€	190,000	€	4,230,000	€	4,229,300	€	4,908,000	€	13,597,300
<i>Product</i>	€	20,000	€	40,000	€	4,080,000	€	4,059,300	€	4,708,000	€	12,907,300
<i>Services</i>	€	20,000	€	150,000	€	150,000	€	170,000	€	200,000	€	690,000
<i>Gross profit (loss)</i>	€	30,000	€	50,000	€	2,850,000	€	3,590,700	€	4,612,000	€	11,132,700
<i>Expenses</i>	€	250,000	€	250,000	€	10,400,000	€	500,000	€	650,000	€	12,050,000
<i>Investment</i>	€	1,000,000	€	15,000,000	€	-	€	-	€	-	€	16,000,000
<i>Net profit</i>	€	(220,000)	€	(200,000)	€	(7,550,000)	€	3,090,700	€	3,962,000	€	(917,300)
<i>Cash</i>	€	780,000	€	15,580,000	€	8,030,000	€	11,120,700	€	15,082,700	€	15,082,700
<i>Gross profit margin</i>		0.43		0.21		0.40		0.46		0.48		0.45
<i>Net profit margin</i>		-3.14		-0.83		-1.07		0.40		0.42		-0.04

In Table 4.10, the 5 years projected costs reveals the change to validation of the business model. Sales of final products will be the main income.

The present business will be profitable from the second half of 2018 with a pay-back time of 6 years.

4.10. RISK ANALYSIS

4.10.1. EXTERNAL ANALYSIS. THREATS AND OPPORTUNITIES

4.10.1.1. *General Environment or Macro-environment*

Table 4.11. Analysis of Macro-Environment.

	Factors	Analysis
Social-Cultural	Labor Legislation	<ul style="list-style-type: none"> ○ Not relevant
	Trade Unions and pressure groups	<ul style="list-style-type: none"> ○ <i>NewCo</i>'s professionals work is well known worldwide for his high impact on aerogel research. ○ <i>NewCo</i> belongs to the main aerogel network in Europe.
	Values and Standards of Living	<ul style="list-style-type: none"> ○ The building insulation with Aerogel will decrease the energy consumption of each family-bill. ○ The European Community is focused into implement Aerogel as the main insulation material for new and old buildings.
Macroeconomic	Policies Sector	<ul style="list-style-type: none"> ○ European Union's new policy will establish superinsulation materials as a requirement for new construction. ○ Slow growth of the European economy can mitigate investment in various sectors of activity.
	Evolution of economic indicators	<ul style="list-style-type: none"> ○ Aerogel global market is expected to grow with a Compound Annual Growth Rate (CAGR) of 35-40% up to 2020.
	Opportunity to buy customers	<ul style="list-style-type: none"> ○ The increase of costumer's purchase encourages the increase of the demand of superior quality's products.
Technologies	Procedures and productive methods	<ul style="list-style-type: none"> ○ Constant evolution of innovative production processes. ○ Growing market of companies dedicated to R&D for specifics applications.
	New Technologies	<ul style="list-style-type: none"> ○ Requirement of insulation market for innovative products and services. ○ Increase of interest on nanotechnology and high-performance technology and products. ○ High European investment in Aerogel research for building insulation.
	Policy in research	<ul style="list-style-type: none"> ○ Increasing private interest in basic research for specifics applications. ○ Extended academic research in basic synthesis and new aerogel-based materials.

4.10.1.2. *Competitive Environment of Industry***Table 4.12.** Analysis of Industry.

Factors	Analysis
Clients/Consumers	<ul style="list-style-type: none"> ○ European SME and large building constructors will be the earlier main client. ○ High-Tech companies for specific applications. ○ Despite the fact that the environment is competitive, there is a great propensity for collaboration between companies. ○ High expectation for the rising of a low-cost and high performance material. ○ The main competitor in Europe will be Cabot and Aspen Aerogel even none of them focus their activity in home insulation.
Competitors	<ul style="list-style-type: none"> ○ A couple of companies are aiming to cover the building insulation sector in Europe but still did not started their activity (ENERSENS, Fixit). ○ There is no competitor capable to make the same product that the <i>NewCO</i> is aiming to produce due to the unique technology advantage.
Sector	<ul style="list-style-type: none"> ○ Main: building and industrial insulation ○ Oil & Gas pipe insulation. ○ Aerospace insulation. ○ Specific High Tech applications

4.10.2. INTERNAL ANALYSIS. STRENGTHS AND WEAKNESS

Table 4.13. Analysis of Weakness and Strengthens.

Factors	Analysis
Historical Situation	<ul style="list-style-type: none"> ○ The <i>NewCo</i> is a SME company with an important background in Aerogel research and supercritical technology.
Economic and Financial Situation	<ul style="list-style-type: none"> ○ The <i>NewCo</i> is a Start-up company which requires of external financial resources for the product development and scale-up.
Information System	<ul style="list-style-type: none"> ○ The <i>NewCo</i> has an important Aerogel Network in Europe composed by researchers and final users. ○ <i>NewCo</i>'s experts participated and organized International and European Congresses of Supercritical Fluids and Aerogel.
Knowledge of Technology	<ul style="list-style-type: none"> ○ <i>NewCo</i> has the knowledge in all the steps of the aerogel manufacturing: <ul style="list-style-type: none"> - Synthesis and applications. - Drying process design and performance. - High pressure equipment design and modification. ○ Exclusive licensed process and products from SEPAREX.
Service Quality	<ul style="list-style-type: none"> ○ When a manufacturing process is developed, certifications of ISO 9001 and 14001 standards are intended to be implemented. ○ Required building and industrial insulation material certification will be also obtained.
Price	<ul style="list-style-type: none"> ○ The main advantage of the business earlier described is the high relationship price/quality that can be offered. This factor is highly superior to the products already in the market due to: <ul style="list-style-type: none"> - Effective production cost. - Supercritical drying quality. - Unique sample size.
Operation Facility	<ul style="list-style-type: none"> ○ The space requirements for the development of the manufacturing activity enclose: <ul style="list-style-type: none"> - Medium warehouse - Standard laboratory - Office

4.10.3. SWOT ANALYSIS

Table 4.14. SWOT Analysis.

		Weakness			Strengthens				
		Company with limited starting financial resources.	Manufactured process still not available.	Not protected IP	Lower price in comparison with the competitors.	High quality services with low prices.	Price in the range of normal insulation materials.	Service customized to client specifications.	Solo company to offer the monolith panels.
Threats	The competitors are strong and have a very high prestige in the sector.	-	-	-	+	+	+	+	+
	Well established competitors in Europe	-	-	-	+	+		+	+
	Difficulties to enter U.S.	-		-	+	+	+	+	+
	Decrease of building construction				+	+	+	+	
	Economic crisis	-	-		+	+	+		
	The building insulation market to enter is huge.	-			+	+	+	+	+
	High investment in equipment	-	-		+				
Opportunities	High investment in building renovation in Europe.	+	-		+	+	+	+	+
	Search of building construction and architect studios partners		-	-	+	+	+	+	+
	High expectation between end-suppliers for a low-cost aerogel material	-	-	-	+	+	+	+	
	Expected low-cost product	+	-		+	+	+		+
	Local partnership	+	-	-		+	+	+	+
	Diversity of products and applications	-	-	-	+	+			+

(+) Interaction positive: Threat or fought exploitation of opportunity.

(-) Interaction negative: Threat or enhanced opportunity wasted.

REFERENCES

- Kistler S.S., Coherent expanded aerogels and jellies, *Nature*, 127: 3211, 741, 1931.
- Jamart-Grégoire B., Allix F., Son S., Pickaert G., Barth D., Degiovanni A.; Elaboration of monolithic organic aerogel from low molecular weight organogel: towards thermal insulators. In: Proceedings of Seminar on Aerogel, Nancy (France), 2012
- Gavillon R., Budtova T., Aerocellulose: New Highly Porous Cellulose Prepared from Cellulose-NaOH Aqueous Solutions, *Biomacromolecules*9, 2008, pp. 269–277.
- Gupta N., Ricci W., Processing and compressive properties of aerogel/epoxy composites, *Journal of Materials Processing Technology*, 198, 2008, pp. 178-182.
- Sun, P.J.; Wu, J.Y.; Zhang, P.; Xu, L.; Jiang, M.L.; Experimental study of the influences of degraded vacuum on multilayer insulation blankets, *Cryogenics*, 49, 719-726, 2009
- AerSUS project. No 284494 (www.spi.pt/aersus/)
- Aspen Aerogel Industrial Insulations Brochure, Aspen Aerogels, May 2010
- Spacecraft Thermal Control Handbook, Gilmore, 2002
- Heinemann 2002, Daten U. Heinemann, ZAE Bayern, 2002
- Swiss-composite, Sales company. www.swiss-composite.ch
- Forest, L.; Gibiat, V.; Hooley, A.; Impedance matching and acoustic absorption on granular layers of silica aerogel, *J. of Non-Crystalline Solids*, 285, 230-235, 2001
- Ricciardi, P.; Gibiat, V.; Hooley, A.; Multilayer absorbers of silica aerogel, In: Proceedings of Forum Acusticum, Sevilla, September, 2002
- Reentry HIAD Flight Demo project (www.nasa.gov)
- www.aspenaerogel.com
- Smirnova, I, Garcia-González, C; Polysaccharide-based Aerogels and their areas of applications, In proceedings of Seminar on Aerogel, Nancy (France), 2012
- Adachi I., Ishii Y., Study of a silica aerogel for a Cherenkov radiator, *Nuclear Instruments and Methods in Physics Research*, 595, pp.180-182, 2008
- Tsou, P.; Silica aerogel captures cosmic dust intact, *J. of Non-Crystalline Solids*, 186, 415-427, 1995
- Pai, RA; Watkins, JJ, "Fabrication of nanostructured metal oxide films by three dimensional replication of structured organic templates in supercritical fluids." *Abstracts of Papers of the American Chemical Society*, 225, U136, 2003.
- Saliger, R.; Fischer, U.; Fricke, J.; High surface area carbon aerogels for supercapacitors; *J. of Non-Crystalline Solids*, 225, 81-85, 1998
- Tenorio, M-J.; Morère, J; Adsorption of PD(HFAC)₂ on mesoporous silica SBA-15 using supercritical CO₂ and its role in catalysis preparation; In proceedings of 13th European Meeting on Supercritical fluids, ISASF, 2011
- Garcia-González, C; Alnaief, M; Smirnova, I; Polysaccharide-based Aerogels: Promising biodegradable matrices for life sciences applications, In proceedings of 13th European Meeting on Supercritical fluids, ISASF, 2011
- Masmoudi, Y; Abdelli, S.; Badens, E.; Supercritical development of sustained drug delivery intraocular lenses; In proceedings of 13th European Meeting on Supercritical fluids, ISASF, 2011
- <http://americanaerogel.com/>
- Kemmerer J., Lu, J., Profitability and royalty rates across industries: Some preliminary evidence, Applied Economics Consulting Group, Inc., Austin, Texas, USA, 2008.
- www.dyecoo.com

GENERAL CONCLUSIONS

The present study aimed to establish the initial guidelines for the techno-economic development of an effective production of aerogels allowing a low cost and high quality product. To achieve this target, it was necessary to have an exhaustive understanding of the existing technology and results derived from each methodology. The study provided a fairly extensive starting knowledge, identifying the benefits and limitations of the three promising approaches: Freeze Drying, Subcritical Pressure Drying and Supercritical Drying; making possible the choice of the technology for the established properties. In this instance the main application is industrial and construction insulation, therefore the properties are mechanical resistance, density and thermal conductivity. It is worth mentioning that for different applications, or more specific, the study will need to be reviewed from the state of the art since other technology might be most appropriate.

The supercritical drying technology was particularly selected because of the numerous benefits related to the quality of the final aerogel's structure as well as the versatility of the process. In the case of Low Temperature Supercritical Drying (LTSCD), it offers a large potential in reducing cycle times and operational expenditures (OPEX). Yet, capital expenditure (CAPEX) would remain higher than for the remainder technologies, however the selection was mainly done as an assumption to be verified at the economic study at larger scale.

The optimization of process operating parameters went through the comprehension and study of the mass transfer mechanisms that govern the process: effective diffusion of solvents through the aerogel's porous medium. This process, described by Fick's second law, was studied for the very first time on aerogels using Raman spectroscopy technology in collaboration with the University of Erlangen-Nuremberg, allowing the outlining of the mixture composition in time and space within the sample. This information might be converted into concentration to calculate the binary diffusion coefficient profile in space and time. The result showed the variation of the diffusion coefficient throughout the process, defining three transition stages. For subsequent scale-up studies, binary diffusion coefficient was computed as $4.7 \cdot 10^{-9} \text{ m}^2/\text{s}$.

Drawing on the versatility of carbon dioxide technology, the functionalization of the aerogel during the LTSCD was a key target in order to diminish the production stages that would require large amounts of chemicals and energy. Therefore, an investigation on the functionalization of aerogel with HMDSO using the supercritical CO₂ as reaction media was performed. Results showed the viability of the process as the tune-ability of the reaction, allowing the control of the hydrophobization rate from humidity-resistant to superhydrophobic. This fact also permits to use lower quantities of chemical (<5% vol.) in comparison to the standard sililation processes (>20% vol.).

Comparing the properties of the hydrophobic aerogel by means of the reaction in CO₂ media with the standard method, it has been observed that in general the degree of hydrophobization is smaller although the reaction was developed similarly. This process is limited to pure silica aerogels, being so far incompatible with aerogels comprising organic precursors such as cellulose. For a better understanding of the process and subsequent

scaling, a study of the composition of the ternary system was carried out for: HMDSO/EtOH/scCO₂ in collaboration with ARMINES. The examination confirmed the solubility boundaries and the appearance of a fourth sub-product: NH₄OH, which has not been included in the present study but should be considered in future analyzes.

Based on the parametrization obtained at laboratory scale, it was performed a scaling up (x100) in a Pilot Plant designed and constructed for the purpose. Integrated to the work of an European granted project, the fluid flow simulation and drying of aerogel for batches comprising <20 aerogel boards (35x35x1 cm³) was performed. Major output comprised the validation of optimal flow as the design of an optimal internal geometry of the vessel. The study also revealed that the minimum process cycle was 5.5 hours.

The optimized manufacturing was validated by producing over 40 m² of aerogel boards. Various quality control methods were developed for the different stages of the process. The characterization of the aerogels properties was conducted to validate both the scaling parameters and product quality. The comparison with similar dried gels produced by Subcritical Pressure Drying technology revealed the justification of the initial assumptions: higher quality product.

After validation of the technology and the assumptions on the product quality, it was performed a techno-economic study of the implantation of different manufacturing levels of aerogels. Production volume and related costs were exposed in order to facilitate the definition of a potential business case. As expected, the reduction of manufacturing costs is proportional to the increasing of plant size.

The major output of this study was the high contribution of the raw material in the final production costs, more specifically the precursor costs. It could achieve up to 80% of the total production costs when high manufacturing levels were considered (>100,000 m²/y).

This fact highlights the absolute need to develop aerogels from low cost precursors, in place of the presently broadly used alkoxisilanes.

Achieving the reduction of production costs while maintaining the high quality of the finished product, a study of the potential market advantage was achieved. Based on the establishment of the semi-industrial production facilities at SEPAREX, the business plan concludes that a production up to 500,000 m² of blankets would require an investment of a straight value of 1 Million €. With a market penetration of 5% annually in industrial and construction insulation markets, this business would acquire a Return of the Investment of 3 years from the beginning of the production.

In conclusion, manufacture of aerogels for insulation applications through LTSCD technology is a clear business opportunity with high growth potential and self-financing.

ANNEXES

ANNEX 1. PREDICTION TERNARY DIAGRAM

A1.1. BINARY MIXTURES

Binary interaction parameters were determined on a selected thermodynamic for the representation of experimental literature data and prediction of the PT envelop. The selected thermodynamic model for the determination of the phase diagram was the software developed by Prosim: Simulis Thermodynamics.

A phi – phi approach was considered to describe the equilibrium condition. The Peng-Robinson Equation of State [1] (PR EoS) was considered (with its generalized alpha function) with the MHV1 mixing rule [2]. The NRTL Excess Gibbs energy model was considered to represent the non-ideality of the mixture.

Equation A1.1 describes the PR EoS.

$$\left(P + \frac{a}{(v^2 + 2bv - b^2)} \right) (v - b) = RT \quad \text{A1.1}$$

where P is the pressure, R the ideal gas constant, T the temperature and v the molar volume. Equations A1.2 and A1.3 describe the MVH1 mixing rules

$$a = b \left[\sum_i x_i \frac{a_i}{b_i} - \frac{RT}{q_1} \sum_i x_i \ln \left(\frac{b_i}{b} \right) + \frac{G_\gamma^E}{q_1} \right] \quad \text{A1.2}$$

With $q_1 = -0.53$

$$b = \sum_i x_i b_i \quad \text{A1.3}$$

Equation A1.4 represents the NRTL Gibbs energy model [3].

$$\ln(\gamma_i) = \frac{\sum_j \tau_{j,i} G_{j,i} x_j}{\sum_j G_{j,i} x_j} + \sum_j \frac{G_{i,j} x_j}{\sum_k G_{k,j} x_k} \left(\tau_{i,j} - \frac{\sum_k G_{k,j} \tau_{k,j} x_k}{\sum_k G_{k,j} x_k} \right) \quad \text{A1.4}$$

with:

$$\tau_{j,i} = \frac{C_{i,j}}{RT}; \quad G_{i,j} = \text{Exp}\left(-\alpha_{j,i} \frac{C_{j,i}}{RT}\right) \quad \text{et} \quad C_{i,i} = 0 \quad \text{A1.5}$$

This model is considered in Simulis Software. For the study, it was considered binary interactions independent of the temperature and an experimental data at 333 K for the determination of each binary interaction parameters.

A1.2. CARBON DIOXIDE (1) – ETHANOL (2) SYSTEM.

Concerning this binary system, we have used the data presented in the paper of Galicia – Luna et al. [4]. The Figure A1.1 presents the result of our data treatment. **¡Error! No se encuentra el origen de la referencia.** presents the deviations. We can also notice that Simulis shows some difficulties to represent the data close to the mixture critical point.

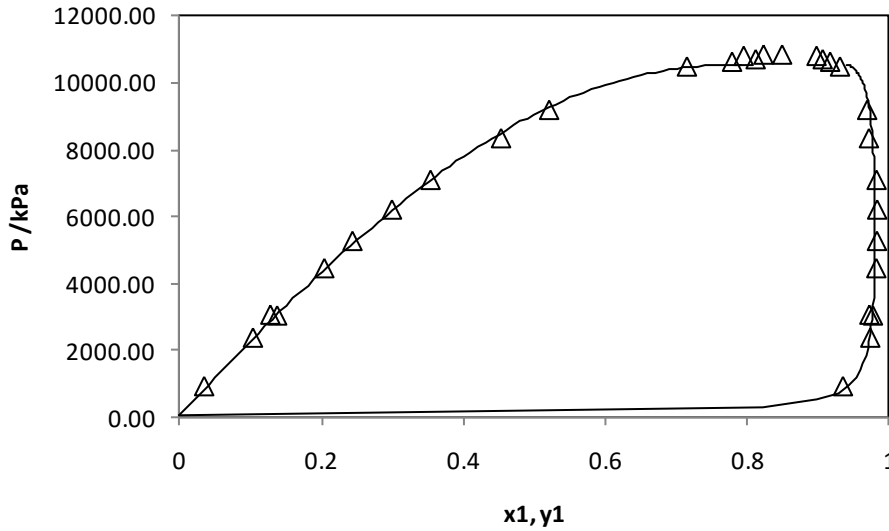


Figure A1.1. Phase diagrams (P-x) for the CO₂ (1) – Ethanol (2) system at 333.82 K. The symbol corresponds to the experimental data. Solid line corresponds to the model calculation.

In order to quantify the accuracy of the model calculations to the experimental data, the deviations, AADU, and BIASU, were determined. The deviations are defined by:

$$AADU = (100 / N) \sum |(U_{cal} - U_{exp}) / U_{exp}| \quad \text{A1.6}$$

$$BIASU = (100 / N) \sum ((U_{exp} - U_{cal}) / U_{exp}) \quad \text{A1.7}$$

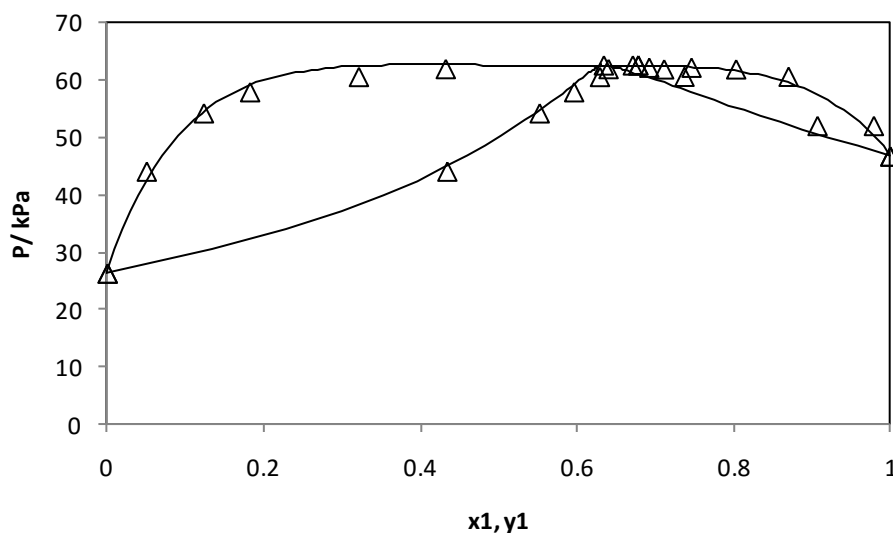
where N is the number of data points, and $U = P$.

These indicators, which give information about the agreement between models and experimental results, are presented in Table A1.1. We can observe that the data are well represented by the model.

Table A1. 1. Relative deviation AADU and BIASU obtained in fitting experimental VLE of CO₂ (1) – Ethanol (2) system at 333.82 K with the model.

T/K	Experimental values					Calculated values					AADP	BIASP
	P/kPa	x1	x2	y1	y2	P/kPa	x1	x2	y1	y2	%	%
333.82	931	0.0344	0.9656	0.9335	0.0665	831	0.0344	0.9656	0.9356	0.0644	11	11
333.82	2382	0.1032	0.8968	0.9721	0.0279	2348	0.1032	0.8968	0.9720	0.0280	1.4	1.4
333.82	3044	0.1373	0.8627	0.9759	0.0241	3072	0.1373	0.8627	0.9763	0.0237	-0.9	0.9
333.82	5272	0.2435	0.7565	0.9815	0.0185	5183	0.2435	0.7565	0.9803	0.0197	1.7	1.7
333.82	4458	0.2038	0.7962	0.9806	0.0194	4421	0.2038	0.7962	0.9797	0.0203	0.8	0.8
333.82	6210	0.2992	0.7008	0.9818	0.0182	6190	0.2992	0.7008	0.9802	0.0198	0.3	0.3
333.82	7096	0.3536	0.6464	0.981	0.019	7093	0.3536	0.6464	0.9793	0.0207	0.0	0.0
333.82	9188	0.5208	0.4792	0.9677	0.0323	9277	0.5208	0.4792	0.9712	0.0288	-1.0	1.0
333.82	10485	0.7151	0.2849	0.9293	0.0707	10458	0.7151	0.2849	0.9485	0.0515	0.3	0.3
333.75	3069	0.1277	0.8723	0.9708	0.0292	2868	0.1277	0.8723	0.9754	0.0246	6.6	6.6
333.75	8342	0.453	0.547	0.9702	0.0298	8502	0.453	0.547	0.9756	0.0244	-1.9	1.9
333.75	10626	0.7787	0.2213	0.9154	0.0846	10536	0.7787	0.2213	0.9409	0.0591	0.8	0.8

A1.3. ETHANOL (1) – HDMS (2) SYSTEM

**Figure A1.2.** Phase diagrams (P-x) for the Ethanol (1) – HDMS (2) system at 333.82 K. The symbol corresponds to the experimental data. Solid line corresponds to the model calculation.

The accuracy of the selected model was evaluated. The Table A1.2 presents the calculated values and the deviations in comparison with the experimental data. *Guzman et al.* [5] was selected as reference data at 333.15 K. The phase diagram is presented in the Figure A1.2. We can observe that the model represent the experimental data. Moreover we can also mention the existence of an azeotrope around a composition of ethanol close to 0.65. This is mainly due to the fact that the two pure component vapour pressure are very close.

Table A1.2. Relative deviation AADU and BIASU obtained in fitting experimental VLE of Ethanol (1) – HDMS (2) system at 333.15 K with our model.

Experimental values						Calculated values					AADP	BIASP
T/K	P/kPa	x1	x2	y1	y2	P/kPa	x1	x2	y1	y2	%	%
333.15	26.2912	0	1	0	1	26.4699	0	1	0	1	-0.68	0.68
333.15	44.1297	0.05	0.95	0.434	0.566	42.3576	0.05	0.95	0.396	0.604	4.02	4.02
333.15	54.3289	0.123	0.877	0.552	0.448	54.4905	0.123	0.877	0.549	0.451	-0.30	0.30
333.15	58.0219	0.182	0.818	0.596	0.404	59.1148	0.182	0.818	0.594	0.406	-1.88	1.88
333.15	60.6884	0.321	0.679	0.629	0.371	62.4951	0.321	0.679	0.628	0.372	-2.98	2.98
333.15	62.0749	0.432	0.568	0.64	0.36	62.6817	0.432	0.568	0.630	0.370	-0.98	0.98
333.15	62.7149	0.634	0.366	0.671	0.329	62.5869	0.634	0.366	0.629	0.371	0.20	0.20
333.15	62.7282	0.678	0.322	0.678	0.322	62.5610	0.678	0.322	0.632	0.368	0.27	0.27
333.15	62.3149	0.746	0.254	0.692	0.308	62.3002	0.746	0.254	0.644	0.356	0.02	0.02
333.15	62.0216	0.803	0.197	0.711	0.289	61.5904	0.803	0.197	0.665	0.335	0.70	0.70
333.15	60.7284	0.87	0.13	0.737	0.263	59.5408	0.87	0.13	0.711	0.289	1.96	1.96
333.15	52.1157	0.979	0.021	0.907	0.093	50.1131	0.979	0.021	0.917	0.083	3.84	3.84
333.15	46.7695	1	0	1	0	46.8364	1	0	1	0	-0.14	0.14

A1.4. CARBON DIOXIDE (1) – HDMS (2) SYSTEM

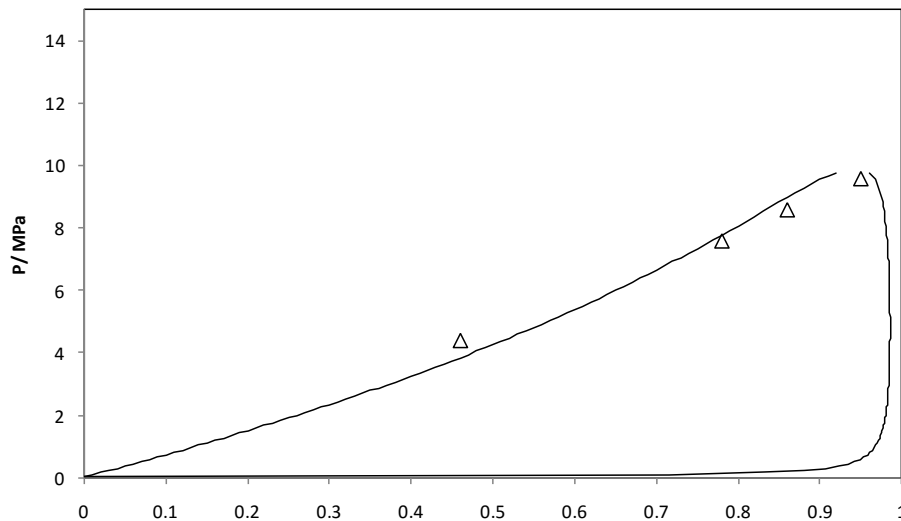


Figure A1.3. Phase diagrams (P-x) for the CO₂ (1) – HDMS (2) system at 333.82 K. The symbol corresponds to the experimental data. Solid line corresponds to the model calculation.

For this system, the data from Sanli et al. [6] was selected as reference at 333.2 K. Even if there are very few experimental data, the phase diagram is typically the one of asymmetric system (gas solvent) if we consider the difference between the two pure component vapor pressure. Concerning the liquid phase, we can consider that we have a Raoult's law behavior with a slight negative deviation (existence of attractive interaction or may be a packing effect).

Figure A1.3 presents the phase diagram. Table A1.3 presents the results of the data treatment (only the data with given liquid phase composition was considered).

Table A1.3. Relative deviation AADU and BIASU obtained in fitting experimental VLE of Ethanol (1) – HDMS (2) system at 333.15 K with the model.

Experimental values						Calculated values					AADP	BIASP
T/K	P/MPa	x1	x2	y1	y2	P/MPa	x1	x2	y1	y2	%	%
333.2	8.3	-	-	0.98	0.02							
333.2	9.2	-	-	0.97	0.03							
333.2	9.6	0.95	0.05			121.6	0.95	0.05	0.95	0.05	-1167	1167
333.2	8.6	0.86	0.14			9.0	0.86	0.14	0.98	0.02	-4.4	4.4
333.2	7.6	0.78	0.22			7.8	0.78	0.22	0.98	0.02	-2.3	2.3
333.2	4.4	0.46	0.54			3.8	0.46	0.54	0.99	0.01	13	13

According to Table A1.3, we can see that the model is not accurate for the representation of the critical point. This can be attributed to the algorithm used in Simulis Thermodynamics.

A1.5. PREDICTION OF PHASE DIAGRAM ON TERNARY SYSTEM

a. Presentation of the parameters.

The Table A1.4 presents the parameters obtained after data treatment using Simulis Thermodynamics (Remark: no Temperature dependence).

Table A1.4. Values of the binary interaction parameters.

Component i	Component j	A _{ij}	A _{ji}
CO ₂	Ethanol	224.1	144.7
CO ₂	HDMS	1035.2	-420.0
Ethanol	HDMS	-209.8	1124.0

b. Definition of PT envelop

Extract from Coquelet and Ramjugernath [7]:

“The Pressure-Temperature (P-T) envelop is a very interesting way to represent phase diagrams. For a mixture (where composition is known), the P-T envelop represents the limits of the phase equilibrium region. An example of a P-T envelop is illustrated in Figure A1.4. The point which corresponds to the maximum of pressure is called the cricondenbar, and with regard to the maximum of temperature, it is called the cricondentherm. Bubble and dew pressures curves are also presented in such a diagram with the critical point. With such a diagram, phenomenon such as retrograde condensation can be easily explained.”

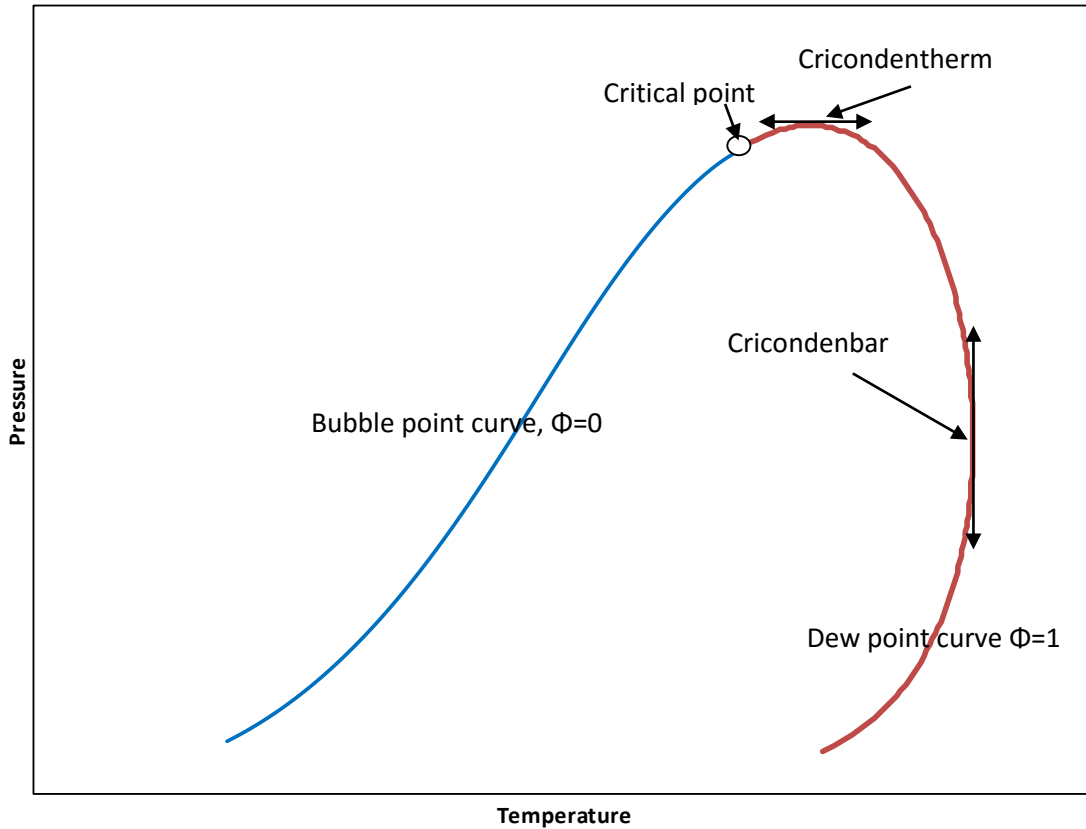


Figure A1.4. Example of P-T envelop of hydrocarbons (C1 to C5).

c. Calculation of the PT envelop

Using the thermodynamic model with the adjusted binary interaction parameters, it was determined the PT envelop of a mixture composed of $z_{CO_2}=0.950$, $z_{Ethanol}=0.045$ and $z_{HDMS}=0.005$.

To solve the model the following functions in excel were applied:

- stCALCriticalTemperatureKij for the determination of the critical temperature of the mixture
- stCALCriticalPressureKij for the determination of the critical pressure of the mixture
- stCALPhaseEnvelopeKij for the determination of the PT envelop

Table A1.5. Calculated bubble and dew point values for the mixture CO₂/ethanol/HDMS (0.9495/0.0472/0.0033)

T/K	P/bar	TVAP									
234.46	10.00	0	344.21	20.00	1	351.30	29.46	1	361.06	78.61	1
239.46	11.93	0	349.21	26.18	1	353.09	32.74	1	360.72	81.89	1
263.21	25.00	0	349.21	26.18	1	354.64	36.01	1	360.26	85.17	1
268.21	28.71	0	349.21	26.18	1	355.98	39.29	1	359.64	88.44	1
269.83	30.00	0	349.21	26.18	1	357.13	42.57	1	358.86	91.72	1
274.83	34.21	0	349.21	26.19	1	358.12	45.84	1	357.87	95.00	1
290.48	50.00	0	349.21	26.19	1	358.96	49.12	1	356.62	98.27	1
295.48	55.89	0	349.22	26.20	1	359.66	52.40	1	355.01	101.55	1
298.79	60.00	0	349.23	26.21	1	360.23	55.67	1	352.78	104.83	1
303.79	66.50	0	349.24	26.23	1	360.68	58.95	1	349.06	108.10	1
306.39	70.00	0	349.28	26.29	1	361.02	62.23	1	344.20	109.44	1
311.39	76.87	0	349.35	26.39	1	361.25	65.50	1	339.06	108.14	1
313.65	80.00	0	349.49	26.59	1	361.37	68.78	1	334.06	104.78	1
318.65	86.86	0	349.76	27.00	1	361.39	70.71	1	331.56	102.46	1
324.90	94.94	0	350.29	27.82	1	361.28	75.34	1	329.06	99.81	1
									327.61	98.17	1
									324.90	94.94	1

REFERENCES

1. Peng, D.-Y. and D.B. Robinson, *A New Two-Constant Equation of State*. Industrial & Engineering Chemistry Fundamentals, 1976. **15**(1): p. 59-64.
2. Michelsen, M.L., *A modified Huron-Vidal mixing rule for cubic equations of state*. Fluid Phase Equilibria, 1990. **60**(1-2): p. 213-219.
3. Renon, H. and J.M. Prausnitz, *Local compositions in thermodynamic excess functions for liquid mixtures*. AIChE journal, 1968. **14**(1): p. 135-144.
4. Galicia-Luna, L.A., A. Ortega-Rodriguez, and D. Richon, *New apparatus for the fast determination of high-pressure vapor-liquid equilibria of mixtures and of accurate critical pressures*. Journal of Chemical & Engineering Data, 2000. **45**(2): p. 265-271.
5. Guzman, J., A.S. Teja, and W.B. Kay, *Vapor-liquid equilibria in binary mixtures formed from hexamethyldisiloxane, toluene and ethanol*. Fluid Phase Equilibria, 1981. **7**(2): p. 187-195.
6. Sanli, D. and C. Erkey, *Bubble point pressures and densities of hexamethyldisiloxane-carbon dioxide binary mixture using a constant volume view cell*. The Journal of Supercritical Fluids, 2013. **74**: p. 52-60.
7. Coquelet, C. and D. Ramjugernath, *Phase Diagrams in Chemical Engineering: Application to Distillation and Solvent Extraction* 2012: Intech.

ANNEX 2. FLUID FLOW SIMULATION

A2.1. SINGLE PLATE CONSIDERATION

Simulation of behavior of one single vertical plate is exposed below. The emphasis of the study is given to a parametric study of velocity, porosity, diffusivity, permeability and viscosity. Parameters considered for this particular case are exposed in Table A2.1.

Table A2.1. Simulation parameters.

Parameter	Units	Values	Range of parameters
Inlet velocity, U	$\text{m}\cdot\text{s}^{-1}$	5.5×10^{-2}	3.6×10^{-4}
Porosity, ε		0.9	0.8 – 0.95
Kinematic viscosity, μ	$\text{m}^2\cdot\text{s}^{-1}$	3.5×10^{-5}	$10^{-6} - 10^{-2}$
Permeability, k	m^2	10^{-10}	$10^{-14} - 10^{-6}$
Binary diffusion coefficient, D_{12}	$\text{m}^2\cdot\text{s}^{-1}$	$6,087\times 10^{-9}$	$10^{-10} - 10^{-6}$

The geometry of the domain and the boundary conditions are shown in Figure 10, left and right, respectively. In red is the area confined for the aerogel, i.e., the porous medium, and in blue is seen medium without porosity. The distance between the vertical walls and the aerogel is equal to the distance between each plate.

The results obtained from these simulations are presented in Figure A2.1, where the left figure presents the stationary velocity profile and right (from left to right) presents the evolution of the concentration of methanol at $t=0$, $t=200$, $t=400$, $t=600$, $t=800$, $t=1,000$ and $t=1,200$ s. The drying time expected for this simulation is approximately 3,800 seconds.

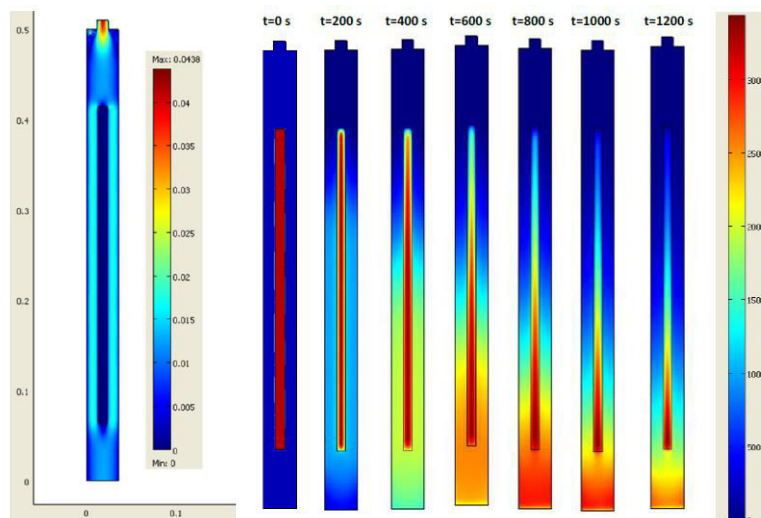


Figure A2.1. Velocity profile ($\text{m}\cdot\text{s}^{-1}$) of single plate (left); Organic solvent concentration [$\text{mol}\cdot\text{m}^{-3}$] evolution of single plate at: $t=0, 200, 400, 600, 800, 1000,$ and $1,200$ s (right).

A2.1. 1. PARAMETERIZATION

The results of this parameterization are presented in Figure A2.2. The red squares are the reference parameters' values of the Separex autoclave; the lines with circles represent the parameterization regarding those reference parameters from literature.

From top to bottom, plots of Figure A2.2 represent the inlet velocity, porosity of the aerogel, binary diffusivity, permeability of aerogel, and viscosity. All parameters in these panels are plotted as a function of time.

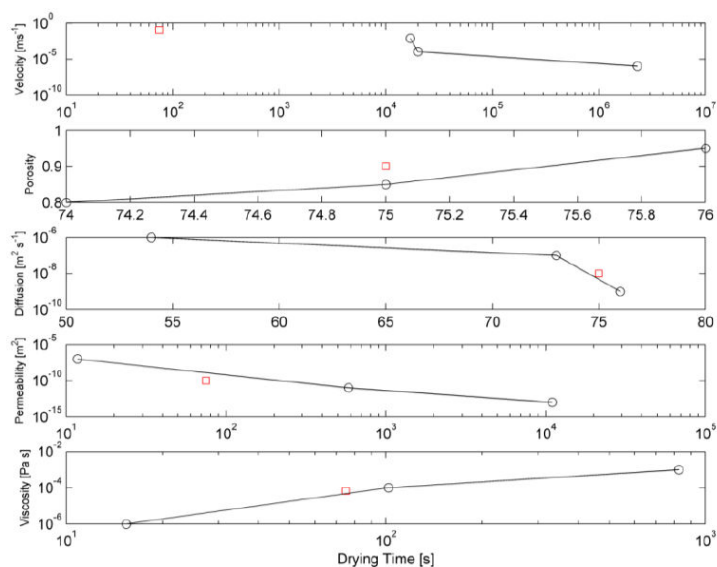


Figure A2.2. Parameterization results. From top to bottom: velocity, porosity, diffusivity, permeability and viscosity as a function of time in seconds.

A2.2. MODULE CONSIDERATION

For the simulation of the full batch drying process in the Pilot Plant, several configurations are simulated in order to test the influence of inlet number and the inlet flow, and to evaluate how these parameters influence the drying time.

The aerogels are displayed in two vertical modules which are able to host around 12 self-supported plates of $35 \times 35 \times 1.5$ cm³ each. Those modules are disposed one over the other with a lapse of 90° from each other. Figure A2.3 shows the individual module of vertical samples and the final display inside the vessel.

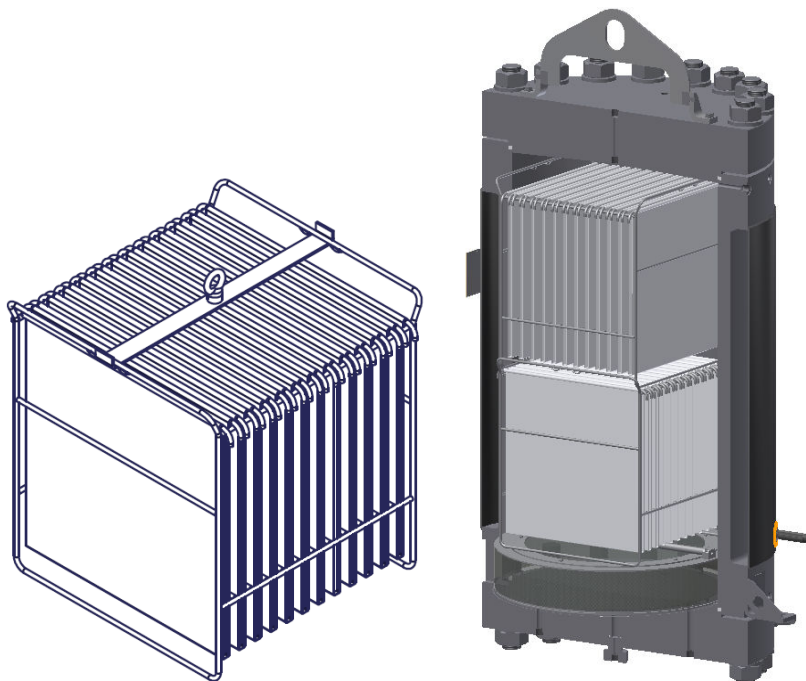


Figure A2.3. Vertical sample holder module (left) and final integration in the vessel (right).

A2.3. ORIGINAL CONFIGURATION

The original configuration consists of the arrangement of the modules containing samples without incurring any change in the internal volume of the reactor. The flow has regarded downstream and transversal to the samples. The modeling parameters are equal to those of Table A2.1.

The obtained results are presented in Figure A2.4, which show the velocity distribution and the concentration of organic solvent at $t=20,000$ s. The expected drying time for this simulation is approximately 6.9×10^5 s.

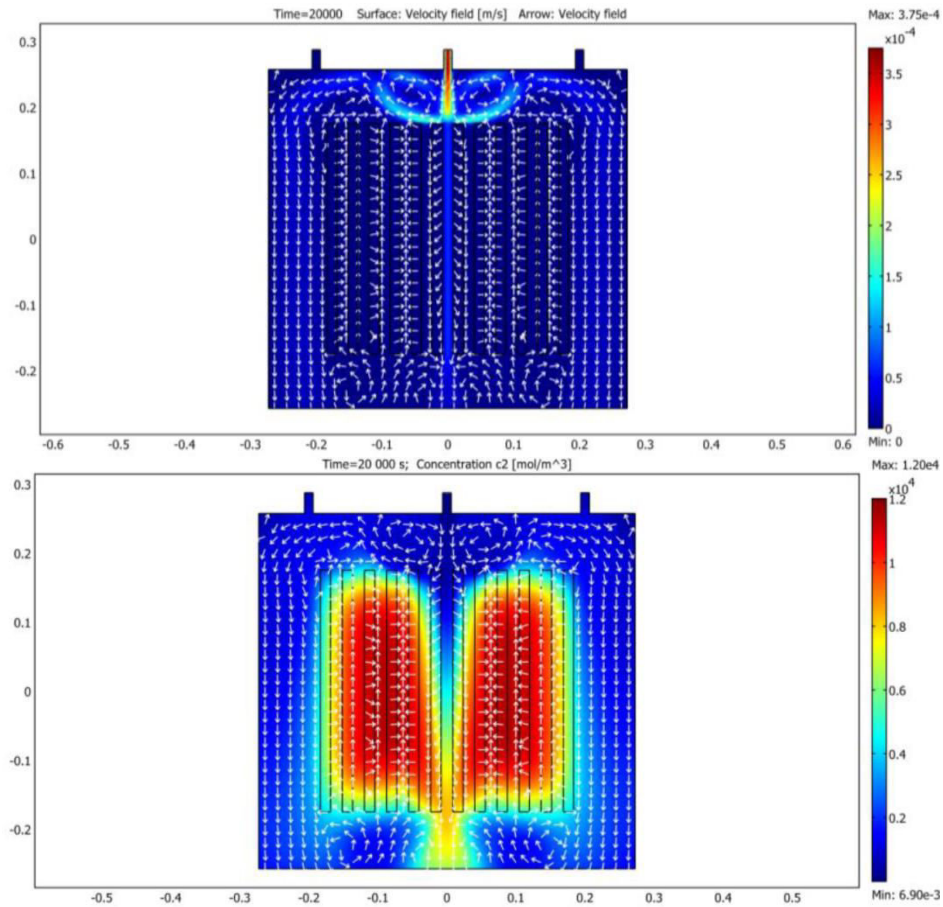


Figure A2.4. Original configuration and single inlet simulation. Velocity profile ($\text{m}\cdot\text{s}^{-1}$) (up); Down: Organic solvent concentration ($\text{mol}\cdot\text{m}^{-3}$) (down).

With this configuration, the velocity between aerogel plates is lower than close to the wall. This fact was expected since there is no restriction to force the solvent to go through the plates. Near the wall, the velocity is zero and is growing in magnitude in the direction perpendicular to the wall, corroborating the no-slip condition. The concentration of organic solvent is decreasing from the center to sideways because of the injection of the CO_2 . The preferred path of the fluid is notable to have an impact on the final drying time.

When three inlets are applied at the same overall flow U_1 , the expected drying time is around 3.69×10^5 s. Velocity within the aerogel plates is lower than the surroundings as the previous case. Concentration of organic solvent is homogeneous in between plates, as shown in Figure A2.5.

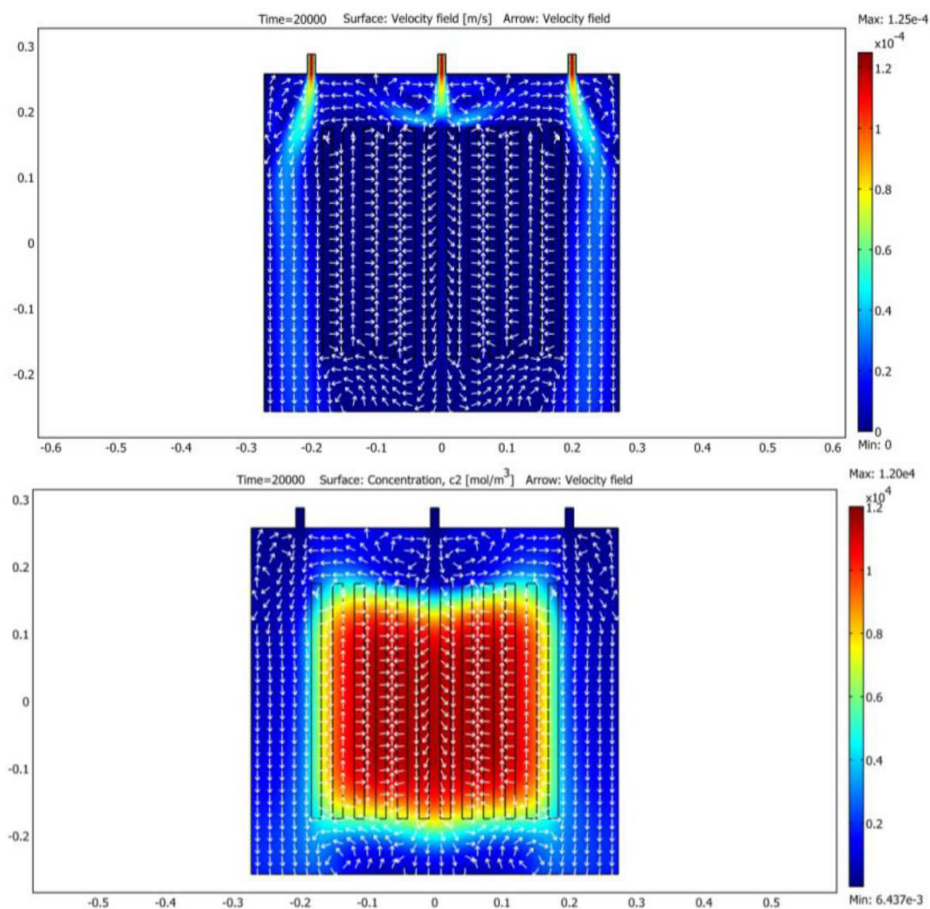


Figure A2.5. Original configuration and three inlets simulation. Velocity profile ($\text{m} \cdot \text{s}^{-1}$) (up); Down: Organic solvent concentration ($\text{mol} \cdot \text{m}^{-3}$) (down).

In the third case, three inlets are applied with a flow velocity of U_1 in each inlet, corresponding with an overall flow of $3 \times U_1$. In this case expected drying time is reduced to 1.8×10^5 s, a 20% of the original single inlet drying time.

The concentration of organic solvent is decreasing from the center to the sideways because the injection of the CO_2 is at the center and the momentum is more pronounced in the middle. In Figure A2.6, one can note two pairs of vortices, one in the top and one in the bottom of the plates.

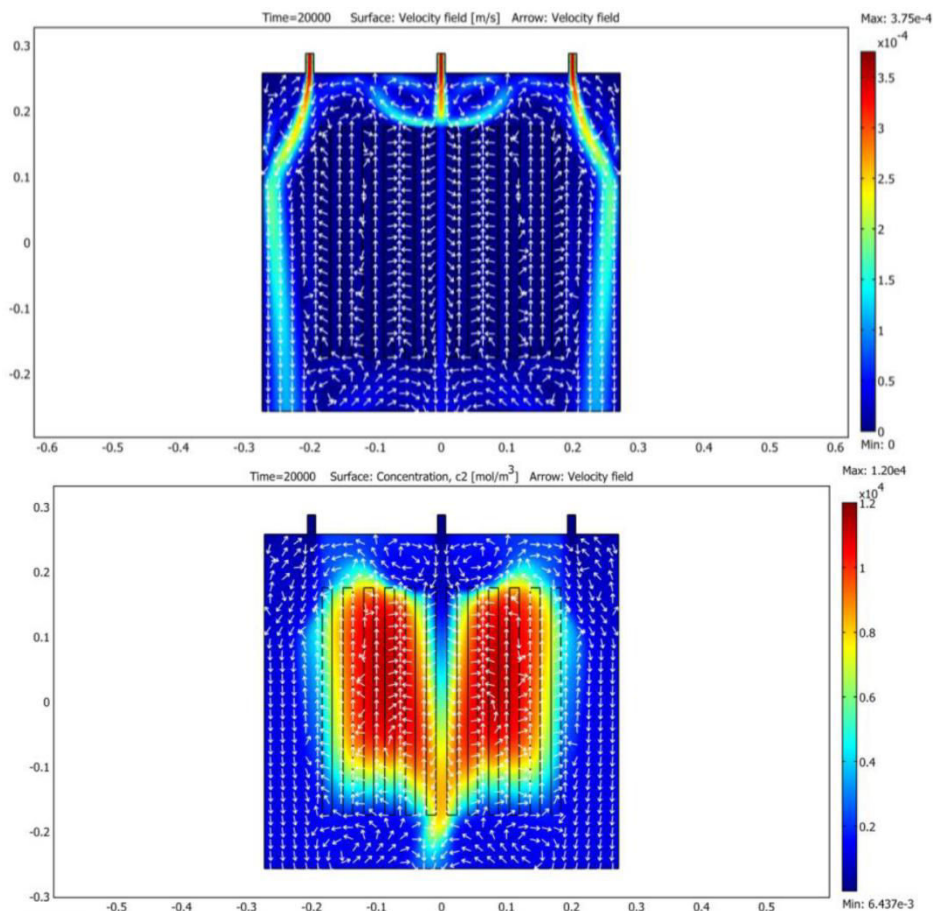


Figure A2.6. Original configuration and three inlets simulation at U_2 velocity. Velocity profile ($\text{m}\cdot\text{s}^{-1}$) (up); Down: Organic solvent concentration ($\text{mol}\cdot\text{m}^{-3}$) (down).

A2.4. MODIFIED CONFIGURATION

As described in *Chapter 3*, the modified configuration is based on the reduction of voids inside the vessel in order to force the solvent flow through the aerogel plates. As shown in Figure A2.7, the velocity in the area filled with aerogel is lower than in the areas where there is no aerogel. Near the wall, the velocity is zero and is growing in magnitude in the direction perpendicular to the wall, corroborating the no-slip condition. The expected drying time for this configuration is approximately 8.05×10^4 s.

The drying of the aerogel is much more uniform than in the previous studies with original configuration. More important than uniformity is the expected drying time, which in this case is approximately 12% of the expected drying time of the first case, representing a significant gain of efficiency of the extraction process and a reduction in the costs associated to manufacturing.

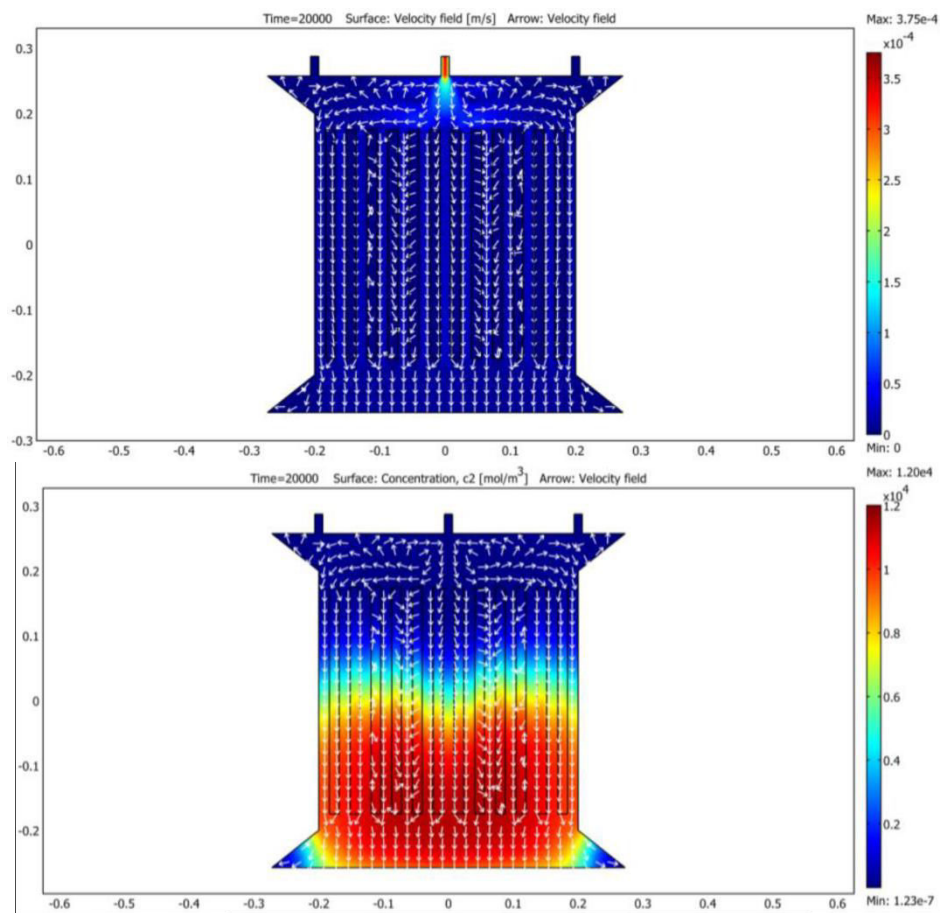
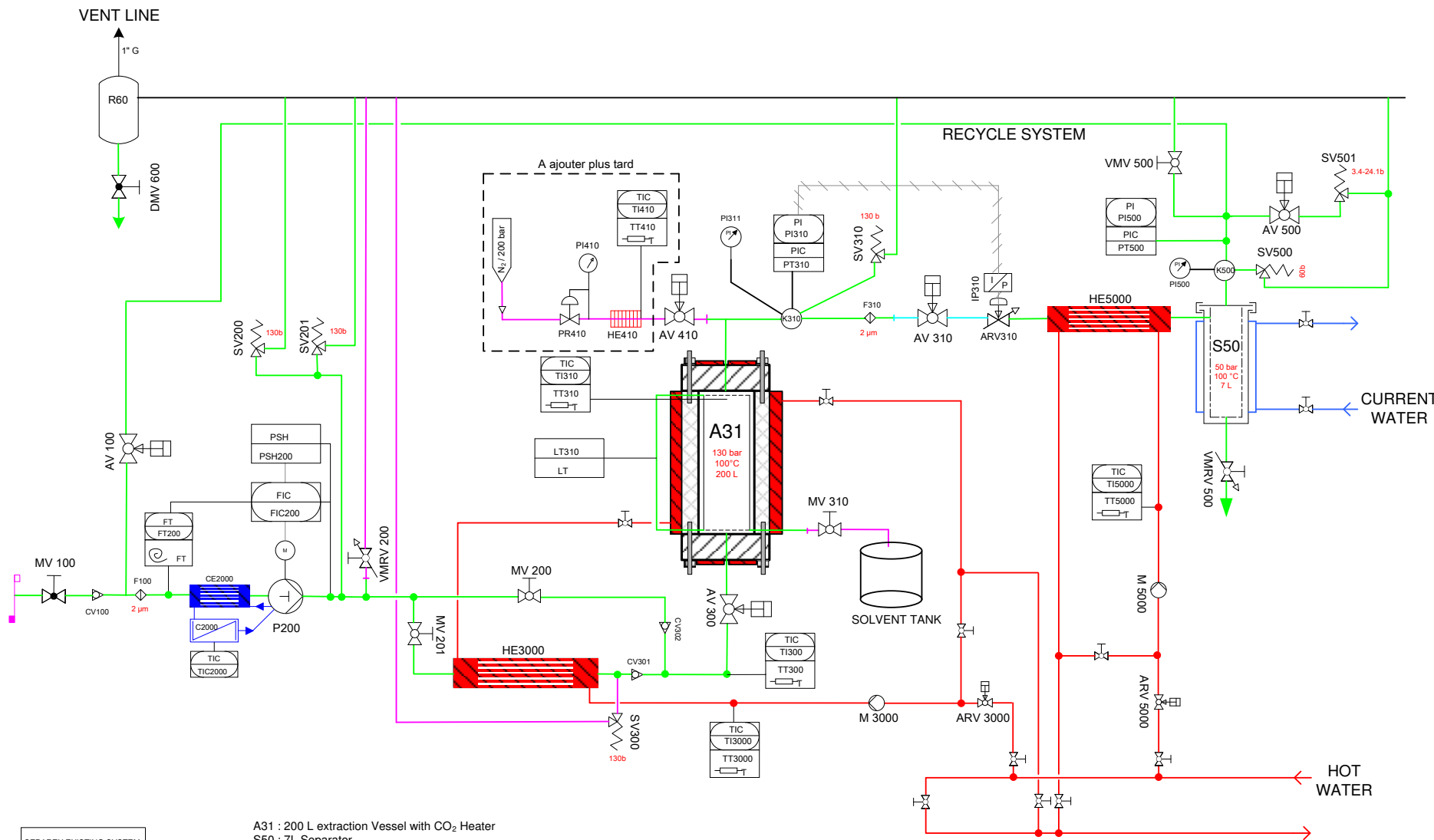


Figure A2.7. Modified configuration and three inlets simulation. Velocity profile ($\text{m} \cdot \text{s}^{-1}$) (up); Down: Organic solvent concentration ($\text{mol} \cdot \text{m}^{-3}$) (down).

ANNEX 3. PILOT PLANT P&ID

A3.1. PILOT PLANT P&ID



SEPREX EXISTING SYSTEM
 NEW INSTALLATION

PIPE 1/2"OD
 PIPE 1/4"OD
 PIPE 3/8"OD

A31 : 200 L extraction Vessel with CO₂ Heater
 S50 : 7L Separator

PUMPS

P200 : SEPREX CO₂ Pump _ 100 Kg/min up to 350 bar
 with Mass Flowmeter Regulation and Pump Head Cooling System

UTILITIES

ARV310 : Kammer Automatic Back Pressure Regulator _ Pneumatic control

SCF AEROGEL DRYING EQUIPMENT		P&ID Ref : 4361-SY40-E Date 15/03/2013
Written by : FR Checked by : JYC Approved by : MP	4361	

ANNEX 4. PILOT PLANT INSTALLATION REQUIREMENTS

The design equipment is installed at SEPAREX workshop in order to use the already existing facilities. Several guidelines for the arrangement of equipment in the workspace are defined.

A4.1. CONNECTIONS

CO₂ inlet

From the high pressure pump placed after the storage tank: ½” OD Line. Minimum thickness of 0.9 mm and maximum thickness of 1.65 mm. ½” Double ring Swagelock connection.

Vent line

The vent line of the plant must be connected to an existing ventilation system attached to a wall and ending into a 20 L pot. This connection have to be realized by an operator and the internal diameter of the ventilation system cannot be inferior to the one installed in the skid.

Connection: Minimum 1” Gas Line, Screwed union.

Compressed air/Nitrogen line

Skid process: 6 bar, non-lubricated dry air to be plugged on the group SEPAREX with a PE tube with a diameter of 8 mm.

Consumption about 2 Nm³/h

A4.2. MECHANICAL SPECIFICATIONS

For the design of the Pilot plant, some specification on the material to be used must be defined in order to be in consistency with the process issued.

Parts in direct contact with CO₂ will only be in stainless steel 316L and in PTFE or PEEK. Parts in direct contact with organic solvent and alcogel/aerogel material will only be in stainless steel 316L. List of material certificate and verification of compliance materials in Annex 2 (see §4361-CM01- A).

A4.3. DESCRIPTION OF INSTALLATION ELEMENTS

Skid: 3.80x1.3x4 m (L x W x H)

To be placed at SEPAREX facilities. It requires free space of 2 m in front of the vessel for the access to the reactor. Hoist of 1 Ton built by SEPAREX over the plant for the elevation of the pieces to be charged in the reactor. Total skid weight until 2 Tons.

Electrical Cabinet: 1.0x0.3x0.8 m (L x W x H)

Installed in the skid must be separated from the process area by a non-conductive barrier.

Power supply in the electrical cabinet: 3 phases + neutral + earth. 50 Hz, 400 V, maximal consumption of 30 kW. A circuit breaker must be installed before the plant in order to protect both the user and the equipment. A cable tray will be installed between the cabinet and the different parts of the system (processes, pump, utilities and 50 L tanks). The cable trays shall be separated by 2 for both the power part and the safety part.

Cold exchanger CE2000

Concentric pipe heat exchange in countercurrent. $Q = -600$ Kcal/h

Inner pipe	¼" OD x 1.22 (max.)
Outer pipe:	14 or 16 mm x 1 mm
Length:	3.7 min. (8m)
Insulation:	Polyisoprene foam
Connections:	16 mm Swagelok line with double ring connections for inlet and outlet for each group.

CO₂ Pump P200

High pressure piston pump.

Flow:	1-100 kg/h
Aspiration pressure:	50 bar
Service pressure:	350 bar
Aspiration temperature:	0 to +5°C
3 head SEPAREX pump with frequency variator.	
Equipped with ATEX eex IIBT4 motor.	

Flow meter FT210

Coriolis mass flow meter.

Flow:	1-600 kg/h
Working pressure:	50 bar

Heat exchanger HE3000

Concentric pipe heat exchange in crosscurrent. $Q = 2,100$ kcal/h

Inner pipe:	¼" OD x 1.22 (max.)
Outer pipe:	14 or 16 mm x 1 mm
Length:	17.4 m min. (20 m)
Insulation:	Polyisoprene foam

Connections: 16 mm Swagelok line with double ring connections for inlet and outlet for each group.

Heat exchanger HE5000

Concentric pipe heat exchange in crosscurrent. Q=5,000 kcal/h

Inner pipe: ¼" OD x 1.22 (max.)
 Outer pipe: 14 or 16 mm x 1 mm
 Length: 18.2 m min. (20 m)
 Insulation: Polyisoprene foam
 Connections: 16 mm Swagelok line with double ring connections for inlet and outlet for each group.

Autoclave A31

High pressure Autoclave.

Diameter: 545 mm
 Height: 956 mm
 Internal Volume: 220 L
 Weight: 1500 kg
 Design Temp.: +20/+100 °C
 Design Pressure: 130 bar
 Operating temperature: -5 to 100°C
 Operating pressure: 120 bar
 Test Pressure: 186 bar

Opening/Closing:

The opening and closing is performed manually with the support of the hoist to elevate the clamp system. Enclosure will be performed by 18 bolt and nuts.

In-line filter with a porosity below 5 microns are positioned upstream of the reactor.

A system of manual hoist allows charge/discharge 500 kg max.loads in/out the autoclave.

The system is equipped with:

- Heating fluid jacket.
- One internal thermocouple is placed at the top and other one in the inlet pipe that controls the temperature of the system and can be used for regulation.
- The seals are composed of PTFE and will be able to resist the range of solvents used.
- Additional connections are furnished in order to add a range of flexibility to the system for further instrumentation. Those additional connections also permit the installation of an agitator in the bottom position (connection M20 x 15).
- Differential pressure sensor allows to controlling both the residual pressure in the autoclave and to ensure a smooth filling with a pressure drop <400 Pa.
- The facility is designed to allow the easy implementation of a second autoclave.

Connections:

- *Top:*
 - ×1 Outlet ½” NPT central connection
 - ×2 Outlet ½” NPT connections
- *Body of the autoclave, at the top:*
 - ×3 ½” NPT tangential inlet connection (type AE SF250).
- *Body of the autoclave on the bottom:*
 - ×3 ½” NPT tangential inlet connection (type AE SF250).
- *Bottom:*
 - ×1 Outlet ½” NPT central connection
 - ×1 Outlet M20 Agitator connection
 - ×2 Outlet ½” NPT connections
- Other specifications/supplies:
 - Bolted top and bottom flanges.

Heating Jacket:

Internal Volume:	75 litre
Design Temp.:	+20/+100 °C
Design Pressure:	5 bar
Test Pressure:	7.4 bar

Drawings and material certificate can be found in ANNEX ...

Separator S50

High pressure separator.

Volume:	7 litre
Inner diameter:	140 mm
Design pressure:	200 bar
Design temperature:	100 °C

50-litre Tanks R50

Dimensions 1.40x.70x1.7 m (L x W x H) for the two tanks transportable by pallet (SEPAREX facilities). 300 mm diameter tank in SS360L.

The system is equipped with:

- 1 Safety valve
- 3 ½” NPT nozzle for connecting one inlet, one outlet and a free flange with a diameter of 220 mm placed in the bottom.
- 3 clamping ears + transportable by pallet
- 1 ½” NPT drain on bottom.

Connections:

- Standard Swagelok double ring fittings will be used.
- ¼" NPT fitting on instrumentation.

The lines will be of ¼" with a thickness of 1.22 mm in the whole system except the suction of the pump that will be of ½".

TABLE OF FIGURES

1.1.	Phase transition routes to pass from liquid to gas phase	9
1.2.	Boris Y et al. FD process system	11
1.3.	Surface representation of hydrophilic (left) and hydrophobic (right) silica aerogel	14
1.4.	SPD rate and shrinkage of porous materials: (a) untreated and (b) treated gel	15
1.5.	Example of continuous process for inorganic xerogel production by Socony Mobil Oil Co.	17
1.6.	Shrinkage during SPD moisture reduction	18
1.7.	Critical point of common solvents	22
1.8.	LTSCD process conditions	24
1.9.	Exchange CO ₂ /ethanol: (x) Shrinkage, (▲) no shrinkage	25
1.10.	Separex S.A.'s semi-continuous LTSCD process with $n+1$ vessels and n steps	28
1.11.	Rapid Supercritical Extraction Process (RSCE) equipment (left – middle) and process conditions (right).	29
2.1.	Hydrolyzation and condensation of alkoxysilanes	47
2.2.	Si(OR) ₄ particle and chain formation at different pH (left), dependence of relative rates of hydrolysis and condensation reactions on pH (right).....	48
2.3.	Synthesis steps diagram	49
2.4.	Flow sheet of lab-scale aerogel dried by LTSCD process with CO ₂ Pressure/Temperature profile	50
2.5.	Appearance of tailored lab-scale equipment	51
2.6.	Drying process diagram	51
2.7.	Standard drying curve for 10-mm thickness P75E20 sample with the image at each stage of the drying. Curve fixed from Fick's second Law with laboratory data	52
2.8.	Raman measurement display and example of three measurements from the sample (SAOT).....	53
2.9.	Concentration of CO ₂ (red), ethanol (blue) and mixture (black) as function of the CO ₂ molar fraction (SAOT).....	55
2.10.	Structure reaction of alkoxisilane with the aerogel backbone. a) Hydrophilic backbone, b) super-hydrophobic backbone and c) moisture-resistant backbone	57

2.11. FTIR measurements. It is clearly observed that treated sample possess more Si – R groups in the place of Si – OH groups (predominant in untreated sample).	58
2.12. FTIR spectra of different concentrations of hydrophobization	59
2.13. a) Precipitation of HMDS inside the sample and b) reaction towards a water droplet for a hydrophilic and an hydrophobic silica aerogel	59
2.14. PT envelop of the mixture CO ₂ /Ethanol/HMDS (0.950/0.045/0.005).	61
2.15. Contact angle measurements on samples a) A1, b) Si_HMDSO-ARMINES and c) B. (<i>ARMINES</i>)	63
2.16. <i>FTIR spectra of samples A2 (blue), B (green), a standard silica aerogel (black), and a standard silica aerogel hydrophobized in HMDS solution (red). (ARMINES)</i>	65
2.17. <i>FTIR spectra of samples Si_HMDS-ARMINES (blue), A2 (orange), A1 (pink), B (light blue), a standard silica aerogel (black), and a standard silica aerogel hydrophobized in HMDS solution (red). (ARMINES)</i>	66
2.18. a) Basic silica Alcolgel, b) Aerogel and c) SEM Image of P75E20 based gel	68
2.19. E Modulus and Compressive Stress of P75E20 based aerogels (<i>AEROCOINs project</i>).....	69
2.20. Tensile Strenght and Compressive Strenght of P75E20 based aerogels (<i>AEROCOINs project</i>).....	69
2.21. Thermal conductivity of P75E20 based aerogel for different densities (<i>AEROCOINs project</i>).....	70
2.22. TEOS58 based aerogel monolith	70
2.23. Waterglass-based aerogel and SEM image	72
2.24. Standard cellulose acetate-based aerogel and SEM image. (<i>ARMINES</i>)	72
2.25. Polyvinyl cross-linked aerogel with different compositions. (<i>AEROCOINs project</i>)	74
2.26. a) Original PES fiber matrix, b) single PES fiber, c) impregnated fiber with waterglass-based aerogel and d) impregnated fiber with P75E20-based aerogel. (<i>LRGP-CNRS</i>)	75
3.1. Process P&ID diagram	84
3.2. Heat exchangers configuration (left); Autoclave A31 connections (right).	86
3.3. Final assembly of the plant	88
3.4. a) Critical Point of the mixture CO ₂ /Water/Ethanol at operating conditions and b) Refraction index of water/Ethanol mixture. Point <i>a</i> (in red), determines the maximal allowance of water in the supercritical mixture in order to acquire one phase.....	90
3.5. a) Boards in the horizontal drying structure, b) aerogel dried board and c) final package and labeling prior sending to partners	91
3.6. Experimental setup for compression testing with two parallel plates. (<i>ZAE</i>)	92
3.7. Black: Stress strain curve recorded for sample SP02-02 (<i>SEPAREX</i>); red: corresponding derivative. (<i>ZAE</i>)	93

3.8. Stress-strain curve for the silica aerogel boards ambient dried (EMPA) and supercritically dried (SEPAREX), as well as the laminated component (ACCIONA). (<i>ZAE</i>)	94
3.9. Set-up of the cup test applied to determine the water vapor permeability under 50 % / 0 % RH humidity condition. (<i>VTT</i>)	95
3.10. Production costs and capacity of aerogel blanket manufacturing at different MLs	99
3.11. Cost contribution on aerogel blankets at different MLs for TEOS based materials	100
3.12. Production costs for different aerogel products	101
4.1. SEPAREX S.A.S. Facilities in Champigneulles France	105
4.2. Total revenues of Aerogel manufacturing	107
4.3. Layer thickness of building insulation material required to reach a U value of 0.5 and 0.2 W/m ² K (<i>AEROCOINS project</i>)	109
4.4. Satellite prototype insulation based on encapsulated aerogel (<i>AerSUS project</i>).	110
4.5. Common insulation of industrial pipes (left). Thickness comparison between normal insulation (lower part), aerogel-based insulation (Aspen Aerogel) (middle part) and row pipe (upper part) (right).....	113
4.6. Powder aerogel sample	115
4.7. Granular aerogel absorbing oil from water.	115
4.8. Inorganic monolith panel	116
4.9. Inorganic aerogel board (left) and blanket (right).	117
4.10. Inorganic Aerogel production cost contribution at different scales	120
4.11. Representation of a desired 5 m ³ scale (DyeCoo Textile Systems B.V.).....	122
4.12. Overview of funding request and development plan	123
A1.1. Phase diagrams (P-x) for the CO ₂ (1) – Ethanol (2) system at 333.82 K. The symbol corresponds to the experimental data. Solid line corresponds to the model calculation	140
A1.2. Phase diagrams (P-x) for the Ethanol (1) – HMDS (2) system at 333.82 K. The symbol corresponds to the experimental data. Solid line corresponds to the model calculation	141
A1.3. Phase diagrams (P-x) for the CO ₂ (1) – HMDS (2) system at 333.82 K. The symbol corresponds to the experimental data. Solid line corresponds to the model calculation	142
A1.4. Example of P-T envelop of hydrocarbons (C1 to C5).	144
A2.1. Velocity profile (m·s ⁻¹) of single plate (left); Organic solvent concentration [mol·m ⁻³] evolution of single plate at: t=0, 200, 400, 600, 800, 1,000, and 1,200 s (right)	148
A2.2. Parameterization results. From top to bottom: velocity, porosity,	

	diffusivity, permeability and viscosity as a function of time in seconds	148
A2.3.	Vertical sample holder module (left) and final integration in the vessel (right).	149
A2.4.	Original configuration and single inlet simulation. Velocity profile ($\text{m}\cdot\text{s}^{-1}$) (up); Down: Organic solvent concentration ($\text{mol}\cdot\text{m}^{-3}$) (down)	150
A2.5.	Original configuration and three inlets simulation. Velocity profile ($\text{m}\cdot\text{s}^{-1}$) (up); Down: Organic solvent concentration ($\text{mol}\cdot\text{m}^{-3}$) (down)	151
A2.6.	Original configuration and three inlets simulation at U_2 velocity. Velocity profile ($\text{m}\cdot\text{s}^{-1}$) (up); Down: Organic solvent concentration ($\text{mol}\cdot\text{m}^{-3}$) (down) ...	152
A2.7.	Modified configuration and three inlets simulation. Velocity profile ($\text{m}\cdot\text{s}^{-1}$) (up); Down: Organic solvent concentration ($\text{mol}\cdot\text{m}^{-3}$) (down)	153

LIST OF TABLES

1.1.	Process and Simulation of Cryogel drying	12
1.2.	Process and Simulation of Xerogel drying	20
1.3.	Different solvent and reactions	20
1.4.	Process and simulation of Aerogel drying	30
1.5.	Different solvent and reactions	31
2.1.	Physical properties of components (Compilation from DIPPR available in Simulis Thermodynamic software from PROSIM France).....	60
2.2.	Values of the binary interaction parameters	60
2.3.	Gels treated and densities	62
2.4.	Contact Angles of HMDS and HMDSO silylated samples	62
2.5.	Water uptake of HMDSO silylated samples	64
2.6.	Experimental thermal conductivity ($W.(mK)^{-1}$) of aerogels from HIPIN58 precursor	71
2.7.	Polyvynil aerogel properties	73
3.1.	Parametrization and variables used in the simulation model	81
3.2.	Organic solvent concentration at 5.5 h of drying time for different configurations	82
3.3.	Dimensional requirements of autoclave A31	87
3.4.	Validated parameters	89
3.5.	Thermal conductivities of supercritically dried boards measured (<i>ZAE</i>).....	91
3.6.	Summary of elastic moduli determined in different regimes of deformation for supercritical dried samples; the boards analyzed had a size of 290 x 290 mm ² and a thickness of about 16 mm. (<i>ZAE</i>).....	93
3.7.	Summary of elastic properties determined	94
3.8.	Water vapor resistance factors μ for test samples. (<i>VTT</i>)	95
3.9.	Manufacture level (ML) assumption	96
3.10.	Inorganic gel raw material cost from different precursors (C_G).....	97
4.1.	Major companies involved in Aerogels production	107
4.2.	Properties of aerospace insulation materials (<i>AerSUS project</i>).....	110
4.3.	Advantages and disadvantages of insulation materials for aerospace applications	111

4.4. Aerogel Nature vs. Shape	114
4.5. Inorganic monolith's main properties	116
4.6. General Aerogel applications and final manufacture	118
4.7. Business assumption for 2017 production.....	123
4.8. Market penetration and annual sales	124
4.9. 3 years profits and costs	124
4.10. 5 years profits and costs	125
4.11. Analysis of Macro-Environment	127
4.12. Analysis of Industry	128
4.13. Analysis of Weakness and Strengthens	129
4.14. SWOT Analysis	130
A1.1. Relative deviation AADU and BIASU obtained in fitting experimental VLE of CO ₂ (1) – Ethanol (2) system at 333.82 K with the model	141
A1.2. Relative deviation AADU and BIASU obtained in fitting experimental VLE of Ethanol (1) – HDMS (2) system at 333.15 K with our model	142
A1.3. Relative deviation AADU and BIASU obtained in fitting experimental VLE of Ethanol (1) – HDMS (2) system at 333.15 K with the model	143
A1.4. Values of the binary interaction parameters	143
A1.5. Calculated bubble and dew point values for the mixture CO ₂ /ethanol/HDMS ...	145
A2.1. Simulation parameters	147

